GOETHE UNIVERSITÄT FRANKFURT AM MAIN

Impact of oxidative stress by hepatitis C virus-mediated Nrf2 inhibition on autophagy and viral particle release

Dissertation

zur Erlangung des Doktorgrades
der Naturwissenschaften (Dr. phil. nat.)

vorgelegt beim Fachbereich
Biochemie, Chemie, Pharmazie
der Johann Wolfgang Goethe-Universität
in Frankfurt am Main

von

Regina Medvedev
aus Tiraspol, Moldawien

Frankfurt (2017)
(D30)

vom Fachbereich Biochemie, Chemie, Pharmazie der
Johann Wolfgang Goethe-Universität als Dissertation angenommen.

Dekan: Prof. Dr. Michael Karas
Gutachter: Prof. Dr. Rolf Marschalek
Prof. Dr. Eberhard Hildt

Datum der Disputation:

"Alles Wissen und alles Vermehren unseres Wissens endet nicht mit einem Schlußpunkt, sondern mit einem Fragezeichen."

Hermann Hesse

Table of contents

1 Introduction

Hepatitis C is an inflammation of the liver caused by the hepatitis C virus (HCV). It can progress to chronic hepatitis, fibrosis and cirrhosis and may ultimately lead to hepatocellular carcinoma (HCC). According to the World Health Organization (WHO), 130—150 million people are chronically infected with HCV worldwide, corresponding to 2 % of the world population (WHO, 2016, Lanini et al., 2016). Even though HCV can nowadays be treated with directly acting antiviral agents (DAA), which are more effective than the old therapies and have revolutionized the treatment, there is still no vaccine available (Jianjun Gao, 2017). As the costs for the treatment with DAAs are prohibitive, the majority of patients are treated with an alternative interferon-α-based therapy, which has certain side effects and is only effective in 50—60 % of the cases. To further develop effective cures and vaccination strategies, a better understanding of the viral life cycle is indispensable.

1.1 History and classification of hepatitis C virus (HCV)

In the 1970s, a so far unknown parenterally-transmitted hepatitis form was identified which was neither caused by the hepatitis A nor the hepatitis B virus (Feinstone et al., 1975). It took over a decade and the development of a diagnostic test to identify in 1988 the hepatitis C virus as cause for the non-A, non-B hepatitis (NANBH) (Choo et al., 1989). Consequently, interferon-α was approved a few years later by the Food and Drug Administration (FDA) as first treatment against HCV (Pawlotsky et al., 2015). Researchers had to face initial limitations to generate a cell culture-based *in vitro* system, in which the virus had the ability to replicate and produce infectious viral particles. Therefore, different systems such as heterologous expression systems (Bartenschlager et al., 1994), subgenomic replicon systems (Lohmann et al., 1999b, Blight et al., 2000) and pseudoparticles (Bartosch et al., 2003) were established to investigate the viral life cycle. The isolation of a clone from the serum of a Japanese patient with fulminant hepatitis (JFH1), which replicated to exceptional high levels without the need of adaptive mutations, as well as the identification of the Huh7.5 cell line being highly permissive for HCV, facilitated the development of a cell culture system to study the complete viral life cycle (Lindenbach et al., 2005, Wakita et al., 2005, Zhong et al., 2005, Pietschmann et al., 2006).

HCV is an RNA virus that belongs to the genus of *Hepacivirus* within the family of *Flaviviridae*. It can be subdivided into 7 genotypes (1−7) and various subtypes (a, b, c, etc.), exhibiting different geographical distributions and medication sensitivities (Simmonds, 2004, Simmonds et al., 2005). The nucleotide sequence within the genotypes differ by about 30−35 % and within the subtypes by another 20−25 % (Irshad et al., 2010). The viral RNA-dependent RNA polymerase (RdRp) lacks a proof-reading function, resulting in high mutation rates of the viral genome. Based on this, a high genetic diversity with different but closely related genomes (so-called quasispecies) is observed within a virus population (Martell et al., 1992, Farci and Purcell, 2000).

1.2 Epidemiology

HCV constitutes a significant health burden worldwide, resulting in rising levels of liver-related mortality and morbidity as a consequence of disease progression (Petruzziello et al., 2016). A recent study including 138 countries estimated a total global HCV prevalence of about 2,5 %, corresponding to 177 million HCV-infected adults (Petruzziello et al., 2016). The highest prevalence is estimated in central Asia and central Africa (>3,5 %), followed by South, East and Southeast Asia, West, East and North Africa and Middle East, Latin America, Australasia, and Eastern Europe with a moderate prevalence (1,5 %−3,5 %). The lowest prevalence was observed in Southern Africa, North America, Pacific Asia and Western and Central Europe (<1,5 %) (Petruzziello et al., 2016). Despite the low prevalence in the first-world countries, HCV represents a tremendous health problem providing the basis for the development of DAAs. Globally, the distribution and appearance of genotypes varies. So far, only one infection with genotype 7 has been reported (Murphy et al., 2007). The geographic distribution is shown in figure 1.1. While genotype 1 is common worldwide, with the highest prevalence in the high income countries, genotype 2 is mostly present in West Africa, while North Africa and the Middle East has the highest genotype 4 population. In Central and Northern Africa and in Southeast Asia genotype 4 and 6 are highly present. Genotype 3 is most prevalent in Asia (Petruzziello et al., 2016).

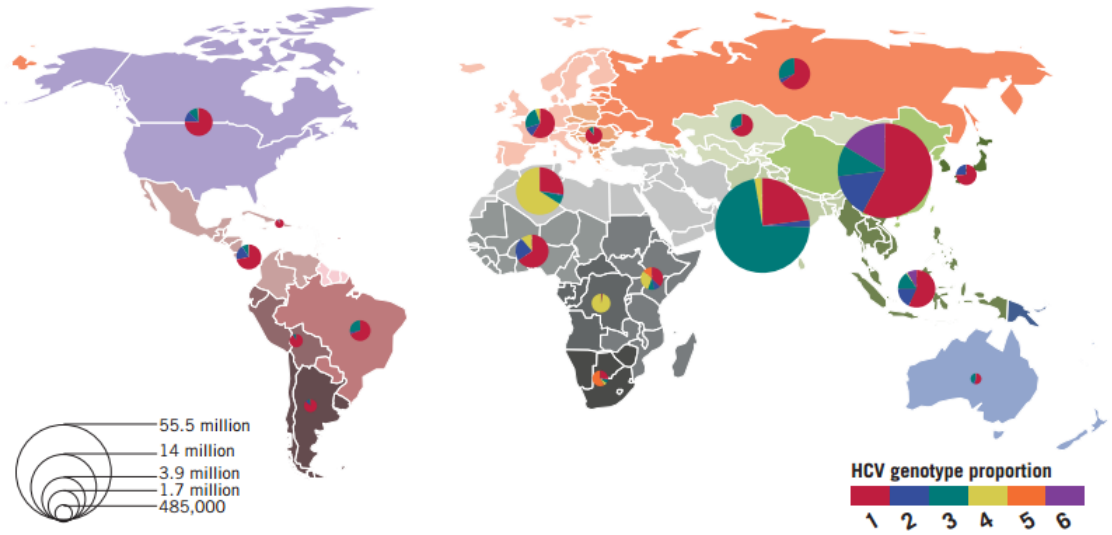

Figure 1.1: Relative prevalence of HCV genotypes worldwide. Size of pie chart is proportional to the number of seroprevalent cases. Adapted from Messina et al., 2014.

HCV is a blood-borne virus. Transmission mostly occurs by intravenous drug infection (67 %) (Nelson et al., 2011). However, the virus can also be transmitted by transfusion of unscreened blood products (Shepard et al., 2005), by an infected mother to her unborn child (Thomas et al., 1998, Mast et al., 2005), tattooing (Jafari et al., 2010) or to a lower extent by sexual activity (Terrault et al., 2013, Tohme and Holmberg, 2010).

1.3 Pathogenesis

The incubation period varies from 2 weeks to 6 months. An acute infection mostly proceeds asymptomatically or shows flu-like symptoms like fever, fatigue, nausea, decreased appetite and jaundice (yellowing of skin and the whites of the eyes). In approximately 15 % of acutely infected patients, HCV infection is cleared spontaneously (Lauer, 2013), while 85 % develop a chronic hepatitis (Nawaz et al., 2015, Alter et al., 1997). The persistent inflammatory activity of the immune system results in the immune-mediated pathogenesis of chronic HCV infection, since HCV itself does not cause a cytopathic effect (Irshad et al., 2013). Thereby, HCV activates natural killer cells (NK cells) and cytotoxic T-cells, which are trying to rehabilitate the original liver structure and hepatic function (Martinez-Esparza et al., 2015). Due to persistent liver damage caused by elevated levels of reactive oxygen species (ROS), liver regeneration is exhausted and gives rise to a replacement of functional tissue with non-functional connective tissue, progressing into fibrosis (Rockey and Bissell, 2006). Thereby, non-parenchymal cells, such as myofibroblasts and activated hepatic stellate cells (HSC), extensively deposit extracellular matrix (ECM) resulting in fibrous scars (Pellicoro et al., 2014). 20 %

of chronic infected patients develop liver cirrhosis within 20 years, which can result in total liver failure (El-Serag, 2002). Furthermore, patients with liver cirrhosis are at high risk of developing hepatocellular carcinoma (HCC), which is the fifth common cancer worldwide and the second most common cause of cancer death (Tang and Grisé, 2009).

1.3.1 HCV-induced oxidative stress

Infection with HCV is often accompanied by elevated levels of reactive oxygen species (ROS) (Ivanov et al., 2013). Several sources of ROS have been identified in HCV-infected hepatocytes which involve ER stress, unfolded protein response (UPR), mitochondrial dysregulation, Ca^{2+} redistribution and NADPH oxidases (NOXs) (Wang and Weinman, 2013, Jheng et al., 2014, Dionisio et al., 2009, de Mochel et al., 2010). Viral infection affects the cellular protein folding machinery, thereby causing an imbalance between strong and fast viral protein processing and the regular ER protein processing output, also termed as ER stress (Jheng et al., 2014). To overcome ER stress, the UPR has evolved, resulting in a reduced protein translation and increased ER folding capacity to reestablish cellular homeostasis (Walter and Ron, 2011). HCV replication (Merquiol et al., 2011, Yao et al., 2014), as well as overexpression of structural proteins E1 and E2 (Chan, 2005) and nonstructural protein NS4B (Zheng et al., 2005), can result in the induction of ER stress and UPR. Mitochondria play a central role in ROS generation upon HCV infection (Wang and Weinman, 2013), as viral proteins are directly associated with mitochondria (Korenaga et al., 2005, Kasprzak et al., 2005, Chu et al., 2011). Particularly, the HCV core protein can bind with its hydrophobic C-terminus to the outer mitochondrial membrane (OMM) (Ivanov et al., 2015, Schwer et al., 2004, Suzuki et al., 2004, Okuda et al., 2002, Korenaga et al., 2005). Consequently, mitochondria are sensitized towards Ca^{2+} influx, resulting in the opening of the mitochondrial permeability transition pore (mPTP) and release of cytochrome c (Wang et al., 2009). Lately, it has been discovered that interaction of NS5A with the phosphatidylinositol-4-kinase IIIα (PI4KA) is necessary for membrane tethering between mitochondria and ER leading to mitochondrial fragmentation (Siu et al., 2016). For the induction of ROS, Ca^{2+} rearrangement between the cytoplasm, ER and mitochondria plays a significant role. Thereby, the core protein exhibits a negative impact on the sarcoplasmic/endoplasmic reticulum calcium ATPase (SERCA), causing an increase of cytolasmic Ca^{2+} concentration (Dionisio et al., 2009). The same holds true for NS5A, which affects Ca^{2+} homeostasis by triggering Ca^{2+} release from the ER into the cytoplasm (Dionisio et al., 2009).

Nox1 and 4 could function as the main source of superoxide anions and H_2O_2 in HCV-infected hepatocytes (Boudreau et al., 2009, de Mochel et al., 2010). The NOX family plays an important role in electron transport through the membrane, thereby transferring electrons from NADPH to molecular

oxygen. As a by-product, superoxide anions ($O_2^{\cdot-}$) and hydrogen peroxide (H_2O_2) are generated (Paik et al., 2014).

1.4 Diagnosis

HCV diagnosis depends on two categories of laboratory tests, direct tests characterizing the viral components like HCV RNA and core antigen, and indirect tests detecting specific antibodies to HCV (anti-HCV) (Bajpai et al., 2014). Furthermore, elevated levels of alanine aminotransferase (ALT) can be detected within 4 to 12 weeks after HCV infection as a consequence of liver injury (Kim et al., 2013).

Anti-HCV antibodies can be first detected about 6 to 8 weeks after the beginning of infection by enzyme-linked immunosorbent assay (ELISA) (Bajpai et al., 2014). Nowadays, fourth generation ELISA tests are available, simultaneously detecting HCV capsid antigen and antibodies against core, NS3, NS4, and NS5. Even though these tests have reduced the time window of HCV detection to 17 days, they still show a lack of sensitivity and specificity (Rouet et al., 2015).

The presence of HCV core antigen is detected by immunoassays like ELISA and chemiluminescence immunoassays (CLIA), independently of HCV genotypes (Seme et al., 2005). These assays detect an HCV infection as effectively as nucleic acid tests (NAT), as the HCV core antigen levels closely follows HCV RNA dynamics in patient's serum (Seme et al., 2005, Gaudy et al., 2005). Limitations arise from its sensitivity compared to NAT (Gaudy et al., 2005).

For detection of active HCV replication, screening of HCV RNA by NAT is regarded as the "gold standard" as it enables an early infection even after 4—6 days (Bajpai et al., 2014, Marwaha and Sachdev, 2014). Due to good sensitivity (99 %) and specificity (98—99 %), quantitative RT-PCR (qRT-PCR) has replaced qualitative PCR, which was utilized to confirm viremia and had a higher limit of detection (Scott and Gretch, 2007).

1.5 Therapy

Over the past two decades, treatment of HCV was based on pegylated interferon (IFN)-α in combination with ribavirin, a guanosine analogue with antiviral effects. To monitor the success of the therapy, sustained virological response is measured (SVR), which is based on an undetectable level of HCV RNA 12 weeks (SVR12) or 24 weeks (SVR24) after completion of treatment (Lynch and Wu, 2016). With a SVR of 42—46 %, the combination therapy of peg-IFN-α with ribavirin is moderately efficient, but has severe side effects like depression, fatigue, flu like symptoms and anaemia

(see figure 1.2) (Pawlotsky et al., 2015). Therefore, new IFN-α free therapeutics are required. In 2011, the two first-wave, first-generation direct-acting antivirals (DAAs) HCV NS3-NS4A protease inhibitors telaprevir and boceprevir were approved in combination with peg-IFN-α and ribavirin and improved the SVR rate to 67−75 % (Ghany et al., 2011). This paved the way for a new generation of HCV therapies. As the HCV life cycle can be blocked at any step (Pawlotsky, 2014), a variety of inhibitors were developed, such as NS3-4A protease inhibitors, inhibitors of the nonstructural 5A protein (NS5A), nucleotide analogue inhibitors of the HCV RNA-dependent RNA polymerase (RdRp) and non-nucleoside inhibitors of the HCV RdRp (Pawlotsky et al., 2015). Nevertheless, activity against different HCV genotypes and barrier to resistance tremendously differs between these drugs (Pawlotsky et al., 2015). While first-wave, first-generation NS3-4A protease inhibitors were mainly active against genotype 1 and exhibited a low barrier to resistance, the development of second-wave, second-generation NS3-NS4A protease inhibitors improved the barrier to resistance. Additionally, these inhibitors showed pangenotypic activity. The group of nucleotide analogues can be applied against every HCV genotype displaying a high barrier to resistance. Non-nucleoside inhibitors of RdRp show only a limited area of application as they are only active against genotype 1 and have a low barrier to resistance. Finally, second-wave NS5A inhibitors have pangenotypic activity but a low barrier to resistance (Pawlotsky et al., 2015). Since 2014, two new IFN-α free DAA combinations have been approved. The combination of sofosbuvir (nucleotide analogue of HCV RdRp NS5B) and ledipasvir (NS5A inhibitor) administered daily in one single pill for 8 to 24 weeks improved the SVR rate to 93−100 % (Pawlotsky et al., 2015). Nowadays, new DAAs and combinations of DAAs are being tested in clinical trials, giving hope to patients, physicians and scientists that HCV can be totally cured and maybe one day globally eliminated (Pawlotsky et al., 2015). One limiting factor of success is the prohibitive pricing for new HCV therapies, which represents a significant limitation in conquering HCV (San Miguel et al., 2015).

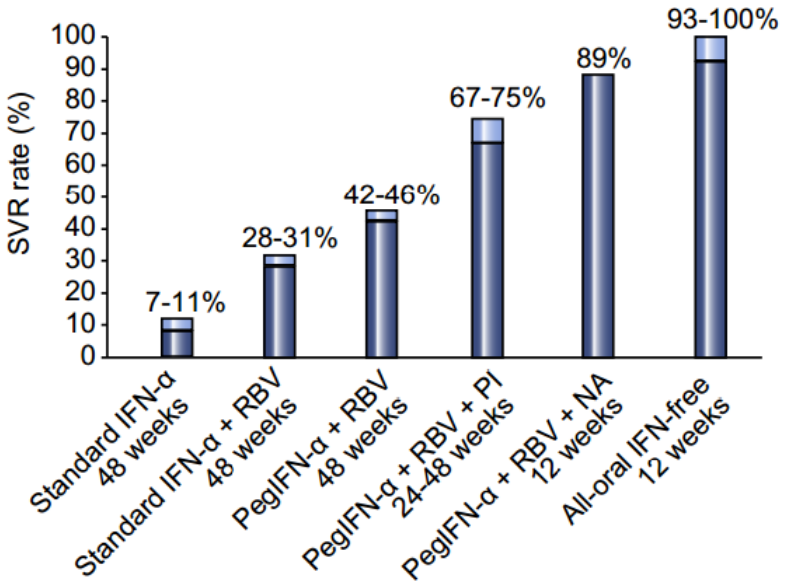

Figure 1.2: Progress in the therapy of chronic hepatitis C genotype 1 as shown by SVR rates with different antiviral regimens. RBV — ribavirin; PI — first-wave, first-generation protease inhibitor (telaprevir or boceprevir); NA — nucleotide analogue (sofosbuvir). (Pawlotsky et al., 2015)

Many efforts have been made to develop both a prophylactic and therapeutic HCV vaccine but to date there is still no vaccine available for clinical use (Ghasemi, 2015). A potential vaccine candidate must be able to provide both, an effective immune response and offer protection against other HCV species (Naderi et al., 2014). Furthermore, it should induce a cellular and humoral immune response against different viral proteins (Zeng et al., 2009). A significant barrier for the generation of an HCV vaccine is the error prone RdRp, as it has no proof-reading activity. The high replication rate gives rise to viral genome mutations, resulting in a heterogeneous virus population within an infected patient (Jawaid and Khuwaja, 2008). Several approaches have been tested so far, including recombinant protein vaccines, peptide vaccines, DNA vaccines, vector-based vaccines and HCV virus-like particles (Swadling et al., 2013). A recombinant protein vaccine has a big safety advantage as it does not contain the pathogen or its genome (Swadling et al., 2013). Several genes encoding viral proteins have been tested for use in HCV vaccines, including the envelope glycoproteins E1 and E2 (Choo et al., 1994). For the development of peptide vaccines, small, synthetic HCV peptides have been applied as potent immunogenic antigens to induce a T cell response as they can be directly presented on MHC class I and II (Firbas et al., 2006, Firbas et al., 2010). A further approach is the DNA-based immunization method, which includes injection of recombinant plasmids showing an effective protein expression *in vivo* followed by an immune response in mouse and primates (Lang Kuhs et al., 2012, Latimer et al., 2014). In these studies, DNA plasmids encoding the antigens NS3, NS4 and NS5A have shown to induce an sustained T cell response. A combination of these plasmids with a plasmid encoding interleukin-28B showed significant immunoadjuvant activity representing a

promising prophylactic vaccine candidate (Lee et al., 2017). However, so far this approach has not been translated well into men (Swadling et al., 2013). Finally, viral vectors are attractive vehicles for the delivery of foreign antigens. Several viral vectors have been tested, including adenovirus, modified vaccinia Ankara and canary pox (Folgori et al., 2006, Barnes et al., 2012, Fattori et al., 2006, Pancholi et al., 2003, Swadling et al., 2014). Many attempts have been made so far to develop a HCV vaccine. Nevertheless, the high genetic variation within populations remains the biggest obstacle that needs to be overcome (Ghasemi, 2015). Even though the prospects for a vaccine have considerably improved, the development of an efficient vaccine with relatively few side effect is still challenging (Swadling et al., 2013, Ghasemi, 2015).

1.6 Hepatitis C virus

1.6.1 Viral genome

HCV has is single-stranded, positive-sensed RNA genome with a size of 9,6 kB, which is composed of one long open reading frame (ORF) flanked by highly structured 5' and 3' untranslated regions (UTR) (figure 1.3) (Bartenschlager et al., 2013). The 5' UTR, that is essential for viral replication, contains an internal ribosomal entry site (IRES), which guides translation of the viral genome in a cap-independent manner (Friebe et al., 2001, Hoffman and Liu, 2011). Furthermore, the miRNA122, which is specifically expressed in the liver, is a host factor that binds to the viral RNA at the 5' UTR, thereby positively regulating the viral life cycle by facilitating viral RNA replication (Roberts et al., 2011). The 3' UTR contains a short variable sequence (VAR), a poly(U/C) region of heterogeneous length and a highly conserved 98 nucleotide sequence (X-tail), which is essential for replication (Kolykhalov et al., 1996). The ORF encodes for a polyprotein of about 3000 amino acids (aa), which is co- and post-translationally processed by viral and host proteases to yield the ten mature viral proteins (Gottwein and Bukh, 2008). The N-terminal encoded structural proteins core, E1 and E2, build up the viral particle. The nonstructural proteins NS3, NS4A, NS4B, NS5A and NS5B form the replication complex, which is essential for viral replication and is involved in the regulation of cellular processes (Lindenbach and Rice, 2013). NS2 together with the ion channel p7 are crucial for the formation of the viral particle. However, both proteins are not part of the viral particle (Bartenschlager et al., 2011).

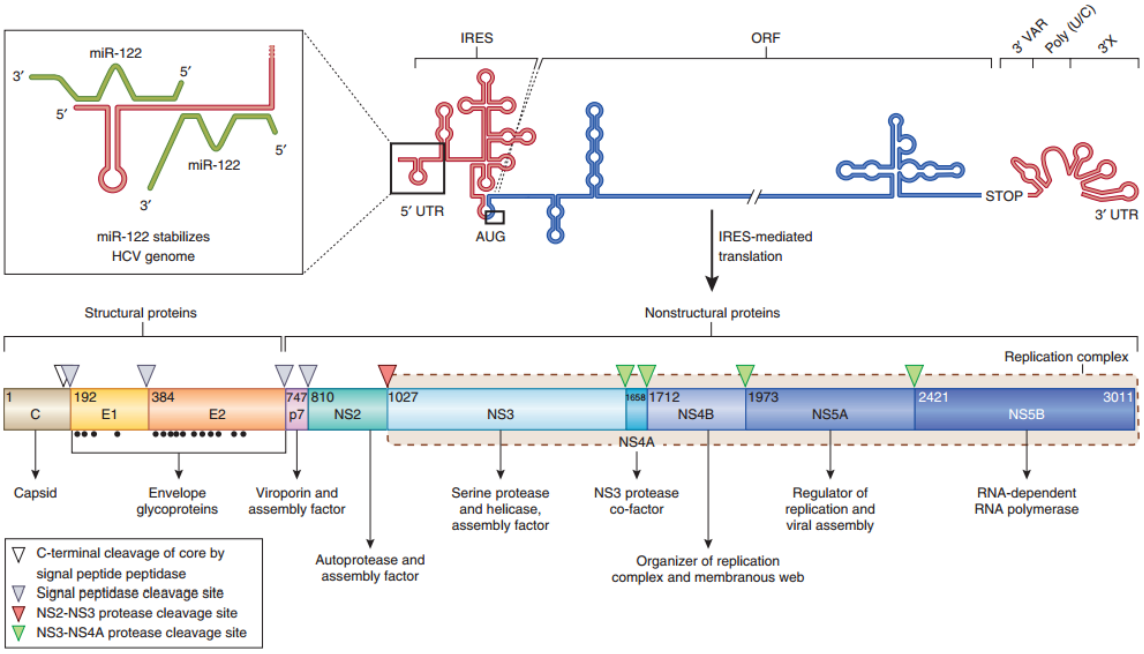

Figure 1.3: The HCV genome and polyprotein processing. The HCV RNA genome (top) consists of one long ORF (blue), which is flanked by 5' and 3' UTR (red). Two copies of miRNA122 (green) bind to the 5' UTR (highlighted in the inset). IRES-mediated translation of the ORF results in a polyprotein (bottom), which is co- and post-translationally processed by viral and host proteases to yield the ten mature viral proteins. Maturation of the core protein involves a cellular signal peptide peptidase cleavage of a C-terminal signal peptide (white triangle) and cleavage from E1 by the cellular signal peptidase which also cleaves E1, E2 and p7 from the polyprotein (gray triangles). The NS2-NS3 protease cleaves itself in an autocleavage-mediated mechanism requiring two identical molecules to form the composite active site (red triangle). The NS3 protease, in combination with its membrane-bound cofactor NS4A , cleaves the remaining proteins NS3, NS4A, NS4B, NS5A and NS5B (green triangles). Glycosylation of the envelope proteins are indicated by the black dots (Scheel and Rice, 2013).

1.6.2 Viral proteins

The ORF encodes for a polyprotein of about 3000 amino acids (aa), which is co- and post-translationally processed in ten mature viral proteins that are invariably associated with intracellular membranes either by transmembrane domains or amphipathic α-helices (Bartenschlager et al., 2013). The membrane topologies and the main functions are shown in figure 1.4.

1.6.2.1 Core

The HCV core protein, which forms the viral capsid, is a highly conserved basic RNA-binding protein with a size of 21 kDa (McLauchlan, 2000). Core can be divided into three domains on the basis of hydrophobicity (Ashfaq et al., 2011). Domain 1 (aa 1—117) mainly contains basic residues and the RNA-binding and self-oligomerization module (Boulant et al., 2005). Domain 2 (aa 118—177) is

more hydrophobic than domain 1 and forms a pair of amphipathic helices that facilitate the peripheral anchoring of core with cellular membranes (Boulant et al., 2006, Kopp et al., 2010, Okamoto et al., 2008). Domain 3 (aa 178—191) is highly hydrophobic and serves as a signal peptide for the translocation of E1 into the endoplasmic reticulum (ER) (McLauchlan, 2000). Initially, core is cleaved by a host signal peptidase from the polyprotein. The removal of domain 3 is mediated by a signal peptide peptidase and yields the mature core protein that forms a homodimer (Boulant et al., 2005, Okamoto et al., 2008, Huessy et al., 1996).

After cleavage, mature core is targeted to the lipid droplets (LD) (Barba et al., 1997, McLauchlan et al., 2002, Moradpour et al., 1996), which are intracellular storage organelles for neutral lipids (Beller et al., 2010). Furthermore, it was observed that core recruits nonstructural proteins as well as replication complexes to close proximity of LDs (Miyanari et al., 2007). However, in life cell imaging analysis an accumulation of core was observed which was transported along microtubules, probably representing viral particles trafficking via the secretory pathway (Counihan et al., 2011). Besides its role in capsid formation, the core protein has certain regulatory functions by interacting with a variety of cellular proteins, thereby affecting host cell functions such as lipid metabolism, oxidative stress responses, gene transcription and many more (Tellinghuisen and Rice, 2002).

1.6.2.2 Envelope glycoproteins E1 and E2

The envelope proteins E1 and E2 are cleaved from the polyprotein by signal peptidase (Scheel and Rice, 2013) and assemble into a non-covalent heterodimer (Deleersnyder et al., 1997). The glycosylation sites are highly conserved with 4—5 N-linked glycans in E1, and 11 glycosylation sites in E2 (Drummer et al., 2003, Goffard et al., 2005). Depending on the glycosylation, E1 has a molecular size of ~33 kDa and E2 ~70 kDa (Deleersnyder et al., 1997). The structure includes a N-terminal ectodomain, which is targeted towards the ER lumen and gets highly glycosylated. The C-terminus forms a transmembrane domain, which harbors a signal sequence and a membrane anchor, and is responsible for the E1E2 heterodimerization and ER-retention of the heterodimer (Voisset and Dubuisson, 2004). The E1E2 complex is embedded in the lipid bilayer of the viral particle, where E2 acts as a receptor binding subunit mediating viral infection (Goffard et al., 2005). It is thought that E1 possesses fusogenic properties, thereby enabling the fusion of the viral and endosomal membrane (Goffard et al., 2005, Drummer et al., 2003). Furthermore, E2 contains two hypervariable regions (HVR), HVR1 and HVR2, that are prone for mutations. This enables the virus to escape neutralizing antibodies (Boulestin et al., 2002, Polyak et al., 1998). However, the genetic heterogeneity of HVR1 may contribute to the evasion of the virus from the immune system, thereby facilitating the development of a chronic infection (Prentoe et al., 2016).

1.6.2.3 p7

p7 is a membrane-spanning, 63-amino acid polypeptide with two transmembrane domains (Griffin et al., 2003). It is located in the ER, where it forms ion channels that play a crucial role for viral infection and the assembly of viral particles (Steinmann et al., 2007).

1.6.2.4 NS2

NS2 is a 21—23 kDa hydrophobic protein forming four transmembrane helices that are incorporated into the ER membrane (Ashfaq et al., 2011). The C-terminus of the protein remains in the cytoplasm, where together with the N-terminal part of NS3 it forms the NS2/3 metalloprotease. As the NS2/3 protease mediates a cleavage at the NS2/NS3 junction, it is also called an autoprotease (Lorenz et al., 2006). Since NS2 is dispensable for viral replication, it is thought that NS2 contributes to the viral particle assembly by attracting the envelope proteins to the assembly site (Popescu et al., 2011).

1.6.2.5 NS3

NS3 is a 67 kDa protein that exhibits various functions. At the N-terminus it harbours a serine protease activity that is involved in the cleavage of the viral polyprotein (Bartenschlager et al., 1993). The C-terminus has NTPase/helicase activity that is essential for viral replication (Gallinari et al., 1998). It is assumed that NS3 initiates the replication by mediating the unwinding of double-stranded RNA intermediates, eliminating secondary structures and separating nucleic acid binding proteins from the viral genome (Serebrov and Pyle, 2004, Levin et al., 2005). Furthermore, NS3 serine protease is able to modulate the innate immune response by inhibiting RIG-I and TLR3 signaling (Gale and Foy, 2005). Through an interaction of NS3 with the protein kinase A (PKA) (Borowski et al., 1997) and the delocalization of sMafs (Carvajal-Yepes et al., 2011), NS3 deregulates a variety of signaling pathways (Ashfaq et al., 2011).

1.6.2.6 NS4A

NS4A is a cofactor for the NS3 protease. It is involved in the targeting of NS3 to the ER membrane and activation of NS3 active site for more efficient protease cleavage (Woelk et al., 2000). A transmembrane helix mediates the anchoring of the NS3/NS4A complex on the ER membrane (Kim et al., 1996). Furthermore, NS4A is supposed to be necessary for the phosphorylation of NS5A (Asabe et al., 1997).

1.6.2.7 NS4B

NS4B has a molecular weight of 27 kDa and is a small hydrophobic protein forming four transmembrane domains that are anchored in the ER membrane (Lundin et al., 2006). It induces the formation of the so-called membranous web, which is composed of ER-derived membranes and LDs (Egger et al., 2002). Through a direct interaction with NS4A, it indirectly interacts with NS3 and NS5A, thereby forming the replication complex (Huegle et al., 2001).

1.6.2.8 NS5A

NS5A is a RNA-binding phosphoprotein with the ability of forming homodimers (Tellinghuisen et al., 2004). It is composed of three domains and a N-terminal amphipathic α-helix that mediates the attachment to the ER membrane (Brass et al., 2002). Domain I is highly structured, forms a dimer and is predominantly interacting with the viral RNA (Tellinghuisen et al., 2004). Domain II is essential for viral genome replication (Tellinghuisen et al., 2007, Ross-Thriepland et al., 2013), while domain III is required for particle assembly (Zayas et al., 2016). N-terminal truncated products of NS5A are able to translocate into the nucleus via the nuclear localization sequence (NLS) located at the C-terminus (Sauter et al., 2009). NS5A exists in two forms, a basally hypophosphorylated form of 56 kDa and a hyperphosphorylated form of 58 kDa (Moradpour et al., 2007). It is assumed that the phosphorylation status of NS5A serves as a molecular switch from viral replication to viral assembly, due to an increased replication after an inhibition of hyperphosphorylation (Appel et al., 2005). Through an interaction with viral RNA and cellular proteins like ApoE and Tip47, NS5A is involved in particle assembly (Ploen et al., 2013b, Cun et al., 2010, Lai et al., 2014). Furthermore, NS5A modulates a variety of cellular signaling pathways and the interferon response (Reed et al., 1997, Macdonald et al., 2004). In case of the genotype 1b, NS5A contains an interferon-α sensitivity-determining region (ISDR), which warrants the resistance of the virus to interferon treatment and interacts directly with the PKR protein kinase, an IFN-α stimulated gene product (Gale et al., 1997). By interaction with numerous cellular partners, NS5A has the ability to modulate MAPK pathways that regulate cellular growth, apoptosis, ROS-dependent pathways and the phosphatidylinositol 3-kinase (PI3K) signaling pathways, which may cause hepatocyte transformation and HCC formation (Macdonald et al., 2004). *In vivo* studies with NS5A-transgenic mice indicate that NS5A impairs the innate and adaptive immune response, contributing to the development of a chronic HCV infection (Kriegs et al., 2009). Additionally, NS5A interacts with the c-Raf kinase by its recruitment to the replication complex, resulting in an activation of the c-Raf, which is essential for the viral replication. Consequently, sequestration of c-Raf to the

replication complex impairs the activation of the MEK/ERK signaling pathway (Burckstummer et al., 2006, Himmelsbach et al., 2009).

1.6.2.9 NS5B

The RNA-dependent RNA polymerase (RdRp) NS5B has a size of 65 kDa and is responsible for the synthesis of new RNA genomes (Behrens et al., 1996). The structure of the enzyme resembles the shape of a right hand with fingers, palm and a thumb subdomain (Lesburg et al., 1999). NS5B is a so-called tail-anchored protein, as it is associated with the ER membrane via the C-terminus which forms an α-helix (Moradpour et al., 2004). Sequence analysis revealed that the amino acids GDD play a crucial role for the polymerase activity (Yamashita et al., 1998). Replication occurs via an intermediate minus-strand RNA using the plus-strand RNA genome as a matrix and the following synthesis of a plus-strand RNA genome from the intermediate minus-strand RNA (De Francesco and Migliaccio, 2005). Given that NS5B has no proof-reading activity, the mutation rate of the viral genome is increased, resulting in the multiplicity of quasispecies (Martell et al., 1992). Furthermore, elevated levels of ROS contribute to the variability and heterogeneity of the HCV genome, as they can act as a mutagen to the viral RNA (Seronello et al., 2011, Forns et al., 1999). As this protein is essential for viral replication, it is a promising target for antiviral strategies (Scheel and Rice, 2013).

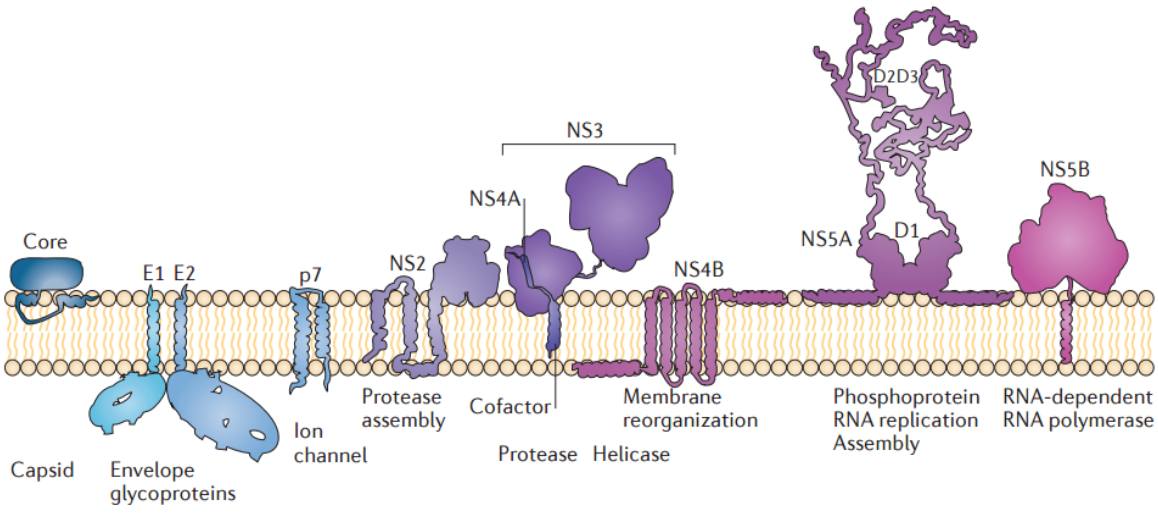

Figure 1.4: Membrane topology and major functions of the cleaved viral proteins. Each protein is tethered to the intracellular membrane by at least one transmembrane domain, formed by an amphipathic α-helix. NS5A is shown as a homodimer, but all HCV proteins form hetero- or homodimers (Bartenschlager et al., 2013).

1.6.3 Viral particle

The HCV particle is surrounded by a host-derived lipid bilayer, containing the two envelope glycoproteins E1 and E2. Beneath the envelope resides the nucleocapsid that is composed of homooligomerized core proteins associated with one copy of viral RNA (figure 1.5) (Lindenbach and Rice, 2013). Electron microscopy studies revealed that HCV particles are 50−80 nm in diameter, pleomorphic and lack distinct symmetry (Bradley et al., 1985, Gastaminza et al., 2010, He et al., 1987, Merz et al., 2011, Catanese et al., 2013). Thereby, Gastaminza et al. observed different populations of particles. While enveloped particles exhibit a mean diameter of 60,7 $\pm$ 10,4 nm, non-enveloped particles show with 44,24 $\pm$ 4,74 nm a smaller diameter (Gastaminza et al., 2010). During particle maturation, virus-associated E1E2 dimers form disulfide-linked complexes (Vieyres et al., 2010), contributing to the acid resistance of the HCV particle (Tscherne et al., 2006). While the immunodominant E2 glycoprotein interacts with host cell receptors (Pileri et al., 1998, Hulst and Moormann, 1997, Scarselli et al., 2002), E1 harbors a putative fusion peptide probably mediating the fusion between the viral and endosomal membrane, resulting in the release of the viral capsid in the cytoplasm (Douam et al., 2014, Lavillette et al., 2007).

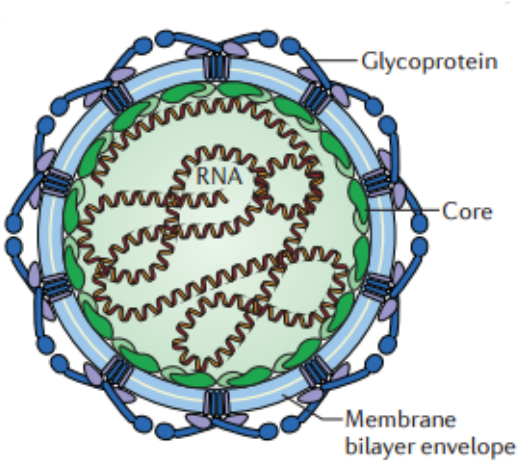

Figure 1.5: Model of the hepatitis C virus particle. The membrane bilayer containing the surface glycoproteins E1-E2 surrounds the nucleocapsid containing core proteins and viral RNA (Lindenbach and Rice, 2013).

Compared to other flaviviruses, the low and heterogeneous buoyant density of HCV poses a challenge to the structural and functional characterization of infectious HCV particles (Andre et al., 2002, Lindenbach et al., 2005). Viral particles derived from the serum of infected patients display a higher density range (1,06 g/ml to 1,25 g/ml), in which particles with lower density are more infectious, and are associated with cellular lipoproteins, such as ApoA, ApoB, ApoC and ApoE (Merz et al.,

2011). In contrast, cell culture-derived infectious viral particles have an average buoyant density of $\leq$1,10 g/ml and show a similar composition, but lack the ApoB lipoprotein (Chang et al., 2007). The lipid composition of a viral particle resembles the one of a very-low density lipoprotein (VLDL) or low density lipoprotein (LDL), which is the reason why they are also depicted as lipoviral particles (LVP) (Lindenbach and Rice, 2013, Merz et al., 2011). Due to the fact that the structure of HCV particles and LVP still remains unresolved, two model systems were proposed to depict the overall architecture, which are shown in figure 1.6. In the two-particle model, virus particles are transiently interacting with divisible serum lipoprotein particles (figure 1.6, left panel), whereas in the hybrid-particle model they share a common envelope (figure 1.6 right panel) (Lindenbach and Rice, 2013, Dubuisson and Cosset, 2014). Independent of which model reflects the reality, both models describe the poor accessibility for specific antibodies against E1 and E2 and the importance of lipoproteins for HCV infection (Dubuisson and Cosset, 2014).

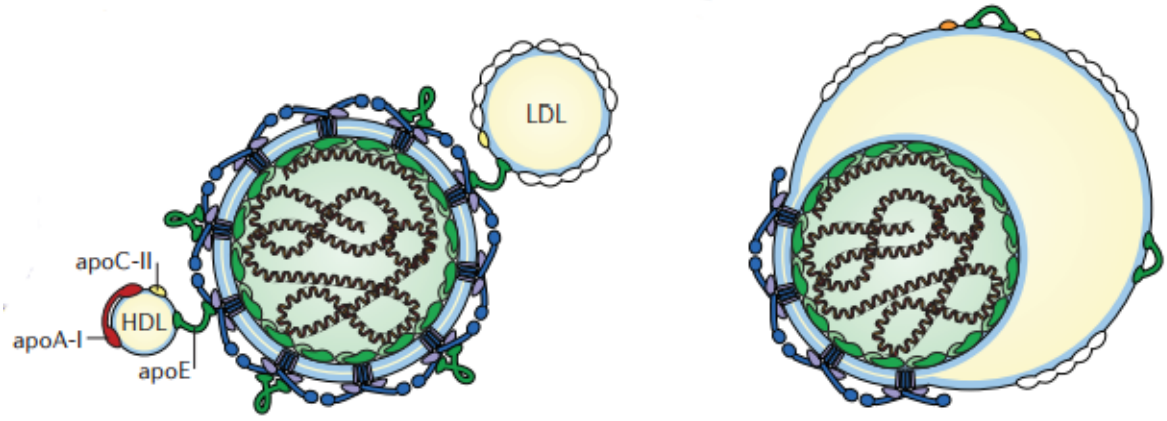

Figure 1.6: Model systems for lipoviral particles. Left, two-particle model for a lipoviral particle, where the virus particle transiently interacts with serum lipoproteins. **Right,** hybrid-particle model, where the virus particle shares an envelope with a low-density lipoprotein particle (Lindenbach and Rice, 2013).

1.6.4 Viral life cycle

1.6.4.1 Entry and uncoating

During a primary infection, HCV particles circulate in the blood and thereby come into contact with the basolateral surface of hepatocytes (Lindenbach and Rice, 2013). This facilitates the interaction with attachment factors and receptors on the surface of these cells (Dubuisson and Cosset, 2014). Initial attachment of HCV particles to hepatocytes happens by low-affinity interaction with glycosaminoglycans (GAGs) present on heparan sulfate proteoglycans (HSPGs) (Barth et al., 2003, Lefevre et al., 2014, Shi et al., 2013) and low-density-lipoprotein receptor (LDLR) (Albecka et al., 2012, Agnello et al., 1999) (figure 1.7). Both, GAGs and LDLR, can interact with ApoE,

that is present on the viral particle (Agnello et al., 1999, Germi et al., 2002, Monazahian et al., 1999). However, interaction with the LDLR is not crucial for viral entry but may play a role for ideal replication of the viral genome (Albecka et al., 2012). Additionally, coordinated activity of four cell surface molecules is essential for HCV entry, including the scavenger receptor B1 (SRB1) (Scarselli et al., 2002), tetraspanin CD81 (Pileri et al., 1998), tight-junction proteins claudin-1 (CLDN1) (Evans et al., 2007) and occludin (OCLN) (Ploss et al., 2009). HCV entry employs the described cell surface molecules in a coordinated chronological and spatial order (Lindenbach and Rice, 2013). Binding of the lipoviral particle to SRB1, which exhibits lipid transfer activity, results in a modified lipid composition of the associated lipoproteins on the viral particle, thereby exposing the CD81 binding site of E2 glycoprotein (Scarselli et al., 2002, Bankwitz et al., 2010, Dao Thi et al., 2012, Zahid et al., 2013). After binding to CD81, a lateral movement of the attached viral particle to tight junctions occurs, where it interacts with CLDN1 (Harris et al., 2010, Harris et al., 2008). CD81-CLDN1 form a co-receptor complex, which is involved in downstream processes of viral entry (Farquhar et al., 2012). The interaction of CD81 and CLDN1 is highly regulated by several signaling pathways, such as protein kinase A (PKA) (Farquhar et al., 2008) and Rho GTPase signaling (Brazzoli et al., 2008, Farquhar et al., 2012), as well as the Ras/MEK/ERK pathway promoted by the epidermal growth factor receptor (EGFR) or the ephrin type A receptor 2 (EphA2) signaling (Lupberger et al., 2011). Additionally, the tight junction protein OCLN is crucial for viral entry, but its precise function remains to be solved (Ploss et al., 2009). It seems to play a role at the late step of HCV entry (Benedicto et al., 2009, Sourisseau et al., 2013). Furthermore, in combination with CD81, OCLN dictates the tropism of HCV for human cells (Evans et al., 2007, Dorner et al., 2011). However, the cholesterol transporter Niemann–Pick C1-like 1 (NPC1L1) (Sainz et al., 2012) and the transferrin receptor 1 (Martin and Uprichard, 2013) were identified as additional entry factors. Bound LVPs are endocytosed together with CD81-OCLD1 complexes in a clathrin-dependent manner (Farquhar et al., 2012, Coller et al., 2009, Blanchard et al., 2006). After internalization, viral particles are transported retrograde along actin filaments to Rab5a-positive early endosomes, where the fusion occurs (Dubuisson and Cosset, 2014, Coller et al., 2009).

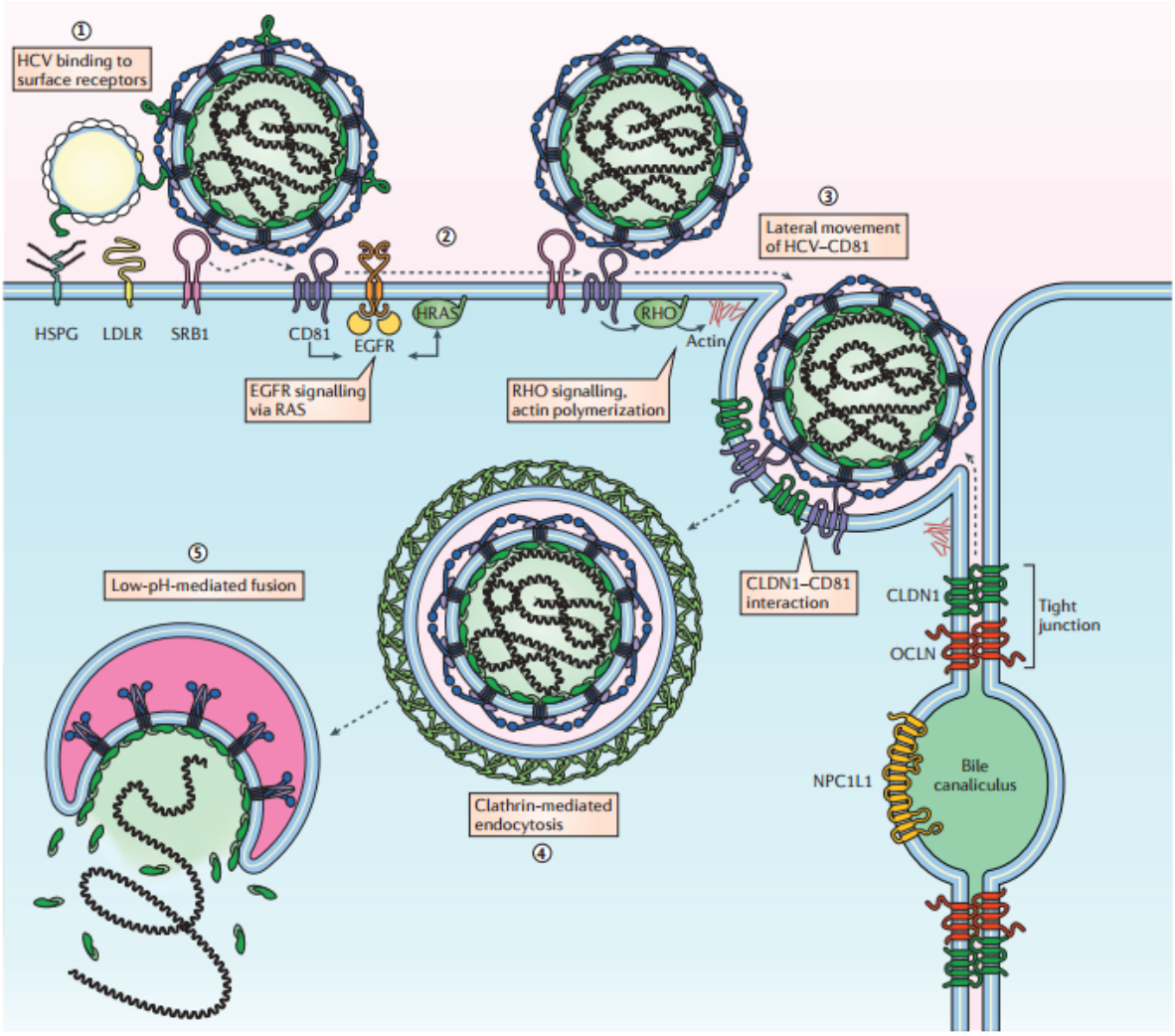

Figure 1.7: HCV entry. Step 1, HCV LVPs bind to the surface of a hepatocyte by interacting with heparan sulfate proteoglycans (HSPGs) and low-density-lipoprotein receptor (LDLR). Scavenger receptor B1 (SRB1) modifies lipid composition of HCV-associated lipoproteins, thereby exposing the CD81 binding site of E2 glycoprotein. **Step 2,** interaction of E2 with CD81 activates signal transduction through epidermal growth factor receptor (EGFR), HRAS and through Rho GTPases. **Step 3,** signaling events induce lateral movement of HCV–CD81 complexes to sites of cell–cell contact. **Step 4,** interaction of CD81 with claudin 1 (CLDN1) results in the internalization of HCV via clathrin-mediated endocytosis. **Step 5,** the low pH of the endosomal compartment induces HCV fusion and the release of HCV genome into the cytoplasm (Lindenbach and Rice, 2013).

1.6.4.2 HCV RNA translation and replication

After binding of the E1E2 glycoproteins to its specific receptors and co-receptors, the viral particle is internalized by clathrin-mediated endocytosis followed by a release of the viral genome into the cytoplasm where it serves as mRNA template for the synthesis of the polyprotein (Dubuisson and Cosset, 2014). IRES-mediated translation located at the rough ER (rER) yields a polyprotein which is co- and post-translationally processed into the mature structural (core, E1, E2) and nonstructural (p7, NS2, NS3, NS4, NS5A, NS5B) proteins (see chapter 1.6.1) (Scheel and Rice, 2013). For

RNA replication, HCV induces tremendous intracellular membrane rearrangements for the formation of the so-called "membranous web", which is composed of ER-derived membranes, lipid droplets (LDs) and double-membrane vesicles (DMVs) (Lohmann, 2013). It is proposed that oligomerized NS4B forms the scaffold of membranous vesicles (Gouttenoire et al., 2010), but the formation of complete membranous web structures requires the presence of all replicase proteins (Dubuisson and Cosset, 2014). A central host factor involved in HCV replication is the phosphatidylinositol-4-kinase-III (PI4KIII) (Reiss et al., 2011). Interaction of NS5A with PI4KIII induces the accumulation of phosphatidylinositol-4-phosphate (PI4P) within the membranous web, which is essential for its formation (Reiss et al., 2011, Reiss et al., 2013). Furthermore, PI4KIII causes the accumulation of cholesterol and other lipids that are crucial for viral replication (Paul et al., 2013, Diamond et al., 2010). Lipid droplets are storage organelles for triacylglycerides (TAG) and cholesterol esters (CE) surrounded by a phospholipid monolayer that is coated with many proteins (Dubuisson and Cosset, 2014). They play a central role in HCV RNA replication and morphogenesis (Targett-Adams et al., 2007). Furthermore, HCV exploits several LD-associated proteins for its life cycle. For instance, Rab18 mediates the interaction of NS5A and other replicase proteins with LDs, thereby promoting viral replication (Salloum et al., 2013). Another LD-associated protein, tail-interacting protein of 47 kDa (TIP47), interacts with NS5A and together with Rab9 is involved in the shuttling of *de novo* synthesized viral RNA from the RC to the LDs, where viral morphogenesis takes place (Ploen et al., 2013a, Ploen et al., 2013b). Several reports have indicated that a variety of host factors are involved in HCV replication. Thereby, several nuclear pore complex (NPC) proteins, like Nup98, and nuclear transport factors (NTFs) have been linked to viral replication (Neufeldt et al., 2013, Levin et al., 2014). In addition, human choline kinase-α (hCKα) was characterized as an essential host factor for membranous web formation and replication (Wong and Chen, 2016). hCKα binds to NS5A thereby enhancing the targeting of the hCKα-NS5A complex to the ER. Here, NS5A binds to NS5B and contributes to the RC formation and replication (Wong and Chen, 2016). In another approach, the cell factor ErbB3 binding protein 1 (Ebp-1) was identified to interact with the viral genome, thereby controlling viral replication and translation (Mishra et al., 2017). Depending on different splicing, Ebp-1 exists in two isoforms, p48 and p42. p48 acts as a proviral factor while p42 exhibits antiviral properties (Mishra et al., 2017). Recently, studies revealed that the human immunity-related GTPase M (IRGM) is involved in Golgi fragmentation upon HCV infection, suggesting that HCV exploits IRGM for the induction of cellular membrane rearrangement to promote its replication (Hansen et al., 2017). Viral translation and replication are schematically shown in figure 1.8.

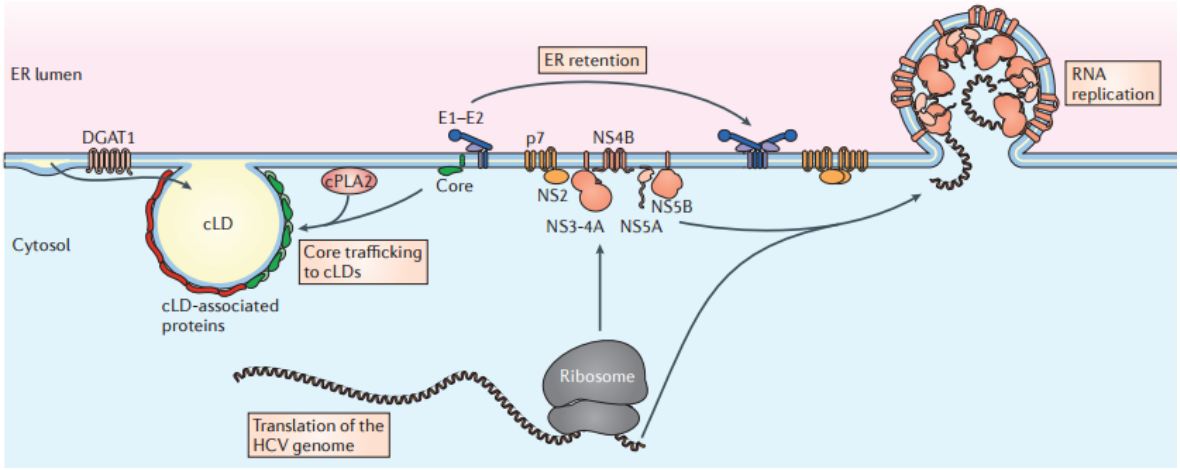

Figure 1.8: HCV translation and replication. In the early phase of the HCV life cycle, viral RNA is translated into the polyprotein. After co- and post-translational processing, mature proteins are associated with ER membranes. The nonstructural proteins form the replication complex where RNA replication takes place. E1, E2, p7 and NS2 remain in the ER membrane, while core is transported by the cytosolic phospholipase A2 (cPLA2) to the surface of cytosolic LDs (cLDs), which are formed by diacylglycerol O-acetyltransferase 1 (DGAT1) (Lindenbach and Rice, 2013).

1.6.4.3 Virus assembly and release

Virus assembly and release are tightly coupled to the host cell metabolism (Bartenschlager et al., 2011). For nucleocapsid formation, homodimerized core protein is transported from the ER to the cytosolic LDs (cLDs) (Boulant et al., 2005, Barba et al., 1997, Moradpour et al., 1996). This transfer is mediated by the host proteins diacylglycerol acyltransferase-1 (DGAT1) and MAPK-regulated cytosolic phospholipase A2 (PLA2G4) (Herker et al., 2010, Menzel et al., 2012). At the surface of LDs, core interacts with viral RNA to form nucleocapsids (Bartenschlager et al., 2011). However, the heterodimerized envelope glycoproteins E1 and E2, which are retained in the ER (Dubuisson et al., 1994), have to migrate in close proximity to the LDs, where viral particle assembly takes place (Miyanari et al., 2007). Interaction of E1E2 heterodimer with NS2 and p7 is essential for the migration to the viral particle assembly site (Jirasko et al., 2010, Ma et al., 2010, Popescu et al., 2011, Stapleford and Lindenbach, 2010). The capsid buds through the ER lumen, where it acquires its envelope (Dubuisson and Cosset, 2014). After particle assembly and budding into the ER, viral particles are released from the cell by transition through the secretory pathway (Coller et al., 2012). LVPs are formed by fusion or interaction with lipoproteins thereby acquiring their low buoytant density (Gastaminza et al., 2008, Gastaminza et al., 2006). A schematic overview of particle assembly and ER-budding is shown in figure 1.9.

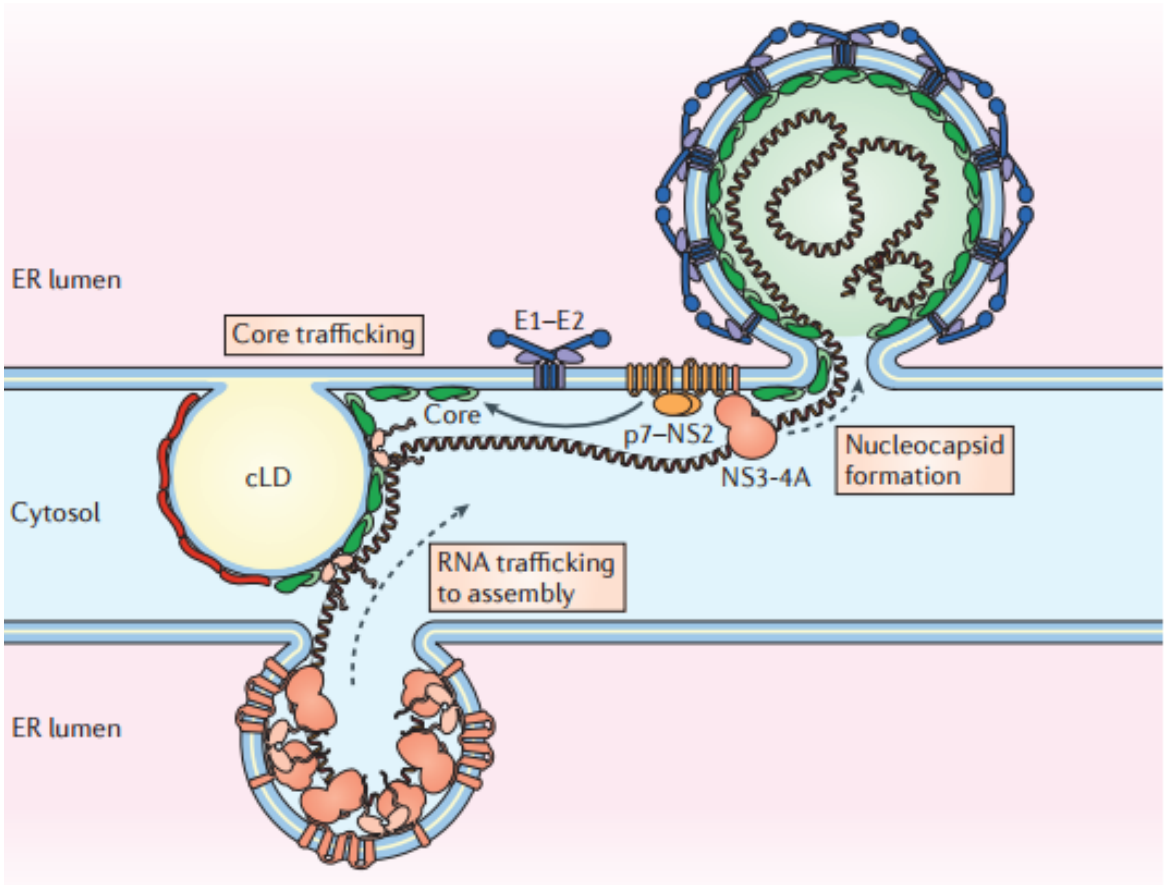

Figure 1.9: HCV particle assembly. In the late phase of particle assembly, viral RNA is shuttled from the RCs to cLDs where viral assembly takes place. HCV core protein is recruited to the particle assembly site by interaction of p7-NS2 with NS3-NS4A. By transition of E1-E2 to the assembly site, the viral particle is formed by budding in the ER (Lindenbach and Rice, 2013).

Nonetheless, there is growing evidence that beside the classical secretory pathway, viral particles can also be released via the endosomal pathway (Elgner et al., 2016, Bayer et al., 2016). Thereby, interfering with the functionality of multivesicular bodies (MVBs) by treatment with the MVB inhibitor U18666A and expression of dominant negative mutants of the ESCRT machinery resulted in an impaired release and intracellular accumulation of infectious viral particles (Elgner et al., 2016). In another study using fluorescent-tagged viral particles, a localization of viral particles and structural proteins on endosomal compartments was observed (Bayer et al., 2016). In line with this, HCV core was found in endosomal structures (Coller et al., 2012, Lai et al., 2010). Additionally, dominant negative mutants of Rab-GTPases involved in the endosomal release pathway were able to inhibit the release of HCV particles (Mankouri et al., 2016). Recently, a study revealed that knockdown of autophagy genes like Beclin1 or Atg7 inhibits the release of infectious viral particles by the exosomal pathway (Shrivastava et al., 2016). Further studies are required to elucidate the release of infectious viral particles.

1.6.5 Model systems for the analysis of HCV

Since the discovery of HCV in 1989, many obstacles had to be overcome in the development of suitable model systems. Historically, HCV isolates derived from patients failed to establish an productive infection in cell culture (Catanese and Dorner, 2015). It took 8 years to develop HCV molecular clones that were able to infect chimpanzees. However, in cell culture these viral genomes failed to produce viral particles (Kolykhalov, 1997, Yanagi et al., 1997). Soon after, the development of a subgenomic replicon system paved the way for *in vitro* studies of HCV (Lohmann et al., 1999b). The subgenomic replicon is a bicistronic RNA construct which expresses an antibiotic resistance gene (e.g. neomycine) under the control of the HCV internal ribosomal entry site (IRES) and HCV nonstructural proteins (NS3-NS5B) from an encephalomyocarditis virus (EMCV) IRES. After transfection of the *in vitro* transcribed RNA in the human hepatoma cell line Huh7, antibiotic selection results in the establishment of stable cell lines replicating HCV at low levels. The subgenomic replicon lacks the coding sequence for the structural proteins E1, E2 and core, hence no infectious particles are formed and released (Lohmann et al., 1999a). Several adaptive cell culture mutations were mapped, resulting in higher replicative fitness (Abe et al., 2007, Blight et al., 2000, Lohmann et al., 2001). Even though the replicon system enabled the studies of viral replication, it was not able to examine early events of viral infection. Therefore, the development of HCV pseudoparticles (HCVpp) and recombinant HCV-like particles facilitated the study of viral entry (Bartosch et al., 2003, Hsu et al., 2003, Baumert et al., 1999). A breakthrough in this field was the isolation of a clone from a Japanese patient with fulminant hepatitis (JFH1), which was able to replicate in Huh7 cells and produced infectious viral particles, so-called HCVcc (Lindenbach et al., 2005, Wakita et al., 2005, Zhong et al., 2005). For the first time, it was possible to study the complete HCV life cycle in cell culture. Based on the JFH1 isolate, several chimeras were developed. For instance, the Jc1 construct is based on a combination of the NS3-NS5B region of JFH1 with the core-NS2 region from another genotype 2a isolate (J6), resulting in an enhanced replicative fitness, thereby producing more infectious viral particles (Pietschmann et al., 2006). By fusion with reporter genes, several reporter constructs were generated, enabling dynamic measurements of viral replication using fluorescent or luminescent readouts (Gottwein et al., 2011, Chan et al., 2013). By a point mutation in the catalytic motif of the viral polymerase NS5B from GDD to GND, a replication deficient virus was developed, which was used as a negative control (Wakita et al., 2005). Viruses used in this study are shown in figure 1.10. The human hepatoma cell line Huh7 and its derivatives are the most permissive cells for HCV replication *in vitro* (Catanese and Dorner, 2015). Nowadays, most of the experiments are carried out in Huh7.5 cells, which exhibit a loss-of-function missense mutation in the retinoic acid-inducible gene I (RIG-I), resulting in defective antiviral signaling (Blight et al., 2002, Sumpter et al., 2005). This results in a

significantly higher production of infectious viral particles and spread in cell culture. A limitation of this system rises from the lack of cell polarity, which does not facilitate the compartmentalization of HCV receptors or the directionality of the secretory pathway observed in polarized hepatocytes (Catanese and Dorner, 2015). A more physiological cell culture model is the use of primary human hepatocytes (PHHs) which can be directly isolated from liver tissues after partial hepatectomy (Ploss et al., 2010, Zeisel et al., 2011, Farquhar and McKeating, 2008). Unfortunately, the use of PHHs has a series of limitations including the loss of differentiation and the poor permissiveness to HCV infection. Consequently, detection of HCV is only possible by highly sensitive qRT-PCR analysis (Catanese and Dorner, 2015). However, further development and improvement of appropriate *in vivo* and *in vitro* models is urgently needed.

Figure 1.10: Schematic overview of used HCV constructs. Based on the JFH1 isolate (genotype 2a), the replication deficient GND mutant was generated. The chimeric construct Jc1 combines the structural proteins, p7 and parts from NS2 from the J6 isolate (genotype 2a) and nonstructural proteins from JFH1. The bicistronic construct Jc1-Luc contains an IRES-dependent luciferase prior to the Jc1 sequence. Adapted from Elgner, 2016.

1.7 Autophagy

Autophagy, also termed as "self-eating" process, is a cellular quality control system to remove damaged proteins or organelles to maintain cellular homeostasis (Mizushima et al., 2008). It is induced in response to cellular stress like nutrient deprivation, elevated levels of ROS or electrophiles, aggregation of damaged proteins and organelles or pathogen infection to ensure cell survival (Eskelinen and Saftig, 2009). Xenophagy is a conserved mechanism that targets and degrades pathogens after invasion of host cells (Gomes and Dikic, 2014, Yuk et al., 2012). However, several mechanisms have evolved how pathogens escape from the xenophagic breakdown, e.g. by avoiding phagocytosis and the autophagic compartment (Radtke and O'Riordan, 2006, Deretic and Levine, 2009, Bauckman et al., 2015). Recently, studies have indicated that pathogens are processed in a more complex

process, termed as LC3-associated phagocytosis (LAP) (Romao and Muenz, 2014, Martinez et al., 2011, Lai and Devenish, 2012). This process is independent from autophagosome sequestration as LC3 directly binds to the phagosome (Romao and Muenz, 2014). More than 32 autophagy-related genes (Atgs) represent the autophagosomal core machinery and orchestrate this highly regulated process (Kroemer et al., 2010). The formation of autophagosomes can be divided into three major steps. The initiation starts with the formation of a membrane crescent, also termed as phagophore assembly site or isolation membranes, followed by nucleation, expansion and enclosure forming double lipid bilayer membrane-bound autophagosomes that have an average size of 300–900 nm (Takeshige et al., 1992). A schematic overview of the autophagosome formation is shown in figure 1.11. The initiation of autophagy is controlled by the serine/threonine kinase mammalian target of rapamycin (mTOR), a key regulator of the nutrient sensing pathway (Sengupta et al., 2010). Under nutrient-rich conditions, mTOR phosphorylates the Unc1-like kinase 1 and 2 (ULK1/2), thereby inhibiting autophagy (Ganley et al., 2009, Hosokawa et al., 2009). During starvation, AMP-activated protein kinase (AMPK) inhibits the kinase activity of mTOR resulting in the activation of the ULK1/2 complex (including ULK1/2, Atg13, FIP200, and Atg101) and the induction of autophagy (Kim et al., 2011). Subsequently, the ULK1/2 complex migrates to certain domains of the ER where it regulates the phosphatidylinositol 3 kinase (PI3K) complex, including Beclin-1, Atg14, Vps15, Vps34, and Ambra1 (Itakura and Mizushima, 2010). The multimembrane-spanning protein Atg9L, which is probably recruited on vesicles, is also participating in the early autophagosome formation (Young et al., 2006). For the formation of a phosphatidylinositol 3-phosphate (PI3P)-enriched environment, the effectors Double FYVE-containing protein 1 (DFCP1) and WD-repeat domain phosphoinositide interacting protein (WIPI) are recruited, promoting the formation of the omegasome, an ER-associated Ω-like structure. The omegasome is an intermediate structure for the formation of the isolation membrane (IM), from which autophagosomes appear to be generated (Axe et al., 2008, Itakura and Mizushima, 2010). After the formation, the IM expands to form the enclosed autophagosome (Suzuki et al., 2007). Therefore, the two ubiquitin-like conjugation systems Atg5-Atg12-Atg16L and Atg4-Atg3-LC3 are required (Mizushima et al., 2011). Initially, Atg12 is first conjugated to Atg5 by an ubiquitination-like reaction mediated by Atg7 (E1-like) and Atg10 (E2-like) followed by interaction with Atg16L, yielding the Atg5-Atg12-Atg16L complex (E3-like) (Nakatogawa and Ohsumi, 2014). Subsequently, the microtubule-associated protein 1 light chain 3 (LC3) is C-terminally processed by Atg4 (Kabeya et al., 2000, Kirisako et al., 2000). Atg3 and Atg7 mediate the conjugation of cytosolic LC3-I to phosphatidylethanolamine (PE), resulting in the lipidated LC3-II form, which is localized to the autophagosomal membrane (Ichimura et al., 2000, Kirisako et al., 1999). Mature and enclosed autophagosomes can either directly fuse with lysosomes to form autophagolysosomes, or prior to

that, fuse with late endosomes/multivesicular bodies (MVBs) to form amphisomes, followed by the fusion with lysosomes (Mizushima et al., 2008, Fader and Colombo, 2009). Due to the low pH in the lysosome, the sequestered cargo is degraded in the autophagolysosomal compartment (Deretic and Levine, 2009). In the process of autophagosome-lysosome fusion, the autophagosomal SNARE (soluble N-ethylmaleimide-sensitive factor attachment) protein syntaxin 17 (Stx17) plays a central role (Itakura et al., 2012). Stx17 is only located on the outer membrane of completed autophagosomes, but not on phagophores, thereby avoiding early fusion with the lysosome (Itakura et al., 2012). In mammals, membrane sources for autophagosome formation can originate, in addition to the ER, from ER mitochondria junctions (Hamasaki et al., 2013), mitochondria (Hailey et al., 2010), the Golgi compartment (Yen et al., 2010), endosomes and the plasma membrane (Ravikumar et al., 2010).

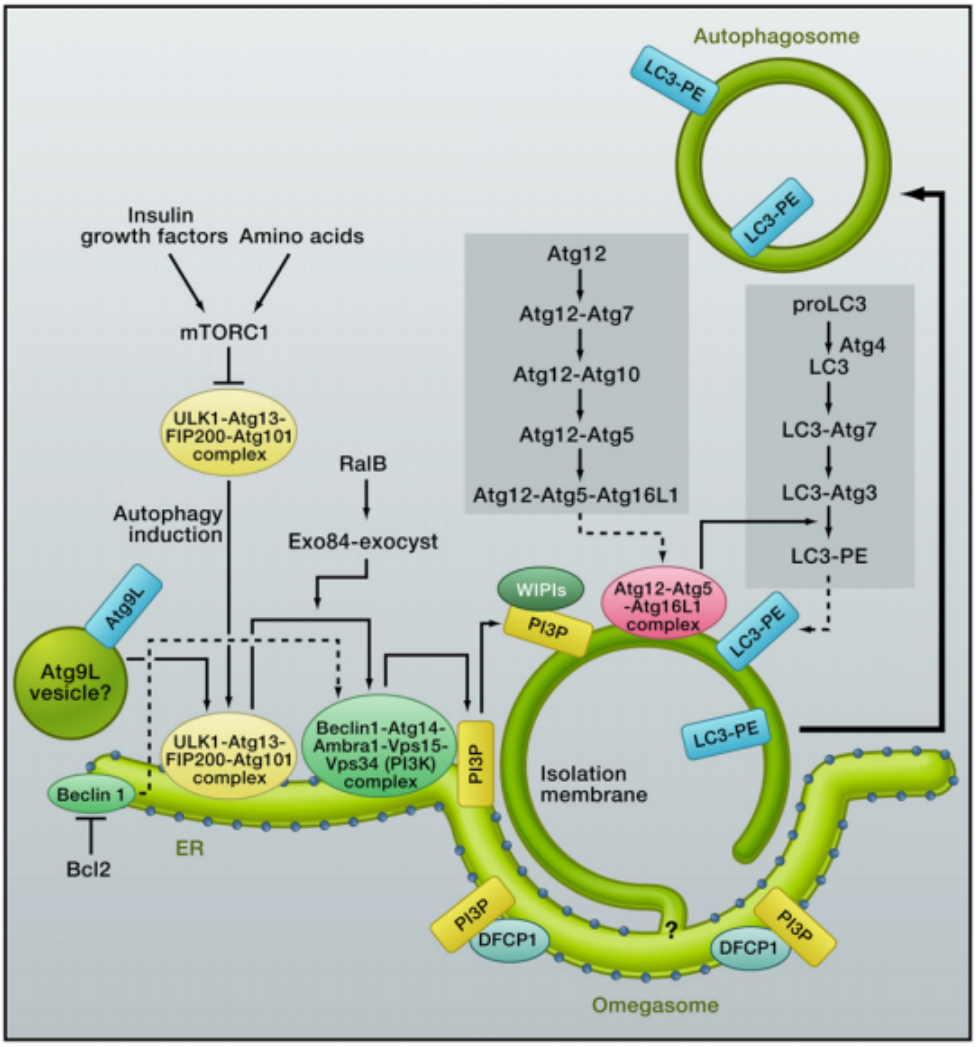

Figure 1.11: Autophagosome formation. Under nutrient-rich conditions, mTOR suppresses the ULK1/2 complex (including ULK1/2, Atg13, FIP200, and Atg101). Upon starvation, mTOR is inhibited, resulting in the activation of the ULK1/2 complex which translocates to a certain domain of the ER, where it regulates the phosphatidylinositol 3 kinase (PI3K) complex, including Beclin-1, Atg14, Vps15, Vps34, and Ambra1. Recruitment of Beclin-1 to the PI3K complex is nutrient-sensitive, as it complexes with ER-associated Bcl-2 under nutrient-rich conditions and is released upon phosphorylation of Bcl-2 by JNK1. Additionally, the PI3P effectors Double FYVE-containing protein 1 (DFCP1) and WD-repeat domain phosphoinositide interacting protein (WIPI) are recruited, promoting the formation of the omegasome. The multimembrane-spanning protein Atg9L is also participating in the early autophagosome formation. For expansion and enclosure of the autophagosome, the two ubiquitin-like conjugation systems Atg5-Atg12-Atg16L and Atg4-Atg3-LC3 are required to mediate the processing and conjugation of LC3 to the autophagosomal membrane. Modified from Mizushima and Komatsu, 2011.

1.7.1 p62 and autophagy

The stress-inducible protein p62 is a signaling hub for a variety of cellular processes and acts as an autophagy adapter and substrate (Taniguchi et al., 2016), which is degraded during the autophagic process. It is a multifunctional scaffolding protein harboring an N-terminal Phox1 and Bem1p (PB1)

domain, a zinc finger (ZZ), two nuclear localization signals (NLS), a tumor necrosis factor receptor-associated factor 6 (TRAF6) binding domain (TB), a nuclear export signal (NES), an LC3-interacting region (LIR), a Keap1-interacting region (KIR), and a C-terminal ubiquitin-associated domain (UBA) (Katsuragi et al., 2015). The domain organization of p62 is shown in figure 1.12. In selective autophagy, p62 functions as a cargo receptor that binds UBA domain-mediated ubiquitinated proteins and organelles, thereby targeting them towards autophagosomal degradation by interacting with LC3 (Johansen and Lamark, 2011). The PB1 domain enables p62 to self-oligomerize and to form heterooligomers with other PB1-containing proteins (Lamark et al., 2003). Furthermore, binding to atypical protein kinase C (aPKC) and extracellular signal-regulated kinase 1 (ERK1) is mediated by PB1 (Sanz et al., 1999, Sanz et al., 2000, Moscat et al., 2006). In addition, p62 binds to receptor-interacting protein 1 (RIP1) and TRAF6 via the ZZ and TB domain. Interaction of p62 with aPKC, RIP1 and TRAF6 is likely to be involved in p62-mediated activation of NF-κB (Sanz et al., 1999, Sanz et al., 2000, Zotti et al., 2014). Raptor belongs to the mTORC1 complex and interacts with p62 in an amino acid dependent manner, resulting in the translocation onto lysosomes upon elevated levels of amino acids (Duran et al., 2011). Finally, p62 is able to induce Nrf2/ARE signaling by direct interaction with Keap1 through the KIR (Copple et al., 2010, Lau et al., 2010). Expression of p62 is regulated on transcriptional as well as on post-transcriptional level (Komatsu et al., 2012, Moscat and Diaz-Meco, 2011), while its activity is affected by phosphorylation (Katsuragi et al., 2015). Both Nrf2 and NF-κB are able to induce p62 transcription and inversely, p62 can activate them both, resulting in a positive feedback loop (Jain et al., 2010, Ling et al., 2012, Zhong et al., 2016, Chen et al., 2014). The phosphorylation of p62 at threonine 269 and serine 272 is mediated by p38δ under nutrient-rich conditions, resulting in recruitment of TRAF6 to p62, thereby activating mTORC1 (Linares et al., 2015, Duran et al., 2011, Linares et al., 2013). Furthermore, a phosphorylation of p62 within the KIR at serine 349 enhances its binding to Keap1 leading to the activation of Nrf2/ARE signaling (see chapter 1.8.1). Finally, a casein kinase 2 (CK2)-mediated phosphorylation of p62 at serine 403 within the UBA domain influences the autophagic breakdown of ubiquitinated proteins by an increased affinity to polyubiquitinated chains (Matsumoto et al., 2011).

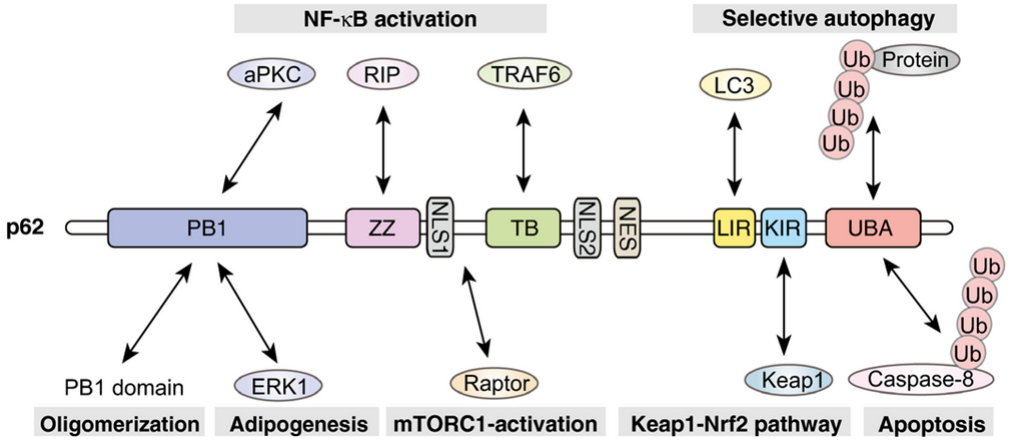

Figure 1.12: Schematic overview of structure and domain organization of p62. p62 harbors an N-terminal Phox1 and Bem1p (PB1) domain, a zinc finger (ZZ), two nuclear localization signals (NLS), a tumor necrosis factor receptor-associated factor 6 (TRAF6) binding domain (TB), a nuclear export signal (NES), an LC3-interacting region (LIR), a Keap1-interacting region (KIR), and a C-terminal ubiquitin-associated domain (UBA). p62 is a signaling hub involved in NF-κB and Nrf2/ARE signaling, autophagy and mTORC1-activation (Katsuragi et al., 2015).

1.7.2 Oxidative stress and autophagy

Eukaryotic cells are continually exposed to the toxic effects of exogenously or endogenously produced highly reactive oxidizing molecules (Filomeni et al., 2015). These can be either radicals ($O_2^{-\cdot}$, $HO^{\cdot}$) or nonradicals (H_2O_2). Both have in common to oxidize cellular biomolecules, resulting in cell structure damage (Filomeni et al., 2015). Reactive oxygen species (ROS) and reactive nitrogen species (RNS) are endogenously produced and have thereby the main biological impact (Kongara and Karantza, 2012). The main source of ROS in the cell is the mitochondrial respiratory chain (Vakifahmetoglu-Norberg et al., 2017). Furthermore, HCV is known to induce oxidative stress (see chapter 1.3.1). Recently, it has been discussed that autophagy, together with the classic antioxidant defenses such as radical-scavenging small molecules and antioxidant enzymes, contributes to alleviate damage resulting from sustained pathophysiological levels of oxidative stress (Giordano et al., 2014). Autophagy induction upon exposure to ROS is very fast, arguing for a rapid response mediated by redox-sensitive proteins (Filomeni et al., 2015). In line with this, AMPK has been proposed as a possible candidate, as it can be activated upon exposure to H_2O_2 (Cardaci et al., 2012, Zmijewski et al., 2010).

1.7.3 HCV and autophagy

Viruses are known to exploit the autophagic machinery to promote their own life cycle (Ke and Chen, 2011a). In case of HCV, autophagy is induced and intervenes with membranous web formation

and translation of incoming RNA, replication, and virus release (Wang et al., 2014, Shrivastava et al., 2016, Wang et al., 2015). Furthermore, induction of autophagy mediates a suppression of the innate immune system, thereby contributing to HCV-associated pathogenesis (Ploen and Hildt, 2015). The mechanisms underlying HCV-mediated induction of autophagy are conflicting and thus far not completely understood (Ploen and Hildt, 2015). Currently, two possible mechanisms are discussed. First, HCV infection is associated with elevated levels of ROS, thereby resulting in oxidative stress which in turn can trigger autophagy (Bartosch et al., 2009). Second, as HCV replication takes place at the membranous web, it is believed that HCV induces ER stress (Sir et al., 2008, Ke and Chen, 2011a, Tardif et al., 2002, Ke and Chen, 2011b). In line with this, the viral glycoproteins E1E2 form a complex retained in the ER membrane that can form aggregates resulting in ER stress (Cocquerel et al., 1998, Choukhi et al., 1998). It was observed that the interaction of NS4B with Rab5 and Vps34 contributes to an activation of autophagy (Su et al., 2011). Furthermore, the formation of double membrane vesicles (DMVs) and multi membrane vesicles (MMVs) is induced by NS5A (Romero-Brey et al., 2012, Romero-Brey and Bartenschlager, 2014), which was recently described to mediate the fusion of the autophagosome with the lysosome (Shrivastava et al., 2012). Indeed, is has been identified that DMVs contain NS3, NS5A, viral RNA and the autophagosomal marker LC3-II, confirming a connection of HCV with the autophagosomal compartment (Ferraris et al., 2010). Additionally, markers of early endosomes (EE), late endosomes (LE), mitochondria, LDs and Rab proteins were identified to be associated with the membranous web, indicating an involvement of autophagosomal factors in the formation of the membranous web (Romero-Brey et al., 2012). Several studies suggested that autophagy favors HCV replication and is crucial for the release of viral particles (Shrivastava et al., 2016, Ren et al., 2016, Tanida et al., 2009, Ploen et al., 2013a). Actually, only a small portion of *de novo* synthesized viral particles are released, while the majority is degraded in the lysosomal compartment (Quinkert et al., 2005, Post et al., 2009). Recently, it was demonstrated that HCV decreased the protein amount of syntaxin 17, thereby preventing the fusion of autophagosome and lysosome (Ren et al., 2016). Hence, reduced amounts of syntaxin17 ensure that the equilibrium between released and lysosomally trapped and degraded viral particles is not completely shifted towards degradation (Ren et al., 2016). Even though, to understand of the interdependency of the HCV life cycle and autophagy increases, further investigations are needed.

1.8 Nrf2/ARE signaling

To counteract oxidative and electrophilic stress, cells have evolved several detoxification mechanisms to maintain cellular homeostasis. The cap 'n' collar basic leucine zipper (bZIP) transcription factor

nuclear factor (erythroid-derived 2)-like-2 (Nrf2) thereby controls the expression of cytoprotective and ROS-detoxifying genes (Levonen et al., 2014, Kensler et al., 2007, Higdon et al., 2012, Kansanen et al., 2013). Under quiescent conditions, Nrf2 resides in its inactive state bound to its inhibitor Kelch-like ECH-associated protein 1 (Keap1) in the cytoplasm and is targeted for ubiquitination and proteasomal degradation. Upon exposure to oxidative and electrophile stress, Keap1 dissociates from Nrf2. Subsequently, Nrf2 translocates into the nucleus where it binds together as a heterodimer with small Maf (sMaf) proteins to antioxidant response elements (ARE), residing in the promoter regions of cytoprotective genes (O'Connell and Hayes, 2015, Harder et al., 2015). These include NAD(P)H quinone oxidoreductase 1 (NQO1), glutathione S-transferases (GSTs), glutamate-cysteine ligase catalytic subunit (GCLc) and the catalytic units of the constitutive proteasome such as PSMB5 (Jaiswal, 2004, Kobayashi and Yamamoto, 2005).

1.8.1 Autophagy and Nrf2/ARE signaling

Recently, a crosstalk between the Nrf2/ARE signaling pathway and autophagy through the direct interaction of p62 and Keap1 was revealed (Komatsu et al., 2010, Lau et al., 2010, Fan et al., 2010, Copple et al., 2010, Jiang et al., 2015a). Thereby, phosphorylation of p62 at serine 349 within its KIR increases the binding affinity of p62 to Keap1. Consequently, p62 binds competitively to Keap1, thereby targeting Keap1 for autophagosomal degradation. Hence, the ubiquitination of Nrf2 is abrogated and results in the translocation of Nrf2 into the nucleus where it activates the expression of cytoprotective genes. Furthermore, the p62 gene harbors an ARE sequence and expression of p62 can thereby be induced by Nrf2 upon exposure to oxidative stress (Jain et al., 2010). Simultaneously, p62 is involved in the activation of Nrf2, thereby creating a positive feedback loop. Performing a chromatin immunoprecipitation (ChIP) screening, 25 presumable ARE sites in 16 autophagy-related genes were identified, pointing to Nrf2 as a crucial factor in regulating the expression of autophagy-related proteins (Pajares et al., 2016). Additionally, Nrf2 knockout mice indicate diminished autophagy gene expression (Pajares et al., 2016). Furthermore, Nrf2 knockout mice exhibit diminished expression of detoxifying enzymes and an impaired liver regeneration which was mediated by an oxidative stress-induced insulin/insulin-like growth factor (IGF) resistance (Beyer et al., 2008). Taken together, Nrf2 plays a crucial role for the regulation of cytoprotective genes as well as for autophagy-related proteins.

1.8.2 HCV and Nrf2/ARE signaling

Several studies have revealed that HCV interferes with the Nrf2/ARE signaling pathway. However, the data are conflicting. On the one hand, it was shown that HCV induces the expression and activation of Nrf2 (Burdette et al., 2010). Furthermore, an increased nuclear localization of Nrf2 was observed (Jiang et al., 2015b). Selective overexpression of the viral proteins core, E1, E2, NS4B, or NS5A in combination with an ARE-dependent luciferase reporter construct indicated that these proteins were able to trigger activation of Nrf2 (Ivanov et al., 2011). On the other hand, previous studies from our group revealed that HCV impairs the Nrf2/ARE signaling pathway and by this prevents the expression of cytoprotective genes. In HCV-positive cells, translocation of the sMaf proteins from the nucleus to the cytoplasm occurs, where they bind to NS3 located at the replication complexes at the ER. This process is core-dependent as it could not be observed in core-deficient mutants. The replicon-bound sMaf traps Nrf2 in the cytoplasm and thereby prevents its translocation into the nucleus leading to an impaired activation of ARE-dependent cytoprotective genes (Carvajal-Yepes et al., 2011). In line with this, transcriptome analysis of HCV-positive cells revealed an impaired expression of a variety of Nrf2-dependent genes such as NQO1, epoxide hydrolase 1 (ephx1), catalase (cat), and glutamate-cysteine ligase catalytic subunit (GCLc) and other enzymes of the glutathione metabolism (Blackham et al., 2010).

2 Thesis objectives

Previous studies from our lab revealed that HCV impairs cytoprotective Nrf2/ARE signaling by inducing a translocation of the sMaf proteins from the nucleus to the cytoplasm. Thereby, Nrf2 is trapped in the cytoplasm and prevented from entering the nucleus. Consequently, the expression of cytoprotective genes is impaired resulting in preserved elevated levels of ROS. Another important cytoprotective mechanism is autophagy. It plays a crucial role in removing damaged proteins and organelles to maintain cellular homeostasis. Furthermore, autophagy is not only induced in response to starvation but as well by elevated levels of ROS. From the literature, it is known that autophagy plays a crucial role in the HCV life cycle. Several studies have revealed that HCV induces autophagy to promote viral replication and the release of infectious viral particles. Hence, this thesis aimed to investigate the relevance of HCV-induced oxidative stress as a possible activator of the autophagic process, which is mediated by inhibition of the Nrf2/ARE signaling. Furthermore, the relevance of autophagy for the release of infectious viral particles was analyzed. Recently, a crosstalk between the Nrf2/ARE signaling pathway and autophagy was revealed. Besides the canonical pathway, Nrf2 can also be activated through a direct interaction of the phosphorylated autophagy adapter protein p62 (pS[349] p62) with Keap1. Based on this, the crosstalk between autophagy and Nrf2/ARE signaling via pS[349] p62 and the effect of HCV was further elucidated.

3 Materials

3.1 Cells

3.1.1 Bacterial cells

Strain	Genotype	Source
***E. coli* TOP10**	F-mcrA Δ(mrr-hsdRMS-mcrBC) ϕ80lacZΔM15 ΔlacX74 deoR nupG recA1 araD139 Δ(ara-leu)7697 galU galK rpsL(StrR) endA1 $\lambda-$	Invitrogen, Karlsruhe, D

3.1.2 Mammalian cells

Strain	Source
Huh7.5	Human hepatoblastoma cell line derived from Huh7 cells (Blight et al., 2002)
Primary human hepatocytes	Isolates from tissue samples obtained from partial hepatectomy

3.2 Plasmids

3.2.1 Plasmids containing the HCV genome

Plasmid	Description	Source
pFK-Jc1	Chimera of genotype 1b and 2a (Lindenbach et al., 2006) producing higher titers of infectious particles	(Pietschmann et al., 2006)
pJFH1dC3	Contains a deletion of core gene in the wildtype sequence	(Miyanari et al., 2007)
pFK-JFH1/GND	Contains mutations in the NS5B gene and is therefore replication-deficient	(Wakita et al., 2005)
pFK-Luc-Jc1	Jc1 sequence containing a Luciferase reporter gene	(Koutsoudakis et al., 2006)

The JFH1 plasmids were kindly provided by Prof. Dr. Ralf Bartenschlager (University Hospital Heidelberg, Institute for Virology) and the pJFH1dC3 was provided by Prof. Dr. Kunitada Shimotohno (Kyoto University, Institute for Virus Research).

3.2.2 Expression plasmids

Plasmid	Description	Source
pUC18	Cloning vector used as a control	Invitrogen, Karlruhe
p(3xARE)TKbasal-hNrf2(1-433)-GL4-Flag (OKD48)	Luciferase reporter construct harboring three repeats of ARE promoter with Nrf2 fragment (aa1–433)	(Oikawa et al., 2012)
pNQO1-Luc	Luciferase reporter construct harboring the ARE promotor region of NQO1	Sabine Werner, ETH Zürich

Plasmid	Description	Source
pGCLc-Luc	Luciferase reporter construct harboring the ARE promotor region of GCS	Sabine Werner, ETH Zürich
p-IRES-puro N3xFlag-Msp62 Wt	Expression construct for Flag-tagged murine wildtype p62	(Komatsu et al., 2010)
p-IRES-puro N3xFlag-Msp62 S351E	Expression construct for Flag-tagged murine p62 with a mutation of serine 351 to glutamic acid (phosphorylation mimicking mutant)	(Ichimura et al., 2013)
EGFP_LC3	LC3 expression construct tagged with EGFP	Addgene (#24920)

Plasmids expressing mouse p62 wild type and the phosphorylation mimicking mutant p62 S351E were kindly provided by Prof. Dr. Masaaki Komatsu (Tokyo Metropolitan Institute of Medical Science), and the OKD48 construct was provided by Takao Iwawaki (Advanced Scientific Research Leaders Development Unit, Gunma University, Maebashi).

3.3 Oligonucleotides

3.3.1 qRT-PCR primer

Number	Name	Sequence (5' → 3')
#26	R6-260-R19 (JFH1-fwd)	atg acc aca agg cct ttc g
#27	R6-130-146 (JFH1-rev)	cgg gag agc cat agt gg
#58	NQO1_fwd	gca ctg atc gta ctg gct ca
#59	NQO1_rev	gaa cac tcg ctc aaa cca g
#60	GCLc_fwd	ccc atg gag gtg caa tta ac
#61	GCLc_rev	tgc gat aaa ctc cct cat cc
#716	LC3_fwd	aga agg cgc tta cag ctc aa
#717	LC3_rev	tct cct ggg agg cat aga cc
#718	p62_fwd	gga gcc aga gaa caa gta cc
#719	p62_rev	ctc gct ctt tca gtt tca tgt tc

#835	RPL27_fwd	aaa gct gtc atc gtg aag aac
#836	RPL27_rev	gct gct act ttg cgg ggg tag
#1033	Beclin-1_fwd	agt gtc aga act aca aac gc
#1034	Beclin-1_rev	ctc ctg atc cag tct cag
#1035	Atg5_fwd	tgc act gtc cat cta agg at
#1036	Atg5_rev	atg agt ttc cga ttg atg gc

3.3.2 siRNA

siRNA	**Target**	**Manufacturer**
p62 siRNA , sc-29679 (10 µM stock solution in RNase-free H_2O)	p62	Santa Cruz Biotechnology, Inc., USA
scrambled RNA, sc-37007 (10 µM stock solution in RNase-free H_2O)	unspecific control	Santa Cruz Biotechnology, Inc., USA

3.4 Antibodies

Antibody	**Species/ Clonality**	**Dilution (WB/IF)**	**Manufacturer**
Primary antibodies			
Anti-ß-actin	Mouse, monoclonal	1:10.000/ -	Sigma-Aldrich, USA
Anti-GCSc	Rabbit, polyclonal	1:300/-	Santa Cruz Biotechnology, USA
Anti-HCV core	Mouse, monoclonal	1:1000/ 1:200	Thermo Fisher Scientific, Schwerte, DE
Anti-HCV NS5A	Rabbit, polyclonal	1:1000/ 1:200	Selfmade (Burckstummer et al., 2006)

Antibody	**Species/ Clonality**	**Dilution (WB/IF)**	**Manufacturer**
Anti-HCV NS3 [8 G-2]	Mouse, monoclonal	1:1000/ -	Abcam, Cambridge, UK
Anti-LC3	Rabbit, polyclonal	1:1000/ 1:100	MBL, Boston, USA
Anti-NQO1	Mouse, monoclonal	1:300/-	Santa Cruz Biotechnology, USA
Anti-p62	Guinea pig, polyclonal	1:1000/ 1:200	Progen Biotechnik, Heidelberg, DE
Anti-Phospho p62 (S351E)	Rabbit, polyclonal	1:500/ 1:500	MBL, Boston, USA
Secondary antibodies			
Anti-mouse IgG-HRP	Donkey, polyclonal	1:2000/ -	GE Healthcare, Freiburg, DE
Anti-rabbit IgG-HRP	Donkey, polyclonal	1:2000/ -	GE Healthcare, Freiburg, DE
Anti-mouse IRDye800CW	Donkey, polyclonal	1:5000/-	LI-COR Biosciences GmbH, Bad Homburg, DE
Anti-rabbit IRDye800CW	Donkey, polyclonal	1:5000/-	LI-COR Biosciences GmbH, Bad Homburg, DE
Anti-mouse IgG-Alexa488	Donkey, polyclonal	-/ 1:1000	Invitrogen, Karlsruhe, DE
Anti-rabbit IgG-Alexa488	Donkey, polyclonal	-/ 1:1000	Invitrogen, Karlsruhe, DE
Anti-mouse IgG-Cy3	Donkey, polyclonal	-/ 1:400	Jackson ImmunoResearch Europe, Suffolk, UK
Anti-rabbit IgG-Cy3	Donkey, polyclonal	-/ 1:400	Jackson ImmunoResearch Europe, Suffolk, UK
Anti-guinea pig IgG-Cy3	Donkey, polyclonal	-/ 1:400	Jackson ImmunoResearch Europe, Suffolk, UK

Antibody	Species/ Clonality	Dilution (WB/IF)	Manufacturer
Anti-mouse IgG-Cy5	Donkey, polyclonal	-/ 1:400	Jackson ImmunoResearch Europe, Suffolk, UK
Anti-rabbit IgG-Cy5	Donkey, polyclonal	-/ 1:400	Jackson ImmunoResearch Europe, Suffolk, UK
DAPI (0.1 mg/ml stock in PBS)		-/1:400	

3.5 Molecular weight markers

Protein markers	
PageRuler^{TM}Prestained Protein Ladder	Thermo Fischer Scientific, Schwerte, DE
DNA marker	
Gene Ruler^{TM}1kb DNA ladder	Thermo Fischer Scientific, Schwerte, DE

3.6 Enzymes

Enzymes	Manufacturer
AseI	NEB, Frankfurt am Main, DE
MluI-HF	NEB, Frankfurt am Main, DE
RevertAid H Minus Reverse Transcriptase	Thermo Fisher Scientific, Schwerte, DE
RQ1 RNase-free DNase	Promega, Fitchburg, USA
T7 RNA-Polymerase	Thermo Fisher Scientific, Schwerte, DE
XbaI	NEB, Frankfurt am Main, DE

3.7 Inhibitors

Inhibitor	Target	Manufacturer
Autophagy inhibitor		
3-Methyladenine	PI3-kinase inhibitor (5 mM)	BIOZOL Diagnostica GmbH, Eching, DE
Lysosomal inhibitor		
Bafilomycin A1 (BFLA-1)	Vacuolar-type H^+-ATPase (100 nM)	Sigma-Aldrich, Sleeze, DE
Protease inhibitors		
Aprotinin	Serine proteases (1 µM)	Sigma-Aldrich, Sleeze, DE
Leupeptin	Serine-, cysteine- protease (4 µM)	Sigma-Aldrich, Sleeze, DE
Peptastin	Acid, aspartatic proteases (1 µM)	Sigma-Aldrich, Sleeze, DE
PMSF	Serine proteases (1 mM)	Carl-Roth, Karlsruhe, DE
Phosphatase inhibitors		
Phosphatase inhibitor cocktail	Phosphatases	Sigma, Seelze, DE
Protein synthesis inhibitor		
Cycloheximide (CHX)	Interferes with the translocation step in protein synthesis	Sigma-Aldrich, Sleeze, DE
RNase inhibtiors		
RNaseOut	RNases	Invitrogen, Karlsruhe, DE

3.8 Reagents for cell culture

Reagent	Manufacturer
DMEM medium (4,5 g/l glucose, L-glutamine)	Lonza, Basel, CHE

PBS without Ca^{2+} und Mg^{2+}	Paul-Ehrlich-Institut, Langen, DE
Fetal calf cerum (FCS)	Biochrom GmbH, Berlin, DE
L-glutamine	Biochrom GmbH, Berlin, DE
Penicillin/streptomycin	Paul-Ehrlich-Institut, Langen, DE
Trypsin/EDTA	Paul-Ehrlich-Institut, Langen, DE
Hepatocyte growth medium	PromoCell GmbH, Heidelberg, DE
Hepatocyte growth medium supplement mix	PromoCell GmbH, Heidelberg, DE

3.9 Chemicals

Chemical	**Manufacturer**
10 mM dNTPs	Thermo Fisher Scientific, Schwerte, DE
5x Reaction buffer for RT	Thermo Fisher Scientific, Schwerte, DE
5x T7 Transcription buffer	Thermo Fisher Scientific, Schwerte, DE
6-Aminohexanoic acid	Carl-Roth, Karlsruhe, DE
GenAgarose LE	Genaxxon, Biberach, DE
Ammoniumperoxodisulfate (APS)	Carl-Roth, Karlsruhe, DE
ATP	ATP Perkin elmer, Waltham, USA
β-mercaptoethanol	Sigma-Aldrich, Seelze, DE
Bovine serum albumin (BSA) fraction V	PAA, Linz, AUT
Bradford reagent	Sigma-Aldrich, Seelze, DE
Bromphenol blue	Merck, Darmstadt, DE
Butanol	Merck, Darmstadt, DE
Cell Lysis Buffer (10x)	Cell Signaling Technology, USA
Chloroform	Carl-Roth, Karlsruhe, DE
Roti-C/I	Carl-Roth, Karlsruhe, DE
Cut smart buffer	NEB, Frankfurt am Main, DE
DEPC-H_2O	Paul-Ehrlich-Institut, Langen, DE
Dithiothreitol (DTT)	Paul-Ehrlich-Institut, Langen, DE
DMSO (Dimethyl sulfoxide)	Genaxxon, Biberach, DE
EDTA (Ethylendiaminotetraacetic acid)	Serva, Heidelberg, DE
EGTA (Ethylene glycol tetraacetic acid)	Serva, Heidelberg, DE
Ethanol (reinst)	Carl-Roth, Karlsruhe, DE
Ethidiumbromide	Applichem, Darmstadt, DE

Formaldehyd (37,5 %)	Carl-Roth, Karlsruhe, DE
Glycerol	Gerbu Biotechnik, Heidelberg, DE
Hydrochloric acid	Carl-Roth, Karlsruhe, DE
Isopropanol	Carl-Roth, Karlsruhe, DE
Luciferin	Sigma-Aldrich, Seelze, DE
Luminata Forte Western HRP Substrat	Merck Millipore
Maxima Probe SYBR Green qPCR Master Mix	Thermo Fisher Scientific, Schwerte, DE
Methanol	Carl-Roth, Karlsruhe, DE
Milk powder	Carl-Roth, Karlsruhe , DE
Mowiol	Sigma-Aldrich, Seelze, DE
N-acetylcysteine (NAC)	Sigma-Aldrich, Seelze, DE
NEB buffer 3	NEB, Frankfurt am Main, DE
NEB buffer 3.1	NEB, Frankfurt am Main, DE
NTP mix	Thermo Fisher Scientific, Schwerte, DE
peqGOLD TriFast	PeqLab, Erlangen, DE
Phenol	Applichem, Darmstadt, DE
Polyethylenimine (PEI)	Polysciences, Eppelheim, DE
Ammonium pyrrolidinedithiocarbamate (PDTC)	Sigma-Aldrich, Sleeze, DE
PrestoBlue® cell viability reagent	Thermo Fisher Scientific, Schwerte, DE
Random hexamer primers	Thermo Fisher Scientific, Schwerte, DE
Roti 40 Acrylamide/Bisacrylamide	Carl-Roth, Karlsruhe , DE
RQ1 DNase 10x reaction buffer	Promega, Fitchburg, USA
RQ1 DNase stop solution	Promega, Fitchburg, USA
SDS	Carl-Roth, Karlsruhe , DE
Sodiumacetate	Carl-Roth, Karlsruhe, DE
Sodiumchloride (NaCl)	Carl-Roth, Karlsruhe, DE
Sodiumdesoxycholat	Carl-Roth, Karlsruhe, DE
SuperSignal West Pico Luminol/Enhancer Solution	Thermo Fisher Scientific, Schwerte, DE
SuperSignal West Pico Stable Peroxide Solution	Thermo Fisher Scientific, Schwerte, DE
tBHQ	Sigma-Aldrich, Seelze, DE
TEMED (Tetramethylethylenediamine)	Merck, Darmstadt, DE
Tris	Carl-Roth, Karlsruhe , DE
Tris-HCl	Carl-Roth, Karlsruhe , DE
Triton X-100	Fluka, Deisenhofen, DE

Tween-20	Genaxxon, Ulm, DE

3.10 Kits

Kit	Manufacturers
artus® HCV RG RT-PCR Kit	Qiagen, Hilden, DE
QIAamp DSP Virus Kit	Qiagen, Hilden, DE
QIAamp DSP Virus Spin Kit	Qiagen, Hilden, DE
Qiagen Plasmid Maxi Kit	Qiagen, Hilden, DE
Qiagen Plasmid Mini Kit	Qiagen, Hilden, DE
N-TER™ Nanoparticle siRNA Transfection System	Sigma-Aldrich, Seelze, DE

3.11 Buffers and solutions

Buffer	Composition
Anode buffer I	20 % Ethanol (v/v) 300 mM Tris
Anode buffer II	20 % Ethanol (v/v) 25 mM Tris
Cathode buffer	20 % Ethanol (v/v) 40 mM 6-aminohexanoic acid
DNA loading dye (6x)	10 mM Tris-HCl pH 7,6 0,03 % Bromphenolblau 0,03 % Xylen Cyanol 60 % Glycerol 60 mM EDTA
Luciferase lysis buffer	25 mM Tris-HCl 2 mM DTT

	2 mM EGTA
	10 % Glycerol (v/v)
	1 % TritonX-100 (v/v)
Luciferase substrate	20 mM Tris-HCl pH 7.8
	5 mM Magnesium chloride
	0,1 mM EDTA
	33,3 mM DTT
	470 µM Luciferin
	530 µM ATP
Lysogeny broth medium (LB)	1% Trypton (w/v)
	0,5 % Yeast extract (w/v)
	1 % Sodium chloride (w/v)
Mowiol	10 % mowiol (w/v)
	25 % Glycerol (w/v)
	2,5 % DABCO
	100 mM Tris/HCl pH 8.5
Phosphate buffered saline (PBS) 10x	80,0 g NaCl
	2.0 g Potassium chloride
	14,4 g Na_2HPO_4
	2,4 g KH_2PO4_4
	pH 7,4
	ad 1 l H2O
PBS-T	PBS without Ca^{2+} and Mg^{2+}
	0,3 % Triton X-100 (v/v)
1x Roti/PBS-T	10x Roti-Block diluted 1:10 in PBS-T
RIPA buffer	50 mM Tris-HCl pH 7,2
	150 mM NaCl
	0,1 % SDS (w/v)
	1 % Sodium desoxycholate (w/v)
	1 % Triton X-100

SDS running buffer (10x)	0,25 M Tris-base 2 M Glycine 1 % SDS (w/v) pH 8,3
SDS loading buffer	4 % SDS (w/v) 125 mM Tris-HCl pH 6,8 10 % Glycerol (v/v) 10 % ß-Mercaptoethanol (v/v) 0,02 % Bromphenol blue (w/v)
Separation gel buffer	1,5 M Tris-HCl 0.4 % SDS (w/v) pH 8,8
Stacking gel buffer	0,5 M Tris 0,4 % SDS (w/v) pH 6,7
TAE buffer (50x)	2 M Tris-Base 1 M NaAc 50 mM EDTA pH 8
TBST (10x)	200 mM Tris-HCl pH 7.8 1,5 M Sodium chloride 0,5 % Tween

3.12 Devices

3.12.1 Electrophoresis

System	Manufacturer
Horizontal electrophoresis system HE33	GE Healthcare Europe GmbH, Freiburg, DE

Hoefer electrophoresis power supply EPS301	GE Healthcare Europe GmbH, Freiburg, DE
Mighty small multiple gel caster SE200 Series	GE Healthcare Europe GmbH, Freiburg, DE
Standard power pack P25	Biometra, Göttingen, DE
TE77 ECL-Semi-Dry Transfer Unit	Amersham BioSciences, DE

3.12.2 Microscopy

Microscope	Manufacturer
Axiovert 40C	Zeiss, Jena, DE
Confocal laser scanning microscope LSM 510	Zeiss, Jena, DE
Leica, Leitz DM RBE	Leica, Wetzlar , DE
Eclipse Ti	Nikon, Tokio, Jp

3.12.3 Imaging

Imaging System	**Manufacturer**
AGFA Curix60 film developer	AGFA, Köln, DE
Hypercassette^{TM}	Amersham Life Science, DE
INTAS-imaging system	Intas, Göttingen, DE
Odyssey infrared imaging system	LI-COR, Bad Homburg, DE

3.12.4 PCR cycler

PCR Cycler	**Manufacturer**
LightCycler ^{R}1.5 instrument	Roche, Mannheim, DE
Rotor-Gene Q	Qiagen, Hilden, DE

3.12.5 Centrifuges

Centrifuge	**Manufacturer**

Eppendorf centrifuge 5415D	Eppendorf, Hamburg, DE
Hereaus Fresco17 Centrifuge	Thermo Scientific, DE
Heraeus Multifuge 1S-R	Thermo Scientific, DE
Thermo Heraeus Multifuge X3 FR	Thermo Scientific, DE
Microcentrifuge	Carl-Roth, Karlsruhe, DE
Sorvall Evolution RC with rotor SLA1500	Sorvall, Bad Homburg, DE

3.12.6 Other devices

Device	**Manufacturer**
Electroporator gene pulser MXcell™	BioRad, USA
Hereaus bacterial incubator Typ B6760	Kendro, Langenselbold, DE
Incubator for cell culture	Heraeus, Osterode, DE
Infinite M1000	Tecan, Männedorf, CHE
Incubator Innova 44	New Brunswick Scientific, Enfield, USA
Nanophotometer P300	IMPLEN, Westlake Village, USA
Neubauer chamber	Marienfeld, Lauda-Königshofen, DE
Orion II microplate Luminometer	Berthold Sys., DE
pH-meter 766 Calimatic	Knick, Berlin, DE
Polymax 1040 Shaker	Heidolph, Kelheim, DE
RCT Classic Magnetic stirrer	IKA, Staufen, DE
Rocking Plattform	Biometra, Göttingen, DE
Satorius balance LP 6000 200S	Satorius, Goettingen, DE
Satorius analytical balance	Satorius, Goettingen, DE
Sonification W-220F	Heat System-Ultrasonic, USA
Sterile bench for cell culture	Heraeus, Osterrode, DE
SterilGard^{R}III Advance	The Baker Company, ME, USA
Stuart roller mixer SRT9	Bibby Scientific, UK
Thermomixer compact	Eppendorf, Hamburg, DE
Vortex-Genie 2	Scientific Industries, USA
Water bath TW12	Julabo, Seelbach, DE

3.12.7 Relevant materials

Material	Manufacturer
Cell culture flasks (T25, T75, T175)	Greiner, Frickenhausen, DE
Cell culture plates (6, 12, 24, 96 wells)	Greiner, Frickenhausen, DE
Cell scraper	A. Hartenstein GmbH, Würzburg, DE
Coverslips, 18 mm	Carl Roth, Karlsruhe, DE
Developer type E 1–3	C & L GmbH, Planegg, DE
Elektroporation cuvettes; 4mm	VWR Collection
Falcon tubes (15 ml, 50 ml)	Greiner, Frickenhausen, DE
Filtered pipette tips (10 µl, 100 µl, 1 ml)	4titude, Berlin, DE
Fixer type F 1–2	C & L GmbH, Planegg, DE
Graduated pipettes (1, 5, 10, 25 ml)	Greiner, Frickenhausen, DE
Hybond-P, PVDF membrane	Millipore, DE
Hyperfilm ECL Chemiluminescence	GE Healthcare, Freiburg, DE
LightCycler capillaries (Polycarbonate)	Genaxxon, Biberach, DE
Microscope slides	Carl Roth, Karlsruhe, DE
MF-MilliporeTM Membrane filters (0.025 µm)	Merck Millipore, Schwalbach, DE
Parafilm	Bemis, Bonn, DE
Phase Lock Gel Heavy, 2ml	5Prime, Aut
SuperSignal West Pico Chemiluminescent Substrate	Thermo scientific, DE
Whatman paper 3 mm	VWR International GmbH, Darmstadt, DE

3.13 Software

Software	Manufacturer
Citavi 5	Swiss Academic Software GmbH, Wädenswil, CHE
GraphPad Prism 7	GraphPad, USA
i-control 1.8	Tecan, Männedorf, CHE
ImageJ	Wayne Rassband
Image Studio	Li-Cor Biosciences, Lincoln, USA

Image Studio Lite	LI-COR, Bad Homburg, DE
INTAS GDS	Intas, Göttingen, DE
LightCycler Software Version 3.5	Roche, Mannheim, DE
LSM Image Browser	Zeiss, Jena, DE
MS Office	Microsoft, Redmond, USA
Photoshop CS2	Adobe, San Jose, USA
Rotor-Gene Q	Qiagen, Hilden, DE
Vector NTI Advance 10	Invitrogen, Karlsruhe, DE
ZEN 2012	Zeiss, Jena, DE

4 Methods

4.1 Cell biology

4.1.1 Prokaryotic cell culture

E.coli strain TOP10 cells were cultivated for 16 h in LB medium with constant shaking in Erlenmeyer flasks. For selection of transformed bacteria, 100 µg/ml ampicillin or 30 µg/ml kanamycin were added to the medium. Glycerol stocks were stored in 30 % (v/v) glycerol at -80 °C.

4.1.2 Eukaryotic cell culture

In this study, the highly permissive human hepatoma-derived cell lines Huh7.5 and Huh7 cell clone 9-13 as well as primary human hepatocytes (PHH) were used. Cells were cultivated at 37 °C, with a content of 5 % CO_2 and $\geq$90 % humidity. Huh7.5 cells were grown in DMEM (4,5 g/l glucose) supplemented with 10 % FCS, 0,1 U/ml penicillin, 100 µg/ml streptomycin and 2 mM L-glutamine (DMEM complete). Huh7 clone 9-13 harboring the HCV subgenomic replicon I377/NS3-3' was cultivated in DMEM complete with 1 mg/ml G418. PHHs were isolated from liver samples obtained from partial hepatectomy and cultured in hepatocyte growth medium with 10 ng/ml epidermal growth factor, 5 µg/ml insulin, 0,5 µg/ml hydrocortisone, 10 µg/ml transferrin, 250 µg/ml ascorbic acid, and 3,75 mg/ml fatty acid free BSA. For passaging, adherent cells were washed once with PBS and detached from the cell culture flask by incubation with 1x trypsin/EDTA for 5 min at 37 °C. Protease activity of trypsin was stopped by adding 8 ml DMEM complete. Cells were resuspended in fresh medium and seeded at different dilutions (1:4–1:10). All experiments with infectious HCV were performed under S3 conditions.

4.1.3 Electroporation of Huh7.5 cells

Huh7.5 cells were passaged 2 days prior to electroporation to obtain a confluence of 80–90 %. Cells were harvested as described in chapter 4.1.2, washed twice with ice cold PBS and diluted to a

concentration of 5 x 10^6 cells/ml in PBS. For electroporation, 800 µl cell suspension were mixed with 10 µg *in vitro* transcribed RNA (see chapter 4.2.12) and transferred into a 4 mm electroporation cuvette. Cells were immediately pulsed by using a Gene Pulser MXcellTM (BioRad, USA) adjusted to deliver one pulse at 300 V and 950 µF. After an incubation period of 10 min at room temperature, electroporated cells were diluted in 12 ml DMEM complete and seeded in the appropriate culture dishes. 4 h after electroporation the medium was changed.

4.1.4 Transfection of Huh7.5 cells

For transfection of Huh7.5 cells, the linear polyethylenimin (PEI) (1 mg/ml) was used. Therefore, 0,5–1 µg plasmid DNA and 6 µl PEI/µg plasmid DNA were resuspended in 200 µl PBS and mixed by vortexing for 15 sec. After incubation for 15 min at room temperature, the transfection mix was added drop wise to 2 ml medium in a six well plate. 16 h after transfection the medium was changed.

4.1.5 Autophagy modulation

48 h after electroporation, cells were treated either with 5 mM 3-methyladenine (3-MA) to inhibit autophagy at an early stage, or 100 nM bafilomycin A1 to inhibit autophagosomal-lysosomal fusion, diluted in DMEM complete for 16 h.

4.1.6 Radical scavenging

For scavenging of ROS, cells were treated with 10 µM pyrrolidine dithiocarbamate (PDTC) or 5 mM N-acetylcysteine (NAC) for 16 h.

4.1.7 Infection of primary human hepatocytes (PHHS)

One day prior to infection, PHHs were seeded into a 6 well plate. Cells were infected with 1 ml supernatant derived from Jc1 replicating Huh7.5 cells. 16 h after infection, cells were washed with PBS and fresh medium was added. 120 h after infection, cells were harvested, total RNA was isolated (see chapter 4.2.7) and analyzed by qRT-PCR (see chapter 4.2.10).

4.1.8 Virus titration

Virus titers were analyzed by determination of the 50 % tissue culture infective dose ($TCID_{50}$/ml) based on limited dilution. Supernatants were dialyzed using 0,025 µm pore size MF-Millipore membrane

filters to get rid of the chemicals. For infection analysis, Huh7.5 cells were seeded in a 96-well plate at a density of 1 x 10^4 cells/well in the morning of infection. After dialysis, 200 µl of serial diluted supernatant were used for infection of Huh7.5 cells for 72 h. For determination of the intracellular $TCID_{50}$, cells were washed with PBS, scraped down in medium and lysed by freeze-thawing 3 times with liquid nitrogen and a 37 °C water bath. Lysed cells were centrifuged for 10 min at 13.300 rpm, and the supernatant was used for $TCID_{50}$ analysis. 72 h after infection, cells were fixed with 4 % formaldehyde. For detection of HCV-positive cells, NS5A-specific serum was used (Burckstummer et al., 2006). Virus titers were calculated based on the method of Spearman and Kärber (Spearman, 1908, Kaerber, 1931).

4.1.9 Cell harvest and lysis

Depending on the subsequent experiments, cells were lysed with different buffers (see chapter 3.11) under different conditions. All steps were carried out on ice.

4.1.9.1 Protein lysates

For western blot analysis, total cell lysates were used. Therefore, cells were washed with PBS and lysed by adding 200 µl of RIPA buffer supplemented with protease- and phosphatase-inhibitors (see chapter 3.7 and 3.11). After an incubation of 10 min on ice, cells were scraped off the wells, transferred to reaction tubes and sonicated (10 sec, 10—20 % intensity) for fragmentation of the chromosomal DNA. Lysates were centrifuged for 5 min at 13.300 rpm and 4 °C. The supernatant was subjected to protein quantification (see chapter 4.3.1).

4.1.9.2 Luciferase lysates

For luciferase reporter gene assays, transfected cells were lysed 48 h after transfection with 200 µl luciferase lysis buffer. Cells electroporated with the pFK-Luc-Jc1 construct were harvested 72 h after electroporation. After 10 min incubation on ice, lysed cells were scraped down, transferred to reaction tubes and centrifuged for 5 min at 13.300 rpm and 4 °C.

4.1.10 Luciferase reporter gene assay

For determination of the luciferase reporter gene activity, lysates (50 µl) were analyzed by automated addition of 50 µl luciferase substrate and subsequent determination of chemiluminescence by an

Orion II microplate Luminometer. Measurements were carried out at room temperature in duplicates. Luciferase levels were referred to the protein concentration of the appropriate lysates.

4.2 Molecular biology

4.2.1 Agarose gel electrophoresis

For analysis of plasmid DNA and RNA, agarose gel electrophoresis was used. Depending on the size of the fragments, 1−2 % (w/v) agarose was dissolved in 1x TAE by heating. After cooling of the solution, 0,1 µg/ml ethidiumbromide was added and the liquid agarose was poured into a horizontal gel chamber complemented with a comb. The solid gel was placed in a gel chamber containing 1x TAE. The DNA samples were supplemented with 6x loading buffer, loaded into the pockets of the gel and separated at 100 V. DNA bands were visualized under UV-light (254/365 nm) using the INTAS imaging system.

4.2.2 Determination of nucleic acid concentration

The concentration of nucleic acids was determined using the NanoPhotometer P300 at a wavelength of 260 nm. At this wavelength, an absorption of 1,0 correlates with a concentration of 50 µg/ml double-stranded DNA and 40 µg/ml RNA. To determine the purity of nucleic acid, the absorbance of proteins at a wavelength of 280 nm was measured. Pure DNA samples should obtain an OD_{260}/OD_{280} ratio of 1,8, pure RNA samples of 2,0. Lower values indicate a contamination with proteins or phenol.

4.2.3 Isolation of plasmid DNA

Plasmid DNA was isolated using the *QIAGEN Plasmid Maxi Kit* according to the manufacturer's instructions. Plasmid DNA was extracted from a 300 ml bacterial culture. The principle relies on the bacterial lysis under alkaline conditions in the presence of SDS (Birnboim and Doly, 1979). DNA was precipitated by isopropanol, followed by washing. After the DNA pellet air-dried, DNA was dissolved in ddH_2O and stored at -20 °C.

4.2.4 Restriction endonuclease digestion

This method was used to linearize circular plasmids containing HCV genomes. Therefore, 40 µg pFK-JFH1/J6 were linearized using *AseI*. pFK-JFH1/GND and pJFH1d3C were linearized usind *XbaI,*

and pFK-Luc-Jc1 was linearized using *MluI*. The DNA was digested according to the manufacturer's instructions.

4.2.5 Transformation of competent bacteria

For transformation of chemical competent TOP10 *E.coli*, 100 ng plasmid were added to 100 µl of competent cells and incubated for 30 min on ice. After a heat shock at 42 °C for 30 sec, cells were incubated for 5 min on ice. 400 µl LB medium were added to the suspension and bacteria were incubated with constant shaking at 37 °C for 1 h. Subsequently, the suspension was added to an Erlenmeyer flask containing 300 ml LB medium with the appropriate antibiotic for resistance selection and incubated with constant shaking at 37 °C for 16 h.

4.2.6 Phenol/chloroform extraction of nucleic acids

To extract nucleic acids from aqueous solution, 1/10 volume 3 M sodium acetate (pH 5,2) and one volume phenol were added to the solution and centrifuged for 5 min at 13.300 rpm and 4 °C. The upper aqueous phase was transferred into a Phase lock tube and mixed with one volume chloroform:isoamylalcohol (24:1), followed by centrifugation for 5 min at 13.300 rpm and 4 °C. To precipitate nucleic acids, the upper phase was transferred into a fresh reaction tube and mixed with 2,5 volumes ice cold absolute ethanol (or 0,7 volumes absolute isopropanol). After a centrifugation for 30 min at 13.300 rpm and 4 °C, the pellet was washed with 75 % ethanol, air dried and resuspended in ddH_2O.

4.2.7 RNA Isolation

Total RNA was isolated using *peqGOLD TriFast* (PeqLab) according to the manufacturer's instructions. RNA was resuspended in DEPC-treated H_2O and the quality was controlled by agarose gel electrophoresis (see chapter 4.2.1).

4.2.8 cDNA synthesis

Before cDNA synthesis, isolated RNA was digested with DNaseI to degrade potential DNA contaminations. Therefore, 5 µg RNA were incubated with DNaseI (PeqLab) in a total volume of 10 µl for 1 h at 37 °C. To inactivate the DNaseI, 1 µl EDTA (25 mM) was added and incubated for 10 min at 65 °C. cDNA synthesis was performed using M-MuIV reverse transcriptase and random hexamer primers. For this, 1 µl random hexamer primers was incubated with the RNA for 5 min at 65 °C. Subsequently,

2 µl dNTPs (10 mM), 4 µl 5x RT buffer, 1 µl H_2O and 1 µl M-MulV reverse transcriptase were added and incubated for 10 min at room temperature and 60 min at 42 °C. For inactivation of the reverse transcriptase, the solution was incubated for 5 min at 72 °C. RNA was stored at -80 °C. For qRT-PCR analysis, cDNA was diluted 1:10.

4.2.9 HCV genome isolation from cell culture supernatant

For the isolation of viral RNA from supernatant, the *QIAamp DSP Virus Kit* was used according to the manufacturer's instructions. Viral genomes were quantified by qRT-PCR using the Rotor Gene cycler (see chapter 4.2.11).

4.2.10 Quantitative real time PCR (qRT-PCR)

The LightCycler 1.5 system and the LightCycler 480 system served for the detection and quantification of specific transcripts using Maxima^{TM}SYBR Green qPCR-Kit (Fermentas). The quantification is based on the intercalation of the DNA binding fluorescent dye SYBR Green during the PCR reaction. Increasing SYBR Green fluorescence intensity is proportional to the amount of amplified DNA. After each cycle, fluorescence intensity is measured. The amount of specific transcripts was calculated as n-fold expression using the $2^{-\Delta\Delta C_P}$ method. The reaction mix, with a total volume of 10 µl, consisted of 5 µl 2x Maxima^{TM}SYBR Green qPCR Master Mix and 0,25 µl of each primer (10 µM) and was filled up with ultrapure ddH_2O. For normalization of the measured values, the house-keeping gene RPL27 was analyzed. The qRT-PCR program is shown in table 4.1.

Table 4.1: Quantitative real time PCR program.

Program	Temperature (°C)	Hold time (sec)	Slope (°C/sec)	Aquisiton Mode	Cycles
denaturating	95	600	20	None	1
cycling	95	15	20	None	45
	56	30	20	None	
	72	30	5	Single	
melting	95	60	20	None	1
	60	30	20	None	
	95	0	0.1	Continous	
cooling	40	30	20	None	

4.2.11 Quantification of HCV genomes in the supernatant by qRT-PCR

Quantification of HCV genomes from cell culture supernatant was performed using the *artus HCV RG RT-PCR Kit* (Qiagen) on the Rotor-Gene Q instrument according to the manufacturer's instructions. In brief, 10 µl of the eluted RNA was added to the master mix, containing 6 µl HCV RG Master A and 9 µl Master B, and was detected by qRT-PCR. For the calculation of total HCV genomes, provided quantification standards were measured.

4.2.12 *In vitro* T7 transcription

In vitro T7 transcription was performed to generate HCV RNA genomes from linearized DNA plasmids containing a T7 promotor for electroporation purposes. The reaction (table 4.2) was incubated for 4 h at 37 °C. To digest the input DNA, 1 U/µg DNaseI was added and incubated for 1—2 h at 37 °C. The transcribed RNA was purified by phenol/chloroform extraction (see chapter 4.2.6), resuspended in DEPC-treated H_2O and frozen in 10 µg aliquots at -80 °C.

Table 4.2: T7 transcription.

	Volume	**Final concentration**
5x transcription buffer	16 µl	1x
10 mM NTPs	3.2 µl	0.4 mM
100 mM DTT	8 µl	10 mM
40 U/ µl RNase Out	2 µl	1 U/ µl
50 U/µl T7 RNA polymerase	4 µl	2.5 U/ µl
DNA template		5 µg
ddH_2O	ad 80 µl	

4.3 Protein biochemistry

4.3.1 Protein quantification by Bradford assay

The protein amount in total cell lysates was quantified using the Bradford reagent. The reagent contains the dye Coomassie Brilliant Blue G250, which shifts in absorbance in the presence of proteins from 465 to 595 nm. Therefore, 2 µl cell lysate were mixed with 200 µl Bradford reagent, and absorbance was measured with the Tecan reader (Infinite M1000).

4.3.2 Polyacrylamide gel electrophoresis

Sodium dodecyl sulfate polyacrylamide gel electrophoresis (SDS-PAGE) was used to separate proteins depending on their molecular weight (Laemmli, 1970). The gel is composed of a stacking gel, in which the proteins get concentrated, and a separation gel, in which the SDS-denatured proteins are separated. For the stacking gel, a polymer density of 4 % was used, while the density of the separation gel varied depending on the expected size of the target protein (10—14 %). The composition of the gels is summarized in table 4.3. Equal amounts of proteins (75—100 µg) were denatured in 1x SDS-PAGE sample buffer by heating the mixture for 5 min at 95 °C. Samples were separated in a vertical chamber at 100—120 V.

Table 4.3: Composition of the stacking and separation gel.

Stacking gel	**4%**	**Separation gel**	**10 %**	**12%**	**14%**
Rotiphorese 40 (29:1)	6 ml	Rotiphorese 40 (29:1)	20 ml	24 ml	28 ml
Stacking gel buffer (4x)	15 ml	Separation gel buffer (4x)	20 ml	20 ml	20 ml
H_2O	45 ml	H_2O	40 ml	36 ml	32 ml
TEMED	60 µl	TEMED	80 µl	80 µl	80 µl
APS (10 %)	600 µl	APS (10%)	800 µl	800 µl	800 µl

4.3.3 Western blot

After separation by SDS-PAGE, proteins were transferred onto a methanol-activated PVDF membrane (Immobilion-P, Millipore), using a semi-dry blotting chamber and a discontinuous buffer system (1,3 mA/ cm^2 for 1 h) (Tobwin et al., 1984) (see picture 4.1). After blotting, the membrane was blocked using 1x Roti®-Block blocking solution, 5 % BSA in 1x TBST or 10 % (w/v) skim milk powder in 1x TBST buffer for 1 h at room temperature, followed by incubation with the primary antibody in blocking solution for 1 h at room temperature or over night at 4 °C. Unspecifically bound antibody was removed by washing with 1x TBST buffer followed by an incubation with secondary antibody coupled with a horseradish peroxidase (HRP)- or IRDye-coupled (Li-Cor) for 1 h at room temperature. After repeated washing to remove unspecifically bound secondary antibody with 1x TBST, protein bands were detected by exposition to a scientific imaging film, using a peroxidase substrate reagent (ECL) or the Li-Cor Odyssee detection system.

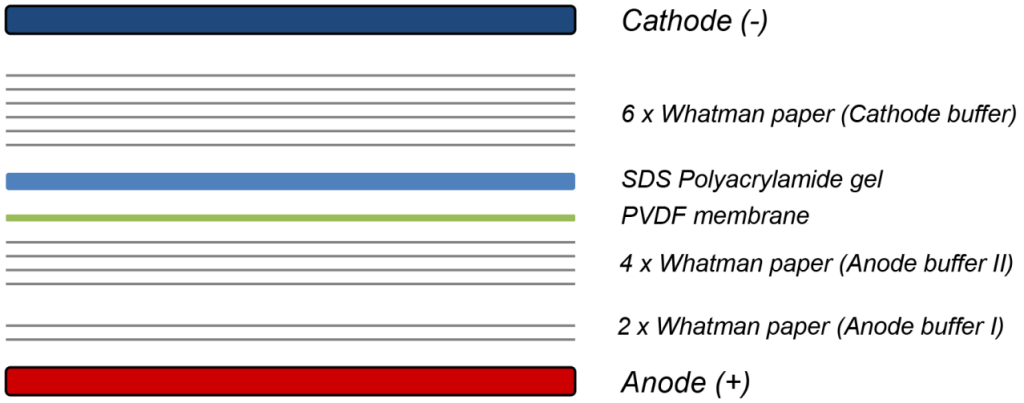

Figure 4.1: Scheme of a semi-dry blot stack. Whatman paper corresponding to the size of the SDS polyacrylamide gel were soaked in the corresponding buffers and arranged together with the SDS polyacrylamide gel and the PVDF membrane as shown in the scheme.

4.3.4 Western blot with phospho-specific antibodies

Western blot analysis with phospho-specific antibodies was performed as described in the previous section (see chapter 4.3.3) with the following exceptions. The methanol-activated PVDF membrane after protein transfer was blocked with 1x Roti®-Block blocking solution in 1x PBS, supplemented with 0,3 % Triton X-100 (PBST). Antibodies were diluted in 1x Roti®-Block solution in PBST overnight at 4 °C. Washing steps were performed three times for 10–15 min each with PBST after each antibody incubation period. As secondary antibodies only HRP-coupled antibodies were used.

4.3.5 Measurement of protein oxidation

4.3.5.1 OxyBlot protein oxidation detection

Carbonylation of proteins by ROS was detected using the *OxyBlot™ protein oxidation detection kit* (Millipore). HCV-positive and HCV-negative cells were harvested 72 h after electroporation, washed with PBS and lysed with RIPA buffer. 20 µg of protein lysate were mixed with the same volume of 12 % SDS, followed by incubation with 2,4-dinitrophenylhydrazine (DNPH) for 15 min at room temperature. Negative controls were incubated with a derivatization control. Reaction was stopped by adding the 1,5 fold volume of neutralization buffer. Protein samples were separated on a 12 % SDS-polyacrylamide gel electrophoresis, followed by western blot analysis, using a DNP-specific antibody.

4.3.5.2 ROS-ID Total ROS detection

Detection of ROS was performed by using the *ROS-ID^{TM} Total ROS Detection Kit* from Enzo Life Sciences. HCV-positive and HCV-negative cells were seeded into 96-well plates after electroporation. After 72 h, cells were washed with PBS and simultaneously treated with pyocyanin as ROS inducer (100 µM) or PDTC (10 µM) as ROS scavenger together with ROS detection solution diluted in washing buffer. After an incubation period of 30 min at 37 °C, cells were washed twice and analyzed by fluorescence microscopy using a Nikon Ti-U E20L80 equipped with a Mono DS-Qi2 camera at 490/525 nm excitation/emission. For comparison of the ROS level of HCV-positive and HCV-negative cells, untreated cells were analyzed. Fluorescence intensity from visual fields was calculated using ImageJ software.

4.3.6 Indirect immunofluorescence microscopy

Cells were grown in 12-well plates on cover slides. After fixation with 4 % formaldehyde in PBS for 10 min, cells were washed twice with PBS and permeabilized with 0,5 % Triton X-100 in PBS for 10 min. Unspecific binding was blocked by incubation with 1 % BSA in PBS for 15 min. Cells were incubated for 1 h at room temperature in a humid chamber with the primary or fluorescence-labeled secondary antibody diluted in PBS. Nuclei were stained with DAPI (4,6- diamidino-2-phenylindole) solution (1 µg/µl). Cells were finally mounted with Mowiol.

4.4 Microscopy

4.4.1 Confocal laser scanning microscopy (CLSM)

Immunofluorescence staining was analyzed using a confocal laser scanning microscope (CLSM 510 Meta; Carl Zeiss) and ZEN 2009 software. The used objectives were 100×, numerical aperture 1,46. Total fluorescence per cell was calculated using ImageJ software and the following formula: corrected total cell fluorescence (CTCF) = integrated density (area of selected cell x mean fluorescence of background readings). In total, a minimum of ten cells were measured.

4.5 Statistical analyses

Results are described as the mean ± standard error of the mean (SEM) from at least 3 independent experiments. The significance of results was analyzed by a two tailed unpaired t test using GraphPad

Prism version 6.07 for Windows (GraphPad Software, San Diego, CA). Error bars in the figures represent SEM. Statistical significance is represented in the figures as follows: *, $P < 0{,}05$; **, $P < 0{,}01$ and ***, $P < 0{,}001$.

5 Results

5.1 HCV induces ROS formation

HCV interferes with a variety of mechanisms, thereby inducing the formation of ROS that are considered as a contributing factor for HCV-associated pathogenesis (Medvedev et al., 2016b, Ivanov et al., 2013, Fu et al., 2016). To analyze the influence of HCV on the intracellular ROS levels, total ROS detection was performed by fluorescence microscopy analysis using DCFH-DA as substrate. Compared to HCV-negative cells, in HCV-positive cells elevated levels of ROS can be observed depicted by enhanced green fluorescence of DCF as shown in figure 5.1. Quantification of fluorescence intensity revealed a significant increase in HCV-positive cells (figure 5.1 lower panel). As controls, cells were treated with the ROS inducer pyocyanin or the ROS scavenger pyrrolidine dithiocarbamate (PDTC). Pyocyanin-treated cells exhibit a bright green fluorescence, due to enhanced ROS formation, while PDTC-treated cells show a decreased green fluorescence due to the scavenging activity of PDTC. To confirm that the observed effect is HCV-dependent, cells were stained with a NS5A-specific antibody. As shown in the right panel of figure 5.1, Jc1 cells are nearly 100 % HCV-positive shown by the cytosolic red staining.

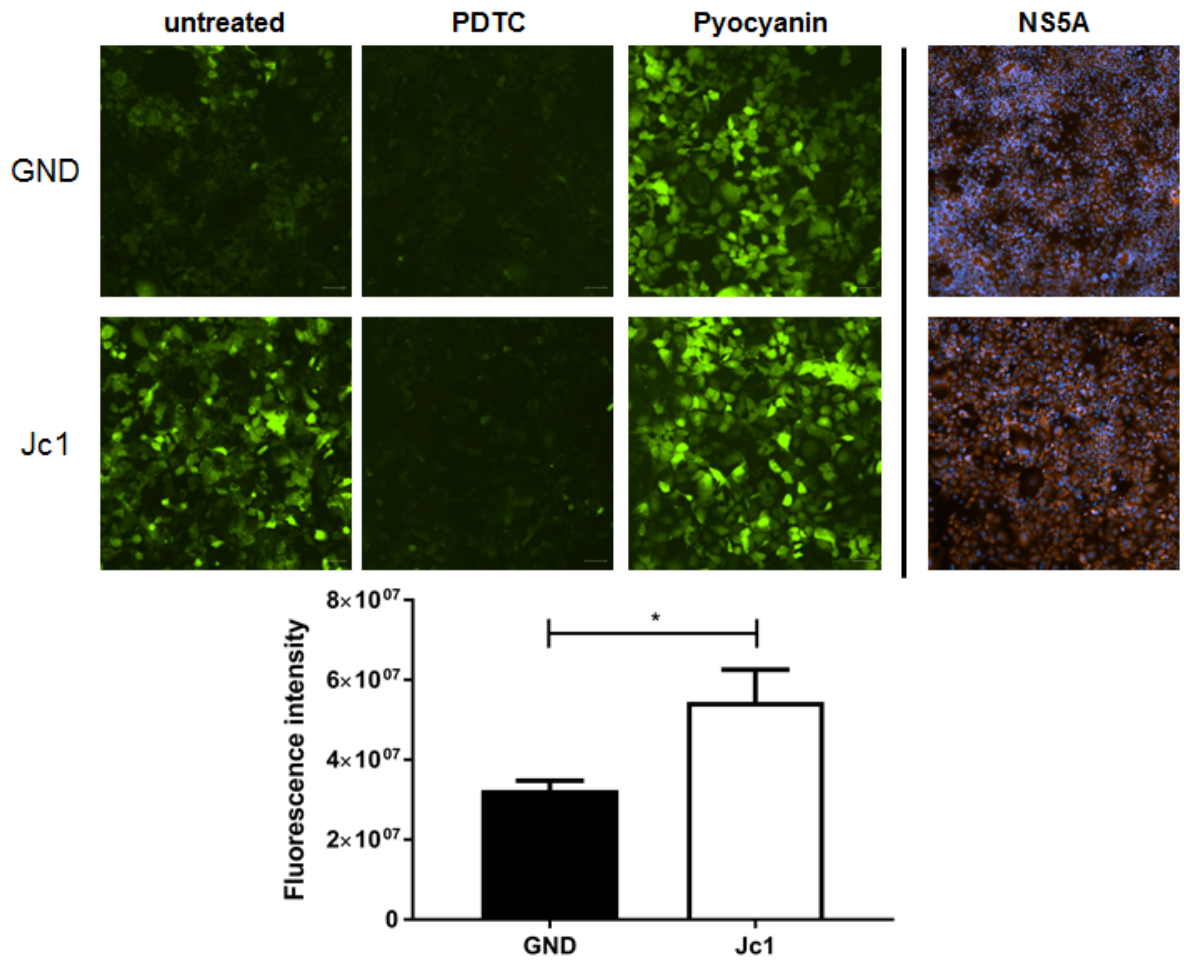

Figure 5.1: HCV induces ROS formation. Detection of cellular ROS levels with ROS-ID^{TM} Total ROS Detection Kit. **Top,** fluorescence analysis of HCV-positive and HCV-negative cells incubated with ROS detection solution. As negative controls, cells were treated with PDTC and as positive control, cells were treated with pyocyanin. **Top right,** HCV-positive and HCV-negative cells were stained with an NS5A-specific antibody. Scale bar represents 100 µm. **Bottom,** quantification of the fluorescence intensity. Results represent the mean of >8 field of views (mean ± SEM). Two-tailed unpaired t-test, *p=0,0114.

To further confirm these findings, OxyBlot analysis was performed. Compared to HCV-negative cells, higher amounts of oxidized proteins are present in HCV-positive DNPH-treated cells (figure 5.2).

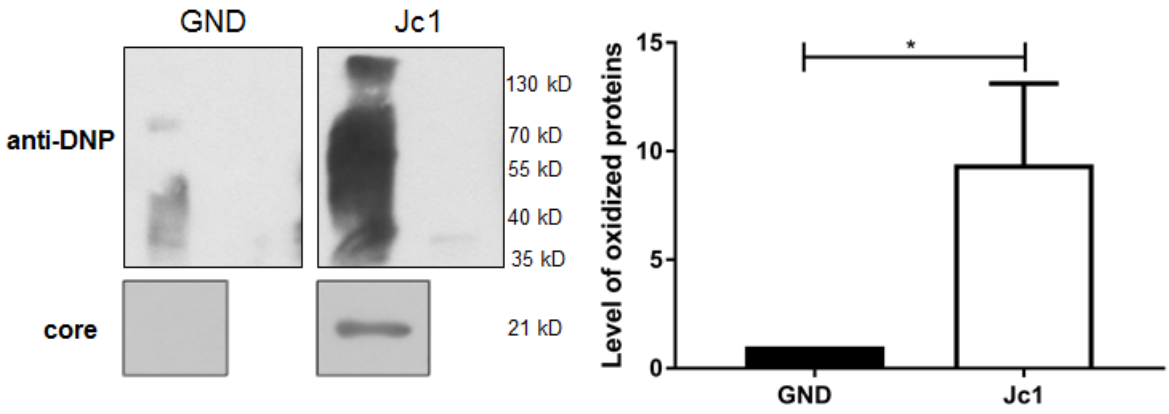

Figure 5.2: Increased amount of oxidized proteins in HCV-positive cells. Left, OxyBlot analysis of cellular lysates derived from HCV-positive or HCV-negative cells. Protein oxidation was analyzed by incubation with 2,4-dinitrophenylhydrazine (DNPH) for covalent modification of oxidized proteins. In lane 2 and 4, lysates were incubated with a derivatization control to reveal the specificity of the observed signals. Detection of core served as control for HCV-positive lysates. **Right,** densitometric quantification of DNP-specific signal from three independent experiments. HCV-negative cells served as control and were set as 1 (n=3, mean ± SEM). Two-tailed unpaired t-test, * p=0,0252.

Taken together, these results demonstrate that in HCV-positive cells elevated amounts of ROS are present, resulting in higher levels of oxidized proteins as compared to HCV-negative control cells.

5.2 HCV induces autophagy

5.2.1 HCV induces the expression of LC3 and p62

Viruses are known to exploit the autophagic machinery for their life cycle (Wang et al., 2015, Elgner et al., 2016, Ren et al., 2016, Dash et al., 2016). The same holds true for HCV, which is known to induce autophagy to promote its own life cycle (Sir et al., 2008, Ke and Chen, 2011a). To verify this effect, HCV-positive cells (Jc1) and the corresponding HCV-negative control cells (GND) were analyzed by western blot and immunofluorescence microscopy, using the two autophagy marker proteins LC3 and p62 (Mizushima et al., 2010). Thereby, LC3-II served as a marker for the induction of autophagy (Mizushima and Yoshimori, 2007). In HCV-positive cells, significantly more LC3-II protein amount was observed by western blot analysis (figure 5.3). Detection of core protein served as a control for HCV-positive cells.

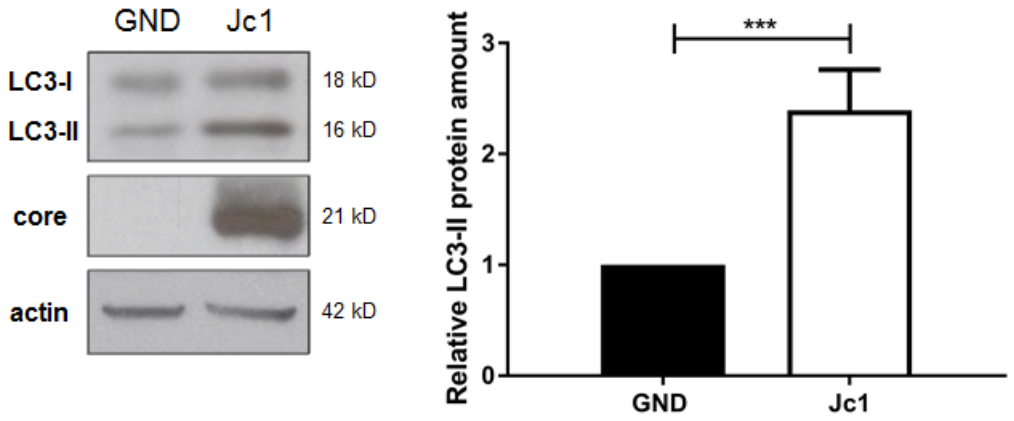

Figure 5.3: Increased amount of LC3-II in HCV-positive cells. Left, western blot analysis of cellular lysates derived from HCV-positive cells (Jc1) and HCV-negative cells (GND), using LC3- and core-specific antibodies. Detection of β-actin served as loading control. **Right,** densitometric quantification of LC3-II expression from five independent experiments. HCV-negative cells served as control and were set as 1 (n=5, mean ± SEM). Two-tailed unpaired t-test, ***p=0,0003.

Similar results were observed by immunofluorescence analysis using LC3- and core-specific antibodies (figure 5.4). Shown in the red channel is the LC3-specific signal, whereas in the green channel HCV-positive cells are detected with a core-specific antibody. Determination of the corrected total cell fluorescence (CTCF) revealed a significant increase in LC3-specific fluorescence signal in HCV-positive cells (figure 5.4 lower panel).

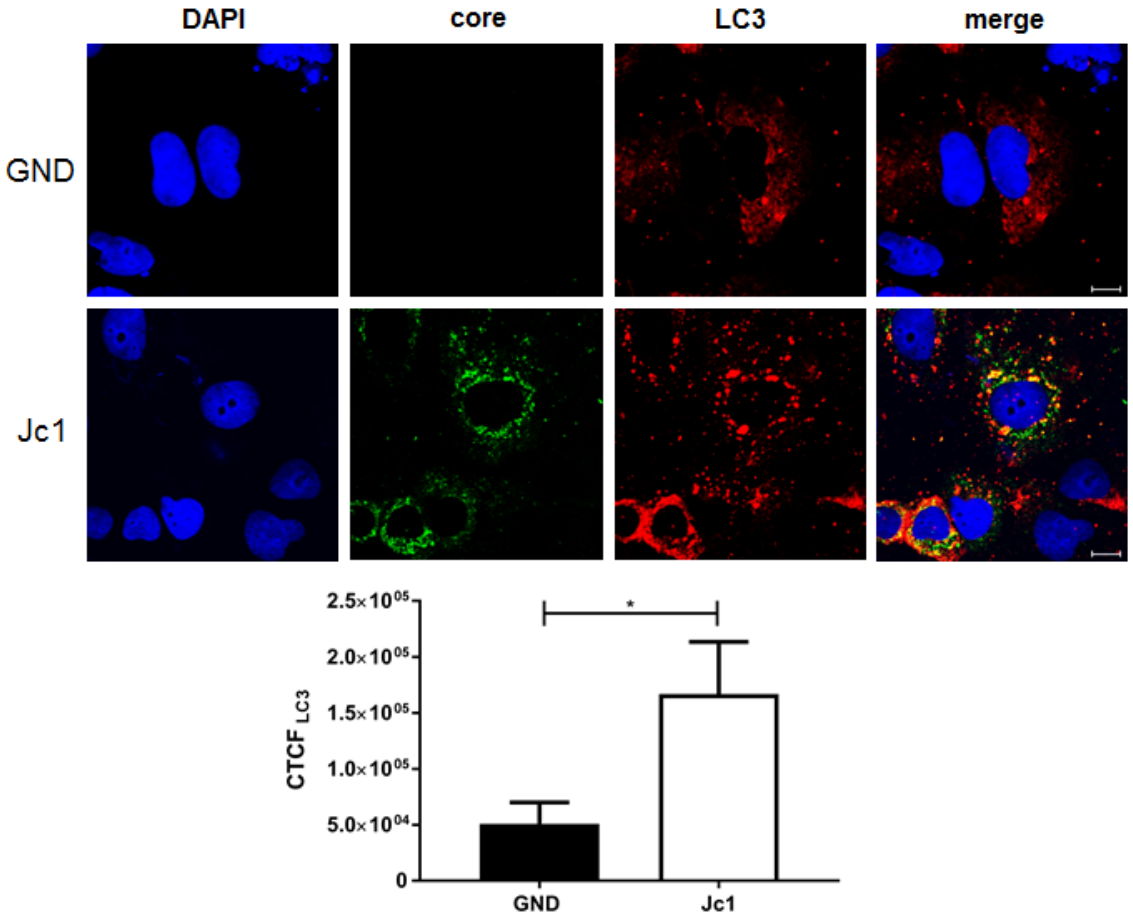

Figure 5.4: Increased amount of LC3-II in HCV-positive cells. Top, CLSM analysis of HCV-positive cells (Jc1) and HCV-negative cells (GND). Cells were stained using core- (green) and LC3-specific (red) antibodies. The nuclei were stained with DAPI (blue). Laser intensity and digital gain were kept constant for GND and Jc1 cells. Magnification 100x. Scale bar represents 10 µm. **Bottom,** quantification of the fluorescence intensity of LC3 by corrected total cell fluorescence (CTCF). Results represent the mean of >7 cells (mean ± SEM). Two-tailed unpaired t-test, *p=0,0455.

For the second autophagy marker protein p62 similar results were observed. Both in western blot analysis (figure 5.5) and in immunofluorescence analysis (figure 5.6), a significant increase in the protein amount of p62 in HCV-positive cells was detected.

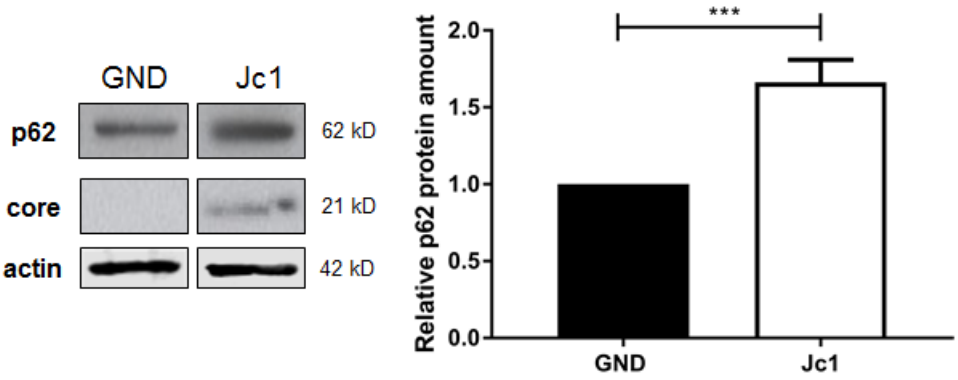

Figure 5.5: Increased amount of p62 in HCV-positive cells. Left, western blot analysis of cellular lysates derived from HCV-positive cells (Jc1) and HCV-negative cells (GND), using p62- and core-specific antibodies. Detection of β-actin served as loading control. **Right,** densitometric quantification of p62 expression from six independent experiments. HCV-negative cells served as control and were set as 1 (n=6, mean ± SEM). Two-tailed unpaired t-test, ***p=0,0003.

Calculating the CTCF, a significantly increased p62-specific signal (red channel) was observed in HCV-positive cells (figure 5.6 lower panel).

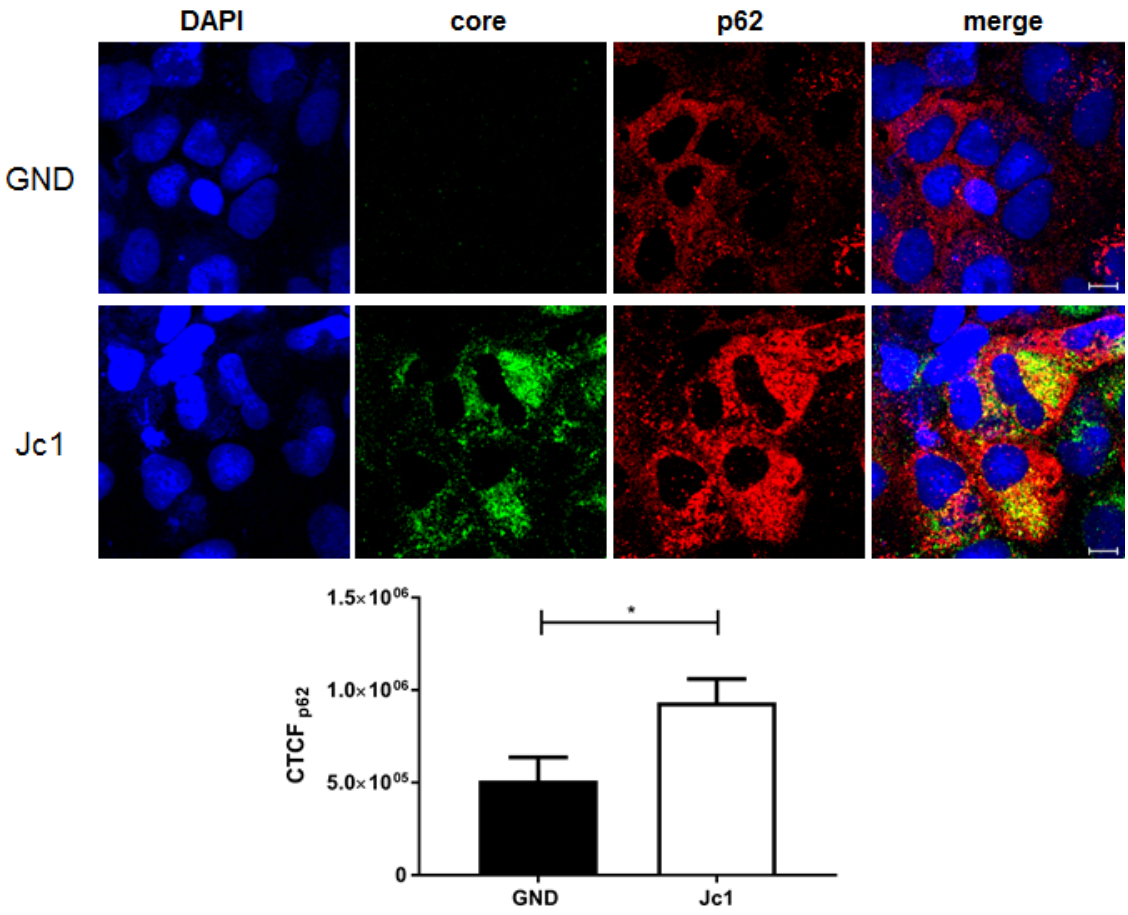

Figure 5.6: Increased amount of p62 in HCV-positive cells. Top, CLSM analysis of HCV-positive cells (Jc1) and HCV-negative cells (GND). Cells were stained using core- (green) and p62-specific (red) antibodies. The nuclei were stained with DAPI (blue). Laser intensity and digital gain were kept constant for GND and Jc1 cells. Magnification 100x. Scale bar represents 10 µm. **Bottom,** quantification of the fluorescence intensity of p62 by corrected total cell fluorescence (CTCF). Results represent the mean of >7 cells (mean ± SEM). Two-tailed unpaired t-test, *p=0,0334.

p62 is a cargo binding protein which is degraded during the autophagic process (Taniguchi et al., 2016). Hence, the induction of autophagy should result in the degradation of p62. But the opposite is the case (figure 5.5). To clarify this discrepancy, alterations of p62 protein amount were studied by western blot analysis within 102 h after electroporation (figure 5.7). Already at an early time point (18 hpe), an increase of p62 protein amount was observed, finally reaching a peak between 42 and 54 h. 102 h after electroporation, elevated amounts of p62 were still detectable.

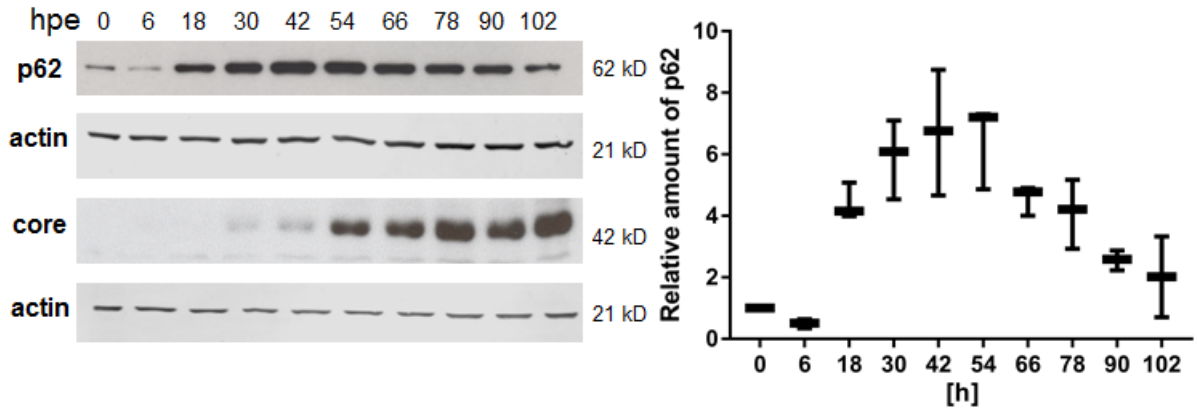

Figure 5.7: p62 protein amount starts to increase 18 h after electroporation. Left, western blot analysis of HCV-positive cells (Jc1) that were harvested at different time points after electroporation. For detection, p62- and core-specific antibodies were used. β-actin served as loading control. **Right**, densitometric quantification of p62 expression from three independent experiments. p62 protein amount before electroporation served as control and was set as 1.

To explain accumulation of p62 in HCV-positive cells, the half-life of p62 was analyzed. Thereby, a significant prolonged half-life of p62 could be observed in HCV-positive cells shifting from 1,5 h to 2,7 h compared to HCV-negative cells (figure 5.8).

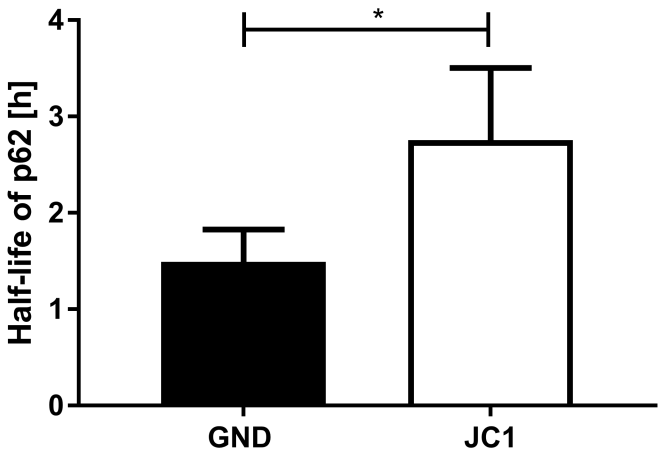

Figure 5.8: Increased half-life of p62 in HCV-positive cells. HCV-positive and negative cells were treated with cycloheximid (CHX) and harvested at different time points. Half-life of p62 was calculated by exponential regression based on western blot analysis. Results represent the mean from three independent experiments (n=3, mean ± SEM). Two-tailed unpaired t-test, *p=0,0421.

5.2.2 HCV induces the phosphorylation of p62 at serine 349

The phosphorylation of p62 at serine 349 (pS[349] p62) plays a significant role in the crosstalk of autophagy and the Nrf2/ARE signaling pathway, as it increases the binding affinity of p62 to

Keap1, resulting in the release of Nrf2 from the complex and thereby inducing the expression of Nrf2/ARE-dependent genes (Komatsu et al., 2010). To investigate the influence of HCV on the phosphorylation of p62, western blot and immunofluorescence microscopy analyses were performed using pS[349] p62- and p62-specific antibodies. In the western blot, a significant increase of pS[349] p62 was observed (figure 5.9). This increase was not caused by increased expression of p62, as the calculation of the ratio of pS[349] p62 to total p62 protein amount still indicates a significant rise (figure 5.9 right panel).

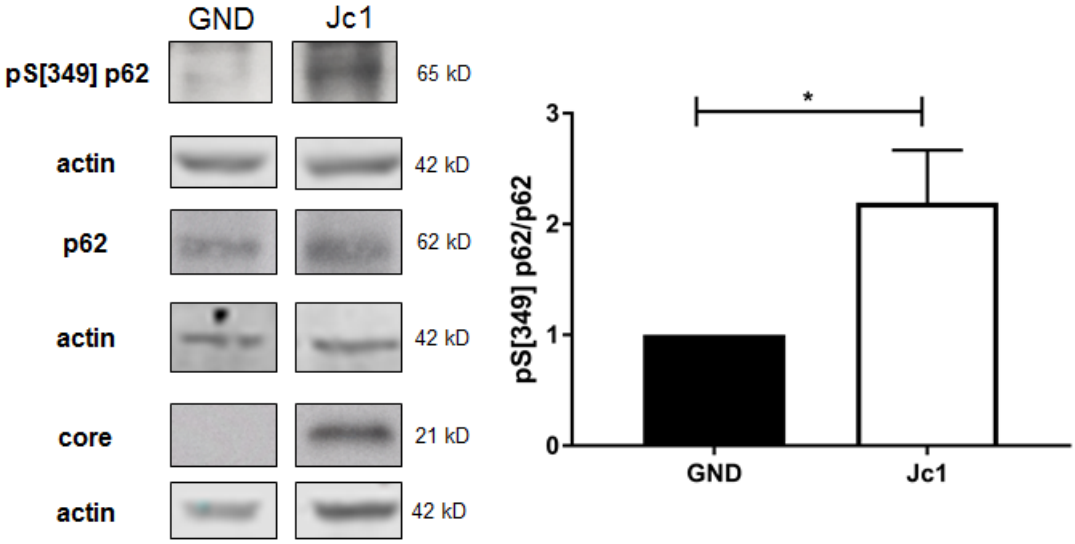

Figure 5.9: HCV induces the phosphorylation of p62 at serine 349. Left, western blot analysis of cellular lysates derived from HCV-positive cells (Jc1) and negative cells (GND) using pS[349] p62-, p62- and core-specific antibodies. Detection of β-actin served as loading control. **Right,** densitometric quantification from four independent experiments. Amount of p[349] p62 was normalized to total p62 amount. HCV-negative cells served as control and were set as 1 (n=4, mean ± SEM). Two-tailed unpaired t-test, *p=0,0159.

Moreover, immunofluorescence analysis confirmed the observation from the western blot (figure 5.10). Cells were stained with a pS[349] p62-specific antibody (green), a p62-specific antibody (red) and a HCV-core-specific antibody (cyan). For quantification, the CTCF of each cell was determined and then the ratio of pS[349] p62 to total p62 was calculated, which is shown in the lower panel of figure 5.10. Thereby, a significant induction of the pS[349] p62 could be observed in HCV-positive cells indicated by a significant higher ratio of pS[349] p62 to p62 compared to HCV-negative cells (figure 5.10 lower panel).

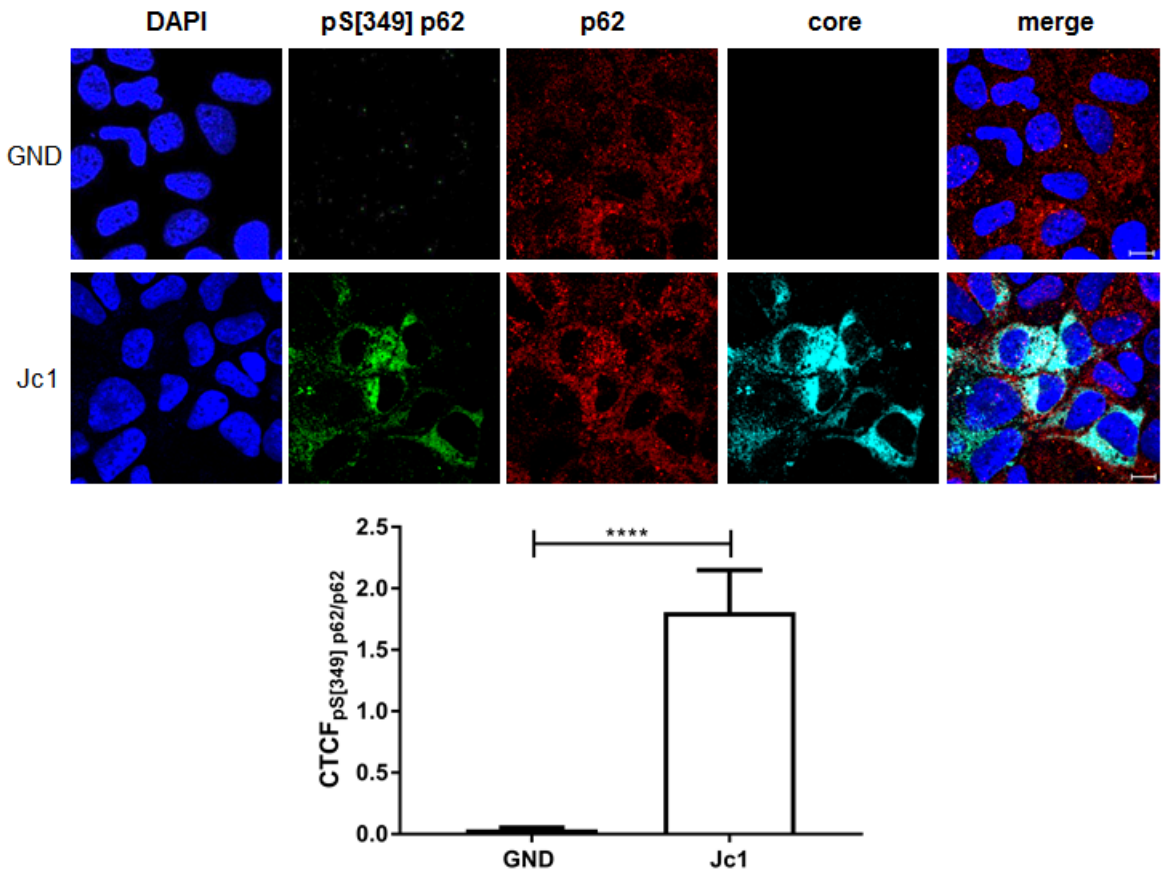

Figure 5.10: HCV induces the phosphorylation of p62 at serine 349. Top, CLSM analysis of HCV-positive cells (Jc1) and HCV-negative cells (GND). Cells were stained with pS[349] p62- (green), p62- (red) and core-specific antibodies (cyan). The nuclei were stained with DAPI (blue). Laser intensity and digital gain were kept constant for GND and Jc1 cells. Magnification 100x. Scale bar represents 10 µm. **Bottom,** quantification of the fluorescence intensity of pS[349] p62 normalized to p62 by (CTCF). Results represent the mean of >9 cells. (mean ± SEM). Two-tailed unpaired t-test, ****p<0,0001.

5.2.3 Induced expression of autophagy marker proteins in HCV-infected PHHs

Primary human hepatocytes (PHHs) are a physiological relevant cell culture model as they support the entire HCV life cycle (Gondeau et al., 2014). To examine the effect of HCV on autophagy in an additional model, PHHs were infected with HCV-positive (Jc1-derived) supernatant for 72 h, total RNA was isolated and analyzed by qRT-PCR (figure 5.11). Using specific primers to detect autophagy marker proteins, an upregulation of LC3, p62, Beclin-1 and Atg5 specific transcripts was observed compared to uninfected cells. Detection of HCV-specific RNA confirmed an effective infection. These findings reveal that autophagy is induced in PHHs in response to an HCV infection.

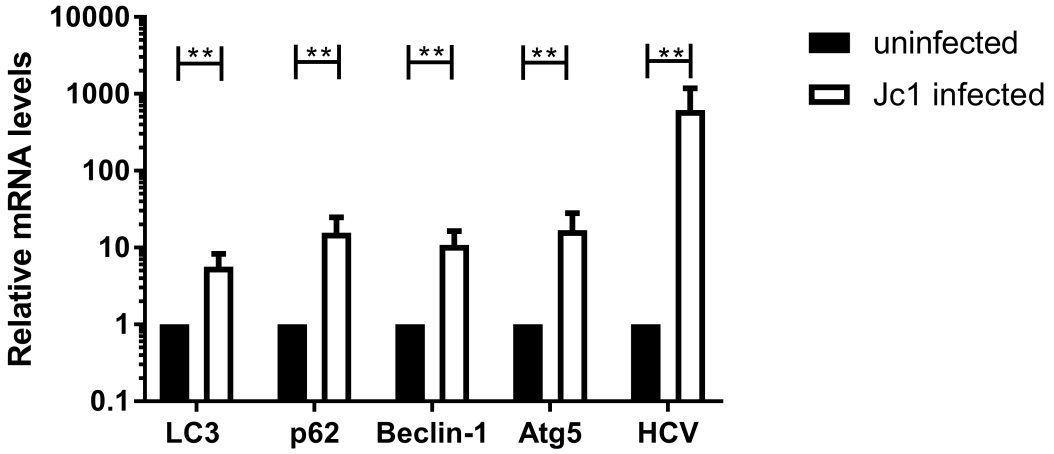

Figure 5.11: Induced expression of autophagy marker proteins in HCV-infected PHHs. qRT-PCR analysis of LC3-, p62-, Beclin-1- and Atg5- specific transcripts derived from Jc1-infected and uninfected PHHs. HCV-specific RNA was detected to monitor efficient infection. Uninfected PHHs served as control and were set as 1 (n=4, mean ± SEM). Two-tailed unpaired t-test, **p=0,0034, **p=0,0022, **p=0,0071, **p=0,0059, **p=0,0080.

Collectively, these results indicate that HCV induces autophagy. This effect is not only restricted to one cell line (Huh7.5 cells) as it could also be observed in HCV-infected PHHs. In addition, in HCV-positive cells elevated amounts of pS[349] p62 are observable in comparison to HCV-negative cells. Despite the fact that HCV-induced autophagy should result in p62 degradation, an early accumulation of p62 and an increased half-life were revealed.

5.3 ROS-induced autophagy is mediated via the phosphorylation of p62

5.3.1 Elevated levels of ROS induce autophagy and the phosphorylation of p62 at serine 349

Autophagy is a known physiological protection system to maintain cellular homeostasis (Mizushima et al., 2008). To test the hypothesis that HCV triggers autophagy via elevated ROS levels, the general potential of ROS to induce autophagy in Huh7.5 cells was studied. Therefore, Huh7.5 cells were treated with glucose oxidase, which is known to induce oxidative stress by oxidizing glucose to D-glucono-1,5-lactone and hydrogen peroxide (Beyer et al., 2008, Schaedler et al., 2010). Initially, the potential of glucose oxidase to induce oxidative stress was studied. Therefore, Huh7.5 cells were treated with different concentrations of glucose oxidase and studied by OxyBlot analysis (figure 5.12) and fluorescence microplate assay using a total ROS detection kit (figure 5.13). As positive control,

cells were treated with the oxidative stressor H_2O_2. As expected, a significant increase of oxidized proteins and relative fluorescence activity were observed indicating an induction of oxidative stress by glucose oxidase.

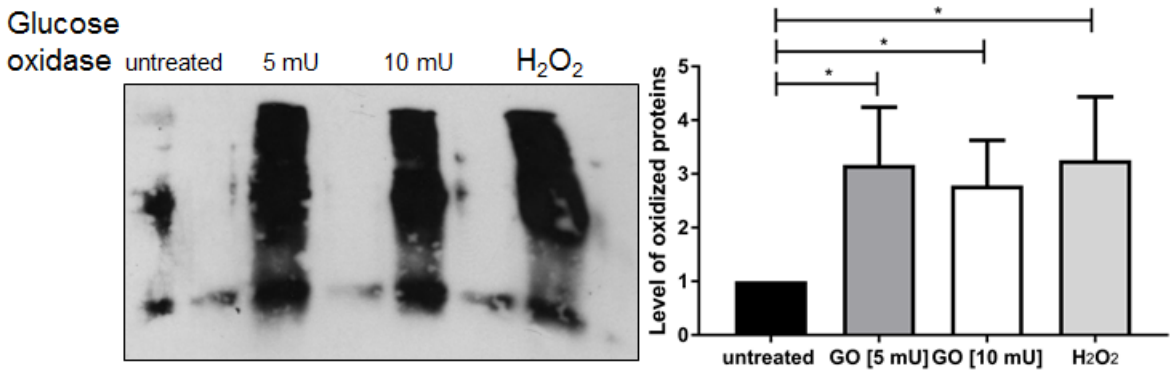

Figure 5.12: Increased levels of oxidized proteins after glucose oxidase treatment. Left, OxyBlot analysis of cellular lysates derived from Huh7.5 cells treated with 5 and 10 mU glucose oxidase (GO). Treatment with 4 mM H_2O_2 served as positive control. In lane 2, 4, 6 and 8 lysates were incubated with a derivatization control. **Right,** densitometric quantification of DNP-specific signal from three independent experiments. Untreated Huh7.5 cells served as control and were set as 1 (n=3, mean ± SEM). Two-tailed unpaired t-test, *p=0,0364, *p=0,0391*p=0,0456.

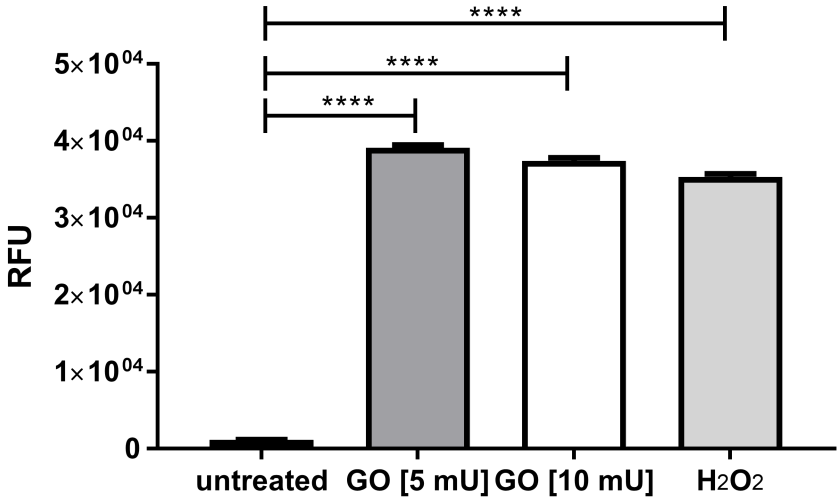

Figure 5.13: Glucose oxidase induces ROS formation. Detection of cellular ROS levels using ROS-ID™ Total ROS Detection Kit. Fluorescence intensity of Huh7.5 cells treated with 5 and 10 mU glucose oxidase (GO) was measured. Treatment with 4 mM H_2O_2 served as positive control. Untreated Huh7.5 cells served as control and were set as 1 (n=3, mean ± SEM). Two-tailed unpaired t-test, ****p<0,0001.

After treatment of Huh7.5 cells with glucose oxidase, significant higher levels of LC3-II were observed by western blot analysis which is shown in figure 5.14.

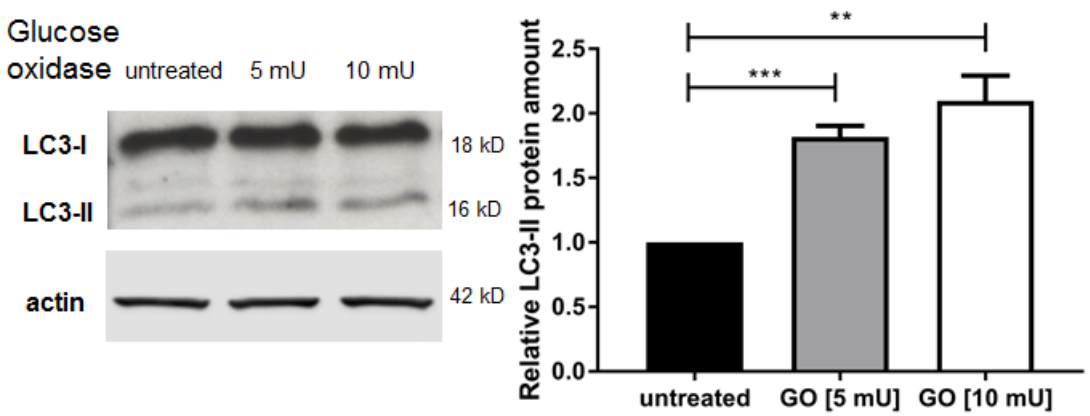

Figure 5.14: Glucose oxidase treatment induces LC3-II formation. Left, western blot analysis of cellular lysates derived from Huh7.5 cells treated with 5 and 10 mU glucose oxidase (GO). For detection, an LC3-specific antibody was used. Detection of β-actin served as loading control. **Right,** densitometric quantification of LC3-II expression from three independent experiments. Untreated Huh7.5 cells served as control and were set as 1 (n=3, mean ± SEM). Two-tailed unpaired t-test, ***p=0,0002, **p=0,0013.

Furthermore, upon glucose oxidase treatment, the amount of phosphorylated pS[349] p62 increased in a linear manner shown in the western blot in figure 5.15.

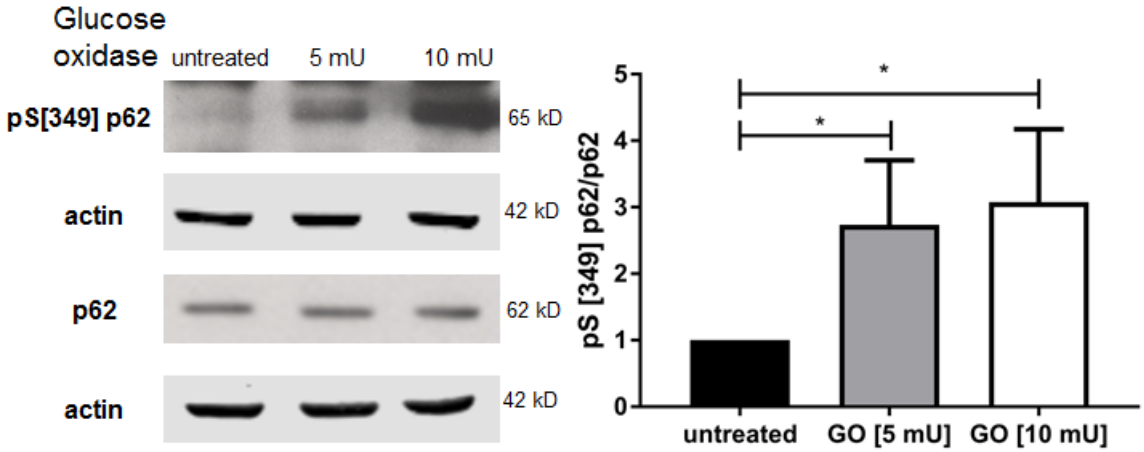

Figure 5.15: Phosphorylation of p62 is induced upon glucose oxidase treatment. Left, western blot analysis of cellular lysates derived from Huh7.5 cells treated with 5 and 10 mU glucose oxidase (GO). For detection, pS[349] p62- and p62-specific antibodies were used. Detection of β-actin served as loading control. **Right,** densitometric quantification from three independent experiments. The amount of p[349] p62 was normalized to total p62 amount. Untreated Huh7.5 cells served as control and were set as 1 (n=3, mean ± SEM). Two-tailed unpaired t-test, *p=0,0285, *p=0,0284.

5.3.2 Increased EGFP_LC3 puncta formation upon glucose oxidase treatment

LC3 is an autophagosome marker protein, which is associated with the isolation membrane and remains on the membrane until a spherical autophagosome is formed (Kabeya et al., 2000, Mizushima et al., 2001). The appearance of EGFP_LC3 puncta is indicative of the ability of ROS to induce autophagy

(Kimura et al., 2009, Kongara and Karantza, 2012). Therefore, Huh7.5 cells were transfected with an EGFP_LC3 encoding plasmid and treated with glucose oxidase to examine EGFP_LC3 puncta formation upon oxidative stress. Immunofluorescence analysis revealed significant higher numbers of EGFP_LC3B puncta per cell after glucose oxidase treatment (figure 5.16).

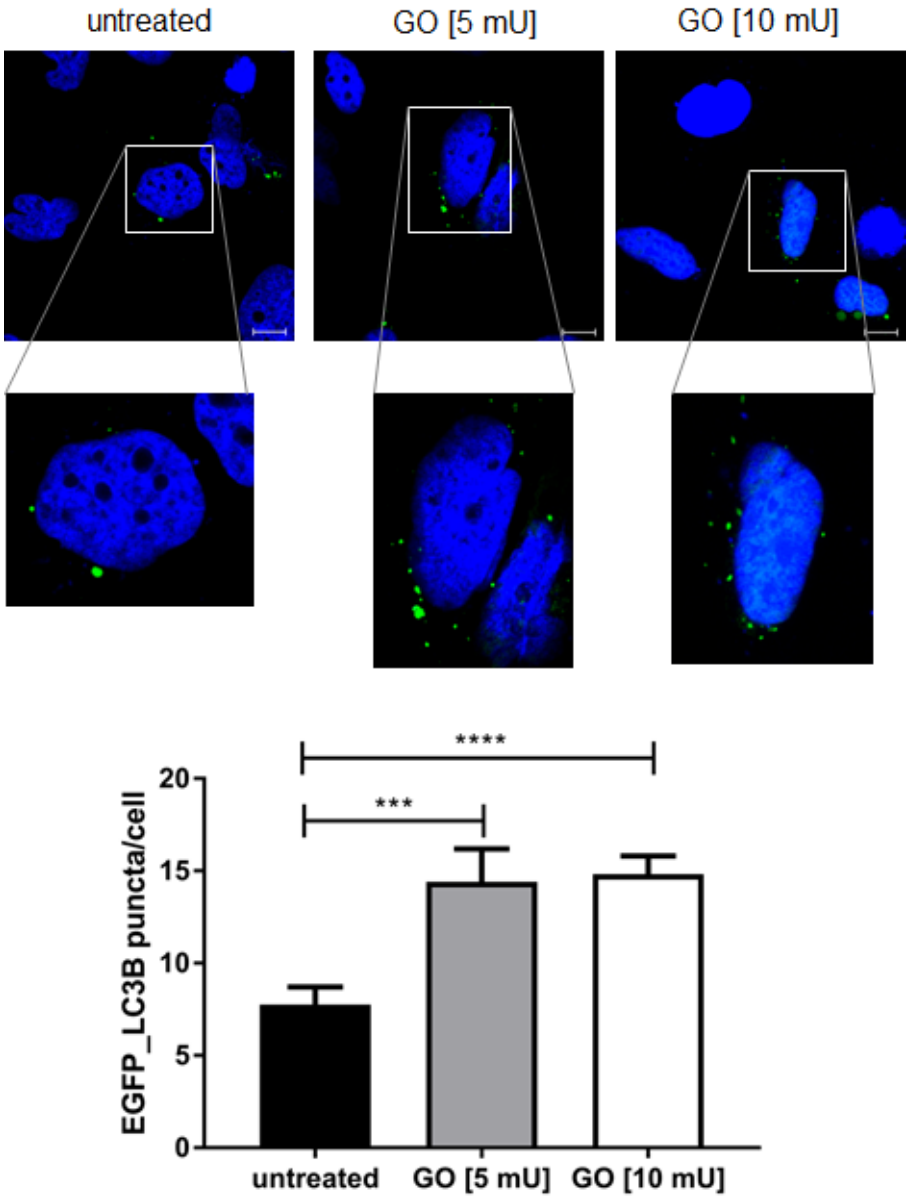

Figure 5.16: Glucose oxidase induces EGFP_LC3 puncta formation. Top, CLSM analysis of EGFP_LC3B-transfected Huh7.5 cells. 40 h after transfection, cells were treated with 5 and 10 mU glucose oxidase for 4 h to induce the formation of ROS. Magnification 100x. Scale bar represents 10 µm. **Bottom,** quantification of the number of EGFP_LC3B puncta per cell. Results represent the mean of >10 cells (mean ± SEM). Two-tailed unpaired t-test, ***p=0,0008, ****p<0,0001.

5.3.3 Phosphorylation mimicking mutant of p62 induces autophagy

HCV induces the phosphorylation of p62 at serine 349 (figure 5.9). To analyze the relevance of pS[349] p62 for induction of autophagy, Huh7.5 cells were either transfected with the FLAG-tagged mouse phosphorylation mimicking mutant p62 [S351E] (corresponding to the human 349-phosphorylated form), mouse p62 wildtype or control transfected with pUC. By western blot analysis increased amounts of LC3-II could be observed in p62 [S351E]-transfected cells, indicating an inducing effect of pS[349] p62 on autophagy (figure 5.17).

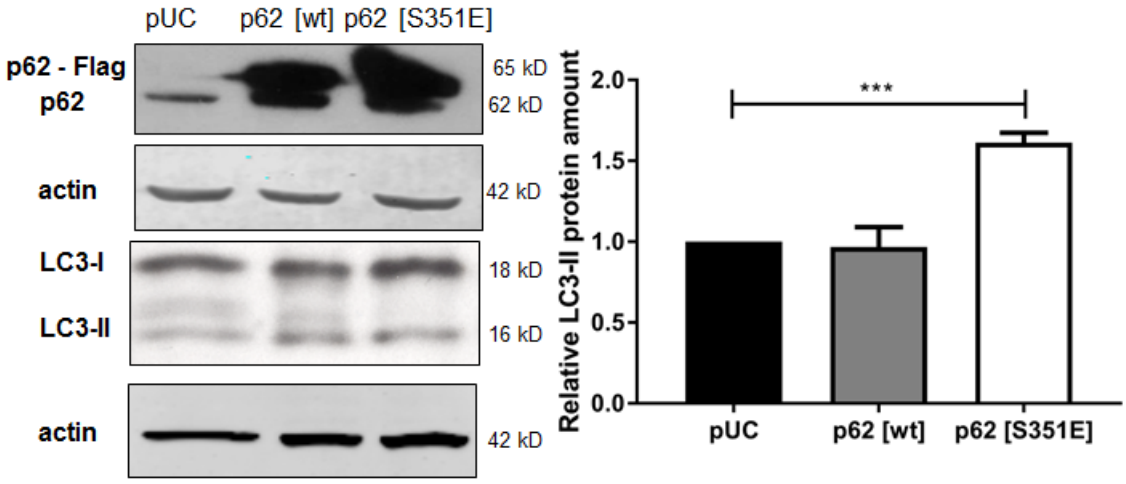

Figure 5.17: Phosphorylation mimicking mutant of p62 induces LC3-II formation. Left, western blot analysis of cellular lysates derived from Huh7.5 cells transfected with the p62 wildtype [wt], the phosphorylation mimicking mutant p62 [S351E] and pUC. For detection, p62- and LC3-specific antibodies were used. Due to the 3xFlag-tag of the exogenous p62, a double-band appears after transfection of the p62 mutants. Detection of β-actin served as loading control. **Right,** densitometric quantification of LC3-II expression from three independent experiments. pUC-transfected Huh7.5 cells served as control and were set as 1 (n=3, mean ± SEM). Two-tailed unpaired t-test, **p=0,0003.

These data reveal that by increasing cellular ROS levels, autophagy can be induced in Huh7.5 cells. Furthermore, it could be observed that by transfecting cells with an expression vector encoding a phosphorylation mimicking mutant of p62, autophagy can be induced, reflecting the ability of pS[349] p62 to induce autophagy in Huh7.5 cells.

5.4 Autophagy is necessary for the release of mature viral particles

5.4.1 Inhibition of autophagy prevents the release of infectious viral particles

To study the impact of autophagy on the viral release, HCV-positive cells were incubated with the autophagy inhibitors 3-methyladenine and bafilomycin which affect different steps in the autophagy

process. 3-methyladenine inhibits the class III phosphoinositide 3-kinase (PI3K), thereby blocking the production of phosphatidylinositol 3-phosphate (PI3P), which is necessary for the initiation of autophagy (Blommaart et al., 1997, Petiot et al., 2000). However, bafilomycin is a specific inhibitor of the vacuolar type H^+-ATPase (V-ATPase), thereby blocking the fusion of autophagosome with lysosome (Yamamoto et al., 1998). The amount of extracellular and intracellular infectious viral particles was quantified by determination of the $TCID_{50}$. An inhibitory effect on the release of infectious viral particles after incubating the cells with 3-methyladenine and bafilomycin was observed (figure 5.18 and 5.19).

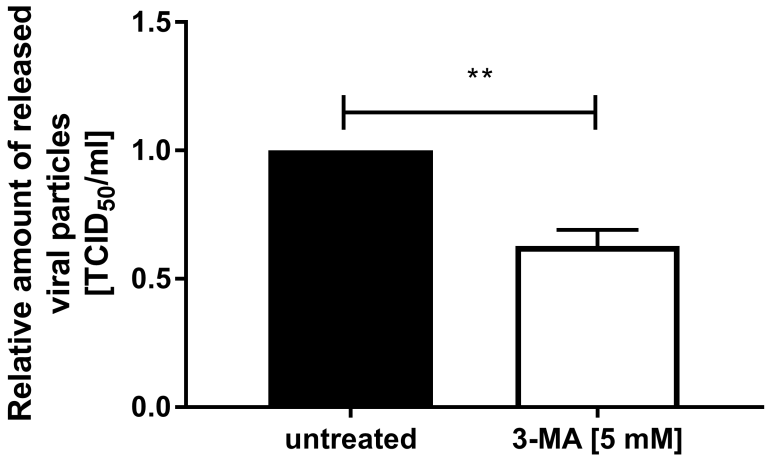

Figure 5.18: Inhibition of autophagy with 3-methyladenine prevents release of infectious viral particles. $TCID_{50}$ analysis of supernatants derived from untreated and 3-methyladenine (3-MA)-treated HCV-positive cells. $TCID_{50}$/ml from untreated supernatants served as control and was set as 1. The graph shows the relative data from three independent experiments (n=3, mean ± SEM). Two-tailed unpaired t-test, **p=0,0078.

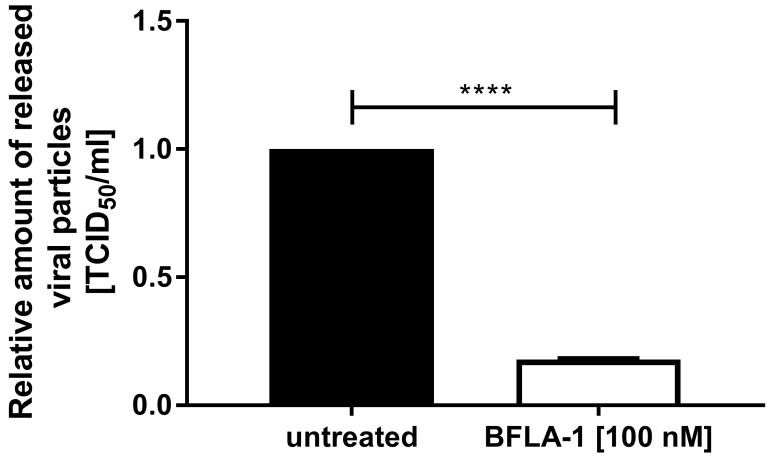

Figure 5.19: Inhibition of autophagy with bafilomycin prevents release of infectious viral particles. $TCID_{50}$ analysis of supernatants derived from untreated and bafilomycin (BFLA)-treated HCV-positive cells. $TCID_{50}$/ml from untreated supernatants served as control and was set as 1. The graph shows the relative data from three independent experiments. (n=3, mean ± SEM). Two-tailed unpaired t-test, ****p<0,0001.

5.4.2 Inhibition of autophagy at different steps has opposing effects on intracellular retained infectious viral particles

Determination of the intracellular $TCID_{50}$ showed different results for the both inhibitors. Incubation with early autophagy inhibitor 3-methyladenine results in decreased amounts of intracellular infectious viral particles (figure 5.20).

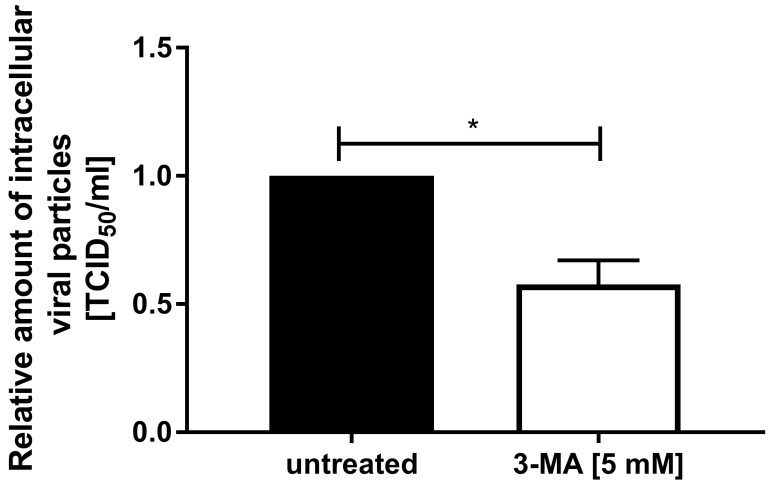

Figure 5.20: Decreased amounts of intracellular infectious viral particles after incubation with 3-methyladenin. Determination of intracellular infectious viral particles by $TCID_{50}$ of HCV-positive cells treated with 3-methyladenine (3-MA) lysed by freeze-thawing. $TCID_{50}$/ml from untreated HCV-positive cells served as control and were set as 1. The graph shows the relative data from three independent experiments (n=3, mean ± SEM). Two-tailed unpaired t-test, *p=0,0249.

However, incubation with bafilomycin is leads to an accumulation of infectious viral particles as shown in figure 5.21.

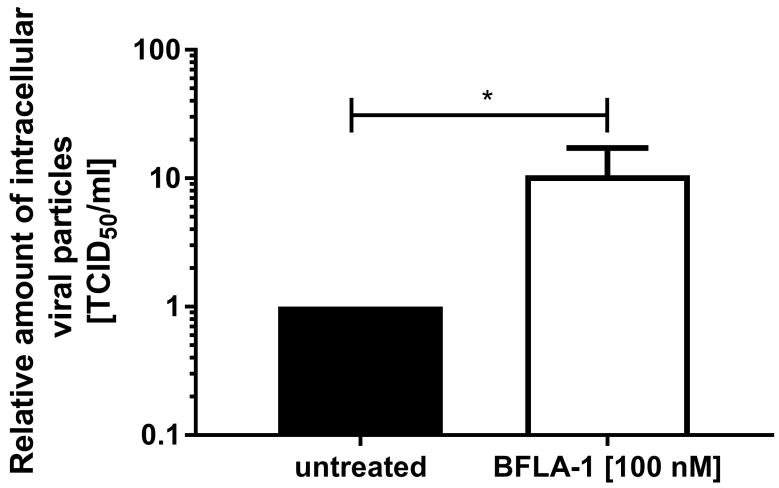

Figure 5.21: Bafilomycin treatment results in intracellular accumulation of infectious viral particles. Determination of intracellular infectious viral particles by $TCID_{50}$ of HCV-positive cells treated with bafilomycin (BFLA) lysed by freeze-thawing. $TCID_{50}$/ml from untreated HCV-positive cells served as control and was set as 1. The graph shows the relative data from three independent experiments (n=3, mean ± SEM). Two-tailed unpaired t-test, *p=0,0461.

5.4.3 Inhibition of autophagy results in intracellular core accumulation

It is supposed that during the viral life cycle only a small fraction of viral particles is released, while the major part is degraded in the autophagosomal/lysosomal department (Quinkert et al., 2005, Post et al., 2009). In line with this, western blot analysis of HCV-positive cells incubated with bafilomycin showed an intracellular accumulation of core (figure 5.22).

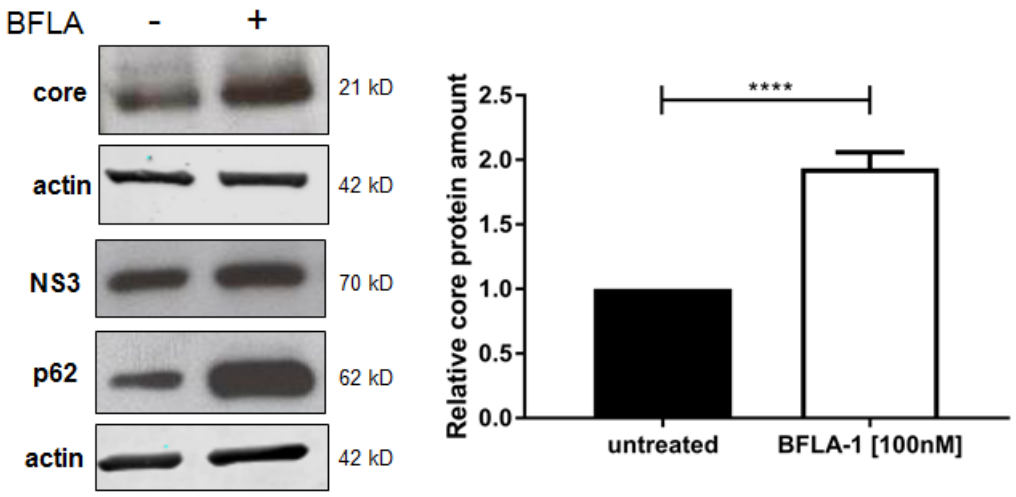

Figure 5.22: Intracellular accumulation of core after bafilomycin treatment. Left, western blot analysis of cellular lysates derived from HCV-positive cells (Jc1) treated with bafilomycin (BFLA). For detection, a core-specific antibody was used. Detection of β-actin served as loading control. **Right,** densitometric quantification of core expression from three independent experiments. Untreated HCV-positive cells served as control and were set as 1 (n=3, mean ± SEM). Two-tailed unpaired t-test, ****p<0,0001.

For immunofluorescence analysis, bafilomycin-treated cells were stained with a core-specific antibody (green) and a LC3-specific antibody (red). Effective bafilomycin-treatment is observed by accumulation of LC3, indicated by the brighter red signal in figure 5.23. Determination of the CTCF revealed a significant increase of core-specific signal after bafilomycin-treatment (figure 5.23 lower panel).

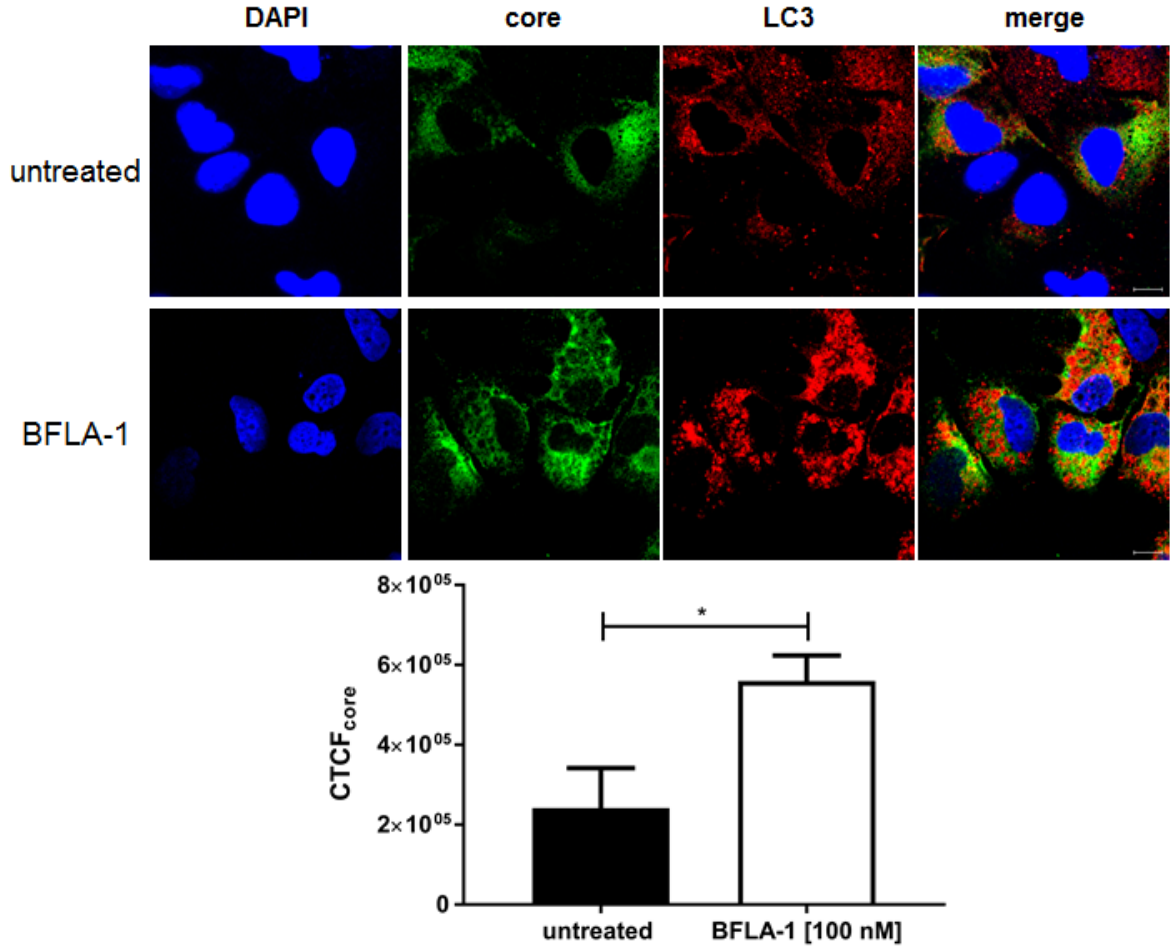

Figure 5.23: Intracellular accumulation of core after bafilomycin treatment. Top, CLSM analysis of HCV-positive cells treated with bafilomycin (BFLA). Cells were stained with a core- (green) and an LC3-specific (red) antibody. The nuclei were stained with DAPI (blue). Laser intensity and digital gain were kept constant for untreated and bafilomycin-treated HCV-positive cells. Magnification 100x. Scale bar represents 10 µm. **Bottom,** quantification of the fluorescence intensity of core by CTCF. Results represent the mean of >5 cells (mean ± SEM). Two-tailed unpaired t-test, *p=0,0137.

5.4.4 Replication is not affected by inhibition of autophagy

To examine the effect of autophagy inhibition by bafilomycin treatment on viral replication, western blot analysis detecting NS3 in HCV-positive cells was performed. Thereby, it was observed that viral replication is not affected by bafilomycin treatment, which is indicated by no significant change of NS3 protein amount (figures 5.22 and 5.24).

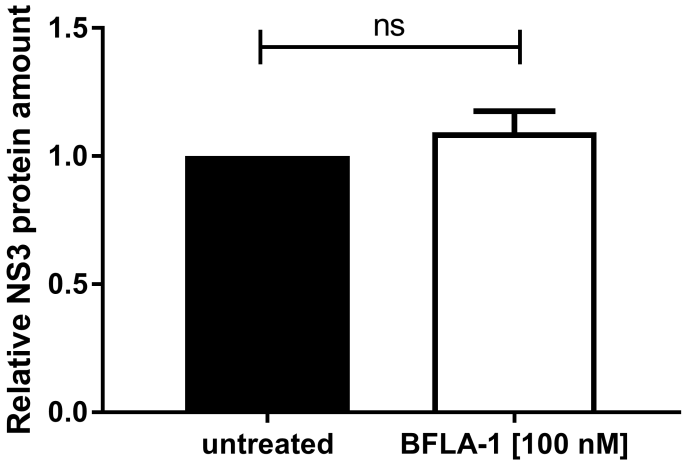

Figure 5.24: Bafilomycin has no effect on NS3 protein amount. Densitometric quantification of NS3 expression from three independent experiments. NS3 blot is shown in figure 5.22. Untreated HCV-positive cells served as control and were set as 1 (n=3, mean ± SEM). Two-tailed unpaired t-test, ns=not significant.

5.4.5 Inhibition of autophagy at different steps has opposing effects on intracellular amount of HCV genomes

To analyze the effect of autophagy inhibition on the amount of viral genomes, intracellular RNA was isolated from HCV-positive cells and analyzed by qRT-PCR. Thereby, a significant intracellular accumulation of HCV genomes after bafilomycin treatment could be observed (figure 5.25), while incubation with 3-methyladenine had no effect on the amount of intracellular viral genomes (figure 5.26).

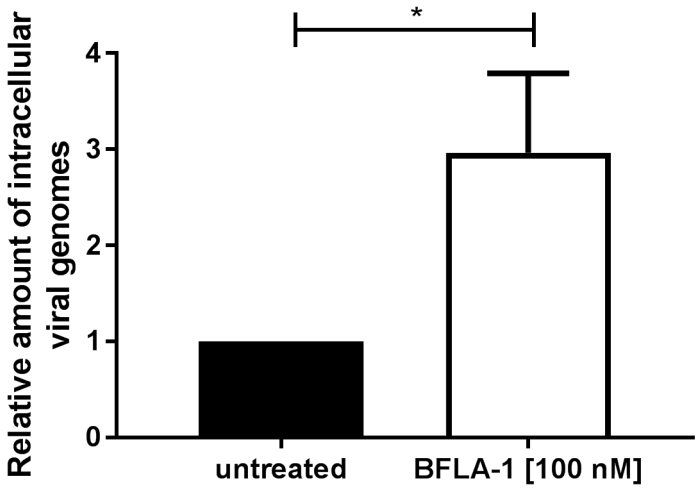

Figure 5.25: Intracellular accumulation of HCV genomes after bafilomycin treatment. qRT-PCR analysis of intracellular viral genomes derived from untreated and bafilomycin-treated HCV-positive cells. Untreated HCV-positive cells served as control and were set as 1 (n=3, mean ± SEM). Two-tailed unpaired t-test, *p=0,0480.

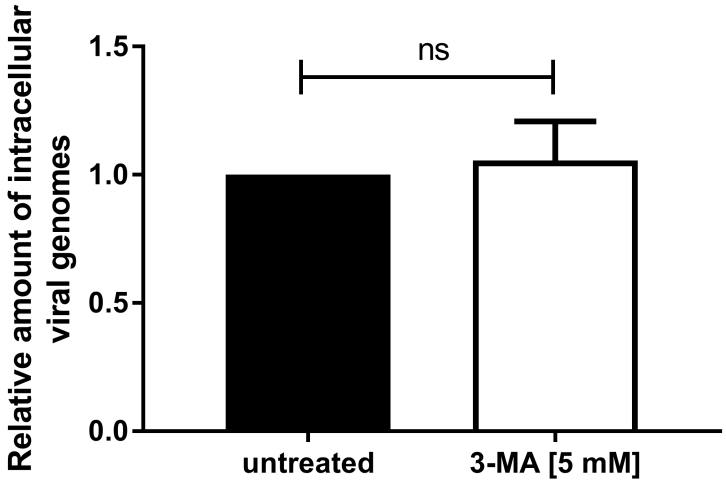

Figure 5.26: 3-Methyladenine has no effect on intracellular HCV genome amount. qRT-PCR analysis of intracellular viral genomes derived from untreated and 3-methyladenine-treated HCV-positive cells. Untreated HCV-positive cells served as control and were set as 1 (n=3, mean ± SEM). Two-tailed unpaired t-test, ns=not significant.

5.4.6 Knockdown of p62 results in intracellular HCV genome accumulation

Further evidence for the importance of autophagy for viral release was assessed by a knockdown of p62 with specific siRNA in HCV-positive cells. As depicted in figure 5.27, the knockdown of p62 results in a significant intracellular accumulation of HCV genomes. Additionally, a decrease of LC3-II was observed.

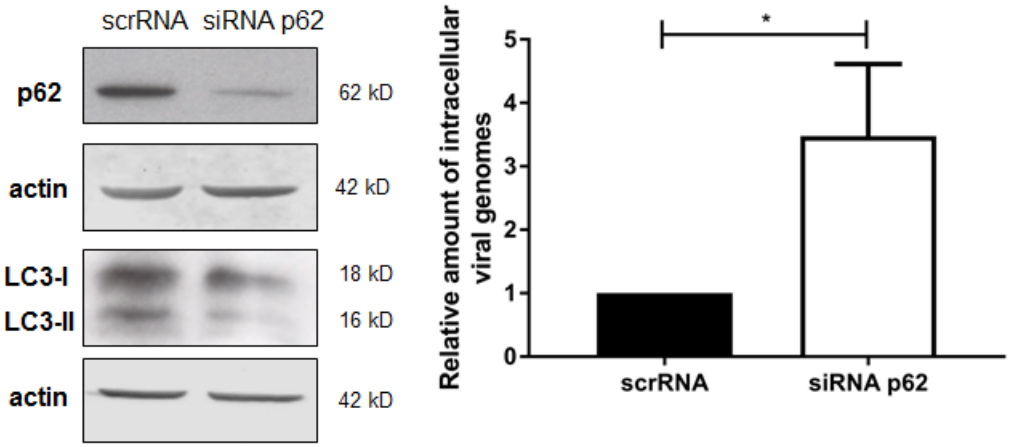

Figure 5.27: p62 knockdown results in intracellular HCV genome accumulation. Left, western blot analysis of cellular lysates derived from HCV-positive cells (Jc1) that were transfected with p62-specific siRNA (siRNA p62) or control siRNA (scrRNA). For detection, p62- and LC3-specific antibodies were used. Detection of β-actin served as loading control. **Right,** qRT-PCR analysis of intracellular viral genomes derived from HCV-positive cells (Jc1) that were transfected with p62-specific siRNA (siRNA p62) or control siRNA (scrRNA). HCV-positive cells transfected with a control siRNA (scrRNA) served as control and were set as 1 (n=4, mean ± SEM). Two-tailed unpaired t-test, *p=0,0226.

Taken together, these data indicate that inhibition of autophagy results in impaired viral particle release. Furthermore, upon inhibition of autophagy, intracellular viral particles either decrease or accumulate within the cell, depending on the step where autophagy is inhibited. In line with this, an accumulation of HCV genomes was observed after the knockdown of p62.

5.5 Scavenging of ROS impairs HCV-dependent induction of autophagy

Elevated levels of ROS can induce autophagy (Kongara and Karantza, 2012). To test the hypothesis that HCV-induced autophagy is mediated by elevated ROS levels via the phosphorylated form of p62, HCV-positive cells were treated with the ROS scavengers PDTC and NAC. Western blot analysis of cell lysates showed a significant decrease in the amount of LC3-II in PDTC- and NAC-treated HCV-positive cells (figure 5.28).

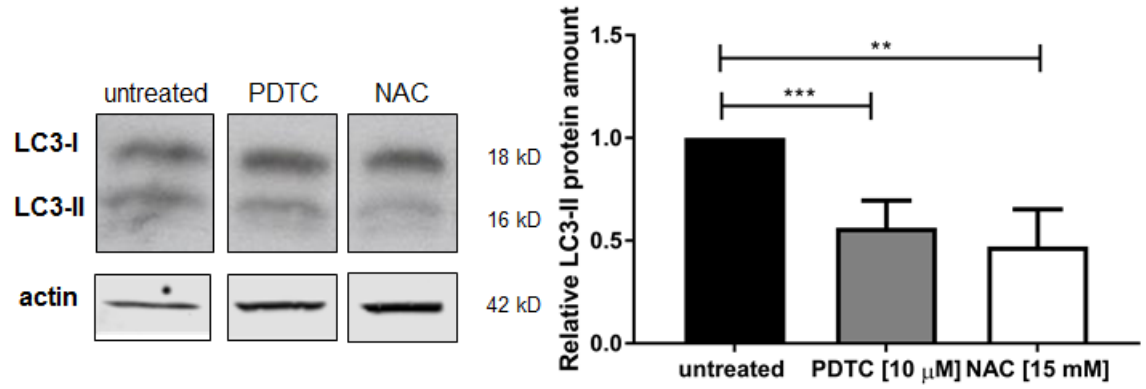

Figure 5.28: Radical scavenging results in decreased amounts of LC3-II. Left, western blot analysis of cellular lysates derived from HCV-positive cells (Jc1) treated with 10 µM PDTC and 15 NAC. For detection, an LC3-specific antibody was used. Detection of β-actin served as loading control. **Right,** densitometric quantification of LC3-II expression from three independent experiments. Untreated HCV-positive cells served as control and were set as 1 (n=3, mean ± SEM). Two-tailed unpaired t-test, ***p= 0,0005, **p=0,0024.

Furthermore, the ratio of pS[349] p62 to p62 significantly decreased in HCV-positive cells after treatment with PDTC and NAC (figure 5.29).

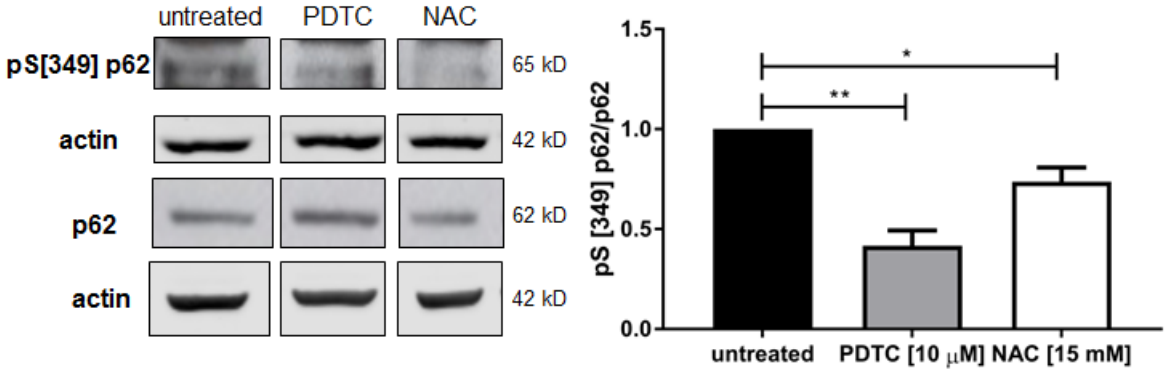

Figure 5.29: Radical scavenging inhibits phosphorylation of p62 at serine 349. Left, western blot analysis of cellular lysates derived from HCV-positive cells treated with 10 µM PDTC and 15 mM NAC using pS[349] p62- and p62-specific antibodies. Detection of β-actin served as loading control. **Right,** densitometric quantification from three independent experiments. Amount of p[349] p62 was normalized to total p62 amount. HCV-negative cells served as control and were set as 1 (n=3, mean ± SEM). Two-tailed unpaired t-test, **p=0,0032, *p=0,0254.

Similar results could be observed in immunofluorescence analysis for pS[349] p62 in HCV-positive cells (figure 5.30). While there was only a moderate effect on total p62 amount (red channel), the ratio of pS[349] p62 (green channel) to a total of p62 significantly decreased after PDTC and NAC treatment.

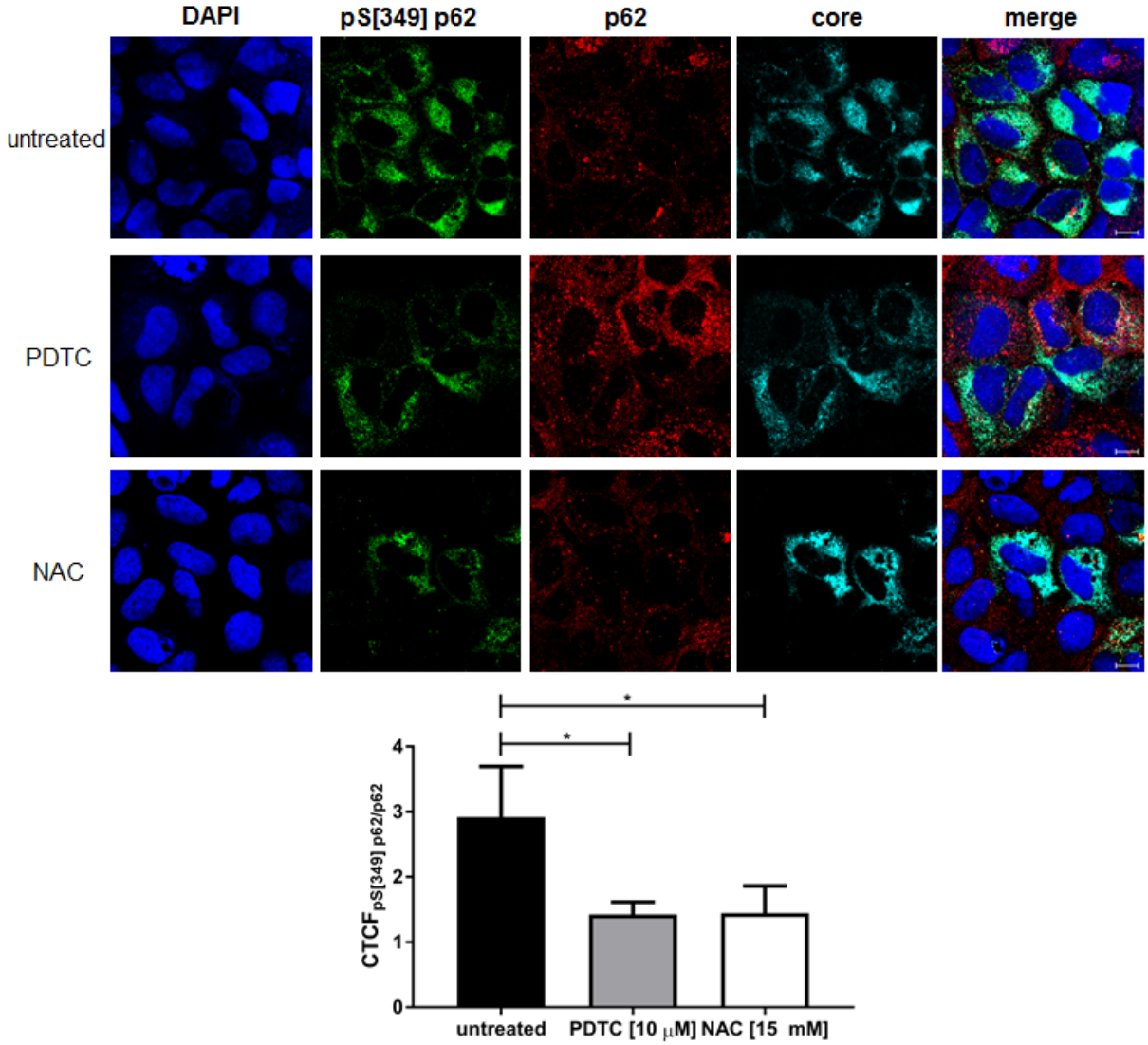

Figure 5.30: Radical scavenging inhibits phosphorylation of p62 at serine 349. Top, CLSM analysis of HCV-positive cells treated with 10 µM PDTC and 15 mM NAC. The cells were stained with pS[349] p62- (green), p62- (red) and core-specific (cyan) antibodies. The nuclei were stained with DAPI (blue). Laser intensity and digital gain were kept constant for untreated, PDTC- and NAC treated Jc1 cells. Magnification 100x. Scale bar represents 10 µm. **Bottom,** quantification of the fluorescence intensity of pS[349] p62 normalized to p62 by (CTCF). Results represent the mean of >9 cells (mean ± SEM). Two-tailed unpaired t-test, *p= 0,0440, *p=0,0410.

Isolation of total RNA revealed no significant effect of PDTC and NAC on p62 and LC3 mRNA levels (figure 5.31 and 5.32).

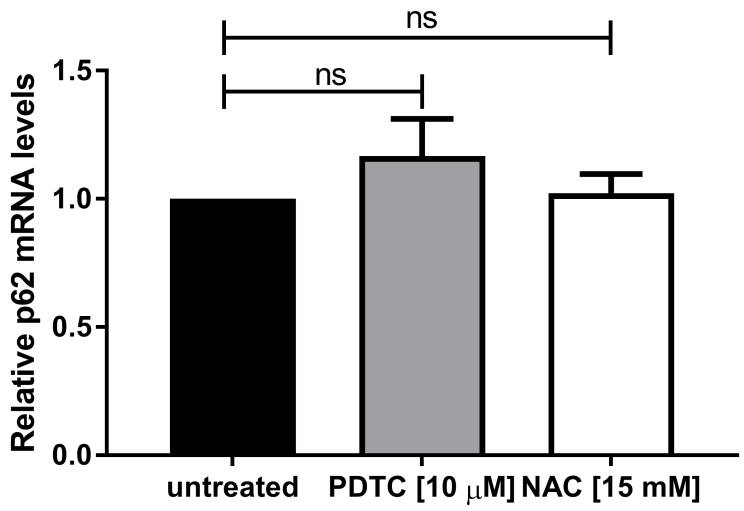

Figure 5.31: PDTC and NAV have no effect on p62 mRNA amount. qRT-PCR analysis of p62-specific transcripts derived from untreated, PDTC- and NAC-treated HCV-positive cells. Untreated HCV-positive cells served as control and were set as 1 (n=4, mean ± SEM). Two-tailed unpaired t-test, ns=not significant.

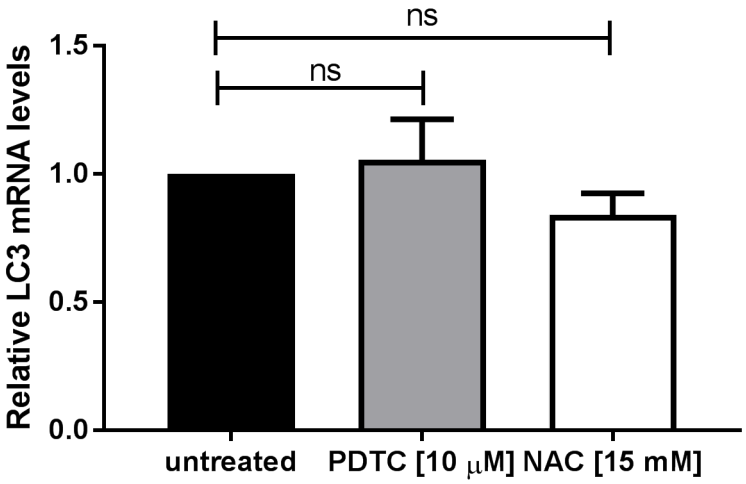

Figure 5.32: PDTC and NAC have no effect on LC3 mRNA amount. qRT-PCR analysis of LC3-specific transcripts derived from untreated, PDTC- and NAC-treated HCV-positive cells. Untreated HCV-positive cells served as control and were set as 1 (n=5, mean ± SEM). Two-tailed unpaired t-test, ns=not significant.

Taken together, these results indicate that ROS are potent inducers of autophagy as it could be observed that the presence of a radical scavengers impairs induction autophagy indicated by the decreased amount of LC3-II and diminished phosphorylation of p62 at serine 349.

5.6 Scavenging of ROS has an impact on the release of mature viral particles

As described above, autophagy plays an essential role for the release of HCV. As radical scavengers negatively affect HCV-induced autophagy by lowering the amount of pS[349] p62, the crosstalk between ROS, phosphorylation of p62, induction of autophagy and viral release was investigated. The impact of the radical scavengers PDTC and NAC on the levels of extra- and intracellular infectious viral particles was analyzed by determination of the $TCID_{50}$. Presence of PDTC and NAC caused a significant decrease of the amount of released viral particles after 16 h (figure 5.33).

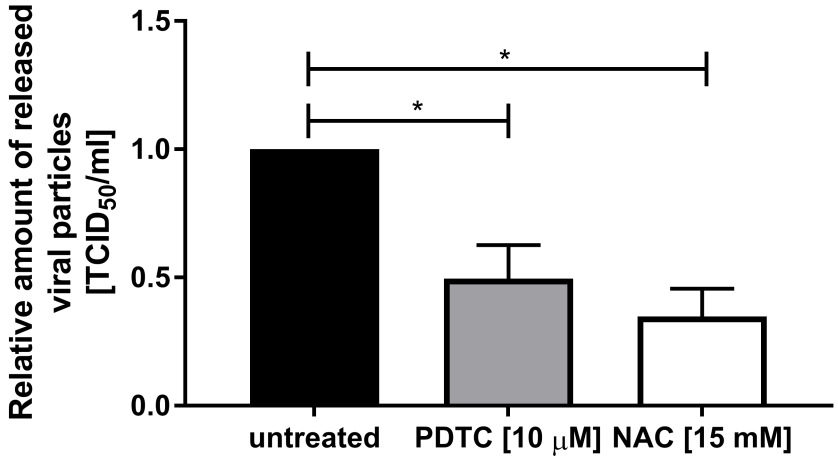

Figure 5.33: Incubation with PDTC and NAC causes a significant decline of released infectious viral particles. $TCID_{50}$ analysis of supernatants derived from untreated, PDTC- and NAC-treated HCV-positive cells. Cells were treated for 16 h with 10 µM PDTC or 15 mM NAC. $TCID_{50}$/ml from untreated supernatants served as control and was set as 1. The graph shows the relative data from three independent experiments (n=3, mean ± SEM). Two-tailed unpaired t-test, *p= 0,0393, *p=0,0161.

Determination of intracellular $TCID_{50}$ revealed no significant effect on the amount of intracellular viral particles after PDTC and NAC treatment (figure 5.34).

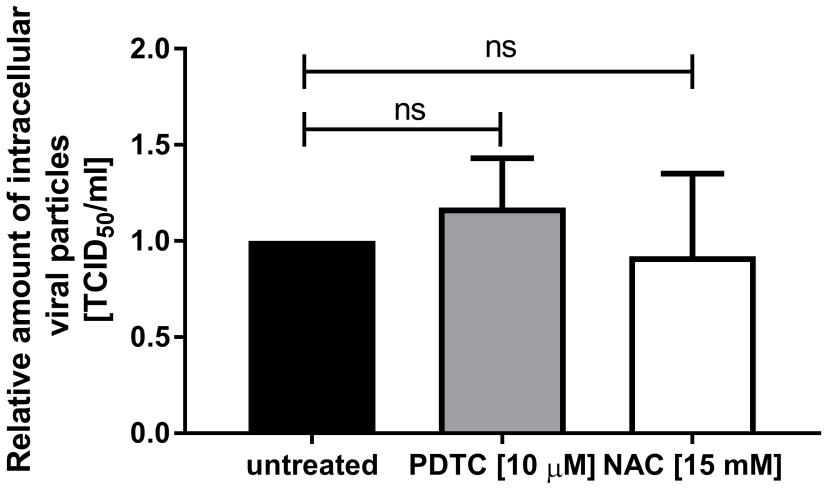

Figure 5.34: PDTC and NAC have no effect on the amount of intracellular infectious viral particles. Determination of intracellular infectious viral particles by $TCID_{50}$ of HCV-positive cells treated with PDTC and NAC lysed by freeze-thawing. $TCID_{50}$/ml from untreated HCV-positive cells served as control and were set as 1. The graph shows the relative data from five independent experiments (n=5, mean ± SEM). Two-tailed unpaired t-test, ns=not significant.

5.6.1 Viral replication is not affected by scavenging of ROS

To examine the effect of radical scavenging on viral replication, a luciferase reporter gene assay was performed by electroporating Huh7.5 cells with a bicistronic reporter construct harboring a luciferase in front of the full length genome (pFK-Luc-Jc1). Thereby, no significant effect was observed in the presence of PDTC and NAC (figure 5.35).

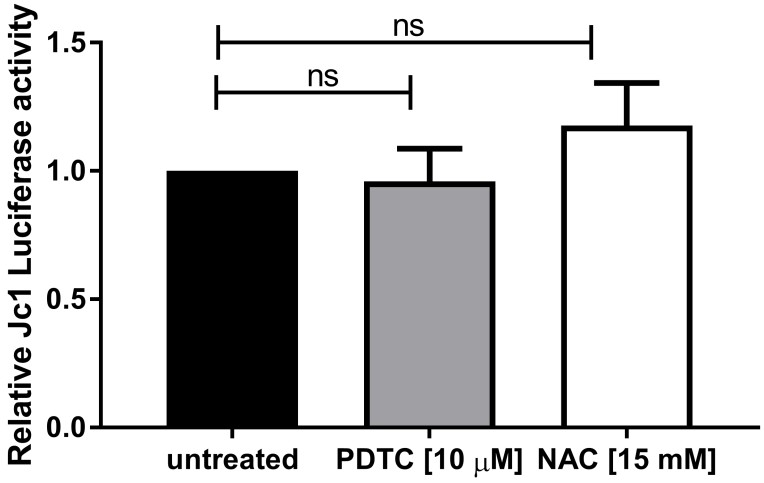

Figure 5.35: Presence of PDTC and NAC has no effect on viral replication. Huh7.5 cells were electroporated with the pFK-Luc-Jc1 construct and treated with 10 µM PDTC and 15 mM NAC. Viral replication was determined by luciferase reporter gene assay. The graph shows the relative data from six independent experiments (n=6, mean ± SEM). Two-tailed unpaired t-test, ns=not significant.

In line with this, determination of the intracellular amount of viral genomes by qRT-PCR revealed no significant influence of PDTC and NAC on the amount of viral RNA (figure 5.36).

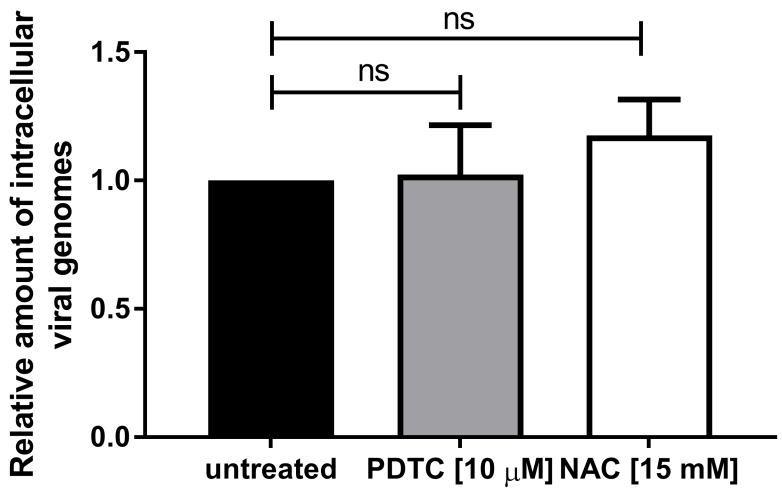

Figure 5.36: Presence of PDTC and NAC has no effect on the amount of intracellular viral RNA. qRT-PCR analysis of intracellular viral genomes derived from untreated, PDTC- and NAC-treated HCV-positive cells. Untreated HCV-positive cells served as control and were set as 1 (n=, mean ± SEM). Two-tailed unpaired t-test, ns=not significant.

These findings could be further verified by western blot analysis of NS3 that revealed no change in the amount of NS3 upon PDTC and NAC treatment (figure 5.37).

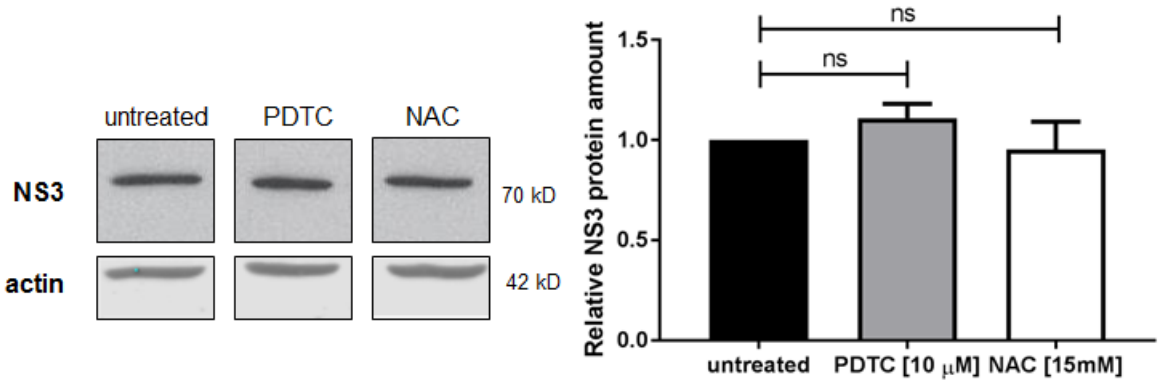

Figure 5.37: Presence of PDTC and NAC has no effect on NS3 protein amount. Left, western blot analysis of cellular lysates derived from HCV-positive cells treated with 10 µM PDTC and 15 mM NAC. For detection, an NS3-specific antibody was used. Detection of β-actin served as loading control. **Right,** densitometric quantification of expression from three independent experiments. Untreated HCV-positive cells served as control and were set as 1 (n=3, mean ± SEM). Two-tailed unpaired t-test, ns=not significant.

Taken together, these data describe a crosstalk between HCV-dependent elevation of ROS-levels, elevated phosphorylation of p62, induction of autophagy and release of viral particles. If this crosstalk

is disturbed by the treatment with radical scavengers, the ratio pS[349] p62 to p62 is decreased and hence the induction of autophagy and release of viral particles is impaired. These findings reveal that HCV-induced oxidative stress is a potent inducer of autophagy, which consequently is essential for viral release.

5.7 HCV exerts a negative effect on Nrf2/ARE-dependent gene expression

5.7.1 Decreased expression of cytoprotective genes in HCV-positive cells

The Nrf2/ARE system plays a central role in counteracting elevated levels of ROS (Osburn et al., 2006). This would result in a breakdown of the previously described crosstalk in HCV-positive cells between ROS, activation of autophagy and the release of infectious viral particles. As described before, HCV interferes with Nrf2/ARE signaling (Carvajal-Yepes et al., 2011). To investigate the influence of HCV on endogenous Nrf2, HCV-positive and HCV-negative cells were transfected with an Nrf2-dependent luciferase reporter construct monitoring Nrf2-activation (OKD48 construct) (figure 5.38). Thereby, a negative effect of HCV on Nrf2 activation was observed indicated by a significant reduced luciferase activity in HCV-positive cells compared to the control cells.

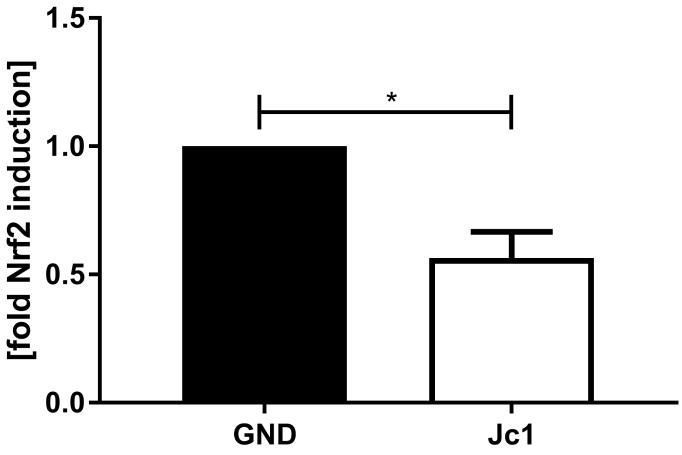

Figure 5.38: Impaired Nrf2 activation in HCV-positive cells. Luciferase activity assay of HCV-positive (Jc1) and HCV-negative (GND) cells transfected with the OKD48 construct. Nrf2 induction was determined by luciferase reporter gene assay. The graph shows the relative data from 3 independent experiments (n=3, mean ± SEM). Two-tailed unpaired t-test, *p=0,0332.

Furthermore, HCV-positive and HCV-negative cells were transfected with a luciferase reporter construct harboring the NQO1- or GCLc-promoter (figure 5.39). Thereby, significant lower expression of the

luciferase reporter gene was observed in HCV-positive cells compared to the HCV-negative control cells.

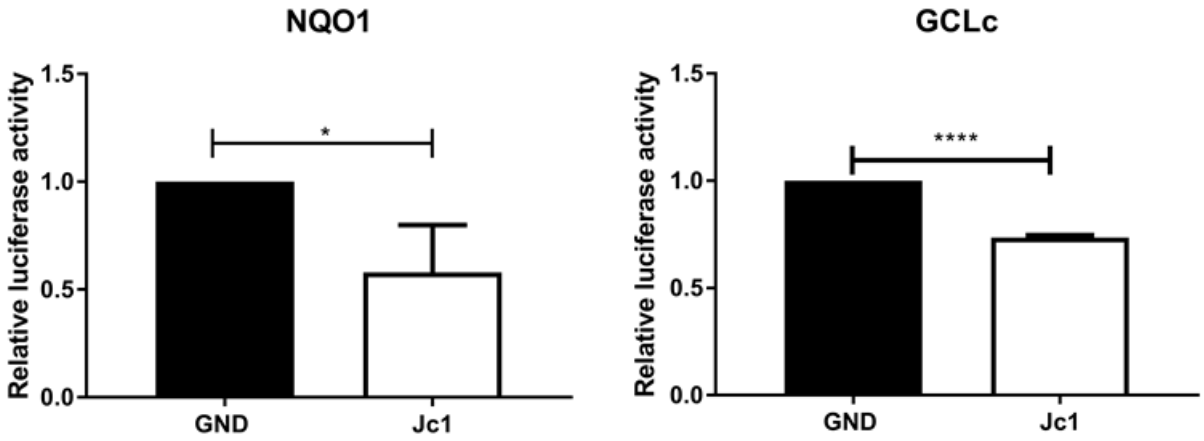

Figure 5.39: Impaired expression of NQO1 and GCLc in HCV-positive cells. Left, luciferase activity assay of HCV-positive (Jc1) and HCV-negative (GND) cells transfected with a NQO1_luciferase construct monitoring NQO1 expression. **Right,** luciferase activity assay of HCV-positive (Jc1) and HCV-negative (GND) cells transfected with a GCLc_luciferase construct monitoring GCLc expression. The graph shows the relative data from 3 independent experiments (n=3, mean ± SEM). Two-tailed unpaired t-test, significant, *p=0,0445, ****p<0,0001.

5.7.2 Despite stress conditions, Nrf2/ARE signaling is not activated in HCV-positive cells

To study Nrf2/ARE-dependent gene expression under stress conditions, HCV-positive and HCV-negative cells were incubated with tBHQ and analyzed by different assays. Rising levels of electrophiles and ROS activate Nrf2 which subsequently induces the expression of cytoprotective enzymes like NQO1, GCLc and GCSc. As expected, luciferase reporter assays revealed that the activation of NQO1 and GCLc is impaired in HCV-positive after tBHQ treatment (figure 5.40).

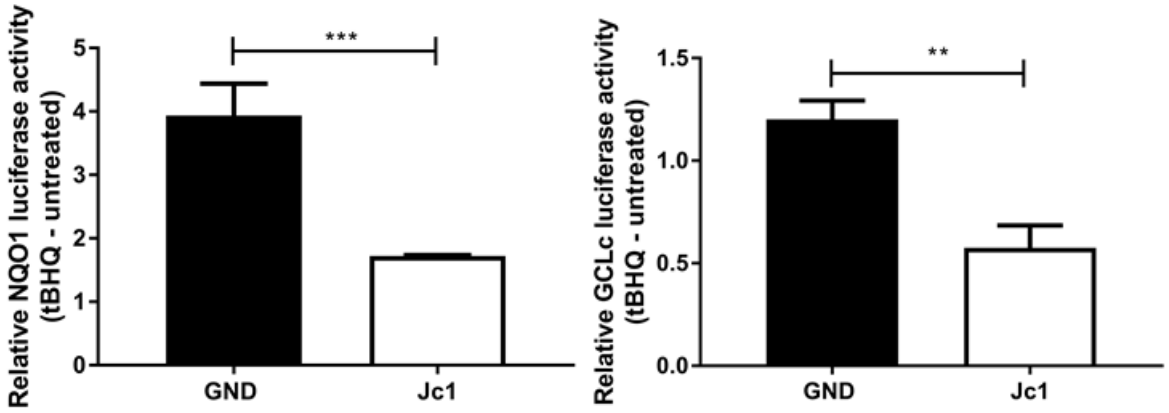

Figure 5.40: HCV impairs Nrf2-dependent gene expression under stress conditions. Right, luciferase activity assay of HCV-positive (Jc1) and HCV-negative (GND) cells transfected with a NQO1_luciferase construct and treated with 50 mM tBHQ. **Left,** luciferase activity assay of HCV-positive (Jc1) and HCV-negative (GND) cells transfected with a GCLc_luciferase construct and treated with 50 mM tBHQ. The difference between tBHQ treated and untreated cells was calculated. The graph shows the relative data from 4 independent experiments (n=4, mean ± SEM). Two-tailed unpaired t-test, significant, ***p=0,0006, **p=0,0097.

Similar results were obtained by qRT-PCR analysis (figure 5.41) and western blot (figure 5.42).

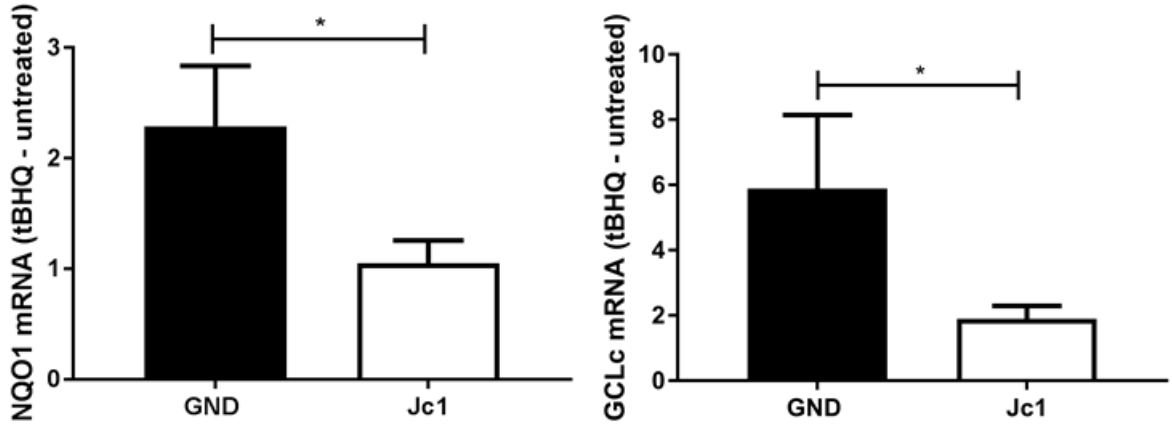

Figure 5.41: HCV impairs activation of Nrf2-dependent genes under stress conditions. Left, qRT-PCR analysis of NQO1-specific transcripts derived from HCV-positive and HCV-negative cells. **Right,** qRT-PCR analysis of GCLc-specific transcripts derived from HCV-positive and HCV-negative cells. The difference between tBHQ treated and untreated cells was calculated (n=6, mean ± SEM). Two-tailed unpaired t-test, *p=0,0242, *p=0,0436.

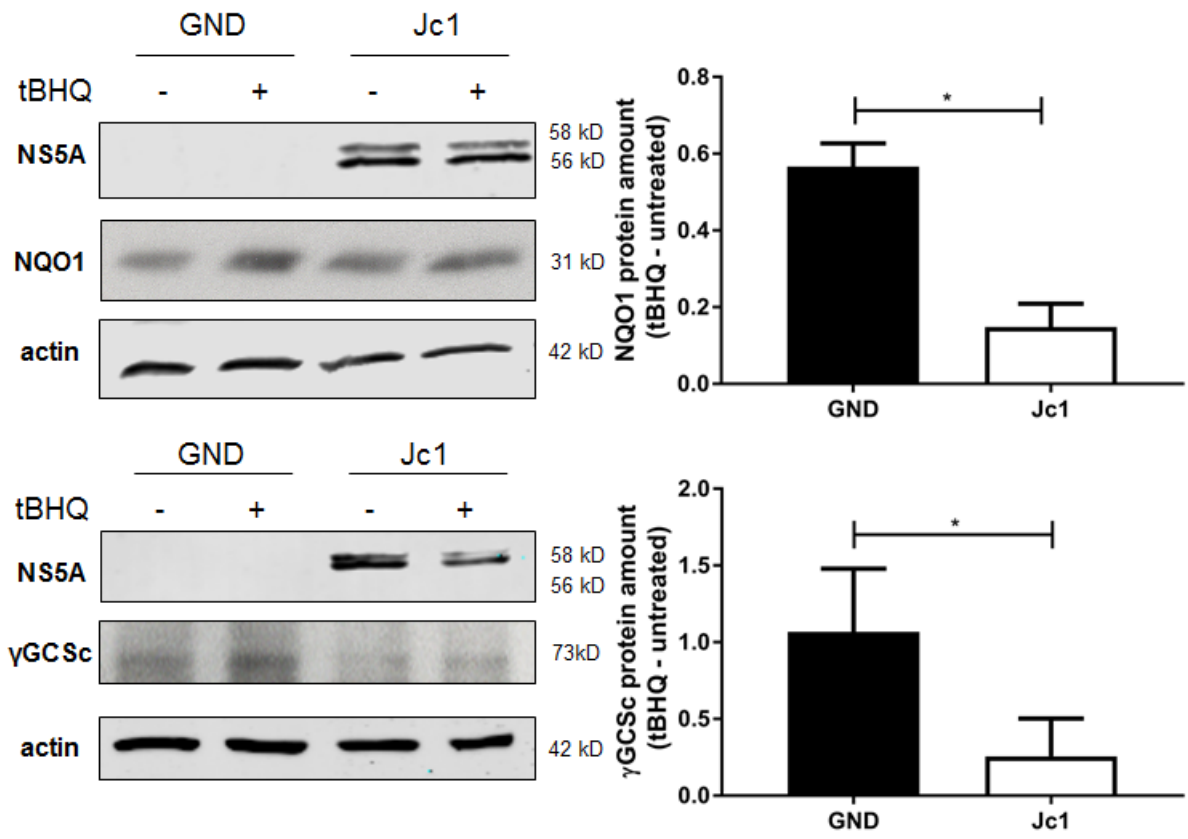

Figure 5.42: Expression of Nrf2-activated proteins is impaired in HCV-positive cells under stress conditions. Top left, western blot analysis of cellular lysates derived from HCV-positive and HCV-negative cells using NQO1- and NS5A-specific antibodies. Detection of β-actin served as loading control. **Top right,** densitometric quantification from three independent experiments. The difference between tBHQ treated and untreated cells was calculated (n=3, mean ± SEM). Two-tailed unpaired t-test, *p=0,0369. **Bottom left,** western blot analysis of cellular lysates derived from HCV-positive and HCV-negative cells using GCSc- and NS5A-specific antibodies. Detection of β-actin served as loading control. **Bottom right,** densitometric quantification from three independent experiments. The difference between tBHQ treated and untreated cells was calculated (n=3, mean ± SEM). Two-tailed unpaired t-test, *p=0,0368.

Taken together, these findings indicate that HCV impairs Nrf2/ARE signaling as it decreases the expression of cytoprotective genes under basal as well as stress conditions and thereby preserves elevated levels of ROS.

5.8 HCV-impaired Nrf2/ARE signaling prevents pS[349] p62-dependently released Nrf2 from entering the nucleus, contributing to an impaired elimination of ROS

Elevated ROS levels can be detoxified by induction of the Nrf2/ARE system (Kensler et al., 2007). As a result, this system would lead to a collapse of the above described crosstalk. However, HCV impairs the activation of Nrf2/ARE-dependent cytoprotective genes by a so far unprecedented mechanism. HCV interferes with the Nrf2/ARE signaling by core-dependent translocation of sMafs from the nucleus to the replication complex on the cytoplasmic face of the ER (Carvajal-Yepes et al., 2011). Thereby, free Nrf2 is trapped in the cytoplasm, leading to an impaired expression of Nrf2/ARE-dependent cytoprotective genes. Based on this, it was hypothesized that in HCV-positive cells this intricate mechanism prevents the pS[349] p62-dependently released Nrf2 from translocation into the nucleus. This in turn leads to impaired expression of Nrf2/ARE-dependent genes and detoxification of ROS. To experimentally evaluate this hypothesis, HCV-positive cells and HCV-negative control cells were cotransfected with either p62 wildtype (p62 [wt]), the phosphorylation mimicking mutant p62 [S351E] or pUC in combination with the OKD48 construct. It was shown that the constitutive active mutant p62 [S351E] activates Nrf2 by binding to Keap1. This binding outcompetes the interaction with Nrf2, resulting in the release of Nrf2 from the complex with Keap1 (Ichimura et al., 2013). While in HCV-negative cells transfection of the p62 [S351E] mutant significantly activates Nrf2 as compared to the wildtype p62, in HCV-positive cells the activation of the Nrf2/ARE-dependent reporter gene by overexpression of the constitutive active mutant p62 [S351E] is impaired (figure 5.43).These results indicate that pS[349] p62-mediated activation of Nrf2 is counteracted in HCV-positive cells due to the trapping of Nrf2 on the ER surface at the replicon complexes (Carvajal-Yepes et al., 2011).

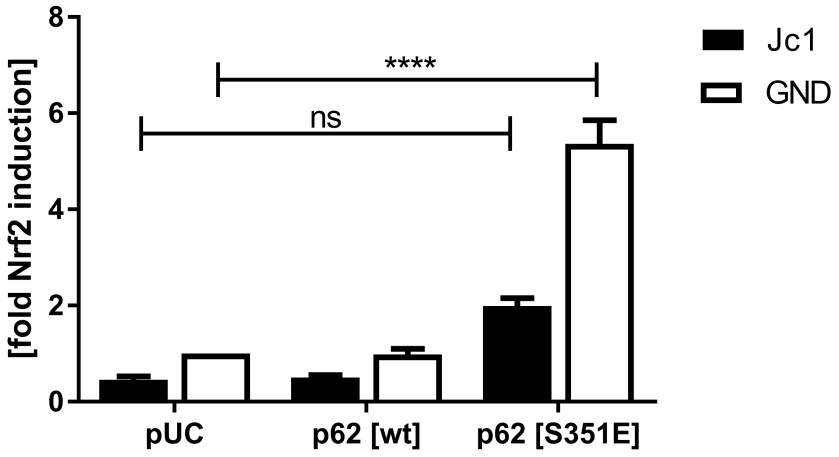

Figure 5.43: p62 [S351E] does not induce Nrf2/ARE signaling in HCV-positive cells. Luciferase activity assay of HCV-positive (black bars) and HCV-negative (white bars) cells cotransfected with the OKD48 construct and p62 wildtype (p62 [wt]), the phosphorylation mimicking mutant (p62 [S351E]) or pUC. Nrf2 induction was determined by luciferase reporter gene assay. The graph shows the relative data from six independent experiments (n=6, mean ± SEM). Two-tailed unpaired t-test, ns=not significant, ****p<0,0001.

To confirm the specificity of the observed effect, a HCV core-deficient construct (dCore) was used. It was found that the trapping of Nrf2 at the replicon complex and the resulting inhibitory effect of HCV on the Nrf2/ARE signaling is core-dependent (Carvajal-Yepes et al., 2011). Therefore, the Nrf2/ARE-dependent gene expression was analyzed upon transfection of the phosphorylation mimicking mutant p62 [S351E] in dCore-expressing cells. Here, in dCore-expressing cells, an activation of the Nrf2/ARE-dependent gene expression comparable to the corresponding HCV-negative control cells could be observed (figure 5.44). This confirms the specificity of the observed effect and indicates that the inhibitory effect of HCV on the pS[349] p62-dependently released Nrf2 depends on the capacity of core to trigger the sequestration of Nrf2 to the replication complex on the cytoplasmic face of the ER.

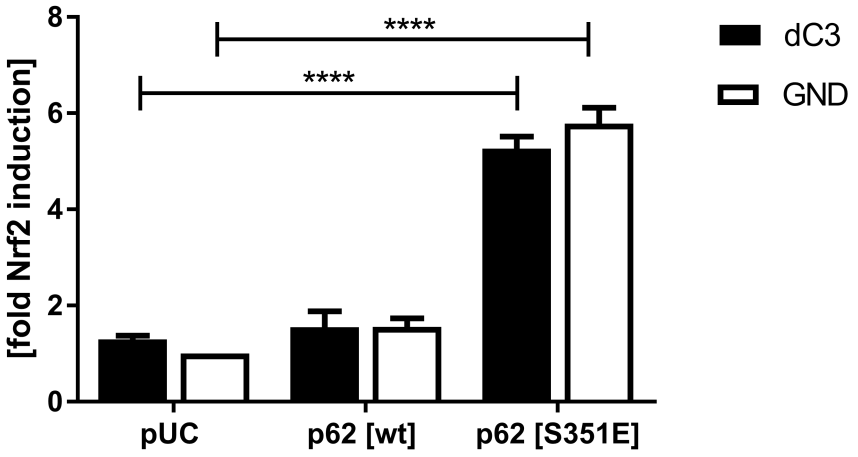

Figure 5.44: Deficiency of core increases Nrf2 activity. Luciferase activity assay in cells replicating the HCV core (dCore)-deficient genome (black bars) and HCV-negative (white bars) cells contransfected with the OKD48 construct and p62 wildtype (p62 [wt]), the phosphorylation mimicking mutant (p62 [S351E]) or pUC. Nrf2 induction was determined by luciferase reporter gene assay. The graph shows the relative data from six independent experiments (n=6, mean ± SEM). Two-tailed unpaired t-test, ****p<0,0001, ****p<0,0001.

In accordance with this, western blot analysis of cells expressing the dCore mutant exhibit an impaired phosphorylation of p62 compared to HCV-positive cells (figure 5.45).

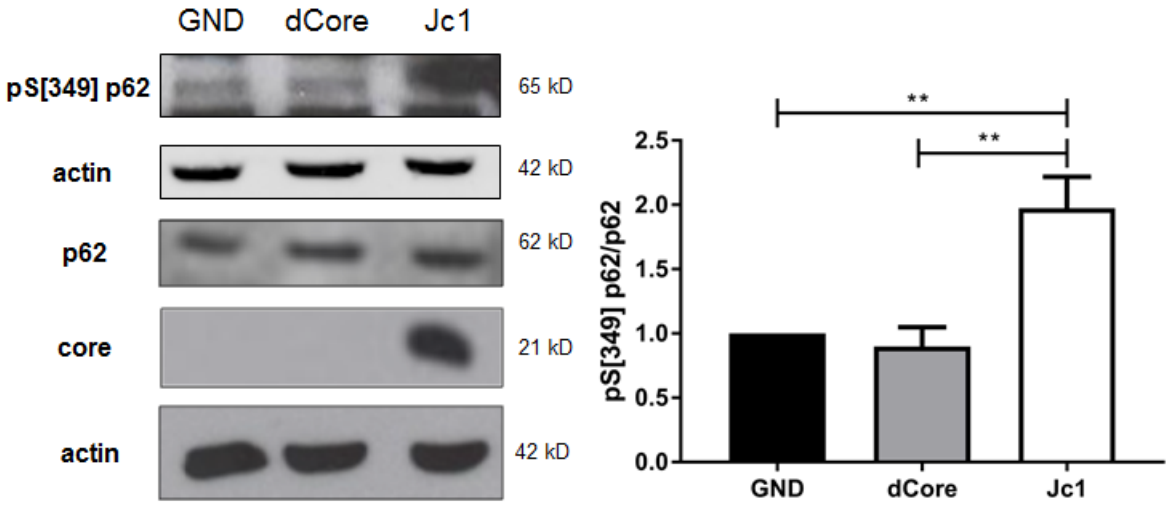

Figure 5.45: Impaired phosphorylation of p62 in cells expressing the dCore mutant. Left, western blot analysis of cellular lysates derived from HCV-positive cells, cells replicating the HCV core (dCore)-deficient genome and HCV-negative cells using pS[349] p62-, p62- and core-specific antibodies. Detection of β-actin served as loading control. **Right,** densitometric quantification from four independent experiments. Amount of p[349] p62 was normalized to total p62 amount. HCV-negative cells served as control and were set as 1 (n=4, mean ± SEM). Two-tailed unpaired t-test, **p=0,0098, **p=0,0012.

In line with this, analysis of total RNA revealed that in dCore-expressing cells no activation of p62 on mRNA levels occurs (figure 5.46).

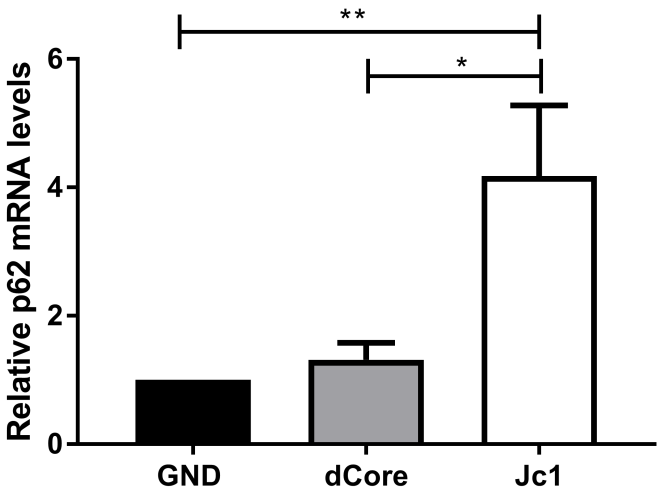

Figure 5.46: dCore-expressing cells exhibit an impaired activation of p62 on mRNA levels. qRT-PCR analysis of p62-specific transcripts derived from HCV-positive cells, cells replicating the HCV core (dCore)-deficient genome and HCV-negative cells. HCV-negative cells served as control and were set as 1 (n=, mean ± SEM). Two-tailed unpaired t-test, **p=0,0019, *p=0,0304.

Taken together, these findings indicate that due to the impaired Nrf2/ARE signaling in HCV-positive the pS[349] p62-dependently released Nrf2 is inhibited from entering the nucleus. This ensures that in HCV-positive cells elevated ROS levels are preserved which can induce autophagy that is required for the release of HCV particles.

6 Discussion

6.1 HCV-induced oxidative stress

HCV-induced oxidative stress plays a central role in the progression and appearance of different pathologies associated with viral infection, such as impaired liver regeneration and the development of fibrosis, cirrhosis and HCC (Bartosch et al., 2009). Therefore, in HCV-positive cells elevated levels of ROS could be observed (figure 5.1). In addition, OxyBlot analysis revealed that higher amounts of oxidized proteins are present in HCV-positive cells (figure 5.2). Previous studies have shown that HCV impairs the Nrf2/ARE signaling by trapping Nrf2 in the cytoplasm (Carvajal-Yepes et al., 2011). Hence, Nrf2 is not able to translocate to the nucleus and the induction of cytoprotective genes is impaired. As detoxifying enzymes are not expressed, this mechanism contributes to the maintenance of elevated ROS levels in HCV-positive cells.

6.2 Impact of HCV on the autophagic machinery

It is well established that HCV interferes with the autophagic machinery to benefit its own life cycle (Ke and Chen, 2011a). In line with this, HCV-positive cells revealed an accumulation of LC3-II in western blot analysis and a total increase of LC3 staining in immunofluorescence analysis (figure 5.3 and 5.4). These observations imply an induction of autophagy in HCV-positive cells, as LC3 is converted from the cytosolic LC3-I to the autophagosome-bound LC3-II during autophagosome formation (Jiang and Mizushima, 2015). Several studies confirmed the occurrence of increased numbers of autophagy vesicles in HCV-positive cells (Dreux et al., 2009, Tanida et al., 2009, Guevin et al., 2010, Ke and Chen, 2011a). In addition, these findings were confirmed in PHHs where an induction of autophagy could be revealed by enhanced expression of autophagy marker proteins, such as Beclin-1 and Atg5, after HCV infection (figure 5.11). In case of p62, a decrease of the protein amount would be expected upon induction of autophagy, as p62 is degraded during the autophagic process (Katsuragi et al., 2015). But the opposite was observed. In western blot and immunofluorescence analyses, increased levels of p62 were detected in HCV-positive cells (figures 5.5

and 5.6). Studying the kinetics of p62 within 102 h after electroporation, already at early time points (18 hpe) an accumulation of p62 was observed (figure 5.7). At the first glance, these findings seem to be conflicting. However, due to the fact that the expression of the catalytic active subunits of the proteasome (PSMB5) is Nrf2-dependent and Nrf2 activation is impaired in HCV-positive cells, the activity of the constitutive proteasome is decreased (Kwak and Kensler, 2006, Carvajal-Yepes et al., 2011). In line with this, analysis of the half-life of p62 revealed that in HCV-positive cells a prolonged half-life could be observed compared to HCV-negative cells as its proteasomal degradation is impaired (figure 5.8). The overlap of these opposite effects in combination could result in elevated amounts of p62 in HCV-positive cells. Similar results were observed by Sir et al. (Sir et al., 2008). Using biochemical assays, they demonstrated that HCV induces the accumulation of autophagosomes without enhancing the autophagic protein degradation. In contrast, Ke and Chen verified that both autophagosome maturation and autolysosome formation takes place in HCV-infected cells (Ke and Chen, 2011a). A possible explanation for this variation is the different experimental set-up. While in the one study, HCV-positive cells were generated by electroporation of Huh7.5 cells, in the other study Huh7.5 cells were infected with infectious supernatant. Thereby, the electroporation process itself can result in the generation of ROS. Nevertheless, additional studies are crucial to clarify this uncertainty. In 2010, several groups uncovered that the Nrf2/ARE signaling pathway can not only be activated by the canonical pathway through the release from Keap1 under stress conditions but also by a direct interaction of p62 and Keap1 (Komatsu et al., 2010, Copple et al., 2010). Thereby, a phosphorylation of p62 within the KIR increases its binding affinity for Keap1, resulting in a competitive binding to Keap1 and the subsequent release of Nrf2. In HCV-positive cells, not only an increase of total p62 could be observed but as well elevated amounts of pS[349] p62 (figures 5.9 and 5.10). Calculating the quotient of pS[349] p62 to total p62, about twice the amount of pS[349] p62 in HCV-positive cells could be observed compared to HCV-negative cells. This was not caused by increased expression of p62 but by significant higher HCV-induced phosphorylation of p62. In line with this, accumulation of p62 and aggregates positive for phosphorylated p62 and Keap1 are frequently found in hepatocellular carcinoma (HCC) (Zatloukal et al., 2002, Ichimura et al., 2013). In autophagy-deficient mice, accumulated pS[351] p62 (homologue of human pS[349] p62) and Keap1 form aggregates resulting in sustained activation of Nrf2 (Ichimura et al., 2013, Inami et al., 2011, Takamura et al., 2011). Furthermore, pS[351] p62-induced activation of Nrf2 contributes to tumor growth as tumor size in liver-specific autophagy-deficient mice is reduced by simultaneous deletion of p62 or Nrf2 (Takamura et al., 2011, Ni et al., 2014). Saito et al. demonstrated that pS[349] 62 influences glucose and glutamine metabolism through persistent activation of Nrf2, providing HCC cells with both tolerance to anti-cancer drugs and proliferation potency (Saito et al., 2016).

6.3 Role of pS[349] p62 in ROS-induced autophagy

Autophagy functions as a quality control system to maintain cellular homeostasis (Mizushima et al., 2008). Hence, it is not surprising that a variety of stress signals are able to induce the autophagic process (Filomeni et al., 2015). To investigate the potential of ROS as autophagy inducer, Huh7.5 cells were treated with glucose oxidase. It was observed that elevated levels of ROS are indeed able to induce autophagy which is reflected by increased amounts of LC3-II (figure 5.14) and the augmented formation of LC3 puncta upon treatment with glucose oxidase (figure 5.16). Furthermore, phosphorylated p62 in Huh7.5 cells is increased (figure 5.15). In line with this, several other studies revealed that the accumulation of ROS can induce autophagy by affecting both the core autophagy machinery and the cellular signaling pathways that regulate autophagy (Li et al., 2012, Scherz-Shouval et al., 2007, Villar et al., 2015). A couple of Atg proteins are known to be redox-sensitive, e.g. Atg4. In its oxidized state, Atg4 avoids the delipidation of LC3-II resulting in maintained autophagy (Scherz-Shouval et al., 2007). Indirectly, ROS can regulate autophagy by activating AMPK and JNK1, thereby resulting in the inactivation of mTORC1 and interference with the Bcl-2-Beclin-1 complex (Li et al., 2013, Wong et al., 2010, Maiuri et al., 2007). Furthermore, the p62 promoter harbors an ARE site. Consequently, p62 gene expression can be induced by oxidative stress mediated by Nrf2 (Jain et al., 2010). Moreover, overexpression of the phosphorylation mimicking mutant p62 [S351E] resulted in an accumulation of LC3-II (figure 5.17), thus reflecting the potential of phosphorylated p62 to induce autophagy.

6.4 Autophagy is crucial to sustain the HCV life cycle

Autophagy is known to be involved in a variety of steps that promote the viral life cycle (Ren et al., 2016, Elgner et al., 2016, Wang et al., 2015, Fahmy and Labonte, 2017). In accordance with this, treatment of HCV-positive cells with the autophagy inhibitors 3-methyladenine (figure 5.18) and bafilomycin (figure 5.19) resulted in an impaired release of infectious viral particles. Nonetheless, intracellular inhibition of autophagy had opposing effects. While treatment with 3-methyladenine decreased the amount of retained infectious viral particles (figure 5.20), bafilomycin leads to an accumulation (figure 5.21). This observation can be explained by the different modes of action of these inhibitors on autophagy. 3-Methyladenine is a PI3K inhibitor, which is crucial for the production of PI3P (Petiot et al., 2000). The key regulator PI3P initiates autophagy by recruiting Atg proteins to the isolation membrane (Pattingre et al., 2008, Zeng et al., 2006). Hence, treatment with 3-methyladenine results in PI3P depletion and suppressed autophagosome formation. Based on this, infectious viral particles are degraded in the cytoplasm as they cannot enter the autophagosomal

compartment resulting in a diminished $TCID_{50}$ after 3-methyladenine treatment. However, the amount of intracellular RNA remained unchanged (figure 5.26). This finding is surprising as Mohl et al. observed that the activity of PI3K is required for HCV RNA replication due to the necessity of an intact autophagosome machinery for the formation of the membranous web (Mohl et al., 2016). Hence, a negative effect of 3-methyladenine on the intracellular viral RNA would be expected. However, the experiments were performed in Huh7 cells expressing the subgenomic replicon. In contrast to this, for our experiments the full-length genome was used, imitating the whole viral life cycle. This differential set-up provides a possible explanation for these contradictory results. During the viral life cycle, the amount of produced viral particles exceeds the amount of released infectious viral particles (Quinkert et al., 2005, Post et al., 2009). The majority of *de novo* synthesized viral particles is degraded in the lysosomal compartment (Ren et al., 2016, Elgner et al., 2016). In line with this, treatment with bafilomycin, a lysosomal inhibitor, traps the viral particles within the autophagosome. Consequently, viral particles cannot longer be degraded within the autolysosome and accumulate within the cell. This is also reflected by the accumulation of the core protein (figure 5.22 and 5.23) and viral RNA (figure 5.25) after bafilomycin treatment. In accordance with this, Ren at al. observed that in HCV-positive cells the expression of the autophagosomal SNARE protein syntaxin 17 is diminished, thereby shifting the equilibrium between viral particle release and lysosomal degradation towards viral particle release (Ren et al., 2016). Nevertheless, viral replication was not affected as bafilomycin had no effect on the NS3 protein amount (figure 5.24). This is not surprising as the proper formation of the membranous web is dependent on autophagosome formation, which is not affected by bafilomycin (Sir et al., 2012). Further insights were gained by knockdown of p62 in HCV-positive cells which results in significant intracellular accumulation of viral genomes (figure 5.27). Additionally, the amount of LC3-II was reduced suggesting that the presence of p62 is required for the formation of autophagosomes. Similar results were obtained by another group where a knockdown of p62 in HeLa and HEK293 cells resulted in decreased LC3-II levels but increased after an overexpression of p62, indicating that p62 is a potential regulator of autophagy (Zhou et al., 2013). Taken together, these findings suggest that the autophagosomal machinery plays a central role in intracellular sorting, degradation and release of viral particles.

6.5 The interdependency of oxidative stress and autophagy for the viral particle release

Oxidative stress is known to play a central role in HCV-associated pathogenesis (Bartosch et al., 2009). In line with this, elevated levels of ROS were detected in HCV-positive cells (discussed in

6.1). Similar results were obtained in previous studies (Ivanov et al., 2015, de Mochel et al., 2010). Furthermore, the potential of ROS to induce autophagy was verified in Huh7.5 cells (discussed in 6.3). HCV infection is accompanied by both elevated levels of ROS and an induction of autophagy. Accordingly, radical scavenging with PDTC and NAC in HCV-positive cells resulted in decreased protein amounts of LC3-II (figure 5.28) and impaired phosphorylation of p62 (figures 5.29 and 5.30), while there was no effect on LC3 and p62 mRNA detectable (figure 5.31 and 5.32). This indicates that HCV-induced oxidative stress has the potential to positively regulate autophagy. It is well established that autophagy plays a central role in the HCV life cycle (Wang et al., 2015, Fahmy and Labonte, 2017). Consequently, radical scavenging reduced the amount of released infectious viral particles (figure 5.33). However, this was not due to an impact on replication, as replication was not influenced by the presence of PDTC and NAC (figures 5.35 - 5.37), but rather by a negative effect on autophagy. These findings suggest a crosstalk between elevated levels of ROS, activation of autophagy and viral particle release. Scavenging of ROS causes a loss of HCV-induced autophagy resulting in impaired viral particle release.

6.6 Negative effect of HCV on Nrf2/ARE-dependent gene expression preserves elevated levels of ROS

Cells are constantly exposed to electrophiles and oxidative stress which can contribute to the development of malignant gene alterations (Kensler et al., 2007, Loboda et al., 2016). To maintain cellular homeostasis, cells have evolved several protective mechanisms. Importantly, the Nrf2/ARE signaling pathway plays a major cytoprotective role (Kansanen et al., 2013, Levonen et al., 2014). Under basal conditions, Nrf2 is bound to Keap1 and thereby targeted for ubiquitination and proteasomal degradation. Upon exposure to oxidative and electrophile stress, Keap1 dissociates from Nrf2. Keap1 is degraded and Nrf2 translocates to the nucleus where it binds together with sMaf proteins, to AREs in the promotor region of cytoprotective genes, resulting in the expression of detoxifying enzymes. Previous studies revealed that HCV impairs Nrf2/ARE signaling by a so far unprecedented mechanism (Carvajal-Yepes et al., 2011). In HCV-replicating cells, a delocalization of sMaf proteins from the nucleus to the cytoplasm occurs, where they bind to the viral protein NS3 localized at the ER. The trapped cytosolic sMafs bind Nrf2 and hinder Nrf2 from entering the nucleus. Consequently, the expression of cytoprotective genes is inhibited resulting in persistent levels of ROS. Analysis of endogenous Nrf2 revealed that both Nrf2 activation (figure 5.38) and the expression of detoxifying enzymes like NQO1 and GCLc are impaired in HCV-positive cells (figure 5.39). In addition, despite the incubation with an electrophilic agent, activation of NQO1 and GCLc on mRNA level (figures 5.40

and 5.41) as well as protein expression of NQO1 and GCSc (figure 5.42) are prevented in HCV-positive cells. It is tempting to say that this intricate mechanisms of Nrf2 inhibition ensures the preservation of elevated levels of ROS as a putative activator of autophagy. Nevertheless, contradictory results were observed by other groups. Burdette et al. revealed an induction of the Nrf2/ARE signaling pathway in HCV-positive cells already on the second day after infection. Additionally, both, enhanced Nrf2 gene transcription and protein synthesis were detected (Burdette et al., 2010). In accordance with this, Ivanov et al. observed an inducing effect of at least five HCV proteins on Nrf2/ARE signaling (Ivanov et al., 2011). In a recent publication, Smirnova et al. mapped the domains of HCV core and NS5A proteins that are involved in the activation of Nrf2/ARE signaling (Smirnova et al., 2016). Even though the experimental set-up partly resembles our experiments, the underlying mechanisms responsible for these variations remain to be elucidated.

6.7 HCV prevents pS[349] p62-dependently released Nrf2 from entering the nucleus, thereby preserving elevated levels of ROS

As discussed before, HCV exerts a negative effect on the Nrf2/ARE signaling pathway. Lately, several groups revealed that Nrf2 is not only activated by the canonical pathway but as well through a direct interaction of p62 with Keap1 (Jiang et al., 2015a). Phosphorylation of p62 within the KIR increases its binding affinity to Keap1. Consequently, p62 competitively binds to Keap1 and thereby sequesters Keap1 into the autophagosomal compartment, guiding Keap1 towards autophagosomal degradation. This event leads to a hindered ubiquitination of Nrf2, which is now able to translocate to the nucleus to induce the transcription of cytoprotective genes (Ichimura et al., 2013). Even though HCV-positive cells were transfected with a phosphorylation mimicking mutant (p62 [S351E]), no Nrf2 activation was observed (figure 5.43). In contrast, in HCV-negative cells a strong activation of Nrf2 was observed. As published by Ichimura et al., the phosphorylation mimicking mutant has the ability to release Nrf2 from the Keap1 complex (Ichimura et al., 2013). Due to the HCV-induced delocalization of sMaf proteins to the replication complexes, the pS[349] p62-dependently released Nrf2 is sequestered to the cytoplasm. Hence, there is a lack of Nrf2 and sMaf proteins in the nucleus and by this, the expression of cytoprotective genes is impaired. Based on the finding that HCV-induced translocation of the sMaf proteins is core-dependent, transfection of core-deficient mutants with the phosphorylation mimicking mutant of p62 revealed that Nrf2/ARE signaling can be activated in the same manner as compared to HCV-negative cells (figure 5.44). Additionally, core deficiency results in a decreased phosphorylation of p62 (figure 5.45) and impaired activation of p62 expression on mRNA level compared to the full-length HCV variant (figure 5.46), suggesting that core plays a crucial role in the generation of

ROS (Ivanov et al., 2015). Consequently, in core-deficient cells the generation of ROS is impaired resulting in a decreased phosphorylation of p62.

6.8 Concluding remarks

HCV interferes with diverse cellular processes causing a negative effect on Nrf2/ARE signaling, thereby preserving elevated levels of ROS. Consequently, phosphorylation of p62 is enhanced leading to an induction of autophagy. In this study, we have proven that despite the pS[349] p62-dependently released Nrf2, the activation of the Nrf2/ARE signaling pathway is impaired due to the fact that Nrf2 is trapped in the cytoplasm by binding to the delocalized sMafs. Based on this, Nrf2 is not able to translocate to the nucleus to ensure the expression of cytoprotective genes. This results in the preservation of elevated levels of ROS that can activate autophagy to promote the viral life cycle.
Taken together, these results describe a so far unique mechanism of how HCV affects the crosstalk between Nrf2/ARE signaling, elevated levels of ROS and autophagy. The results of this thesis are summarized in figure 6.1.
Oxidative stress is known to play a central role in HCV-associated pathogenesis, as it can induce a variety of metabolic disorders. Elevated levels of ROS can cause DNA damage leading to chromosome instability giving rise to malignant transformation (Shawki et al., 2014, Tsukiyama-Kohara, 2012). Additionally, elevated levels of ROS exert a negative effect on the insulin receptor signaling pathway, resulting in insulin resistance and impaired liver regeneration (Barthel et al., 2016, Beyer et al., 2008). Conclusively, this thesis highlights a so far unprecedented target structure, which is equally relevant for viral replication as well as for virus-associated pathogenesis. Considering this, reconstitution of the Nrf2/ARE signaling pathway that results in ROS detoxification would affect both viral life cycle and virus-associated pathogenesis.

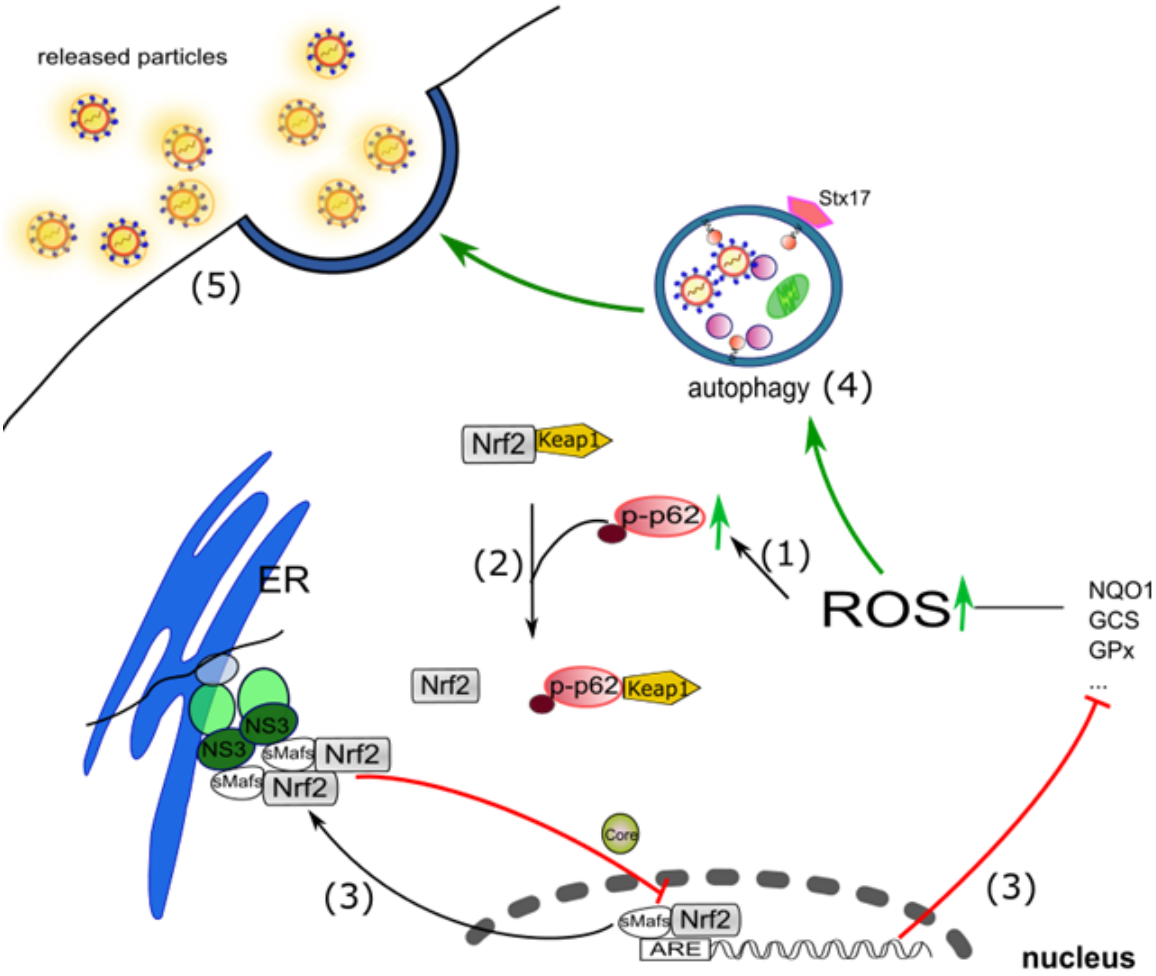

Figure 6.1: Schematic overview illustrating the crosstalk of HCV-impaired Nrf2/ARE signaling autophagy and via pS[349] p62. (1) HCV infection is associated with elevated levels of ROS that are capable of inducing the phosphorylation of p62 on serine 349 (pS[349] p62). **(2)** pS[349] p62 competitively binds to Keap1 concurrently activating Nrf2. **(3)** HCV inhibits Nrf2/ARE signaling by inducing a delocalization of sMafs from the nucleus to the cytoplasm where they bind to the viral protein NS3 localized at the ER. The trapped cytosolic sMafs bind Nrf2 and prevent it from entering the nucleus resulting in an impaired expression of cytoprotective genes. **(4)** Hence, elevated levels of ROS are preserved triggering the induction of autophagy. **(5)** Autophagy is essential for the release of infectious viral particles. Adapted from Medvedev et al., 2016a.

7 Summary

The hepatitis C virus (HCV) can cause an inflammation of the liver (hepatitis). According to the World Health Organization (WHO), 130-150 million people are chronically infected with HCV worldwide. Even though HCV can nowadays be cured with directly acting antiviral agents (DAA), which are more effective than the old therapies and have revolutionized the treatment, there is still no vaccine available. Infection with HCV is often accompanied by elevated levels of reactive oxygen species (ROS), which are known to play a central role in progression and appearance of different pathologies associated with an infection, such as impaired liver regeneration and the development of fibrosis, cirrhosis and HCC. To counteract oxidative and electrophilic stress, cells have evolved several detoxification mechanisms to maintain cellular homeostasis. Thereby, the redox-sensitive transcription factor Nrf2 controls the expression of cytoprotective and ROS-detoxifying genes. Previous studies from our group revealed that HCV impairs the Nrf2/ARE signaling pathway and by this prevents the expression of cytoprotective genes preserving elevated levels of ROS. Another important cellular defense mechanism is autophagy. It plays a crucial role in removing damaged proteins and organelles to maintain cellular homeostasis. Furthermore, autophagy is not only induced in response to starvation but as well by elevated levels of ROS. Several studies have revealed that autophagy plays a crucial role in the HCV life cycle as it intervenes with membranous web formation, translation of incoming RNA, replication as well as virus release. Hence, the aim of this thesis was to investigate the relevance of HCV-induced oxidative stress as a possible activator of the autophagic process, which is preserved by inhibition of the Nrf2/ARE signaling. In HCV-positive cells an induction of autophagy was observed, reflected by LC3-II accumulation and enhanced expression of autophagy marker proteins in HCV-infected PHHs. Upon induction of autophagy, p62 is degraded which should result in a decrease of p62 protein amount. But surprisingly, an accumulation of p62 was detected as a consequence of HCV-induced prolonged half-life. Recently, a crosstalk between the Nrf2/ARE signaling pathway and autophagy was revealed. Besides the canonical pathway, Nrf2 can also be activated through a direct interaction of the phosphorylated autophagy adapter protein p62 (pS[349] p62) with Keap1. In HCV-positive cells not only an increase of total p62 could be observed but as well elevated amounts of pS[349] p62. Calculating the quotient of pS[349] p62 to total p62, about twice the amount of pS[349]

p62 in HCV-positive cells could be observed compared to HCV-negative cells. This was not caused by increased expression of p62 but by significant higher HCV-induced phosphorylation of p62. By investigating the role of pS[349] p62 in ROS-induced autophagy, it was observed that elevated levels of ROS, induced by glucose oxidase treatment, increased the amount of LC3-II and caused formation of LC3 puncta. Additionally, phosphorylation of p62 in Huh7.5 cells was increased. Moreover, overexpression of the phosphorylation mimicking mutant p62 [S351E] resulted in an accumulation of LC3-II, reflecting the capacity of phosphorylated p62 in inducing autophagy. Modulation of autophagy with bafilomycin and 3-methyladenine impaired the release of infectious viral particles, pointing out the importance of the autophagic machinery for the morphogenesis of HCV. An HCV infection is accompanied by both elevated levels of ROS and an induction of autophagy. Accordingly, radical scavenging with PDTC and NAC in HCV-positive cells resulted in decreased protein amounts of LC3-II and impaired phosphorylation of p62. It was further observed that scavenging of ROS reduced the amount of released infectious viral particles, suggesting a crosstalk between elevated levels of ROS, activation of autophagy and viral particle release. Elevated ROS levels can be detoxified by the induction of the Nrf2/ARE system. As a result, this system would lead to a collapse of the above-described crosstalk. As HCV impairs the activation of Nrf2/ARE-dependent cytoprotective genes, it was hypothesized that in HCV-positive cells this intricate mechanism prevents the pS[349] p62-dependently released Nrf2 from translocation into the nucleus. This in turn leads to impaired expression of Nrf2/ARE-dependent genes and detoxification of ROS. To experimentally evaluate this hypothesis, HCV-positive cells and HCV-negative control cells were cotransfected with either p62 wildtype (p62 [wt]), the phosphorylation mimicking mutant p62 [S351E] or pUC in combination with a Nrf2-dependent luciferase reporter construct monitoring Nrf2-activation (OKD48 construct). While in HCV-negative cells transfection of the p62 [S351E] mutant significantly activated Nrf2 as compared to the wildtype p62, in HCV-positive cells the activation of the Nrf2/ARE-dependent reporter gene by overexpression of the constitutive active mutant p62 [S351E] was impaired. These results indicated that pS[349] p62-mediated activation of Nrf2 is counteracted in HCV-positive cells due to the trapping of Nrf2 on the ER surface at the replicon complexes. Taken together, these results describe a so far unique mechanism of how HCV affects the crosstalk between the Nrf2/ARE signaling, elevated levels of ROS and autophagy. HCV negatively affects the Nrf2/ARE signaling to escape the pS[349] p62-dependent released Nrf2. Consequently, elevated levels of ROS are preserved facilitating the induction of autophagy, which in turn is essential for the release of infectious viral particles. This mechanism represents a potential target structure which affects both, viral life cycle and HCV-associated pathogenesis.

8 Zusammenfassung

Das Hepatitis-C-Virus (HCV) ist ein behülltes RNA-Virus aus der Familie der *Flaviviridae*. Es trägt ein positiv orientiertes, einzelsträngiges RNA-Genom mit einer Länge von 9600 Nukleotiden, welches für 10 virale Proteine kodiert. Eine Infektion erfolgt meist parenteral. Dadurch gelangt das Virus in die Leber, wo es spezifisch Hepatozyten infiziert. Eine Infektion mit HCV ruft eine entzündliche Lebererkrankung (Hepatitis) hervor, die einen akuten oder chronischen Verlauf nehmen kann. Mit etwa 130-150 Millionen infizierten Patienten weltweit, stellt HCV eine bedeutende Infektionskrankheit dar. Trotz vieler Bemühungen ist heutzutage immer noch keine prophylaktische Vakzinierung verfügbar. Dennoch versprechen neuartige Therapien eine hohe Heilungsrate, diese sind jedoch mit hohen Kosten verbunden. Eine akute Hepatitis-C-Infektion verläuft in der Regel asymptomatisch oder mit grippeähnlichen Symptomen und erschwert damit eine Diagnose. HCV induziert oxidativen Stress, welcher für das Auftreten und die Progression der Pathogenese eine zentrale Rolle spielt. Dabei entwickelt der Großteil der Betroffenen, etwa 75−85 %, eine chronische Hepatitis, die durch eine wiederkehrende Leberschädigung gekennzeichnet ist. Die persistierende inflammatorische Aktivität des Immunsystems führt zu einer immunvermittelten Pathogenese der chronischen HCV-Infektion, da HCV *per se* keine zytopathogene Wirkung hat. Durch die Leberregeneration kann zwar geschädigtes Lebergewebe wiederhergestellt werden, diese ist jedoch nach bestimmter Zeit durch die anhaltende Leberschädigung erschöpft, was eine Fibrosierung der Leber zur Folge hat. Dabei wird funktionelles Gewebe durch nichtfunktionelles Bindegewebe ersetzt. 20 % der chronisch infizierten Patienten entwickeln innerhalb von 20 Jahren eine Leberzirrhose, die durch eine Vernarbung der Leber charakterisiert ist und in einem Leberversagen enden kann. Des Weiteren haben Patienten mit einer Leberzirrhose ein erhöhtes Risiko, ein hepatozelluläres Karzinom zu entwickeln, welches die zweithäufigste Krebsart weltweit ist. Große Fortschritte wurden im Verständnis des Lebenszyklus von HCV in den letzten Jahren erzielt. Nach einer Bindung der struktuellen HCV-Glykoproteine E1E2 an die spezifischen Rezeptoren und Corezeptoren auf der Zelloberfläche von Hepatozyten wird das Virus durch Clathrin-vermittelte Endozytose internalisiert. Dabei wird das virale Genom pH-abhängig in das Cytoplasma freigesetzt und dient als Matrize für die IRES-vermittelte Translation am rauen ER. Das entstandene Polyprotein wird in die reifen Struktur- und Nichtstrukturproteine prozessiert. Für die RNA-Replikation induziert HCV

eine weitreichende intrazelluläre Membranumstrukturierung, die zur Ausbildung des *membranous web* führt, welches aus ER-abstammenden Membranen, *lipid droplets* und Doppelmembranvesikeln besteht. Nach der Formierung des Nukleokapsids auf der Oberfläche der *lipid droplets* und Reifung wird das Virus entweder über den klassischen sekretorischen oder über den endosomalen Weg freigesetzt. Dabei konnte mittels Inkubation mit dem MVB-Inhibitor U18666A oder Expression von dominant-negativen Mutanten der ESCRT-Maschinerie eine beeinträchtige Freisetzung und eine intrazelluläre Akkumulation viraler Partikel beobachtet werden. Des Weiteren wurde unter Verwendung von Fluoreszenz-markierten viralen Partikeln eine Lokalisation von viralen Partikeln und Strukturproteinen an endosomalen Strukturen nachgewiesen. In Übereinstimmung damit wurde das Core-Protein an endosomalen Strukturen lokalisiert. Zusätzlich konnten dominant-negative Rab-GTPase-Mutanten, die involviert sind im endosomalen Freisetzungsweg, die Freisetzung von viralen Partikeln inhibieren. Um den viralen Lebenszyklus aufrechtzuerhalten, induzieren viele RNA-Viren, darunter auch HCV, Autophagie um autophagosomale Strukturen und Prozesse zu nutzen. Die Autophagie dient der Aufrechterhaltung der zellulären Homöostase durch den Abbau von defekten Proteinen und Organellen. Dieser hochkonservierte Prozess wird in Folge eines Nährstoffmangels, durch die Inhibition der Kinase mTOR, induziert. Die Biogenese von Autophagosomen kann in drei wesentliche Schritte unterteilt werden: die Inititation, welche mit der Entstehung der Isolationsmembran beginnt, die Nukleation und Ausdehnung der Isolationsmembran, bis ein reifes und geschlossenes Autophagosom entsteht. Das Protein LC3 ist ein oft verwendeter Marker der Autophagie, welcher im Laufe des autophagosomalen Prozesses lipidiert wird und sowohl auf der inneren als auch äußeren Seite des Autophagosoms lokalisiert ist. Reife Autophagosomen können mit Lysosomen zu Autophagolysosomen fusionieren, in denen der Abbau der eingeschlossenen Komponenten statt findet. Einen wichtigen Cargo-bindenden Rezeptor stellt das Stress-induzierte Protein p62 dar, welches an ubiquitinierte Proteine bindet, diese zum Autophagosom lenkt und dort zusammen mit dem Bindungspartner angebaut wird. In sämtlichen Studien konnte beobachtet werden, dass Autophagie mit der Ausbildung des *membranous web*, der Translation, Replikation und Freisetzung des Virus interveniert. Des Weiteren ist bekannt, dass Autophagie nicht nur im Laufe von Nährstoffmangel induziert wird, sondern auch durch erhöhte Mengen an ROS. Sie dient als Teil des zellulären Abwehrmechanismus. Um oxidativen und elektrophilen Stress entgegenzuwirken, haben Zellen detoxifizierende Mechanismen entwickelt, die zelluläre Homöostase aufrechterhalten. Dabei kontrolliert der redoxsensitive Transkriptionsfaktor Nrf2 als Heterodimer mit den sMaf-Proteinen, die Expression von zytoprotektiven und ROS-detoxifizierenden Genen. Vorherige Studien haben gezeigt, dass HCV den Nrf2/ARE-Signalweg beeinträchtigt. Dabei induziert HCV eine Translokation der sMaf-Proteine aus dem Zellkern in das Cytoplasma, wo sie das virale Protein NS3 binden. Im Cytoplasma lokalisierte sMaf-Proteine verhindern eine Translokation von Nrf2 in

den Zellkern. Folglich ist die Expression von zytoprotektiven Genen inhibiert, was zu dauerhaft erhöhten ROS-Spiegeln beiträgt. Ausgehend davon sollte zunächst die Relevanz von HCV-induziertem oxidativen Stress, resultierend aus der Inhibition des Nrf2/ARE-Signalwegs, als möglicher Aktivator der Autophagie untersucht werden. Dazu wurde zunächst nachgewiesen, dass HCV oxidativen Stress induziert (Abbildung 5.1 und 5.2). Des Weiteren konnte in HCV-positiven Zellen eine Akkumulation von LC3-II beobachtet werden (Abbildung 5.3 und 5.4), was auf eine Induktion der Autophagie schließen lässt. In Übereinstimmung damit wurde eine erhöhte Expression von Autophagie-Markerproteinen in HCV-infizierten PHHs detektiert (Abbildung 5.11). Im Laufe der Autophagie wird p62 abgebaut. Somit sollte eine Induktion der Autophagie zu einer Verminderung der Menge an p62 führen. Nichtsdestotrotz ist eine Akkumulation von p62 in HCV-positiven Zellen nachzuweisen (Abbildung 5.9 und 5.10), die schon 18 h nach der Elektroporation detektierbar war (Abbildung 5.7). Dies erscheint zunächst widersprüchlich. Aber aufgrund der Tatsache, dass die Expression der katalytischen Untereinheit des Proteasoms (PSMB5) Nrf2-abhängig ist, führte die beeinträchtigte Nrf2-Aktivität in HCV-positiven Zellen zu einer verringerten Aktivität des konstitutiven Proteasoms, was auch die erhöhte Halbwertzeit von p62 in HCV-positiven Zellen erklärt (Abbildung 5.8). Kürzlich wurde ein Zusammenspiel des Nrf2/ARE-Signalwegs und der Autophagie beobachtet. Dabei kann Nrf2 nicht nur über den kanonischen Signalweg aktiviert werden, sondern auch durch eine direkte Interaktion von p62 mit Keap1. Eine Phosphorylierung von p62 innerhalb der Keap1-Interaktionsdomäne (pS[349] p62) erhöhte seine Bindungsaffinität zu Keap1. Infolgedessen bindet pS[349] p62 kompetitiv an Keap1 und führt zu dessen autophagosomalen Abbau. Dadurch wird Nrf2 aus dem Komplex mit Keap1 freigesetzt. Somit kann Nrf2 in den Zellkern wandern und die Expression zytoprotektiver Gene aktivieren. In HCV-positiven Zellen konnte nicht nur eine Zunahme der Gesamtmenge von p62 beobachtet werden, sondern auch erhöhte Mengen an pS[349] p62 (Abbildung 5.9 und 5.10). Die Berechnung des Quotienten aus pS[349] p62 und p62 zeigte in etwa eine Verdopplung der Menge an pS[349] p62, die nicht allein durch die Zunahme der Gesamtmenge von p62 erklärt werden kann, sondern auf eine vermehrte Phosphorylierung von p62 in HCV-positiven Zellen rückschließen lässt. Des Weiteren konnte beobachtet werden, dass erhöhte Mengen an ROS, wie sie auch in HCV-positiven Zellen vorkommen, eine Induktion der Autophagie auslösen können, die durch eine Akkumulation von LC3-II und die Zunahme von LC3-Puncta charakterisiert ist (Abbildung 5.14 und 5.16). Zusätzlich stieg die Menge an pS[349] p62 durch erhöhte ROS-Spiegel (Abbildung 5.15). Ferner resultierte die Überexpression der phosphomimetischen Mutante (p62 [S351E]) in einer Akkumulation von LC3-II, was auf die Fähigkeit von pS[349] p62 rückschließen lässt, Autophagie zu induzieren (Abbildung 5.17). Eine Modulation der Autophagie mittels der Inhibitoren 3-Methyladenin und Bafilomycin führte zu einer inhibierten Freisetzung von infektiösen viralen Partikeln (Abbildung 5.18 und 5.19).

Intrazellulär konnten hingegen gegensätzliche Effekte beobachtet werden. Während die Inkubation mit 3-Methyladenin zu einer Verminderung der intrazellulären infektiösen viralen Partikel führte (Abbildung 5.20), konnte nach einer Inkubation mit Bafilomycin eine Akkumulation beobachtet werden (Abbildung 5.21). In Übereinstimmung damit führte die Inkubation mit Bafilomycin zu einer intrazellulären Akkumulation des Core-Proteins (Abbildung 5.23). Auch auf die Menge der intrazellulären viralen RNA zeigten die Inhibitoren unterschiedliche Auswirkungen. Im Falle von Bafilomycin ließ sich eine Akkumulation nachweisen, jedoch war in 3-Methyladenin-behandelten Zellen keine signifikante Änderung zu erkennen (Abbildung 5.25 und 5.26). Die verschiedenen Beobachtungen sind auf die unterschiedlichen Wirkmechanismen der Modulatoren zurückzuführen. Während 3-Methyladenin, als PI3P-Inhibitor, die Initiation der Autophagie und damit die Bildung von Autophagosomen inhibiert, verhindert Bafilomycin als lysosomaler Inhibitor die Ansäuerung von Lysosomen und wirkt damit einer Verschmelzung von Autophagosomen und Lysosomen entgegen. Im Laufe des viralen Lebenszyklus werden deutlich mehr virale Partikel produziert als von der Zelle freigesetzt. Der Großteil der *de novo* synthetisierten viralen Partikel wird intrazellulär lysosomal abgebaut. Somit führt Bafilomycin dazu, dass die viralen Partikel im Autophagosom gefangen bleiben und nicht mehr lysosomal abgebaut werden können. Ein Knockdown von p62 in HCV-positiven Zellen resultierte in einer Akkumulation der viralen Genome (Abbildung 5.27). Des Weiteren konnte eine Abnahme von LC3-II beobachtet werden, die darauf schließen lässt, dass p62 für die Bildung von Autophagosomen notwendig ist. Ausgehend von diesen Beobachtungen kann darauf geschlossen werden, dass der Autophagie eine essentielle Bedeutung bei der Sortierung und Freisetzung viraler Partikel zukommt. Eine HCV-Infektion wird sowohl von erhöhten Mengen an ROS als auch von einer Induktion der Autophagie begleitet. Dementsprechend führte eine Verminderung des intrazellulären Radikalspiegels durch eine Inkubation mit den Radikalfängern PDTC und NAC zu geringeren Mengen an LC3-II und pS[349] p62 (Abbildungen 5.28 - 5.30). Auch konnte unter denselben Bedingungen eine Abnahme der freigesetzten infektiösen viralen Partikel beobachtet werden (Abbildung 5.33), was ein Zusammenspiel zwischen erhöhten Mengen an ROS, Induktion der Autophagie und Virusfreisetzung nahelegt. Des Weiteren konnte ausgeschlossen werden, dass die verminderte Freisetzung viraler Partikel durch einen negativen Einfluss der Radikalfänger auf die Replikation hervorgerufen wird (Abbildungen 5.35 - 5.37). Erhöhte Mengen an ROS können durch eine Aktivierung des Nrf2/ARE-Systems detoxifiziert werden, welches in einem Zusammenbruch des zuvor beschriebenen Mechanismus resultieren würde. Da HCV die Aktivierung Nrf2/ARE-regulierter Gene beeinträchtigt (Abbildungen 5.38 - 5.42), wurde die Hypothese aufgestellt, dass in HCV-positiven Zellen dieser komplexe Mechanismus dazu dient, die Translokation des pS[349] p62-abhängig freigesetzten Nrf2 in den Zellkern zu verhindern. Das wiederum hat eine eingeschränkte Expression von Nrf2/ARE-abhängigen Genen und Detoxifizierung

von ROS zur Folge. Um diese Hypothese experimentell zu untersuchen, wurden HCV-positive und -negative Zellen cotransfiziert mit dem p62-Wildtyp (p62 [wt]), der p62 phosphomimetischen Mutante (p62 [S351E]) oder einem Kontrollplasmid in Kombination mit einem Reporterkonstrukt, welches die Nrf2-Aktivierung darstellt (OKD48). Während in HCV-negativen Zellen eine Transfektion mit p62 [S351E] im Vergleich zum p62 [wt] in einer signifikanten Nrf2-Aktivierung resultierte, konnte dies in HCV-positiven Zellen nicht beobachtet werden (Abbildung 5.43). Des Weiteren konnte mittels Transfektion von p62 [S351E] in Core-defizienten Mutanten eine Aktivierung von Nrf2, vergleichbar mit der in HCV-negativen Zellen, beobachtet werden (Abbildung 5.44). Auch eine Abnahme der p62-Phosphorylierung und Expression konnte in diesen Zellen beobachtet werden (Abbildungen 5.45 und 5.46), was eine zentrale regulatorische Rolle von Core nahelegt. Zusammengenommen beschreiben diese Ergebnisse einen bisher unbekannten Mechanismus, wie HCV das Zusammenspiel zwischen dem Nrf2/ARE-Signalweg, erhöhten Mengen an ROS und Autophagie beeinflusst. Dabei übt HCV einen negativen Effekt auf den Nrf2/ARE-Signalweg aus, um dem pS[349] p62-abhängig freigesetzten Nrf2 zu entkommen. Folglich werden erhöhte Mengen an ROS aufrechterhalten, die eine Induktion der Autophagie ermöglichen, welche für die Freisetzung viraler Partikel essentiell ist. Die in dieser Arbeit gewonnenen Erkenntnisse beschreiben eine einzigartige Zielstruktur, die sowohl für die virale Replikation als auch für die virus-assoziierte Pathogenese relevant ist. In Anbetracht dieser Tatsache, könnte eine Wiederherstellung des Nrf2/ARE-Signalwegs den erhöhten Mengen an ROS entgegenwirken und damit sowohl den viralen Lebenszyklus als auch die virus-assoziierte Pathogenese beeinträchtigen. Eine schematische Zusammenfassung der Ergebnisse ist in Abbildung 8.1 dargestellt.

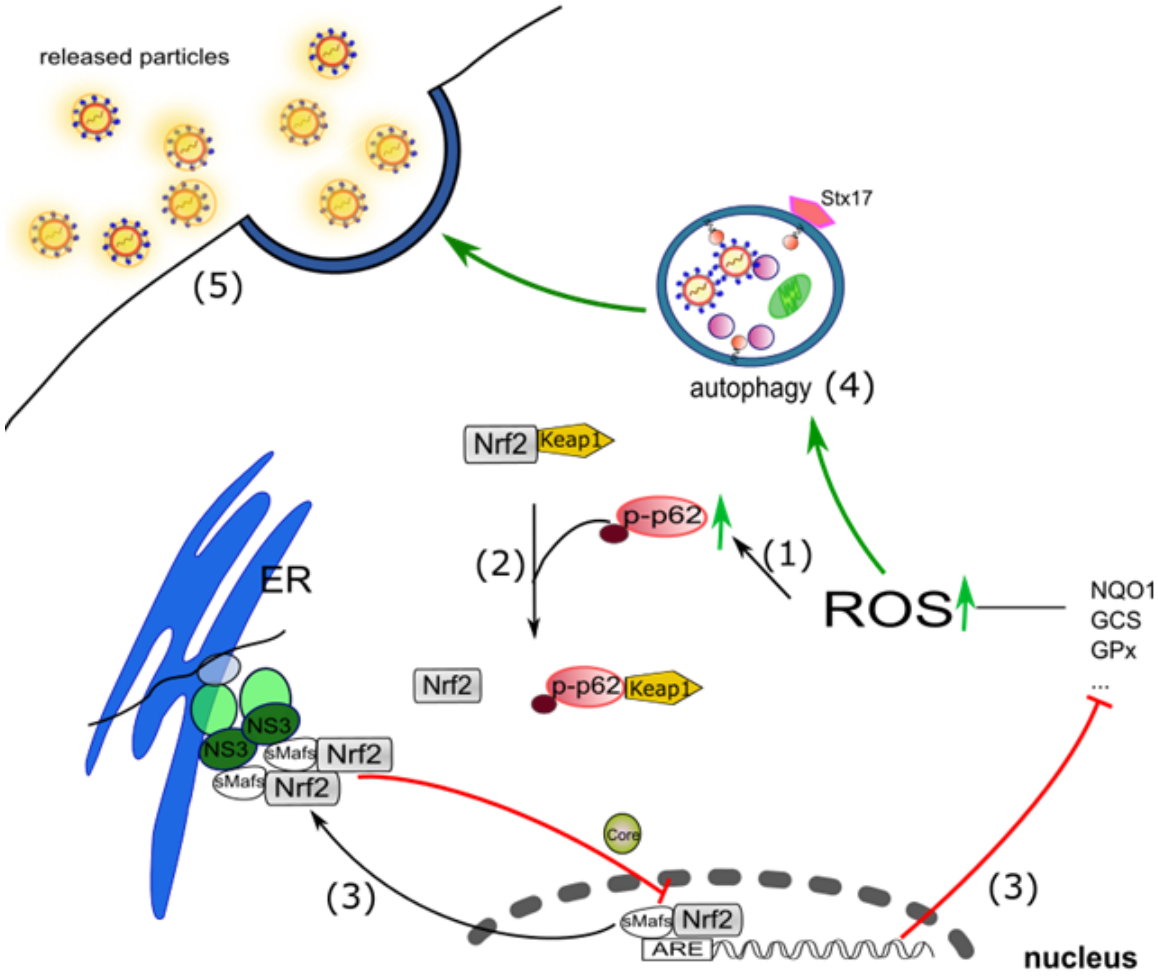

Figure 8.1: Schematische Darstellung des Zusammenspiels des durch HCV-beeinträchtigten Nrf2/ARE-Signalwegs und der Autophagie über pS[349] p62. **(1)** Eine HCV-Infektion ist assoziiert mit erhöhten Mengen an ROS, die in der Lage sind, eine Phosphorylierung von p62 an Serin 349 (pS[349] p62) zu induzieren. **(2)** pS[349] p62 bindet kompetitiv an Keap1 und aktiviert damit Nrf2. **(3)** HCV inhibiert den Nrf2/ARE-Signalweg, indem es eine Translokation der sMaf aus dem Zellkern in das Cytoplasma induziert, wo diese an das virale Protein NS3 am ER binden. Cytosolische sMaf-Proteine binden an Nrf2 im Cytoplasma und verhindern damit, dass Nrf2 in den Zellkern wandern und die Expression von zytoprotektiven Genen induzieren kann. **(4)** Dadurch werden erhöhte Mengen an ROS aufrechterhalten, die eine Induktion der Autophagie auslösen. **(5)** Autophagie wiederum ist essentiell für die Freisetzung viraler Partikel. Modifiziert nach Medvedev et al., 2016a.

9 References

Abe, K., Ikeda, M., Dansako, H., Naka, K., and Kato, N. 2007. Cell culture-adaptive ns3 mutations required for the robust replication of genome-length hepatitis c virus rna. *Virus Research*, 125(1):88–97.

Agnello, V., Abel, G., Elfahal, M., Knight, G. B., and Zhang, Q. X. 1999. Hepatitis c virus and other flaviviridae viruses enter cells via low density lipoprotein receptor. *Proceedings of the National Academy of Sciences of the United States of America*, 96(22):12766–12771.

Albecka, A., Belouzard, S., Op de Beeck, A., Descamps, V., Goueslain, L., Bertrand-Michel, J., Terce, F., Duverlie, G., Rouille, Y., and Dubuisson, J. 2012. Role of low-density lipoprotein receptor in the hepatitis c virus life cycle. *Hepatology (Baltimore, Md.)*, 55(4):998–1007.

Alter, H. J., Conry-Cantilena, C., Melpolder, J., Tan, D., Van Raden, M., Herion, D., Lau, D., and Hoofnagle, J. H. 1997. Hepatitis c in asymptomatic blood donors. *Hepatology (Baltimore, Md.)*, 26:29S–33S.

Andre, P., Komurian-Pradel, F., Deforges, S., Perret, M., Berland, J. L., Sodoyer, M., Pol, S., Brechot, C., Paranhos-Baccala, G., and Lotteau, V. 2002. Characterization of low- and very-low-density hepatitis c virus rna-containing particles. *Journal of virology*, 76(14):6919–6928.

Appel, N., Pietschmann, T., and Bartenschlager, R. 2005. Mutational analysis of hepatitis c virus nonstructural protein 5a: Potential role of differential phosphorylation in rna replication and identification of a genetically flexible domain. *Journal of virology*, 79(5):3187–3194.

Asabe, S. I., Tanji, Y., Satoh, S., Kaneko, T., Kimura, K., and Shimotohno, K. 1997. The n-terminal region of hepatitis c virus-encoded ns5a is important for ns4a-dependent phosphorylation. *Journal of virology*, 71:790–796.

Ashfaq, U. A., Javed, T., Rehman, S., Nawaz, Z., and Riazuddin, S. 2011. An overview of hcv molecular biology, replication and immune responses. *Virology journal*, 8:161.

Axe, E. L., Walker, S. A., Manifava, M., Chandra, P., Roderick, H. L., Habermann, A., Griffiths, G., and Ktistakis, N. T. 2008. Autophagosome formation from membrane compartments enriched in

phosphatidylinositol 3-phosphate and dynamically connected to the endoplasmic reticulum. *The Journal of cell biology*, 182(4):685–701.

Bajpai, M., Gupta, E., and Choudhary, A. 2014. Hepatitis c virus: Screening, diagnosis, and interpretation of laboratory assays. *Asian Journal of Transfusion Science*, 8(1):19.

Bankwitz, D., Steinmann, E., Bitzegeio, J., Ciesek, S., Friesland, M., Herrmann, E., Zeisel, M. B., Baumert, T. F., Keck, Z.-y., Foung, S. K. H., Pecheur, E.-I., and Pietschmann, T. 2010. Hepatitis c virus hypervariable region 1 modulates receptor interactions, conceals the cd81 binding site, and protects conserved neutralizing epitopes. *Journal of virology*, 84:5751–5763.

Barba, G., Harper, F., Harada, T., Kohara, M., Goulinet, S., Matsuura, Y., Eder, G., Schaff, Z., Chapman, M. J., Miyamura, T., and Brechot, C. 1997. Hepatitis c virus core protein shows a cytoplasmic localization and associates to cellular lipid storage droplets. *Proceedings of the National Academy of Sciences of the United States of America*, 94(4):1200–1205.

Barnes, E., Folgori, A., Capone, S., Swadling, L., Aston, S., Kurioka, A., Meyer, J., Huddart, R., Smith, K., Townsend, R., Brown, A., Antrobus, R., Ammendola, V., Naddeo, M., O'Hara, G., Willberg, C., Harrison, A., Grazioli, F., Esposito, M. L., Siani, L., Traboni, C., Oo, Y., Adams, D., Hill, A., Colloca, S., Nicosia, A., Cortese, R., and Klenerman, P. 2012. Novel adenovirus-based vaccines induce broad and sustained t cell responses to hcv in man. *Science translational medicine*, 4:115ra1.

Bartenschlager, R., Ahlborn-Laake, L., Mous, J., and Jacobsen, H. 1993. Nonstructural protein 3 of the hepatitis c virus encodes a serine-type proteinase required for cleavage at the ns3/4 and ns4/5 junctions. *Journal of virology*, 67(7):3835–3844.

Bartenschlager, R., Ahlborn-Laake, L., Mous, J., and Jacobsen, H. 1994. Kinetic and structural analyses of hepatitis c virus polyprotein processing. *Journal of virology*, 68:5045–5055.

Bartenschlager, R., Lohmann, V., and Penin, F. 2013. The molecular and structural basis of advanced antiviral therapy for hepatitis c virus infection. *Nature reviews. Microbiology*, 11(7):482–496.

Bartenschlager, R., Penin, F., Lohmann, V., and Andre, P. 2011. Assembly of infectious hepatitis c virus particles. *Trends in microbiology*, 19(2):95–103.

Barth, H., Schafer, C., Adah, M. I., Zhang, F., Linhardt, R. J., Toyoda, H., Kinoshita-Toyoda, A., Toida, T., Van Kuppevelt, T. H., Depla, E., von Weizsacker, F., Blum, H. E., and Baumert, T. F. 2003. Cellular binding of hepatitis c virus envelope glycoprotein e2 requires cell surface heparan sulfate. *The Journal of biological chemistry*, 278(42):41003–41012.

Barthel, S. R., Medvedev, R., Heinrich, T., Buechner, S. M., Kettern, N., and Hildt, E. 2016. Hepatitis b virus inhibits insulin receptor signaling and impairs liver regeneration via intracellular retention of the insulin receptor. *Cellular and molecular life sciences : CMLS*, 73:4121–4140.

Bartosch, B., Dubuisson, J., and Cosset, F.-L. 2003. Infectious hepatitis c virus pseudo-particles containing functional e1-e2 envelope protein complexes. *The Journal of experimental medicine*, 197(5):633–642.

Bartosch, B., Thimme, R., Blum, H. E., and Zoulim, F. 2009. Hepatitis c virus-induced hepatocarcinogenesis. *Journal of hepatology*, 51(4):810–820.

Bauckman, K. A., Owusu-Boaitey, N., and Mysorekar, I. U. 2015. Selective autophagy: Xenophagy. *Methods*, 75:120–127.

Baumert, T. F., Vergalla, J., Satoi, J., Thomson, M., Lechmann, M., Herion, D., Greenberg, H. B., Ito, S., and Liang, T. J. 1999. Hepatitis c virus-like particles synthesized in insect cells as a potential vaccine candidate. *Gastroenterology*, 117(6):1397–1407.

Bayer, K., Banning, C., Bruss, V., Wiltzer-Bach, L., and Schindler, M. 2016. Hepatitis c virus is released via a non-canonical secretory route. *Journal of virology*.

Behrens, S. E., Tomei, L., and De Francesco, R. 1996. Identification and properties of the rna-dependent rna polymerase of hepatitis c virus. *The EMBO journal*, 15:12–22.

Beller, M., Thiel, K., Thul, P. J., and Jäckle, H. 2010. Lipid droplets: a dynamic organelle moves into focus. *FEBS letters*, 584(11):2176–2182.

Benedicto, I., Molina-Jimenez, F., Bartosch, B., Cosset, F.-L., Lavillette, D., Prieto, J., Moreno-Otero, R., Valenzuela-Fernandez, A., Aldabe, R., Lopez-Cabrera, M., and Majano, P. L. 2009. The tight junction-associated protein occludin is required for a postbinding step in hepatitis c virus entry and infection. *Journal of Virology*, 83(16):8012–8020.

Beyer, T. A., Xu, W., Teupser, D., auf dem Keller, Ulrich, Bugnon, P., Hildt, E., Thiery, J., Kan, Y. W., and Werner, S. 2008. Impaired liver regeneration in nrf2 knockout mice: role of ros-mediated insulin/igf-1 resistance. *The EMBO journal*, 27(1):212–223.

Birnboim, H. and Doly, J. 1979. A rapid alkaline extraction procedure for screening recombinant plasmid DNA. *Nucleic Acids Research*, 7(6):1513–1523.

Blackham, S., Baillie, A., Al-Hababi, F., Remlinger, K., You, S., Hamatake, R., and McGarvey, M. J. 2010. Gene expression profiling indicates the roles of host oxidative stress, apoptosis, lipid metabolism, and intracellular transport genes in the replication of hepatitis c virus. *Journal of virology*, 84(10):5404–5414.

Blanchard, E., Belouzard, S., Goueslain, L., Wakita, T., Dubuisson, J., Wychowski, C., and Rouille, Y. 2006. Hepatitis c virus entry depends on clathrin-mediated endocytosis. *Journal of virology*, 80(14):6964–6972.

Blight, K. J., Kolykhalov, A. A., and Rice, C. M. 2000. Efficient initiation of hcv rna replication in cell culture. *Science*, 290(5498):1972–1974.

Blight, K. J., McKeating, J. A., and Rice, C. M. 2002. Highly permissive cell lines for subgenomic and genomic hepatitis c virus rna replication. *Journal of virology*, 76(24):13001–13014.

Blommaart, E. F., Krause, U., Schellens, J. P., Vreeling-Sindelarova, H., and Meijer, A. J. 1997. The phosphatidylinositol 3-kinase inhibitors wortmannin and ly294002 inhibit autophagy in isolated rat hepatocytes. *European journal of biochemistry*, 243:240–246.

Borowski, P., Oehlmann, K., Heiland, M., and Laufs, R. 1997. Nonstructural protein 3 of hepatitis c virus blocks the distribution of the free catalytic subunit of cyclic amp-dependent protein kinase. *Journal of virology*, 71:2838–2843.

Boudreau, H. E., Emerson, S. U., Korzeniowska, A., Jendrysik, M. A., and Leto, T. L. 2009. Hepatitis c virus (hcv) proteins induce nadph oxidase 4 expression in a transforming growth factor beta-dependent manner: a new contributor to hcv-induced oxidative stress. *Journal of Virology*, 83(24):12934–12946.

Boulant, S., Montserret, R., Hope, R. G., Ratinier, M., Targett-Adams, P., Lavergne, J.-P., Penin, F., and McLauchlan, J. 2006. Structural determinants that target the hepatitis c virus core protein to lipid droplets. *The Journal of biological chemistry*, 281:22236–22247.

Boulant, S., Vanbelle, C., Ebel, C., Penin, F., and Lavergne, J.-P. 2005. Hepatitis c virus core protein is a dimeric alpha-helical protein exhibiting membrane protein features. *Journal of virology*, 79:11353–11365.

Boulestin, A., Sandres-Saune, K., Payen, J.-L., Alric, L., Dubois, M., Pasquier, C., Vinel, J.-P., Pascal, J.-P., Puel, J., and Izopet, J. 2002. Genetic heterogeneity of the envelope 2 gene and eradication of hepatitis c virus after a second course of interferon-alpha. *Journal of medical virology*, 68:221–228.

Bradley, D. W., McCaustland, K. A., Cook, E. H., Schable, C. A., Ebert, J. W., and Maynard, J. E. 1985. Posttransfusion non-a, non-b hepatitis in chimpanzees. physicochemical evidence that the tubule-forming agent is a small, enveloped virus. *Gastroenterology*, 88:773–779.

Brass, V., Bieck, E., Montserret, R., Wolk, B., Hellings, J. A., Blum, H. E., Penin, F., and Moradpour, D. 2002. An amino-terminal amphipathic alpha-helix mediates membrane association of the hepatitis c virus nonstructural protein 5a. *The Journal of biological chemistry*, 277(10):8130–8139.

Brazzoli, M., Bianchi, A., Filippini, S., Weiner, A., Zhu, Q., Pizza, M., and Crotta, S. 2008. Cd81 is a central regulator of cellular events required for hepatitis c virus infection of human hepatocytes. *Journal of virology*, 82:8316–8329.

Burckstummer, T., Kriegs, M., Lupberger, J., Pauli, E. K., Schmittel, S., and Hildt, E. 2006. Raf-1 kinase associates with hepatitis c virus ns5a and regulates viral replication. *FEBS letters*, 580(2):575–580.

Burdette, D., Olivarez, M., and Waris, G. 2010. Activation of transcription factor nrf2 by hepatitis c virus induces the cell-survival pathway. *The Journal of general virology*, 91(Pt 3):681–690.

Cardaci, S., Filomeni, G., and Ciriolo, M. R. 2012. Redox implications of ampk-mediated signal transduction beyond energetic clues. *Journal of cell science*, 125:2115–2125.

Carvajal-Yepes, M., Himmelsbach, K., Schaedler, S., Ploen, D., Krause, J., Ludwig, L., Weiss, T., Klingel, K., and Hildt, E. 2011. Hepatitis c virus impairs the induction of cytoprotective nrf2 target genes by delocalization of small maf proteins. *The Journal of biological chemistry*, 286(11):8941–8951.

Catanese, M. T. and Dorner, M. 2015. Advances in experimental systems to study hepatitis c virus in vitro and in vivo. *Virology*, 479-480:221–233.

Catanese, M. T., Uryu, K., Kopp, M., Edwards, T. J., Andrus, L., Rice, W. J., Silvestry, M., Kuhn, R. J., and Rice, C. M. 2013. Ultrastructural analysis of hepatitis c virus particles. *Proceedings of the National Academy of Sciences of the United States of America*, 110(23):9505–9510.

Chan, K., Robinson, M., Yang, H., Cornew, S., and IV, W. E. D. 2013. Development of a robust luciferase reporter 1b/2a hepatitis c virus hcv for characterization of early stage hcv life cycle inhibitors. *Antiviral Research*, 98(1):85–92.

Chan, S.-W. 2005. Hepatitis c virus envelope proteins regulate CHOP via induction of the unfolded protein response. *The FASEB Journal*.

Chang, K.-S., Jiang, J., Cai, Z., and Luo, G. 2007. Human apolipoprotein e is required for infectivity and production of hepatitis c virus in cell culture. *Journal of virology*, 81(24):13783–13793.

Chen, C., Deng, M., Sun, Q., Loughran, P., Billiar, T. R., and Scott, M. J. 2014. Lipopolysaccharide stimulates p62-dependent autophagy-like aggregate clearance in hepatocytes. *BioMed Research International*, 2014:1–13.

Choo, Q. L., Kuo, G., Ralston, R., Weiner, A., Chien, D., Van Nest, G., Han, J., Berger, K., Thudium, K., and Kuo, C. 1994. Vaccination of chimpanzees against infection by the hepatitis c virus. *Proceedings of the National Academy of Sciences of the United States of America*, 91:1294–1298.

Choo, Q. L., Kuo, G., Weiner, A. J., Overby, L. R., Bradley, D. W., and Houghton, M. 1989. Isolation of a cdna clone derived from a blood-borne non-a, non-b viral hepatitis genome. *Science (New York, N.Y.)*, 244:359–362.

Choukhi, A., Ung, S., Wychowski, C., and Dubuisson, J. 1998. Involvement of endoplasmic reticulum chaperones in the folding of hepatitis c virus glycoproteins. *Journal of virology*, 72(5):3851–3858.

Chu, V. C., Bhattacharya, S., Nomoto, A., Lin, J., Zaidi, S. K., Oberley, T. D., Weinman, S. A., Azhar, S., and Huang, T.-T. 2011. Persistent expression of hepatitis c virus non-structural proteins leads to increased autophagy and mitochondrial injury in human hepatoma cells. *PLoS ONE*, 6(12):e28551.

Cocquerel, L., Meunier, J. C., Pillez, A., Wychowski, C., and Dubuisson, J. 1998. A retention signal necessary and sufficient for endoplasmic reticulum localization maps to the transmembrane domain of hepatitis c virus glycoprotein e2. *Journal of virology*, 72(3):2183–2191.

Coller, K. E., Berger, K. L., Heaton, N. S., Cooper, J. D., Yoon, R., and Randall, G. 2009. Rna interference and single particle tracking analysis of hepatitis c virus endocytosis. *PLoS Pathogens*, 5(12):e1000702.

Coller, K. E., Heaton, N. S., Berger, K. L., Cooper, J. D., Saunders, J. L., and Randall, G. 2012. Molecular determinants and dynamics of hepatitis c virus secretion. *PLoS Pathogens*, 8(1):e1002466.

Copple, I. M., Lister, A., Obeng, A. D., Kitteringham, N. R., Jenkins, R. E., Layfield, R., Foster, B. J., Goldring, C. E., and Park, B. K. 2010. Physical and functional interaction of sequestosome 1 with keap1 regulates the keap1-nrf2 cell defense pathway. *The Journal of biological chemistry*, 285(22):16782–16788.

Counihan, N. A., Rawlinson, S. M., and Lindenbach, B. D. 2011. Trafficking of hepatitis c virus core protein during virus particle assembly. *PLoS Pathogens*, 7(10):e1002302.

Cun, W., Jiang, J., and Luo, G. 2010. The c-terminal alpha-helix domain of apolipoprotein e is required for interaction with nonstructural protein 5a and assembly of hepatitis c virus. *Journal of virology*, 84(21):11532–11541.

Dao Thi, V. L., Granier, C., Zeisel, M. B., Guerin, M., Mancip, J., Granio, O., Penin, F., Lavillette, D., Bartenschlager, R., Baumert, T. F., Cosset, F.-L., and Dreux, M. 2012. Characterization of hepatitis c virus particle subpopulations reveals multiple usage of the scavenger receptor bi for entry steps. *The Journal of biological chemistry*, 287:31242–31257.

Dash, S., Chava, S., Aydin, Y., Chandra, P. K., Ferraris, P., Chen, W., Balart, L. A., Wu, T., and Garry, R. F. 2016. Hepatitis c virus infection induces autophagy as a prosurvival mechanism to alleviate hepatic er-stress response. *Viruses*, 8.

De Francesco, R. and Migliaccio, G. 2005. Challenges and successes in developing new therapies for hepatitis c. *Nature*, 436:953–960.

de Mochel, N. S. R., Seronello, S., Wang, S. H., Ito, C., Zheng, J. X., Liang, T. J., Lambeth, J. D., and Choi, J. 2010. Hepatocyte nad(p)h oxidases as an endogenous source of reactive oxygen species during hepatitis c virus infection. *Hepatology (Baltimore, Md.)*, 52:47–59.

Deleersnyder, V., Pillez, A., Wychowski, C., Blight, K., Xu, J., Hahn, Y. S., Rice, C. M., and Dubuisson, J. 1997. Formation of native hepatitis c virus glycoprotein complexes. *Journal of virology*, 71:697–704.

Deretic, V. and Levine, B. 2009. Autophagy, immunity, and microbial adaptations. *Cell host & microbe*, 5:527–549.

Diamond, D. L., Syder, A. J., Jacobs, J. M., Sorensen, C. M., Walters, K.-A., Proll, S. C., McDermott, J. E., Gritsenko, M. A., Zhang, Q., Zhao, R., Metz, T. O., Camp, D. G., Waters, K. M., Smith, R. D., Rice, C. M., and Katze, M. G. 2010. Temporal proteome and lipidome profiles reveal hepatitis c virus-associated reprogramming of hepatocellular metabolism and bioenergetics. *PLoS Pathogens*, 6(1):e1000719.

Dionisio, N., Garcia-Mediavilla, M. V., Sanchez-Campos, S., Majano, P. L., Benedicto, I., Rosado, J. A., Salido, G. M., and Gonzalez-Gallego, J. 2009. Hepatitis c virus ns5a and core proteins induce oxidative stress-mediated calcium signalling alterations in hepatocytes. *Journal of Hepatology*, 50(5):872–882.

Dorner, M., Horwitz, J. A., Robbins, J. B., Barry, W. T., Feng, Q., Mu, K., Jones, C. T., Schoggins, J. W., Catanese, M. T., Burton, D. R., Law, M., Rice, C. M., and Ploss, A. 2011. A genetically humanized mouse model for hepatitis c virus infection. *Nature*, 474(7350):208–211.

Douam, F., Thi, V. L. D., Maurin, G., Fresquet, J., Mompelat, D., Zeisel, M. B., Baumert, T. F., Cosset, F.-L., and Lavillette, D. 2014. Critical interaction between e1 and e2 glycoproteins determines binding and fusion properties of hepatitis c virus during cell entry. *Hepatology*, 59(3):776–788.

Dreux, M., Gastaminza, P., Wieland, S. F., and Chisari, F. V. 2009. The autophagy machinery is required to initiate hepatitis c virus replication. *Proceedings of the National Academy of Sciences of the United States of America*, 106(33):14046–14051.

Drummer, H. E., Maerz, A., and Poumbourios, P. 2003. Cell surface expression of functional hepatitis c virus e1 and e2 glycoproteins. *FEBS letters*, 546:385–390.

Dubuisson, J. and Cosset, F.-L. 2014. Virology and cell biology of the hepatitis c virus life cycle–an update. *Journal of hepatology*, 61(1 Suppl):S3–S13.

Dubuisson, J., Hsu, H. H., Cheung, R. C., Greenberg, H. B., Russell, D. G., and Rice, C. M. 1994. Formation and intracellular localization of hepatitis c virus envelope glycoprotein complexes expressed by recombinant vaccinia and sindbis viruses. *Journal of virology*, 68:6147–6160.

Duran, A., Amanchy, R., Linares, J. F., Joshi, J., Abu-Baker, S., Porollo, A., Hansen, M., Moscat, J., and Diaz-Meco, M. T. 2011. p62 is a key regulator of nutrient sensing in the mtorc1 pathway. *Molecular cell*, 44:134–146.

Egger, D., Wolk, B., Gosert, R., Bianchi, L., Blum, H. E., Moradpour, D., Bienz, K., Egger, D., Wolk, B., Gosert, R., Bianchi, L., Blum, H. E., Moradpour, D., and Bienz, K. 2002. Expression of hepatitis c virus proteins induces distinct membrane alterations including a candidate viral replication complex. *Journal of virology*, 76(12):5974–5984.

El-Serag, H. B. 2002. Hepatocellular carcinoma and hepatitis c in the united states. *Hepatology (Baltimore, Md.)*, 36:S74–S83.

Elgner, F. 2016. *Charakterisierung des endosomalen Freisetzungswegs von Hepatitis-C-Virionen*. PhD thesis.

Elgner, F., Ren, H., Medvedev, R., Ploen, D., Himmelsbach, K., Boller, K., and Hildt, E. 2016. The intra-cellular cholesterol transport inhibitor u18666a inhibits the exosome-dependent release of mature hepatitis c virus. *Journal of virology*.

Eskelinen, E.-L. and Saftig, P. 2009. Autophagy: a lysosomal degradation pathway with a central role in health and disease. *Biochimica et biophysica acta*, 1793(4):664–673.

Evans, M. J., von Hahn, T., Tscherne, D. M., Syder, A. J., Panis, M., Wolk, B., Hatziioannou, T., McKeating, J. A., Bieniasz, P. D., and Rice, C. M. 2007. Claudin-1 is a hepatitis c virus co-receptor required for a late step in entry. *Nature*, 446(7137):801–805.

Fader, C. M. and Colombo, M. I. 2009. Autophagy and multivesicular bodies: two closely related partners. *Cell death and differentiation*, 16(1):70–78.

Fahmy, A. M. and Labonte, P. 2017. The autophagy elongation complex (atg5-12/16l1) positively regulates hcv replication and is required for wild-type membranous web formation. *Scientific reports*, 7:40351.

Fan, W., Tang, Z., Chen, D., Moughon, D., Ding, X., Chen, S., Zhu, M., and Zhong, Q. 2010. Keap1 facilitates p62-mediated ubiquitin aggregate clearance via autophagy. *Autophagy*, 6(5):614–621.

Farci, P. and Purcell, R. H. 2000. Clinical significance of hepatitis c virus genotypes and quasispecies. *Seminars in liver disease*, 20:103–126.

Farquhar, M. J., Harris, H. J., Diskar, M., Jones, S., Mee, C. J., Nielsen, S. U., Brimacombe, C. L., Molina, S., Toms, G. L., Maurel, P., Howl, J., Herberg, F. W., van Ijzendoorn, S. C. D., Balfe, P., and McKeating, J. A. 2008. Protein kinase a-dependent step(s) in hepatitis c virus entry and infectivity. *Journal of virology*, 82:8797–8811.

Farquhar, M. J., Hu, K., Harris, H. J., Davis, C., Brimacombe, C. L., Fletcher, S. J., Baumert, T. F., Rappoport, J. Z., Balfe, P., and McKeating, J. A. 2012. Hepatitis c virus induces cd81 and claudin-1 endocytosis. *Journal of virology*, 86(8):4305–4316.

Farquhar, M. J. and McKeating, J. A. 2008. Primary hepatocytes as targets for hepatitis c virus replication. *Journal of viral hepatitis*, 15:849–854.

Fattori, E., Zampaglione, I., Arcuri, M., Meola, A., Ercole, B. B., Cirillo, A., Folgori, A., Bett, A., Cappelletti, M., Sporeno, E., Cortese, R., Nicosia, A., and Colloca, S. 2006. Efficient immunization of rhesus macaques with an hcv candidate vaccine by heterologous priming-boosting with novel adenoviral vectors based on different serotypes. *Gene therapy*, 13:1088–1096.

Feinstone, S. M., Kapikian, A. Z., Purcell, R. H., Alter, H. J., and Holland, P. V. 1975. Transfusion-associated hepatitis not due to viral hepatitis type a or b. *Reviews in medical virology*, 11:3–8; discussion 8–9.

Ferraris, P., Blanchard, E., and Roingeard, P. 2010. Ultrastructural and biochemical analyses of hepatitis c virus-associated host cell membranes. *The Journal of general virology*, 91(Pt 9):2230–2237.

Filomeni, G., de Zio, D., and Cecconi, F. 2015. Oxidative stress and autophagy: the clash between damage and metabolic needs. *Cell death and differentiation*, 22(3):377–388.

Firbas, C., Boehm, T., Buerger, V., Schuller, E., Sabarth, N., Jilma, B., and Klade, C. S. 2010. Immunogenicity and safety of different injection routes and schedules of ic41, a hepatitis c virus (hcv) peptide vaccine. *Vaccine*, 28:2397–2407.

Firbas, C., Jilma, B., Tauber, E., Buerger, V., Jelovcan, S., Lingnau, K., Buschle, M., Frisch, J., and Klade, C. S. 2006. Immunogenicity and safety of a novel therapeutic hepatitis c virus (hcv) peptide vaccine: a randomized, placebo controlled trial for dose optimization in 128 healthy subjects. *Vaccine*, 24:4343–4353.

Folgori, A., Capone, S., Ruggeri, L., Meola, A., Sporeno, E., Ercole, B. B., Pezzanera, M., Tafi, R., Arcuri, M., Fattori, E., Lahm, A., Luzzago, A., Vitelli, A., Colloca, S., Cortese, R., and Nicosia, A. 2006. A t-cell hcv vaccine eliciting effective immunity against heterologous virus challenge in chimpanzees. *Nature medicine*, 12:190–197.

Forns, X., Purcell, R. H., and Bukh, J. 1999. Quasispecies in viral persistence and pathogenesis of hepatitis c virus. *Trends in microbiology*, 7:402–410.

Friebe, P., Lohmann, V., Krieger, N., and Bartenschlager, R. 2001. Sequences in the 5' nontranslated region of hepatitis c virus required for rna replication. *Journal of virology*, 75:12047–12057.

Fu, N., Yao, H., Nan, Y., and Qiao, L. 2016. Role of oxidative stress in hepatitis c virus induced hepatocellular carcinoma. *Current cancer drug targets*.

Gale, M. and Foy, E. M. 2005. Evasion of intracellular host defence by hepatitis c virus. *Nature*, 436:939–945.

Gale, M. J., Korth, M. J., Tang, N. M., Tan, S. L., Hopkins, D. A., Dever, T. E., Polyak, S. J., Gretch, D. R., and Katze, M. G. 1997. Evidence that hepatitis c virus resistance to interferon is mediated through repression of the pkr protein kinase by the nonstructural 5a protein. *Virology*, 230(2):217–227.

Gallinari, P., Brennan, D., Nardi, C., Brunetti, M., Tomei, L., Steinkuehler, C., and De Francesco, R. 1998. Multiple enzymatic activities associated with recombinant ns3 protein of hepatitis c virus. *Journal of virology*, 72:6758–6769.

Ganley, I. G., Du Lam, H., Wang, J., Ding, X., Chen, S., and Jiang, X. 2009. Ulk1.atg13.fip200 complex mediates mtor signaling and is essential for autophagy. *The Journal of biological chemistry*, 284(18):12297–12305.

Gastaminza, P., Cheng, G., Wieland, S., Zhong, J., Liao, W., and Chisari, F. V. 2008. Cellular determinants of hepatitis c virus assembly, maturation, degradation, and secretion. *Journal of virology*, 82(5):2120–2129.

Gastaminza, P., Dryden, K. A., Boyd, B., Wood, M. R., Law, M., Yeager, M., and Chisari, F. V. 2010. Ultrastructural and biophysical characterization of hepatitis c virus particles produced in cell culture. *Journal of virology*, 84(21):10999–11009.

Gastaminza, P., Kapadia, S. B., and Chisari, F. V. 2006. Differential biophysical properties of infectious intracellular and secreted hepatitis c virus particles. *Journal of Virology*, 80(22):11074–11081.

Gaudy, C., Thevenas, C., Tichet, J., Mariotte, N., Goudeau, A., and Dubois, F. 2005. Usefulness of the hepatitis c virus core ntigen assay for screening of a population undergoing routine medical checkup. *Journal of Clinical Microbiology*, 43(4):1722–1726.

Germi, R., Crance, J.-M., Garin, D., Guimet, J., Lortat-Jacob, H., Ruigrok, R. W. H., Zarski, J.-P., and Drouet, E. 2002. Cellular glycosaminoglycans and low density lipoprotein receptor are involved in hepatitis c virus adsorption. *Journal of medical virology*, 68(2):206–215.

Ghany, M. G., Nelson, D. R., Strader, D. B., Thomas, D. L., Seeff, L. B., and for Study of Liver Diseases, A. A. 2011. An update on treatment of genotype 1 chronic hepatitis c virus infection: 2011 practice guideline by the american association for the study of liver diseases. *Hepatology (Baltimore, Md.)*, 54:1433–1444.

Ghasemi, F. 2015. Progress in the development of vaccines for hepatitis c virus infection. *World Journal of Gastroenterology*, 21(42):11984.

Giordano, S., Darley-Usmar, V., and Zhang, J. 2014. Autophagy as an essential cellular antioxidant pathway in neurodegenerative disease. *Redox biology*, 2:82–90. Original DateCompleted: 20140624.

Goffard, A., Callens, N., Bartosch, B., Wychowski, C., Cosset, F.-L., Montpellier, C., and Dubuisson, J. 2005. Role of n-linked glycans in the functions of hepatitis c virus envelope glycoproteins. *Journal of virology*, 79:8400–8409.

Gomes, L. C. and Dikic, I. 2014. Autophagy in antimicrobial immunity. *Molecular cell*, 54:224–233.

Gondeau, C., Briolotti, P., Razafy, F., Duret, C., Rubbo, P.-A., Helle, F., Reme, T., Ripault, M.-P., Ducos, J., Fabre, J.-M., Ramos, J., Pecheur, E.-I., Larrey, D., Maurel, P., and Daujat-Chavanieu, M. 2014. In vitro infection of primary human hepatocytes by hcv-positive sera: insights on a highly relevant model. *Gut*, 63:1490–1500.

Gottwein, J. M. and Bukh, J. 2008. Cutting the gordian knot-development and biological relevance of hepatitis c virus cell culture systems. *Advances in virus research*, 71:51–133.

Gottwein, J. M., Jensen, T. B., Mathiesen, C. K., Meuleman, P., Serre, S. B. N., Lademann, J. B., Ghanem, L., Scheel, T. K. H., Leroux-Roels, G., and Bukh, J. 2011. Development and application of hepatitis c reporter viruses with genotype 1 to 7 core-nonstructural protein 2 ns2 expressing fluorescent proteins or luciferase in modified jfh1 ns5a. *Journal of Virology*, 85(17):8913–8928.

Gouttenoire, J., Roingeard, P., Penin, F., and Moradpour, D. 2010. Amphipathic alpha-helix ah2 is a major determinant for the oligomerization of hepatitis c virus nonstructural protein 4b. *Journal of Virology*, 84(24):12529–12537.

Griffin, S. D. C., Beales, L. P., Clarke, D. S., Worsfold, O., Evans, S. D., Jaeger, J., Harris, M. P. G., and Rowlands, D. J. 2003. The p7 protein of hepatitis c virus forms an ion channel that is blocked by the antiviral drug, amantadine. *FEBS letters*, 535(1-3):34–38.

Guevin, C., Manna, D., Belanger, C., Konan, K. V., Mak, P., and Labonte, P. 2010. Autophagy protein atg5 interacts transiently with the hepatitis c virus rna polymerase ns5b early during infection. *Virology*, 405(1):1–7.

Hailey, D. W., Rambold, A. S., Satpute-Krishnan, P., Mitra, K., Sougrat, R., Kim, P. K., and Lippincott-Schwartz, J. 2010. Mitochondria supply membranes for autophagosome biogenesis during starvation. *Cell*, 141(4):656–667.

Hamasaki, M., Furuta, N., Matsuda, A., Nezu, A., Yamamoto, A., Fujita, N., Oomori, H., Noda, T., Haraguchi, T., Hiraoka, Y., Amano, A., and Yoshimori, T. 2013. Autophagosomes form at er-mitochondria contact sites. *Nature*, 495(7441):389–393.

Hansen, M. D., Johnsen, I. B., Stiberg, K. A., Sherstova, T., Wakita, T., Richard, G. M., Kandasamy, R. K., Meurs, E. F., and Anthonsen, M. W. 2017. Hepatitis c virus triggers golgi fragmentation and autophagy through the immunity-related gtpase m. *Proceedings of the National Academy of Sciences of the United States of America*.

Harder, B., Jiang, T., Wu, T., Tao, S., de la Vega, M. R., Tian, W., Chapman, E., and Zhang, D. D. 2015. Molecular mechanisms of nrf2 regulation and how these influence chemical modulation for disease intervention. *Biochemical Society transactions*, 43(4):680–686.

Harris, H. J., Davis, C., Mullins, J. G. L., Hu, K., Goodall, M., Farquhar, M. J., Mee, C. J., McCaffrey, K., Young, S., Drummer, H., Balfe, P., and McKeating, J. A. 2010. Claudin association with cd81 defines hepatitis c virus entry. *The Journal of biological chemistry*, 285(27):21092–21102.

Harris, H. J., Farquhar, M. J., Mee, C. J., Davis, C., Reynolds, G. M., Jennings, A., Hu, K., Yuan, F., Deng, H., Hubscher, S. G., Han, J. H., Balfe, P., and McKeating, J. A. 2008. Cd81 and claudin 1 coreceptor association: Role in hepatitis c virus entry. *Journal of Virology*, 82(10):5007–5020.

He, L. F., Alling, D., Popkin, T., Shapiro, M., Alter, H. J., and Purcell, R. H. 1987. Determining the size of non-a, non-b hepatitis virus by filtration. *The Journal of infectious diseases*, 156:636–640.

Herker, E., Harris, C., Hernandez, C., Carpentier, A., Kaehlcke, K., Rosenberg, A. R., Farese, R. V., and Ott, M. 2010. Efficient hepatitis c virus particle formation requires diacylglycerol acyltransferase-1. *Nature Medicine*, 16(11):1295–1298.

Higdon, A., Diers, A. R., Oh, J. Y., Landar, A., and Darley-Usmar, V. M. 2012. Cell signalling by reactive lipid species: new concepts and molecular mechanisms. *The Biochemical journal*, 442:453–464.

Himmelsbach, K., Sauter, D., Baumert, T. F., Ludwig, L., Blum, H. E., and Hildt, E. 2009. New aspects of an anti-tumour drug: sorafenib efficiently inhibits hcv replication. *Gut*, 58(12):1644–1653.

Hoffman, B. and Liu, Q. 2011. Hepatitis c viral protein translation: mechanisms and implications in developing antivirals. *Liver international : official journal of the International Association for the Study of the Liver*, 31:1449–1467.

Hosokawa, N., Hara, T., Kaizuka, T., Kishi, C., Takamura, A., Miura, Y., Iemura, S.-i., Natsume, T., Takehana, K., Yamada, N., Guan, J.-L., Oshiro, N., and Mizushima, N. 2009. Nutrient-dependent mtorc1 association with the ulk1–atg13–fip200 complex required for autophagy. *Molecular biology of the cell*, (20):1981–1991.

Hsu, M., Zhang, J., Flint, M., Logvinoff, C., Cheng-Mayer, C., Rice, C. M., and McKeating, J. A. 2003. Hepatitis c virus glycoproteins mediate ph-dependent cell entry of pseudotyped retroviral particles. *Proceedings of the National Academy of Sciences of the United States of America*, 100(12):7271–7276.

Huegle, T., Fehrmann, F., Bieck, E., Kohara, M., Kraeusslich, H. G., Rice, C. M., Blum, H. E., and Moradpour, D. 2001. The hepatitis c virus nonstructural protein 4b is an integral endoplasmic reticulum membrane protein. *Virology*, 284:70–81.

Huessy, P., Langen, H., Mous, J., and Jacobsen, H. 1996. Hepatitis c virus core protein: carboxy-terminal boundaries of two processed species suggest cleavage by a signal peptide peptidase. *Virology*, 224:93–104.

Hulst, M. M. and Moormann, R. J. 1997. Inhibition of pestivirus infection in cell culture by envelope proteins e(rns) and e2 of classical swine fever virus: E(rns) and e2 interact with different receptors. *The Journal of general virology*, 78 (Pt 11):2779–2787.

Ichimura, Y., Kirisako, T., Takao, T., Satomi, Y., Shimonishi, Y., Ishihara, N., Mizushima, N., Tanida, I., Kominami, E., Ohsumi, M., Noda, T., and Ohsumi, Y. 2000. A ubiquitin-like system mediates protein lipidation. *Nature*, 408:488–492.

Ichimura, Y., Waguri, S., Sou, Y.-S., Kageyama, S., Hasegawa, J., Ishimura, R., Saito, T., Yang, Y., Kouno, T., Fukutomi, T., Hoshii, T., Hirao, A., Takagi, K., Mizushima, T., Motohashi, H., Lee, M.-S., Yoshimori, T., Tanaka, K., Yamamoto, M., and Komatsu, M. 2013. Phosphorylation of p62 activates the keap1-nrf2 pathway during selective autophagy. *Molecular cell*, 51(5):618–631.

Inami, Y., Waguri, S., Sakamoto, A., Kouno, T., Nakada, K., Hino, O., Watanabe, S., Ando, J., Iwadate, M., Yamamoto, M., Lee, M.-S., Tanaka, K., and Komatsu, M. 2011. Persistent activation of nrf2 through p62 in hepatocellular carcinoma cells. *The Journal of cell biology*, 193(2):275–284.

Irshad, M., Ansari, M. A., Singh, A., Nag, P., Raghvendra, L., Singh, S., and Badhal, S. S. 2010. Hcv-genotypes: a review on their origin, global status, assay system, pathogenecity and response to treatment. *Hepato-gastroenterology*, 57:1529–1538.

Irshad, M., Mankotia, D. S., and Irshad, K. 2013. An insight into the diagnosis and pathogenesis of hepatitis c virus infection. *World journal of gastroenterology*, 19:7896–7909.

Itakura, E., Kishi-Itakura, C., and Mizushima, N. 2012. The hairpin-type tail-anchored snare syntaxin 17 targets to autophagosomes for fusion with endosomes/lysosomes. *Cell*, 151(6):1256–1269.

Itakura, E. and Mizushima, N. 2010. Characterization of autophagosome formation site by a hierarchical analysis of mammalian atg proteins. *Autophagy*, 6:764–776.

Ivanov, A. V., Bartosch, B., Smirnova, O. A., Isaguliants, M. G., and Kochetkov, S. N. 2013. Hcv and oxidative stress in the liver. *Viruses*, 5(2):439–469.

Ivanov, A. V., Smirnova, O. A., Ivanova, O. N., Masalova, O. V., Kochetkov, S. N., and Isaguliants, M. G. 2011. Hepatitis c virus proteins activate nrf2/are pathway by distinct ros-dependent and independent mechanisms in huh7 cells. *PLoS ONE*, 6(9):e24957.

Ivanov, A. V., Smirnova, O. A., Petrushanko, I. Y., Ivanova, O. N., Karpenko, I. L., Alekseeva, E., Sominskaya, I., Makarov, A. A., Bartosch, B., Kochetkov, S. N., and Isaguliants, M. G. 2015. Hcv core protein uses multiple mechanisms to induce oxidative stress in human hepatoma huh7 cells. *Viruses*, 7(6):2745–2770.

Jafari, S., Copes, R., Baharlou, S., Etminan, M., and Buxton, J. 2010. Tattooing and the risk of transmission of hepatitis c: a systematic review and meta-analysis. *International journal of infectious diseases : IJID : official publication of the International Society for Infectious Diseases*, 14:e928–e940.

Jain, A., Lamark, T., Sjottem, E., Larsen, K. B., Awuh, J. A., Overvatn, A., McMahon, M., Hayes, J. D., and Johansen, T. 2010. p62/sqstm1 is a target gene for transcription factor nrf2 and creates a positive feedback loop by inducing antioxidant response element-driven gene transcription. *The Journal of biological chemistry*, 285(29):22576–22591.

Jaiswal, A. K. 2004. Nrf2 signaling in coordinated activation of antioxidant gene expression. *Free radical biology & medicine*, 36:1199–1207.

Jawaid, A. and Khuwaja, A. K. 2008. Treatment and vaccination for hepatitis c: present and future. *Journal of Ayub Medical College, Abbottabad : JAMC*, 20:129–133.

Jheng, J.-R., Ho, J.-Y., and Horng, J.-T. 2014. Er stress, autophagy, and rna viruses. *Frontiers in microbiology*, 5:388.

Jiang, P. and Mizushima, N. 2015. Lc3- and p62-based biochemical methods for the analysis of autophagy progression in mammalian cells. *Methods (San Diego, Calif.)*, 75:13–18.

Jiang, T., Harder, B., Vega, M. R. d. l., Wong, P. K., Chapman, E., and Zhang, D. D. 2015a. p62 links autophagy and nrf2 signaling. *Free radical biology & medicine*.

Jiang, Y., Bao, H., Ge, Y., Tang, W., Cheng, D., Luo, K., Gong, G., and Gong, R. 2015b. Therapeutic targeting of gsk3beta enhances the nrf2 antioxidant response and confers hepatic cytoprotection in hepatitis c. *Gut*, 64(1):168–179.

Jianjun Gao, C. J. 2017. Research progress on the direct antiviral drugs for hepatitis c virus. *BioScience Trends*.

Jirasko, V., Montserret, R., Lee, J. Y., Gouttenoire, J., Moradpour, D., Penin, F., and Bartenschlager, R. 2010. Structural and functional studies of nonstructural protein 2 of the hepatitis c virus reveal its key role as organizer of virion assembly. *PLoS Pathogens*, 6(12):e1001233.

Johansen, T. and Lamark, T. 2011. Selective autophagy mediated by autophagic adapter proteins. *Autophagy*, 7(3):279–296.

Kabeya, Y., Mizushima, N., Ueno, T., Yamamoto, A., Kirisako, T., Noda, T., Kominami, E., Ohsumi, Y., and Yoshimori, T. 2000. Lc3, a mammalian homologue of yeast apg8p, is localized in autophagosome membranes after processing. *The EMBO journal*, 19:5720–5728.

Kaerber, G. 1931. Beitrag zur kollektiven behandlung pharmakologischer reihenversuche. *Naunyn-Schmiedebergs Archiv fuer Experimentelle Pathologie und Pharmakologie*, 162(4):480–483.

Kansanen, E., Kuosmanen, S. M., Leinonen, H., and Levonen, A.-L. 2013. The keap1-nrf2 pathway: Mechanisms of activation and dysregulation in cancer. *Redox biology*, 1:45–49. Original DateCompleted: 20140624.

Kasprzak, A., Seidel, J., Biczysko, W., Wysocki, J., Spachacz, R., and Zabel, M. 2005. Intracellular localization of NS3 and c proteins in chronic hepatitis c. *Liver International*, 25(4):896–903.

Katsuragi, Y., Ichimura, Y., and Komatsu, M. 2015. p62/sqstm1 functions as a signaling hub and an autophagy adaptor. *The FEBS journal*.

Ke, P.-Y. and Chen, S. S.-L. 2011a. Activation of the unfolded protein response and autophagy after hepatitis c virus infection suppresses innate antiviral immunity in vitro. *The Journal of clinical investigation*, 121(1):37–56.

Ke, P.-Y. and Chen, S. S.-L. 2011b. Autophagy: A novel guardian of hcv against innate immune response. *Autophagy*, 7(5):533–535.

Kensler, T. W., Wakabayashi, N., and Biswal, S. 2007. Cell survival responses to environmental stresses via the keap1-nrf2-are pathway. *Annual review of pharmacology and toxicology*, 47:89–116.

Kim, A. Y., Nagami, E. H., Birch, C. E., Bowen, M. J., Lauer, G. M., and McGovern, B. H. 2013. A simple strategy to identify acute hepatitis c virus infection among newly incarcerated injection drug users. *Hepatology*, 57(3):944–952.

Kim, J., Kundu, M., Viollet, B., and Guan, K.-L. 2011. Ampk and mtor regulate autophagy through direct phosphorylation of ulk1. *Nature Cell Biology*, 13(2):132–141.

Kim, J. L., Morgenstern, K. A., Lin, C., Fox, T., Dwyer, M. D., Landro, J. A., Chambers, S. P., Markland, W., Lepre, C. A., O'Malley, E. T., Harbeson, S. L., Rice, C. M., Murcko, M. A., Caron, P. R., and Thomson, J. A. 1996. Crystal structure of the hepatitis c virus ns3 protease domain complexed with a synthetic ns4a cofactor peptide. *Cell*, 87(2):343–355.

Kimura, S., Fujita, N., Noda, T., and Yoshimori, T. 2009. Monitoring autophagy in mammalian cultured cells through the dynamics of lc3. *Methods in enzymology*, 452:1–12.

Kirisako, T., Baba, M., Ishihara, N., Miyazawa, K., Ohsumi, M., Yoshimori, T., Noda, T., and Ohsumi, Y. 1999. Formation process of autophagosome is traced with apg8/aut7p in yeast. *The Journal of cell biology*, 147:435–446.

Kirisako, T., Ichimura, Y., Okada, H., Kabeya, Y., Mizushima, N., Yoshimori, T., Ohsumi, M., Takao, T., Noda, T., and Ohsumi, Y. 2000. The reversible modification regulates the membrane-binding state of apg8/aut7 essential for autophagy and the cytoplasm to vacuole targeting pathway. *The Journal of cell biology*, 151:263–276.

Kobayashi, M. and Yamamoto, M. 2005. Molecular mechanisms activating the nrf2-keap1 pathway of antioxidant gene regulation. *Antioxidants & redox signaling*, 7:385–394.

Kolykhalov, A. A. 1997. Transmission of hepatitis c by intrahepatic inoculation with transcribed rna. *Science*, 277(5325):570–574.

Kolykhalov, A. A., Feinstone, S. M., and Rice, C. M. 1996. Identification of a highly conserved sequence element at the 3' terminus of hepatitis c virus genome rna. *Journal of virology*, 70:3363–3371.

Komatsu, M., Kageyama, S., and Ichimura, Y. 2012. p62/sqstm1/a170: physiology and pathology. *Pharmacological research : the official journal of the Italian Pharmacological Society*, 66(6):457–462.

Komatsu, M., Kurokawa, H., Waguri, S., Taguchi, K., Kobayashi, A., Ichimura, Y., Sou, Y.-S., Ueno, I., Sakamoto, A., Tong, K. I., Kim, M., Nishito, Y., Iemura, S.-i., Natsume, T., Ueno, T., Kominami, E., Motohashi, H., Tanaka, K., and Yamamoto, M. 2010. The selective autophagy substrate p62 activates the stress responsive transcription factor nrf2 through inactivation of keap1. *Nature Cell Biology*, 12(3):213–223.

Kongara, S. and Karantza, V. 2012. The interplay between autophagy and ros in tumorigenesis. *Frontiers in Oncology*, 2.

Kopp, M., Murray, C. L., Jones, C. T., and Rice, C. M. 2010. Genetic analysis of the carboxy-terminal region of the hepatitis c virus core protein. *Journal of virology*, 84:1666–1673.

Korenaga, M., Wang, T., Li, Y., Showalter, L. A., Chan, T., Sun, J., and Weinman, S. A. 2005. Hepatitis c virus core protein inhibits mitochondrial electron transport and increases reactive oxygen species (ROS) production. *Journal of Biological Chemistry*, 280(45):37481–37488.

Koutsoudakis, G., Kaul, A., Steinmann, E., Kallis, S., Lohmann, V., Pietschmann, T., and Bartenschlager, R. 2006. Characterization of the early steps of hepatitis c virus infection by using luciferase reporter viruses. *Journal of virology*, 80(11):5308–5320.

Kriegs, M., Burckstummer, T., Himmelsbach, K., Bruns, M., Frelin, L., Ahlen, G., Sallberg, M., and Hildt, E. 2009. The hepatitis c virus non-structural ns5a protein impairs both the innate and adaptive hepatic immune response in vivo. *The Journal of biological chemistry*, 284(41):28343–28351.

Kroemer, G., Marino, G., and Levine, B. 2010. Autophagy and the integrated stress response. *Molecular cell*, 40(2):280–293.

Kwak, M.-K. and Kensler, T. W. 2006. Induction of 26s proteasome subunit psmb5 by the bifunctional inducer 3-methylcholanthrene through the nrf2-are, but not the ahr/arnt-xre, pathway. *Biochemical and biophysical research communications*, 345(4):1350–1357.

Laemmli, U. K. 1970. Cleavage of structural proteins during the assembly of the head of bacteriophage t4. *Nature*, 227(5259):680–685.

Lai, C.-K., Jeng, K.-S., Machida, K., and Lai, M. M. C. 2010. Hepatitis c virus egress and release depend on endosomal trafficking of core protein. *Journal of virology*, 84(21):11590–11598.

Lai, C.-K., Saxena, V., Tseng, C.-H., Jeng, K.-S., Kohara, M., and Lai, M. M. C. 2014. Nonstructural protein 5a is incorporated into hepatitis c virus low-density particle through interaction with core protein and microtubules during intracellular transport. *PLoS ONE*, 9(6):e99022.

Lai, S.-C. and Devenish, R. J. 2012. Lc3-associated phagocytosis (lap): Connections with host autophagy. *Cells*, 1:396–408.

Lamark, T., Perander, M., Outzen, H., Kristiansen, K., overvatn, A., Michaelsen, E., Bjorkoy, G., and Johansen, T. 2003. Interaction codes within the family of mammalian phox and bem1p domain-containing proteins. *The Journal of biological chemistry*, 278:34568–34581.

Lang Kuhs, K. A., Ginsberg, A. A., Yan, J., Wiseman, R. W., Khan, A. S., Sardesai, N. Y., O'Connor, D. H., and Weiner, D. B. 2012. Hepatitis c virus ns3/ns4a dna vaccine induces multiepitope t cell responses in rhesus macaques mimicking human immune responses [corrected]. *Molecular therapy : the journal of the American Society of Gene Therapy*, 20:669–678.

Lanini, S., Easterbrook, P. J., Zumla, A., and Ippolito, G. 2016. Hepatitis c: Global epidemiology and strategies for control. *Clinical microbiology and infection : the official publication of the European Society of Clinical Microbiology and Infectious Diseases*.

Latimer, B., Toporovski, R., Yan, J., Pankhong, P., Morrow, M. P., Khan, A. S., Sardesai, N. Y., Welles, S. L., Jacobson, J. M., Weiner, D. B., and Kutzler, M. A. 2014. Strong hcv ns3/4a, ns4b, ns5a, ns5b-specific cellular immune responses induced in rhesus macaques by a novel hcv genotype 1a/1b consensus dna vaccine. *Human vaccines & immunotherapeutics*, 10:2357–2365.

Lau, A., Wang, X.-J., Zhao, F., Villeneuve, N. F., Wu, T., Jiang, T., Sun, Z., White, E., and Zhang, D. D. 2010. A noncanonical mechanism of nrf2 activation by autophagy deficiency: direct interaction between keap1 and p62. *Molecular and cellular biology*, 30(13):3275–3285.

Lauer, G. M. 2013. Immune responses to hepatitis c virus (hcv) infection and the prospects for an effective hcv vaccine or immunotherapies. *The Journal of infectious diseases*, 207 Suppl 1:S7–S12.

Lavillette, D., Pecheur, E.-I., Donot, P., Fresquet, J., Molle, J., Corbau, R., Dreux, M., Penin, F., and Cosset, F.-L. 2007. Characterization of fusion determinants points to the involvement of three discrete regions of both e1 and e2 glycoproteins in the membrane fusion process of hepatitis c virus. *Journal of Virology*, 81(16):8752–8765.

Lee, H., Jeong, M., Oh, J., Cho, Y., Shen, X., Stone, J., Yan, J., Rothkopf, Z., Khan, A. S., Cho, B. M., Park, Y. K., Weiner, D. B., Son, W.-C., and Maslow, J. N. 2017. Preclinical evaluation of multi antigenic hcv dna vaccine for the prevention of hepatitis c virus infection. *Scientific Reports*, 7:43531.

Lefevre, M., Felmlee, D. J., Parnot, M., Baumert, T. F., and Schuster, C. 2014. Syndecan 4 is involved in mediating hcv entry through interaction with lipoviral particle-associated apolipoprotein e. *PLoS ONE*, 9(4):e95550.

Lesburg, C. A., Cable, M. B., Ferrari, E., Hong, Z., Mannarino, A. F., and Weber, P. C. 1999. Crystal structure of the rna-dependent rna polymerase from hepatitis c virus reveals a fully encircled active site. *Nature structural biology*, 6(10):937–943.

Levin, A., Neufeldt, C. J., Pang, D., Wilson, K., Loewen-Dobler, D., Joyce, M. A., Wozniak, R. W., and Tyrrell, D. L. J. 2014. Functional characterization of nuclear localization and export signals in hepatitis c virus proteins and their role in the membranous web. *PloS one*, 9:e114629.

Levin, M. K., Gurjar, M., and Patel, S. S. 2005. A brownian motor mechanism of translocation and strand separation by hepatitis c virus helicase. *Nature structural & molecular biology*, 12:429–435.

Levonen, A.-L., Hill, B. G., Kansanen, E., Zhang, J., and Darley-Usmar, V. M. 2014. Redox regulation of antioxidants, autophagy, and the response to stress: implications for electrophile therapeutics. *Free radical biology & medicine*, 71:196–207.

Li, L., Chen, Y., and Gibson, S. B. 2013. Starvation-induced autophagy is regulated by mitochondrial reactive oxygen species leading to ampk activation. *Cellular signalling*, 25:50–65.

Li, L., Ishdorj, G., and Gibson, S. B. 2012. Reactive oxygen species regulation of autophagy in cancer: implications for cancer treatment. *Free radical biology & medicine*, 53:1399–1410.

Linares, J. F., Duran, A., Reina-Campos, M., Aza-Blanc, P., Campos, A., Moscat, J., and Diaz-Meco, M. T. 2015. Amino acid activation of mtorc1 by a pb1-domain-driven kinase complex cascade. *Cell Reports*, 12(8):1339–1352.

Linares, J. F., Duran, A., Yajima, T., Pasparakis, M., Moscat, J., and Diaz-Meco, M. T. 2013. K63 polyubiquitination and activation of mtor by the p62-traf6 complex in nutrient-activated cells. *Molecular Cell*, 51(3):283–296.

Lindenbach, B. D., Evans, M. J., Syder, A. J., Wolk, B., Tellinghuisen, T. L., Liu, C. C., Maruyama, T., Hynes, R. O., Burton, D. R., McKeating, J. A., and Rice, C. M. 2005. Complete replication of hepatitis c virus in cell culture. *Science (New York, N.Y.)*, 309(5734):623–626.

Lindenbach, B. D., Meuleman, P., Ploss, A., Vanwolleghem, T., Syder, A. J., McKeating, J. A., Lanford, R. E., Feinstone, S. M., Major, M. E., Leroux-Roels, G., and Rice, C. M. 2006. Cell culture-grown hepatitis c virus is infectious in vivo and can be recultured in vitro. *Proceedings of the National Academy of Sciences of the United States of America*, 103(10):3805–3809.

Lindenbach, B. D. and Rice, C. M. 2013. The ins and outs of hepatitis c virus entry and assembly. *Nature Reviews Microbiology*, 11(10):688–700.

Ling, J., Kang, Y., Zhao, R., Xia, Q., Lee, D.-F., Chang, Z., Li, J., Peng, B., Fleming, J. B., Wang, H., Liu, J., Lemischka, I. R., Hung, M.-C., and Chiao, P. J. 2012. Krasg12d-induced

ikk2/beta/nf-kappab activation by il-1palpha and p62 feedforward loops is required for development of pancreatic ductal adenocarcinoma. *Cancer Cell*, 21(1):105–120.

Loboda, A., Damulewicz, M., Pyza, E., Jozkowicz, A., and Dulak, J. 2016. Role of nrf2/ho-1 system in development, oxidative stress response and diseases: an evolutionarily conserved mechanism. *Cellular and molecular life sciences : CMLS*, 73:3221–3247.

Lohmann, V. 2013. Hepatitis c virus rna replication. *Curr.Top.Microbiol.Immunol.*, 369:167–198.

Lohmann, V., Koerner, F., Koch, J., Herian, U., Theilmann, L., and Bartenschlager, R. 1999a. Replication of subgenomic hepatitis c virus rnas in a hepatoma cell line. *Science (New York, N.Y.)*, 285:110–113.

Lohmann, V., Korner, F., Dobierzewska, A., and Bartenschlager, R. 2001. Mutations in hepatitis c virus rnas conferring cell culture adaptation. *Journal of Virology*, 75(3):1437–1449.

Lohmann, V., Korner, F., Koch, J., Herian, U., Theilmann, L., and Bartenschlager, R. 1999b. Replication of subgenomic hepatitis c virus rnas in a hepatoma cell line. *Science (New York, N.Y.)*, 285(5424):110–113.

Lorenz, I. C., Marcotrigiano, J., Dentzer, T. G., and Rice, C. M. 2006. Structure of the catalytic domain of the hepatitis c virus ns2-3 protease. *Nature*, 442:831–835.

Lundin, M., Lindstrom, H., Gronwall, C., and Persson, M. A. A. 2006. Dual topology of the processed hepatitis c virus protein ns4b is influenced by the ns5a protein. *The Journal of general virology*, 87:3263–3272.

Lupberger, J., Zeisel, M. B., Xiao, F., Thumann, C., Fofana, I., Zona, L., Davis, C., Mee, C. J., Turek, M., Gorke, S., Royer, C., Fischer, B., Zahid, M. N., Lavillette, D., Fresquet, J., Cosset, F.-L., Rothenberg, S. M., Pietschmann, T., Patel, A. H., Pessaux, P., Doffoel, M., Raffelsberger, W., Poch, O., McKeating, J. A., Brino, L., and Baumert, T. F. 2011. Egfr and epha2 are host factors for hepatitis c virus entry and possible targets for antiviral therapy. *Nature Medicine*, 17(5):589–595.

Lynch, S. M. and Wu, G. Y. 2016. Hepatitis c virus: A review of treatment guidelines, cost-effectiveness, and access to therapy. *Journal of clinical and translational hepatology*, 4:310–319.

Ma, Y., Anantpadma, M., Timpe, J. M., Shanmugam, S., Singh, S. M., Lemon, S. M., and Yi, M. 2010. Hepatitis c virus ns2 protein serves as a scaffold for virus assembly by interacting with both structural and nonstructural proteins. *Journal of Virology*, 85(1):86–97.

Macdonald, A., Crowder, K., Street, A., McCormick, C., and Harris, M. 2004. The hepatitis c virus ns5a protein binds to members of the src family of tyrosine kinases and regulates kinase activity. *The Journal of general virology*, 85:721–729.

Maiuri, M. C., Le Toumelin, G., Criollo, A., Rain, J.-C., Gautier, F., Juin, P., Tasdemir, E., Pierron, G., Troulinaki, K., Tavernarakis, N., Hickman, J. A., Geneste, O., and Kroemer, G. 2007. Functional and physical interaction between bcl-x(l) and a bh3-like domain in beclin-1. *The EMBO journal*, 26:2527–2539.

Mankouri, J., Walter, C., Stewart, H., Bentham, M., Park, W. S., Heo, W. D., Fukuda, M., Griffin, S., and Harris, M. 2016. Release of infectious hepatitis c virus from huh7 cells occurs via a trans-golgi network to endosome pathway independent of vldl. *Journal of virology*.

Martell, M., Esteban, J. I., Quer, J., Genesca, J., Weiner, A., Esteban, R., Guardia, J., and Gomez, J. 1992. Hepatitis c virus circulates as a population of different but closely related genomes: quasispecies nature of hcv genome distribution. *Journal of virology*, 66(5):3225–3229.

Martin, D. N. and Uprichard, S. L. 2013. Identification of transferrin receptor 1 as a hepatitis c virus entry factor. *Proceedings of the National Academy of Sciences of the United States of America*, 110(26):10777–10782.

Martinez, J., Almendinger, J., Oberst, A., Ness, R., Dillon, C. P., Fitzgerald, P., Hengartner, M. O., and Green, D. R. 2011. Microtubule-associated protein 1 light chain 3 alpha (lc3)-associated phagocytosis is required for the efficient clearance of dead cells. *Proceedings of the National Academy of Sciences of the United States of America*, 108:17396–17401.

Martinez-Esparza, M., Tristan-Manzano, M., Ruiz-Alcaraz, A. J., and Garcia-Penarrubia, P. 2015. Inflammatory status in human hepatic cirrhosis. *World journal of gastroenterology*, 21:11522–11541.

Marwaha, N. and Sachdev, S. 2014. Current testing strategies for hepatitis c virus infection in blood donors and the way forward. *World journal of gastroenterology*, 20:2948–2954.

Mast, E. E., Hwang, L.-Y., Seto, D. S. Y., Nolte, F. S., Nainan, O. V., Wurtzel, H., and Alter, M. J. 2005. Risk factors for perinatal transmission of hepatitis c virus (hcv) and the natural history of hcv infection acquired in infancy. *The Journal of infectious diseases*, 192:1880–1889.

Matsumoto, G., Wada, K., Okuno, M., Kurosawa, M., and Nukina, N. 2011. Serine 403 phosphorylation of p62/sqstm1 regulates selective autophagic clearance of ubiquitinated proteins. *Molecular cell*, 44:279–289.

McLauchlan, J. 2000. Properties of the hepatitis c virus core protein: a structural protein that modulates cellular processes. *Journal of viral hepatitis*, 7:2–14.

McLauchlan, J., Lemberg, M. K., Hope, G., and Martoglio, B. 2002. Intramembrane proteolysis promotes trafficking of hepatitis c virus core protein to lipid droplets. *The EMBO journal*, 21(15):3980–3988.

Medvedev, R., Hildt, E., and Ploen, D. 2016a. Look who's talking—the crosstalk between oxidative stress and autophagy supports exosomal-dependent release of HCV particles. *Cell Biology and Toxicology*.

Medvedev, R., Ploen, D., and Hildt, E. 2016b. Hcv and oxidative stress: Implications for hcv life cycle and hcv-associated pathogenesis. *Oxidative medicine and cellular longevity*, 2016:9012580.

Menzel, N., Fischl, W., Hueging, K., Bankwitz, D., Frentzen, A., Haid, S., Gentzsch, J., Kaderali, L., Bartenschlager, R., and Pietschmann, T. 2012. Map-kinase regulated cytosolic phospholipase a2 activity is essential for production of infectious hepatitis c virus particles. *PLoS Pathogens*, 8(7):e1002829.

Merquiol, E., Uzi, D., Mueller, T., Goldenberg, D., Nahmias, Y., Xavier, R. J., Tirosh, B., and Shibolet, O. 2011. HCV causes chronic endoplasmic reticulum stress leading to adaptation and interference with the unfolded protein response. *PLoS ONE*, 6(9):e24660.

Merz, A., Long, G., Hiet, M.-S., Brugger, B., Chlanda, P., Andre, P., Wieland, F., Krijnse-Locker, J., and Bartenschlager, R. 2011. Biochemical and morphological properties of hepatitis c virus particles and determination of their lipidome. *The Journal of biological chemistry*, 286(4):3018–3032.

Messina, J. P., Humphreys, I., Flaxman, A., Brown, A., Cooke, G. S., Pybus, O. G., and Barnes, E. 2014. Global distribution and prevalence of hepatitis c virus genotypes. *Hepatology (Baltimore, Md.)*.

Mishra, P., Dixit, U., Pandey, A. K., Upadhyay, A., and Pandey, V. N. 2017. Modulation of hcv replication and translation by erbb3 binding protein1 isoforms. *Virology*, 500:35–49.

Miyanari, Y., Atsuzawa, K., Usuda, N., Watashi, K., Hishiki, T., Zayas, M., Bartenschlager, R., Wakita, T., Hijikata, M., and Shimotohno, K. 2007. The lipid droplet is an important organelle for hepatitis c virus production. *Nature Cell Biology*, 9(9):1089–1097.

Mizushima, N. and Komatsu, M. 2011. Autophagy: renovation of cells and tissues. *Cell*, 147(4):728–741.

Mizushima, N., Levine, B., Cuervo, A. M., and Klionsky, D. J. 2008. Autophagy fights disease through cellular self-digestion. *Nature*, 451(7182):1069–1075.

Mizushima, N., Yamamoto, A., Hatano, M., Kobayashi, Y., Kabeya, Y., Suzuki, K., Tokuhisa, T., Ohsumi, Y., and Yoshimori, T. 2001. Dissection of autophagosome formation using apg5-deficient mouse embryonic stem cells. *The Journal of cell biology*, 152(4):657–668.

Mizushima, N. and Yoshimori, T. 2007. How to interpret lc3 immunoblotting. *Autophagy*, 3:542–545.

Mizushima, N., Yoshimori, T., and Levine, B. 2010. Methods in mammalian autophagy research. *Cell*, 140(3):313–326.

Mizushima, N., Yoshimori, T., and Ohsumi, Y. 2011. The role of atg proteins in autophagosome formation. *Annual review of cell and developmental biology*, 27:107–132.

Mohl, B.-P., Bartlett, C., Mankouri, J., and Harris, M. 2016. Early events in the generation of autophagosomes are required for the formation of membrane structures involved in hepatitis c virus genome replication. *The Journal of general virology*, 97(3):680–693.

Monazahian, M., Boehme, I., Bonk, S., Koch, A., Scholz, C., Grethe, S., and Thomssen, R. 1999. Low density lipoprotein receptor as a candidate receptor for hepatitis c virus. *Journal of medical virology*, 57:223–229.

Moradpour, D., Brass, V., Bieck, E., Friebe, P., Gosert, R., Blum, H. E., Bartenschlager, R., Penin, F., and Lohmann, V. 2004. Membrane association of the rna-dependent rna polymerase is essential for hepatitis c virus rna replication. *Journal of virology*, 78(23):13278–13284.

Moradpour, D., Englert, C., Wakita, T., and Wands, J. R. 1996. Characterization of cell lines allowing tightly regulated expression of hepatitis c virus core protein. *Virology*, 222:51–63.

Moradpour, D., Penin, F., and Rice, C. M. 2007. Replication of hepatitis c virus. *Nature reviews. Microbiology*, 5(6):453–463.

Moscat, J. and Diaz-Meco, M. T. 2011. Feedback on fat: p62-mtorc1-autophagy connections. *Cell*, 147(4):724–727.

Moscat, J., Diaz-Meco, M. T., Albert, A., and Campuzano, S. 2006. Cell signaling and function organized by pb1 domain interactions. *Molecular cell*, 23:631–640.

Murphy, D. G., Willems, B., DeschÃªnes, M., Hilzenrat, N., Mousseau, R., and Sabbah, S. 2007. Use of sequence analysis of the ns5b region for routine genotyping of hepatitis c virus with reference to c/e1 and 5' untranslated region sequences. *Journal of clinical microbiology*, 45:1102–1112.

Naderi, M., Gholipour, N., Zolfaghari, M. R., Moradi Binabaj, M., Yegane Moghadam, A., and Motalleb, G. 2014. Hepatitis c virus and vaccine development. *International journal of molecular and cellular medicine*, 3:207–215.

Nakatogawa, H. and Ohsumi, Y. 2014. Autophagy: close contact keeps out the uninvited. *Current biology : CB*, 24:R560–R562.

Nawaz, A., Zaidi, S. F., Usmanghani, K., and Ahmad, I. 2015. Concise review on the insight of hepatitis c. *Journal of Taibah University Medical Sciences*, 10(2):132–139.

Nelson, P. K., Mathers, B. M., Cowie, B., Hagan, H., Des Jarlais, D., Horyniak, D., and Degenhardt, L. 2011. Global epidemiology of hepatitis b and hepatitis c in people who inject drugs: results of systematic reviews. *Lancet (London, England)*, 378:571–583.

Neufeldt, C. J., Joyce, M. A., Levin, A., Steenbergen, R. H., Pang, D., Shields, J., Tyrrell, D. L. J., and Wozniak, R. W. 2013. Hepatitis c virus-induced cytoplasmic organelles use the nuclear transport machinery to establish an environment conducive to virus replication. *PLoS pathogens*, 9:e1003744.

Ni, H.-M., Woolbright, B. L., Williams, J., Copple, B., Cui, W., Luyendyk, J. P., Jaeschke, H., and Ding, W.-X. 2014. Nrf2 promotes the development of fibrosis and tumorigenesis in mice with defective hepatic autophagy. *Journal of hepatology*, 61:617–625.

O'Connell, M. A. and Hayes, J. D. 2015. The keap1/nrf2 pathway in health and disease: from the bench to the clinic. *Biochemical Society transactions*, 43:687–689.

Oikawa, D., Akai, R., Tokuda, M., and Iwawaki, T. 2012. A transgenic mouse model for monitoring oxidative stress. *Scientific reports*, 2:229.

Okamoto, K., Mori, Y., Komoda, Y., Okamoto, T., Okochi, M., Takeda, M., Suzuki, T., Moriishi, K., and Matsuura, Y. 2008. Intramembrane processing by signal peptide peptidase regulates the membrane localization of hepatitis c virus core protein and viral propagation. *Journal of virology*, 82:8349–8361.

Okuda, M., Li, K., Beard, M. R., Showalter, L. A., Scholle, F., Lemon, S. M., and Weinman, S. A. 2002. Mitochondrial injury, oxidative stress, and antioxidant gene expression are induced by hepatitis c virus core protein. *Gastroenterology*, 122:366–375.

Osburn, W. O., Wakabayashi, N., Misra, V., Nilles, T., Biswal, S., Trush, M. A., and Kensler, T. W. 2006. Nrf2 regulates an adaptive response protecting against oxidative damage following diquat-mediated formation of superoxide anion. *Archives of biochemistry and biophysics*, 454:7–15.

Paik, Y.-H., Kim, J., Aoyama, T., Minicis, S. D., Bataller, R., and Brenner, D. A. 2014. Role of nadph oxidases in liver fibrosis. *Antioxidants Redox Signaling*, 20(17):2854–2872.

Pajares, M., Jimenez-Moreno, N., Garcia-Yague, A. J., Escoll, M., de Ceballos, M. L., Van Leuven, F., Rabano, A., Yamamoto, M., Rojo, A. I., and Cuadrado, A. 2016. Transcription factor nfe2l2/nrf2 is a regulator of macroautophagy genes. *Autophagy*, 12:1902–1916.

Pancholi, P., Perkus, M., Tricoche, N., Liu, Q., and Prince, A. M. 2003. Dna immunization with hepatitis c virus (hcv) polycistronic genes or immunization by hcv dna priming-recombinant canarypox virus boosting induces immune responses and protection from recombinant hcv-vaccinia virus infection in hla-a2.1-transgenic mice. *Journal of virology*, 77:382–390.

Pattingre, S., Espert, L., Biard-Piechaczyk, M., and Codogno, P. 2008. Regulation of macroautophagy by mtor and beclin 1 complexes. *Biochimie*, 90:313–323.

Paul, D., Hoppe, S., Saher, G., Krijnse-Locker, J., and Bartenschlager, R. 2013. Morphological and biochemical characterization of the membranous hepatitis c virus replication compartment. *Journal of virology*, 87(19):10612–10627.

Pawlotsky, J.-M. 2014. New hepatitis c therapies: the toolbox, strategies, and challenges. *Gastroenterology*, 146(5):1176–1192.

Pawlotsky, J.-M., Feld, J. J., Zeuzem, S., and Hoofnagle, J. H. 2015. From non-a, non-b hepatitis to hepatitis c virus cure. *Journal of Hepatology*, 62(1):S87–S99.

Pellicoro, A., Ramachandran, P., Iredale, J. P., and Fallowfield, J. A. 2014. Liver fibrosis and repair: immune regulation of wound healing in a solid organ. *Nature reviews. Immunology*, 14:181–194.

Petiot, A., Ogier-Denis, E., Blommaart, E. F., Meijer, A. J., and Codogno, P. 2000. Distinct classes of phosphatidylinositol 3'-kinases are involved in signaling pathways that control macroautophagy in ht-29 cells. *The Journal of biological chemistry*, 275:992–998.

Petruzziello, A., Marigliano, S., Loquercio, G., Cozzolino, A., and Cacciapuoti, C. 2016. Global epidemiology of hepatitis c virus infection: An up-date of the distribution and circulation of hepatitis c virus genotypes. *World journal of gastroenterology*, 22:7824–7840.

Pietschmann, T., Kaul, A., Koutsoudakis, G., Shavinskaya, A., Kallis, S., Steinmann, E., Abid, K., Negro, F., Dreux, M., Cosset, F.-L., and Bartenschlager, R. 2006. Construction and characterization of infectious intragenotypic and intergenotypic hepatitis c virus chimeras. *Proceedings of the National Academy of Sciences of the United States of America*, 103(19):7408–7413.

Pileri, P., Uematsu, Y., Campagnoli, S., Galli, G., Falugi, F., Petracca, R., Weiner, A. J., Houghton, M., Rosa, D., Grandi, G., and Abrignani, S. 1998. Binding of hepatitis c virus to cd81. *Science (New York, N.Y.)*, 282(5390):938–941.

Ploen, D., Hafirassou, M. L., Himmelsbach, K., Sauter, D., Biniossek, M. L., Weiss, T. S., Baumert, T. F., Schuster, C., and Hildt, E. 2013a. Tip47 plays a crucial role in the life cycle of hepatitis c virus. *Journal of hepatology*, 58(6):1081–1088.

Ploen, D., Hafirassou, M. L., Himmelsbach, K., Schille, S. A., Biniossek, M. L., Baumert, T. F., Schuster, C., and Hildt, E. 2013b. Tip47 is associated with the hepatitis c virus and its interaction with rab9 is required for release of viral particles. *European journal of cell biology*, 92(12):374–382.

Ploen, D. and Hildt, E. 2015. Hepatitis c virus comes for dinner: How the hepatitis c virus interferes with autophagy. *World journal of gastroenterology : WJG*, 21(28):8492–8507.

Ploss, A., Evans, M. J., Gaysinskaya, V. A., Panis, M., You, H., de Jong, Y. P., and Rice, C. M. 2009. Human occludin is a hepatitis c virus entry factor required for infection of mouse cells. *Nature*, 457(7231):882–886.

Ploss, A., Khetani, S. R., Jones, C. T., Syder, A. J., Trehan, K., Gaysinskaya, V. A., Mu, K., Ritola, K., Rice, C. M., and Bhatia, S. N. 2010. Persistent hepatitis c virus infection in microscale primary human hepatocyte cultures. *Proceedings of the National Academy of Sciences of the United States of America*, 107:3141–3145.

Polyak, S. J., McArdle, S., Liu, S. L., Sullivan, D. G., Chung, M., Hofgaertner, W. T., Carithers, R. L., McMahon, B. J., Mullins, J. I., Corey, L., and Gretch, D. R. 1998. Evolution of hepatitis c virus quasispecies in hypervariable region 1 and the putative interferon sensitivity-determining region during interferon therapy and natural infection. *Journal of virology*, 72:4288–4296.

Popescu, C.-I., Callens, N., Trinel, D., Roingeard, P., Moradpour, D., Descamps, V., Duverlie, G., Penin, F., Heliot, L., Rouille, Y., and Dubuisson, J. 2011. Ns2 protein of hepatitis c virus interacts with structural and non-structural proteins towards virus assembly. *PLoS Pathogens*, 7(2):e1001278.

Post, J., Ratnarajah, S., and Lloyd, A. R. 2009. Immunological determinants of the outcomes from primary hepatitis c infection. *Cellular and molecular life sciences*, 66(5):733–756.

Prentoe, J., Velazquez-Moctezuma, R., Foung, S. K. H., Law, M., and Bukh, J. 2016. Hypervariable region 1 shielding of hepatitis c virus is a main contributor to genotypic differences in neutralization sensitivity. *Hepatology (Baltimore, Md.)*, 64:1881–1892.

Quinkert, D., Bartenschlager, R., and Lohmann, V. 2005. Quantitative analysis of the hepatitis c virus replication complex. *Journal of virology*, 79(21):13594–13605.

Radtke, A. L. and O'Riordan, M. X. D. 2006. Intracellular innate resistance to bacterial pathogens. *Cellular microbiology*, 8:1720–1729.

Ravikumar, B., Moreau, K., Jahreiss, L., Puri, C., and Rubinsztein, D. C. 2010. Plasma membrane contributes to the formation of pre-autophagosomal structures. *Nature Cell Biology*, 12(8):747–757.

Reed, K. E., Xu, J., and Rice, C. M. 1997. Phosphorylation of the hepatitis c virus ns5a protein in vitro and in vivo: properties of the ns5a-associated kinase. *Journal of virology*, 71:7187–7197.

Reiss, S., Harak, C., Romero-Brey, I., Radujkovic, D., Klein, R., Ruggieri, A., Rebhan, I., Bartenschlager, R., and Lohmann, V. 2013. The lipid kinase phosphatidylinositol-4 kinase iii alpha regulates the phosphorylation status of hepatitis c virus ns5a. *PLoS Pathogens*, 9(5):e1003359.

Reiss, S., Rebhan, I., Backes, P., Romero-Brey, I., Erfle, H., Matula, P., Kaderali, L., Poenisch, M., Blankenburg, H., Hiet, M.-S., Longerich, T., Diehl, S., Ramirez, F., Balla, T., Rohr, K., Kaul,

A., Buhler, S., Pepperkok, R., Lengauer, T., Albrecht, M., Eils, R., Schirmacher, P., Lohmann, V., and Bartenschlager, R. 2011. Recruitment and activation of a lipid kinase by hepatitis c virus ns5a is essential for integrity of the membranous replication compartment. *Cell host & microbe*, 9(1):32–45.

Ren, H., Elgner, F., Jiang, B., Himmelsbach, K., Medvedev, R., Ploen, D., and Hildt, E. 2016. The autophagosomal snare protein syntaxin 17 is an essential factor for the hepatitis c virus life cycle. *Journal of virology*, 90(13):5989–6000.

Roberts, A. P. E., Lewis, A. P., and Jopling, C. L. 2011. mir-122 activates hepatitis c virus translation by a specialized mechanism requiring particular rna components. *Nucleic acids research*, 39(17):7716–7729.

Rockey, D. C. and Bissell, D. M. 2006. Noninvasive measures of liver fibrosis. *Hepatology (Baltimore, Md.)*, 43:S113–S120.

Romao, S. and Muenz, C. 2014. Lc3-associated phagocytosis. *Autophagy*, 10:526–528.

Romero-Brey, I. and Bartenschlager, R. 2014. Membranous replication factories induced by plus-strand rna viruses. *Viruses*, 6(7):2826–2857.

Romero-Brey, I., Merz, A., Chiramel, A., Lee, J.-Y., Chlanda, P., Haselman, U., Santarella-Mellwig, R., Habermann, A., Hoppe, S., Kallis, S., Walther, P., Antony, C., Krijnse-Locker, J., and Bartenschlager, R. 2012. Three-dimensional architecture and biogenesis of membrane structures associated with hepatitis c virus replication. *PLoS Pathogens*, 8(12):e1003056.

Ross-Thriepland, D., Amako, Y., and Harris, M. 2013. The c terminus of ns5a domain ii is a key determinant of hepatitis c virus genome replication, but is not required for virion assembly and release. *The Journal of general virology*, 94:1009–1018.

Rouet, F., Deleplancque, L., Mboumba, B. B., Sica, J., Mouinga-Ondémé, A., Liégeois, F., Goudeau, A., Dubois, F., and Gaudy-Graffin, C. 2015. Usefulness of a fourth generation elisa assay for the reliable identification of hcv infection in hiv-positive adults from gabon (central africa). *PLOS ONE*, 10(1):e0116975.

Sainz, B., Barretto, N., Martin, D. N., Hiraga, N., Imamura, M., Hussain, S., Marsh, K. A., Yu, X., Chayama, K., Alrefai, W. A., and Uprichard, S. L. 2012. Identification of the niemann-pick c1-like 1 cholesterol absorption receptor as a new hepatitis c virus entry factor. *Nature Medicine*, 18(2):281–285.

Saito, T., Ichimura, Y., Taguchi, K., Suzuki, T., Mizushima, T., Takagi, K., Hirose, Y., Nagahashi, M., Iso, T., Fukutomi, T., Ohishi, M., Endo, K., Uemura, T., Nishito, Y., Okuda, S., Obata,

M., Kouno, T., Imamura, R., Tada, Y., Obata, R., Yasuda, D., Takahashi, K., Fujimura, T., Pi, J., Lee, M.-S., Ueno, T., Ohe, T., Mashino, T., Wakai, T., Kojima, H., Okabe, T., Nagano, T., Motohashi, H., Waguri, S., Soga, T., Yamamoto, M., Tanaka, K., and Komatsu, M. 2016. p62/sqstm1 promotes malignancy of hcv-positive hepatocellular carcinoma through nrf2-dependent metabolic reprogramming. *Nature communications*, 7:12030.

Salloum, S., Wang, H., Ferguson, C., Parton, R. G., and Tai, A. W. 2013. Rab18 binds to hepatitis c virus ns5a and promotes interaction between sites of viral replication and lipid droplets. *PLoS Pathogens*, 9(8):e1003513.

San Miguel, R., Gimeno-Ballester, V., Blazquez, A., and Mar, J. 2015. Cost-effectiveness analysis of sofosbuvir-based regimens for chronic hepatitis c. *Gut*, 64:1277–1288.

Sanz, L., Diaz-Meco, M. T., Nakano, H., and Moscat, J. 2000. The atypical pkc-interacting protein p62 channels nf-kappab activation by the il-1-traf6 pathway. *The EMBO journal*, 19:1576–1586.

Sanz, L., Sanchez, P., Lallena, M. J., Diaz-Meco, M. T., and Moscat, J. 1999. The interaction of p62 with rip links the atypical pkcs to nf-kappab activation. *The EMBO journal*, 18:3044–3053.

Sauter, D., Himmelsbach, K., Kriegs, M., Carvajal Yepes, M., and Hildt, E. 2009. Localization determines function: N-terminally truncated ns5a fragments accumulate in the nucleus and impair hcv replication. *Journal of hepatology*, 50(5):861–871.

Scarselli, E., Ansuini, H., Cerino, R., Roccasecca, R. M., Acali, S., Filocamo, G., Traboni, C., Nicosia, A., Cortese, R., and Vitelli, A. 2002. The human scavenger receptor class b type i is a novel candidate receptor for the hepatitis c virus. *The EMBO journal*, 21(19):5017–5025.

Schaedler, S., Krause, J., Himmelsbach, K., Carvajal-Yepes, M., Lieder, F., Klingel, K., Nassal, M., Weiss, T. S., Werner, S., and Hildt, E. 2010. Hepatitis b virus induces expression of antioxidant response element-regulated genes by activation of nrf2. *The Journal of biological chemistry*, 285(52):41074–41086.

Scheel, T. K. H. and Rice, C. M. 2013. Understanding the hepatitis c virus life cycle paves the way for highly effective therapies. *Nature Medicine*, 19(7):837–849.

Scherz-Shouval, R., Shvets, E., Fass, E., Shorer, H., Gil, L., and Elazar, Z. 2007. Reactive oxygen species are essential for autophagy and specifically regulate the activity of atg4. *The EMBO journal*, 26:1749–1760.

Schwer, B., Ren, S., Pietschmann, T., Kartenbeck, J., Kaehlcke, K., Bartenschlager, R., Yen, T. S. B., and Ott, M. 2004. Targeting of hepatitis c virus core protein to mitochondria through a novel c-terminal localization motif. *Journal of Virology*, 78(15):7958–7968.

Scott, J. D. and Gretch, D. R. 2007. Molecular diagnostics of hepatitis c virus infection: a systematic review. *JAMA*, 297:724–732.

Seme, K., Poljak, M., Babic, D. Z., Mocilnik, T., and Vince, A. 2005. The role of core antigen detection in management of hepatitis c: a critical review. *Journal of clinical virology : the official publication of the Pan American Society for Clinical Virology*, 32:92–101.

Sengupta, S., Peterson, T. R., and Sabatini, D. M. 2010. Regulation of the mtor complex 1 pathway by nutrients, growth factors, and stress. *Molecular cell*, 40(2):310–322.

Serebrov, V. and Pyle, A. M. 2004. Periodic cycles of rna unwinding and pausing by hepatitis c virus ns3 helicase. *Nature*, 430:476–480.

Seronello, S., Montanez, J., Presleigh, K., Barlow, M., Park, S. B., and Choi, J. 2011. Ethanol and reactive species increase basal sequence heterogeneity of hepatitis c virus and produce variants with reduced susceptibility to antivirals. *PloS one*, 6:e27436.

Shawki, S. M., Meshaal, S. S., El Dash, A. S., Zayed, N. A., and Hanna, M. O. F. 2014. Increased dna damage in hepatitis c virus-related hepatocellular carcinoma. *DNA and cell biology*, 33:884–890.

Shepard, C. W., Finelli, L., and Alter, M. J. 2005. Global epidemiology of hepatitis c virus infection. *The Lancet. Infectious diseases*, 5:558–567.

Shi, Q., Jiang, J., and Luo, G. 2013. Syndecan-1 serves as the major receptor for attachment of hepatitis c virus to the surfaces of hepatocytes. *Journal of virology*, 87(12):6866–6875.

Shrivastava, S., Bhanja Chowdhury, J., Steele, R., Ray, R., and Ray, R. B. 2012. Hepatitis c virus upregulates beclin1 for induction of autophagy and activates mtor signaling. *Journal of virology*, 86(16):8705–8712.

Shrivastava, S., Devhare, P., Sujijantarat, N., Steele, R., Kwon, Y.-C., Ray, R., and Ray, R. B. 2016. Knockdown of autophagy inhibits infectious hepatitis c virus release by the exosomal pathway. *Journal of virology*, 90(3):1387–1396.

Simmonds, P. 2004. Genetic diversity and evolution of hepatitis c virus–15 years on. *The Journal of general virology*, 85(Pt 11):3173–3188.

Simmonds, P., Bukh, J., Combet, C., Deléage, G., Enomoto, N., Feinstone, S., Halfon, P., Inchauspé, G., Kuiken, C., Maertens, G., Mizokami, M., Murphy, D. G., Okamoto, H., Pawlotsky, J.-M., Penin, F., Sablon, E., Shin-I, T., Stuyver, L. J., Thiel, H.-J., Viazov, S., Weiner, A. J., and Widell, A. 2005. Consensus proposals for a unified system of nomenclature of hepatitis c virus genotypes. *Hepatology (Baltimore, Md.)*, 42(4):962–973.

Sir, D., Chen, W.-L., Choi, J., Wakita, T., Yen, T. S. B., and Ou, J.-h. J. 2008. Induction of incomplete autophagic response by hepatitis c virus via the unfolded protein response. *Hepatology (Baltimore, Md.)*, 48(4):1054–1061.

Sir, D., Kuo, C.-f., Tian, Y., Liu, H. M., Huang, E. J., Jung, J. U., Machida, K., and Ou, J.-h. J. 2012. Replication of hepatitis c virus rna on autophagosomal membranes. *The Journal of biological chemistry*, 287(22):18036–18043.

Siu, G. K. Y., Zhou, F., Yu, M. K., Zhang, L., Wang, T., Liang, Y., Chen, Y., Chan, H. C., and Yu, S. 2016. Hepatitis c virus ns5a protein cooperates with phosphatidylinositol 4-kinase iiialpha to induce mitochondrial fragmentation. *Scientific Reports*, 6:23464.

Smirnova, O. A., Ivanova, O. N., Mukhtarov, F. S., Tunitskaya, V. L., Jansons, J., Isaguliants, M. G., Kochetkov, S. N., and Ivanov, A. V. 2016. Analysis of the domains of hepatitis c virus core and ns5a proteins that activate the nrf2/are cascade. *Acta naturae*, 8:123–127.

Sourisseau, M., Michta, M. L., Zony, C., Israelow, B., Hopcraft, S. E., Narbus, C. M., Martin, A. P., and Evans, M. J. 2013. Temporal analysis of hepatitis c virus cell entry with occludin directed blocking antibodies. *PLoS Pathogens*, 9(3):e1003244.

Spearman, C. 1908. The method of right and wrong cases (constant stimuli) without gauss's formulae. *British Journal of Psychology, 1904-1920*, 2(3):227–242.

Stapleford, K. A. and Lindenbach, B. D. 2010. Hepatitis c virus ns2 coordinates virus particle assembly through physical interactions with the e1-e2 glycoprotein and ns3-ns4a enzyme complexes. *Journal of Virology*, 85(4):1706–1717.

Steinmann, E., Penin, F., Kallis, S., Patel, A. H., Bartenschlager, R., and Pietschmann, T. 2007. Hepatitis c virus p7 protein is crucial for assembly and release of infectious virions. *PLoS pathogens*, 3:e103.

Su, W.-C., Chao, T.-C., Huang, Y.-L., Weng, S.-C., Jeng, K.-S., and Lai, M. M. C. 2011. Rab5 and class iii phosphoinositide 3-kinase vps34 are involved in hepatitis c virus ns4b-induced autophagy. *Journal of virology*, 85(20):10561–10571.

Sumpter, R., Loo, Y.-M., Foy, E., Li, K., Yoneyama, M., Fujita, T., Lemon, S. M., and Gale, M. 2005. Regulating intracellular antiviral defense and permissiveness to hepatitis c virus rna replication through a cellular rna helicase, rig-i. *Journal of Virology*, 79(5):2689–2699.

Suzuki, K., Kubota, Y., Sekito, T., and Ohsumi, Y. 2007. Hierarchy of atg proteins in pre-autophagosomal structure organization. *Genes to cells : devoted to molecular & cellular mechanisms*, 12:209–218.

Suzuki, R., Sakamoto, S., Tsutsumi, T., Rikimaru, A., Tanaka, K., Shimoike, T., Moriishi, K., Iwasaki, T., Mizumoto, K., Matsuura, Y., Miyamura, T., and Suzuki, T. 2004. Molecular determinants for subcellular localization of hepatitis c virus core protein. *Journal of Virology*, 79(2):1271–1281.

Swadling, L., Capone, S., Antrobus, R. D., Brown, A., Richardson, R., Newell, E. W., Halliday, J., Kelly, C., Bowen, D., Fergusson, J., Kurioka, A., Ammendola, V., Del Sorbo, M., Grazioli, F., Esposito, M. L., Siani, L., Traboni, C., Hill, A., Colloca, S., Davis, M., Nicosia, A., Cortese, R., Folgori, A., Klenerman, P., and Barnes, E. 2014. A human vaccine strategy based on chimpanzee adenoviral and mva vectors that primes, boosts, and sustains functional hcv-specific t cell memory. *Science translational medicine*, 6:261ra153.

Swadling, L., Klenerman, P., and Barnes, E. 2013. Ever closer to a prophylactic vaccine for hcv. *Expert Opinion on Biological Therapy*, 13(8):1109–1124.

Takamura, A., Komatsu, M., Hara, T., Sakamoto, A., Kishi, C., Waguri, S., Eishi, Y., Hino, O., Tanaka, K., and Mizushima, N. 2011. Autophagy-deficient mice develop multiple liver tumors. *Genes & development*, 25:795–800.

Takeshige, K., Baba, M., Tsuboi, S., Noda, T., and Ohsumi, Y. 1992. Autophagy in yeast demonstrated with proteinase-deficient mutants and conditions for its induction. *The Journal of cell biology*, 119:301–311.

Tang, H. and Grisé, H. 2009. Cellular and molecular biology of HCV infection and hepatitis. *Clinical Science*, 117(2):49–65.

Tanida, I., Fukasawa, M., Ueno, T., Kominami, E., Wakita, T., and Hanada, K. 2009. Knockdown of autophagy-related gene decreases the production of infectious hepatitis c virus particles. *Autophagy*, 5(7):937–945.

Taniguchi, K., Yamachika, S., He, F., and Karin, M. 2016. p62sqstm1-dr. jekyll and mr. hyde that prevents oxidative stress but promotes liver cancer. *FEBS Letters*, 590(15):2375–2397.

Tardif, K. D., Mori, K., and Siddiqui, A. 2002. Hepatitis c virus subgenomic replicons induce endoplasmic reticulum stress activating an intracellular signaling pathway. *Journal of virology*, 76(15):7453–7459.

Targett-Adams, P., Boulant, S., and McLauchlan, J. 2007. Visualization of double-stranded rna in cells supporting hepatitis c virus rna replication. *Journal of Virology*, 82(5):2182–2195.

Tellinghuisen, T. L., Foss, K. L., Treadaway, J. C., and Rice, C. M. 2007. Identification of residues required for rna replication in domains ii and iii of the hepatitis c virus ns5a protein. *Journal of Virology*, 82(3):1073–1083.

Tellinghuisen, T. L., Marcotrigiano, J., Gorbalenya, A. E., and Rice, C. M. 2004. The ns5a protein of hepatitis c virus is a zinc metalloprotein. *The Journal of biological chemistry*, 279(47):48576–48587.

Tellinghuisen, T. L. and Rice, C. M. 2002. Interaction between hepatitis c virus proteins and host cell factors. *Current opinion in microbiology*, 5:419–427.

Terrault, N. A., Dodge, J. L., Murphy, E. L., Tavis, J. E., Kiss, A., Levin, T. R., Gish, R. G., Busch, M. P., Reingold, A. L., and Alter, M. J. 2013. Sexual transmission of hepatitis c virus among monogamous heterosexual couples: the hcv partners study. *Hepatology (Baltimore, Md.)*, 57:881–889.

Thomas, D. L., Villano, S. A., Riester, K. A., Hershow, R., Mofenson, L. M., Landesman, S. H., Hollinger, F. B., Davenny, K., Riley, L., Diaz, C., Tang, H. B., and Quinn, T. C. 1998. Perinatal transmission of hepatitis c virus from human immunodeficiency virus type 1-infected mothers. women and infants transmission study. *The Journal of infectious diseases*, 177:1480–1488.

Tohme, R. A. and Holmberg, S. D. 2010. Is sexual contact a major mode of hepatitis c virus transmission? *Hepatology (Baltimore, Md.)*, 52:1497–1505.

Tscherne, D. M., Jones, C. T., Evans, M. J., Lindenbach, B. D., McKeating, J. A., and Rice, C. M. 2006. Time- and temperature-dependent activation of hepatitis c virus for low-ph-triggered entry. *Journal of virology*, 80:1734–1741.

Tsukiyama-Kohara, K. 2012. Role of oxidative stress in hepatocarcinogenesis induced by hepatitis c virus. *International journal of molecular sciences*, 13:15271–15278. Original DateCompleted: 20121204.

Vakifahmetoglu-Norberg, H., Ouchida, A. T., and Norberg, E. 2017. The role of mitochondria in metabolism and cell death. *Biochemical and biophysical research communications*, 482:426–431.

Vieyres, G., Thomas, X., Descamps, V., Duverlie, G., Patel, A. H., and Dubuisson, J. 2010. Characterization of the envelope glycoproteins associated with infectious hepatitis c virus. *Journal of virology*, 84(19):10159–10168.

Villar, V. H., Merhi, F., Djavaheri-Mergny, M., and Duran, R. V. 2015. Glutaminolysis and autophagy in cancer. *Autophagy*, 11:1198–1208.

Voisset, C. and Dubuisson, J. 2004. Functional hepatitis c virus envelope glycoproteins. *Biology of the cell*, 96:413–420.

Wakita, T., Pietschmann, T., Kato, T., Date, T., Miyamoto, M., Zhao, Z., Murthy, K., Habermann, A., Krausslich, H.-G., Mizokami, M., Bartenschlager, R., and Liang, T. J. 2005. Production

of infectious hepatitis c virus in tissue culture from a cloned viral genome. *Nature Medicine*, 11(7):791–796.

Walter, P. and Ron, D. 2011. The unfolded protein response: From stress pathway to homeostatic regulation. *Science*, 334(6059):1081–1086.

Wang, J., Kang, R., Huang, H., Xi, X., Wang, B., Wang, J., and Zhao, Z. 2014. Hepatitis c virus core protein activates autophagy through eif2ak3 and atf6 upr pathway-mediated map1lc3b and atg12 expression. *Autophagy*, 10:766–784.

Wang, L., Tian, Y., and Ou, J.-h. J. 2015. Hcv induces the expression of rubicon and uvrag to temporally regulate the maturation of autophagosomes and viral replication. *PLoS pathogens*, 11(3):e1004764.

Wang, T., Campbell, R. V., Yi, M. K., Lemon, S. M., and Weinman, S. A. 2009. Role of hepatitis c virus core protein in viral-induced mitochondrial dysfunction. *Journal of Viral Hepatitis*, 17(11):784–793.

Wang, T. and Weinman, S. A. 2013. Interactions between hepatitis c virus and mitochondria: Impact on pathogenesis and innate immunity. *Current pathobiology reports*, 1(3):179–187.

WHO 2016. *Guidelines for the screening, care and treatment of persons with chronic hepatitis C infection. Updated Version*.

Woelk, B., Sansonno, D., Kraeusslich, H. G., Dammacco, F., Rice, C. M., Blum, H. E., and Moradpour, D. 2000. Subcellular localization, stability, and trans-cleavage competence of the hepatitis c virus ns3-ns4a complex expressed in tetracycline-regulated cell lines. *Journal of virology*, 74:2293–2304.

Wong, C. H., Iskandar, K. B., Yadav, S. K., Hirpara, J. L., Loh, T., and Pervaiz, S. 2010. Simultaneous induction of non-canonical autophagy and apoptosis in cancer cells by ros-dependent erk and jnk activation. *PloS one*, 5:e9996.

Wong, M.-T. and Chen, S. S. 2016. Human choline kinase-alpha promotes hepatitis c virus rna replication through modulation of membranous viral replication complex formation. *Journal of virology*, 90:9075–9095.

Yamamoto, A., Tagawa, Y., Yoshimori, T., Moriyama, Y., Masaki, R., and Tashiro, Y. 1998. Bafilomycin a1 prevents maturation of autophagic vacuoles by inhibiting fusion between autophagosomes and lysosomes in rat hepatoma cell line, h-4-ii-e cells. *Cell structure and function*, 23:33–42.

Yamashita, T., Kaneko, S., Shirota, Y., Qin, W., Nomura, T., Kobayashi, K., and Murakami, S. 1998. Rna-dependent rna polymerase activity of the soluble recombinant hepatitis c virus ns5b protein truncated at the c-terminal region. *The Journal of biological chemistry*, 273:15479–15486.

Yanagi, M., Purcell, R. H., Emerson, S. U., and Bukh, J. 1997. Transcripts from a single full-length cdna clone of hepatitis c virus are infectious when directly transfected into the liver of a chimpanzee. *Proceedings of the National Academy of Sciences of the United States of America*, 94:8738–8743.

Yao, W., Cai, H., Li, X., Li, T., Hu, L., and Peng, T. 2014. Endoplasmic reticulum stress links hepatitis c virus RNA replication to wild-type PGC-1 /liver-specific PGC-1 upregulation. *Journal of Virology*, 88(15):8361–8374.

Yen, W.-L., Shintani, T., Nair, U., Cao, Y., Richardson, B. C., Li, Z., Hughson, F. M., Baba, M., and Klionsky, D. J. 2010. The conserved oligomeric golgi complex is involved in double-membrane vesicle formation during autophagy. *The Journal of cell biology*, 188(1):101–114.

Young, A. R. J., Chan, E. Y. W., Hu, X. W., Kochl, R., Crawshaw, S. G., High, S., Hailey, D. W., Lippincott-Schwartz, J., and Tooze, S. A. 2006. Starvation and ulk1-dependent cycling of mammalian atg9 between the tgn and endosomes. *Journal of cell science*, 119:3888–3900.

Yuk, J. M., Yoshimori, T., and Jo, E. K. 2012. Autophagy and bacterial infectious diseases. *Experimental & molecular medicine*, 44:99–108.

Zahid, M. N., Turek, M., Xiao, F., Thi, V. L. D., Guerin, M., Fofana, I., Bachellier, P., Thompson, J., Delang, L., Neyts, J., Bankwitz, D., Pietschmann, T., Dreux, M., Cosset, F.-L., Grunert, F., Baumert, T. F., and Zeisel, M. B. 2013. The postbinding activity of scavenger receptor class b type i mediates initiation of hepatitis c virus infection and viral dissemination. *Hepatology (Baltimore, Md.)*, 57:492–504.

Zatloukal, K., Stumptner, C., Fuchsbichler, A., Heid, H., Schnoelzer, M., Kenner, L., Kleinert, R., Prinz, M., Aguzzi, A., and Denk, H. 2002. p62 is a common component of cytoplasmic inclusions in protein aggregation diseases. *The American journal of pathology*, 160:255–263.

Zayas, M., Long, G., Madan, V., and Bartenschlager, R. 2016. Coordination of hepatitis c virus assembly by distinct regulatory regions in nonstructural protein 5a. *PLOS Pathogens*, 12(1):e1005376.

Zeisel, M. B., Fofana, I., Fafi-Kremer, S., and Baumert, T. F. 2011. Hepatitis c virus entry into hepatocytes: molecular mechanisms and targets for antiviral therapies. *Journal of hepatology*, 54:566–576.

Zeng, R., Li, G., Ling, S., Zhang, H., Yao, Z., Xiu, B., He, F., Huang, R., and Wei, L. 2009. A novel combined vaccine candidate containing epitopes of hcv ns3, core and e1 proteins induces multi-specific immune responses in balb/c mice. *Antiviral research*, 84:23–30.

Zeng, X., Overmeyer, J. H., and Maltese, W. A. 2006. Functional specificity of the mammalian beclin-vps34 pi 3-kinase complex in macroautophagy versus endocytosis and lysosomal enzyme trafficking. *Journal of cell science*, 119:259–270.

Zheng, Y., Gao, B., Ye, L., Kong, L., Jing, W., Yang, X., Wu, Z., and Ye, L. 2005. Hepatitis c virus non-structural protein ns4b can modulate an unfolded protein response. *Journal of microbiology (Seoul, Korea)*, 43:529–536.

Zhong, J., Gastaminza, P., Cheng, G., Kapadia, S., Kato, T., Burton, D. R., Wieland, S. F., Uprichard, S. L., Wakita, T., and Chisari, F. V. 2005. Robust hepatitis c virus infection in vitro. *Proceedings of the National Academy of Sciences of the United States of America*, 102(26):9294–9299.

Zhong, Z., Umemura, A., Sanchez-Lopez, E., Liang, S., Shalapour, S., Wong, J., He, F., Boassa, D., Perkins, G., Ali, S. R., McGeough, M. D., Ellisman, M. H., Seki, E., Gustafsson, A. B., Hoffman, H., Diaz-Meco, M. T., Moscat, J., and Karin, M. 2016. Nf-kappab restricts inflammasome activation via elimination of damaged mitochondria. *Cell*, 164(5):896–910.

Zhou, L., feng Wang, H., gang Ren, H., Chen, D., Gao, F., song Hu, Q., Fu, C., jie Xu, R., Ying, Z., and hui Wang, G. 2013. Bcl-2-dependent upregulation of autophagy by sequestosome 1/p62 in vitro. *Acta Pharmacologica Sinica*, 34(5):651–656.

Zmijewski, J. W., Banerjee, S., Bae, H., Friggeri, A., Lazarowski, E. R., and Abraham, E. 2010. Exposure to hydrogen peroxide induces oxidation and activation of amp-activated protein kinase. *The Journal of biological chemistry*, 285:33154–33164.

Zotti, T., Scudiero, I., Settembre, P., Ferravante, A., Mazzone, P., D'Andrea, L., Reale, C., Vito, P., and Stilo, R. 2014. Traf6-mediated ubiquitination of nemo requires p62/sequestosome-1. *Molecular Immunology*, 58(1):27–31.

10 Abbreviations

3-MA	3-Methyladenine
aa	Amino acids
ALT	Alanine aminotransferase
AMPK	AMP-activated protein kinase
aPKC	Atypical protein kinase C
apoE	Apolipoprotein E
APS	Ammonium persulfate
ARE	Antioxidant response element
Atg	Autophagy-related gene
ATP	Adenosine triphosphate
Bcl-2	B-cell lymphoma 2
BFLA	Bafilomycin-A1
bp	Base pairs
BSA	Bovine serum albumine
cat	Catalase
CE	Cholesterol ester
ChIP	Chromatin immunoprecipitation
CK2	Casein kinase 2
CLDN-1	Claudine-1
CLIA	Chemiluminescence immunoassay
CLSM	Confocal laser scanning microscopy
cPLA2	Cytosolic phospholipase A2
CTCF	Corrected total cell fluorescence
DAA	Directly acting antiviral agent
DCFH-DA	2´,7´-Dichlorofluorescin diacetate
DFCP1	Double FYVE-containing protein 1
DGAT-1	Diacylglycerol acyltransferase-1
DMEM	Dulbecco´s Modified Eagle Medium
DMSO	Dimethyl sulfoxid
DMV	Double membrane vesicle
DTT	1,4-Dithiothreitol
Ebp-1	ErbB3 binding protein 1
ECL	Enhanced chemiluminescence
ECM	Extracellular matrix
E. coli	Escherichia coli
EDTA	Ethylenediaminetetraacetic acid
EE	Early endosome
EGFR	Epidermal growth factor receptor
ELISA	Enzyme-linked immunosorbent assay
EMCV	Encephalomyocarditis virus
EphA1	Ephrin type A receptor 2
ephx1	Epoxide hydrolase 1
ER	Endoplasmatic reticulum
ERK1	Extracellular signal-regulated kinase 1

ESCRT	Endosomal sorting complexes required for sorting	**Keap1**	Kelch-like ECH-associated protein 1
FCS	Fetal calf serum	**KIR**	Keap1-interacting region
FDA	Food and Drug Administration	**LAP**	LC3-associated phagocytosis
GAG	Glycosaminoglycan	**Keap1**	Kelch-like ECH-associated protein 1
GCLc	Glutamate-cysteine ligase catalytic subunit	**KIR**	Keap1-interacting region
GCSc	Glutamate-cysteine synthetase catalytic subunit	**LAP**	LC3-associated phagocytosis
GO	Glucose oxidase	**LC3**	Microtubule-associated protein 1 light chain 3
GST	Glutathione S-transferase	**LD**	Lipid droplets
HCC	Hepatocellular carcinoma	**LDLR**	Low-density-lipoprotein receptor
hCKα	Human choline kinase-α	**LE**	Late endosome
HCVcc	HCV cell culture	**LIR**	LC3-interacting region
HCV	Hepatitis C virus	**MAPK**	Mitogen-activated protein kinase
HCVpp	HCV pseudoparticles	**MEK**	MAP-ERK kinase
hpe	hours post electroporation	**MHC**	Major histocompatibility complex
HRP	Horseradish peroxidase	**MMV**	Multi membrane vesicle
HSC	Hepatic stellate cell	**mPTP**	Mitochondrial permeability transition pore
HSPG	Heparan sulfate proteoglycan	**mRNA**	Messenger RNA
Huh7.5	Human hepatoma cell line	**mTOR**	Mammalian target of rapamycin
HVR	Hypervariable region	**MVB**	Multivesicular body
IFN	Interferon	**NAC**	N-acetylcysteine
IL	Interleukin	**NaCl**	Sodiumchloride
IM	Isolation membrane	**NANBH**	Non-A, non-B hepatitis
IRES	Internal ribosomal entry site	**NAT**	Nucleic acid test
IRGM	Immunity-related GTPase M	**NES**	Nuclear export signal
ISDR	Interferon-α sensitivity-determining region	**NFκB**	Nuclear factor kappa-light-chain-enhancer of activated B-cells
IU	International units	**NK cells**	Natural killer cells

NLS	Nuclear localization sequence	**RIP1**	Receptor-interacting protein 1
nm	Nanometer	**RNS**	Reactive nitrogen species
NOX	NADPH oxidase	**ROS**	Reactive oxygen species
NPC	Nuclear pore complex	**PAGE**	Polyacrylamide gel electrophoresis
NPC1L1	Niemann–Pick C1-like 1	**qRT-PCR**	Quantitative Real time PCR
NQO1	NAD(P)H quinone oxidoreductase 1	**SDS**	Sodium dodecyl sulfate
Nrf2	Nuclear factor (erythroid-derived 2)-like-2	**SEM**	Standard error of the mean
NS	Nonstructural	**SERCA**	Sarcoplasmic/endoplasmic reticulum calcium ATPase
NTF	Nuclear transport factor	**siRNA**	Small interfering RNA
OCLN	Occludin	**sMaf**	Small Maf
OMM	Outer mitochondrial membrane	**SNARE**	Soluble N-ethylmaleimide-sensitive factor receptor
ORF	Open reading frame	**SRB1**	Scavenger receptor B1
PB1	Phox1 and Bem1p	**Stx17**	Syntaxin 17
PBS	Phosphate buffered saline	**SVR**	Sustained virological response
PDTC	Pyrrolidinedithiocarbamate	**TAG**	Triacylglyceride
PEI	Polyethylenimine	**tBHQ**	tert-Butylhydroquinone
PHH	Primary human hepatocytes	**TBS**	Tris buffered saline
PI3K	Phosphatidylinositol 3-kinase	**TBST**	Tris buffered saline-Tween 20
PI4KA	Phosphatidylinositol-4-kinase IIIα	**$TCID_{50}$**	50 % tissue culture infective dose
PI4P	Phosphatidylinositol-4-phosphate	**TIP47**	Tail-interacting protein of 47 kDa
PKA	Protein kinase A	**TRAF6**	Tumor necrosis factor receptor-associated factor 6
PKR	Phosphate buffered saline	**UBA**	Ubiquitin-associated domain
PLA2G4	Phospholipase A2	**ULK1/2**	Unc1-like kinase 1 and 2
PSMB5	Proteasomal subunit beta 5	**UPR**	Unfolded protein response
PVDF	Polyvinylidene fluoride	**UTR**	Untranslated region
RBV	Ribavirin	**VAR**	Variable sequence
RC	Replication complex	**V-ATPase**	Vacuolar type H^+-ATPase
RdRp	RNA-dependent RNA polymerase	**VLDL**	Very-low density lipoprotein
RIG-I	Retinoic acid-inducible gene I	**WHO**	World Health Organization

WIPI	WD-repeat domain phosphoinositide interacting protein
ZZ	Zinc finger

11 Eidesstaatliche Erklärung

Hiermit erkläre ich an Eides statt, dass ich die vorliegende Dissertation selbstständig und ohne unerlaubte Hilfe angefertigt und andere als die in der Arbeit angegebenen Hilfsmittel nicht benutzt habe. Alle Stellen, die wörtlich oder sinngemäß aus anderen Schriften entnommen sind, habe ich als solche kenntlich gemacht. Diese Arbeit hat in gleicher oder ähnlicher Form noch keiner Prüfungsbehörde vorgelegen. Des Weiteren bin ich mit der späteren Ausleihe meiner Doktorarbeit an die Fachbereichsbibliothek einverstanden.

Frankfurt, den 03.05.2017

Regina Medvedev